



The  
University  
Of  
Sheffield.

# One Dimensional Mean Line Performance Prediction Program for Turbocharger Axial Turbines

**Alan Martin Taylor**

A thesis submitted in partial fulfilment of the requirements for the degree of  
Master of Philosophy

The University of Sheffield  
Faculty of Engineering  
Department of Mechanical Engineering

July 2021

## **Acknowledgements**

First of all, I would like to thank Dr Robert Howell for all of his kind support and guidance during my time at the University of Sheffield. Similarly, I wish to thank Napier Turbochargers and my colleagues at Napier Turbochargers for their continued support and assistance during my course.

Finally, I would like to thank my family for their unwavering support throughout my course, thank you.

## Abstract

Mean line turbine performance prediction calculations are commonplace in the early stages of the turbine design process and are used to predict turbine performance and estimate geometric parameters before committing to CFD analysis. Napier Turbochargers also use such a tool for turbine performance map generation, turbine maps which are used in engine simulation software to predict engine performance. Periodically it is necessary to update the loss mechanisms used in the 1D tool based on current experimental data and research to ensure the accuracy and relevance of the results are maintained. The current performance prediction code used by Napier Turbochargers requires updating, it is necessary to review suitable, more recent axial turbine loss mechanisms with the aim of increasing the accuracy of efficiency prediction over a wide range of operating conditions for families of turbine geometries.

The results retrieved from the new program in conjunction with the selected loss models are compared to CFD results in order to validate the performance code and assess the chosen loss correlations. A number of productionised turbine geometries have been selected from the Napier Turbocharger portfolio to test the suitability of each loss correlation.

Analysis of the results revealed the governing parameters of each loss correlation and their applicability to a turbocharger turbine stage. The results were also assessed with the goal of possibly creating a selective tool to select the optimum loss correlation based on the required operating condition or turbine geometry.

# List of Contents

|   |                |
|---|----------------|
| Acknowledgements                            | page 2         |
| Abstract                                    | page 3         |
| List of Contents                            | page 4         |
| List of Tables                              | page 9         |
| List of Figures                             | page 9         |
| Nomenclature                                | page 17        |
| Declaration                                 | page 22        |
| <b>1 Introduction</b>                       | <b>page 24</b> |
| 1.1 Turbocharging and Performance           | page 24        |
| 1.2 Scope of Work                           | page 26        |
| 1.3 Thesis Outline and Synopses of Chapters | page 27        |
| <b>2 Literature Review</b>                  | <b>page 28</b> |
| 2.1 Introduction                            | page 28        |
| 2.2 Turbocharger Turbine Fundamentals       | page 29        |
| 2.3 Operating Characteristics               | page 33        |
| 2.3.1 Stage Loading Coefficient             | page 34        |
| 2.3.2 Flow coefficient                      | page 34        |
| 2.3.3 Velocity Ratio                        | page 35        |
| 2.3.4 Degree of Reaction                    | page 35        |
| 2.3.5 Smith Chart                           | page 36        |
| 2.4 Flow Field in Axial Turbines            | page 37        |
| 2.5 Loss Classification                     | page 40        |
| 2.5.1 Profile Loss                          | page 40        |
| 2.5.2 Trailing Edge Loss                    | page 40        |
| 2.5.3 Annulus Loss                          | page 41        |
| 2.5.4 Secondary loss                        | page 41        |

|         |                                  |         |
|---------|----------------------------------|---------|
| 2.5.5   | Tip clearance loss               | page 41 |
| 2.6     | Loss Correlations                | page 42 |
| 2.6.1   | Ainley and Mathieson Loss Model  | page 42 |
| 2.6.1.1 | Total Loss                       | page 42 |
| 2.6.1.2 | Profile Loss                     | page 42 |
| 2.6.1.3 | Secondary Loss                   | page 45 |
| 2.6.1.4 | Tip Clearance loss               | page 46 |
| 2.6.1.5 | Trailing Edge Correction         | page 46 |
| 2.6.2   | Dunham and Came Loss Model       | page 47 |
| 2.6.2.1 | Total Loss                       | page 47 |
| 2.6.2.2 | Profile Loss                     | page 47 |
| 2.6.2.3 | Secondary and tip clearance loss | page 47 |
| 2.6.2.4 | Tip Clearance loss               | page 48 |
| 2.6.3   | Kacker and Okapuu Loss Model     | page 48 |
| 2.6.3.1 | Total Loss                       | page 48 |
| 2.6.3.2 | Profile Loss                     | page 48 |
| 2.6.3.3 | Secondary Loss                   | page 50 |
| 2.6.3.4 | Trailing Edge Loss               | page 51 |
| 2.6.3.5 | Tip Clearance Loss               | page 52 |
| 2.6.4   | Craig and Cox Loss Model         | page 53 |
| 2.6.4.1 | Total Loss                       | page 53 |
| 2.6.4.2 | Profile Loss                     | page 53 |
| 2.6.4.3 | Secondary Loss                   | page 61 |
| 2.6.4.4 | Tip Clearance Loss               | page 63 |
| 2.6.4.5 | Annulus loss                     | page 63 |
| 2.6.4.6 | Cavity Loss                      | page 64 |
| 2.6.4.7 | Leakage Flow Through Glands      | page 65 |

|          |  |                |
|----------|--|----------------|
|          | 2.6.4.8 Other Loss                           | page 65        |
|          | 2.6.5 Denton Loss Model                      | page 65        |
|          | 2.6.5.1 Boundary layer Loss                  | page 65        |
|          | 2.6.5.2 Trailing Edge Loss                   | page 67        |
|          | 2.6.5.3 Tip Leakage Loss                     | page 68        |
|          | 2.6.5.4 Endwall Loss                         | page 68        |
|          | 2.6.5.5 Shock loss                           | page 68        |
| 2.7      | Loss Model Accuracy                          | page 69        |
|          | 2.7.1 Ainley and Mathieson Loss Model        | page 69        |
|          | 2.7.2 Dunham and Came Loss Model             | page 69        |
|          | 2.7.3 Kacker and Okapuu Loss Model           | page 70        |
|          | 2.7.4 Craig and Cox Loss Model               | page 71        |
|          | 2.7.5 Discussion                             | page 71        |
| <b>3</b> | <b>Mean Line Performance Prediction Tool</b> | <b>page 73</b> |
|          | 3.1 Introduction                             | page 73        |
|          | 3.2 Mean Line Tool Structure                 | page 74        |
|          | 3.3 Mean line Tool Inputs                    | page 75        |
|          | 3.4 Loss Correlation Implementation          | page 78        |
|          | 3.3.1 Kacker and Okapuu                      | page 79        |
|          | 3.3.2 Craig and Cox                          | page 79        |
|          | 3.3.3 Denton                                 | page 80        |
|          | 3.3.3.1 Profile Loss                         | page 80        |
|          | 3.3.3.2 Trailing Edge Loss                   | page 81        |
|          | 3.3.3.3 Secondary Loss                       | page 81        |
|          | 3.3.3.4 Tip Clearance Loss                   | page 81        |
| <b>4</b> | <b>CFD and Results Comparison</b>            | <b>page 83</b> |
|          | 4.1 Introduction                             | page 83        |

|     |                                    |          |
|-----|------------------------------------|----------|
| 4.2 | MULTALL CFD Code                   | page 84  |
|     | 4.2.1 CFD Mesh Study               | page 87  |
| 4.3 | MULTALL CFD Validation             | page 87  |
| 4.4 | MULTALL Boundary Conditions        | page 88  |
| 4.5 | Results Comparison and Analysis    | page 88  |
|     | 4.5.1 Geometry for Simulation      | page 89  |
|     | 4.5.2 Geometry 1                   | page 90  |
|     | 4.5.3 Geometry 2                   | page 102 |
|     | 4.5.4 Geometry 3                   | page 113 |
| 4.6 | Individual Loss Mechanism Analysis | page 119 |
|     | 4.6.1 Profile Loss                 | page 119 |
|     | 4.6.1.1 Kacker and Okapuu          | page 119 |
|     | 4.6.1.2 Craig and Cox              | page 120 |
|     | 4.6.1.3 Denton                     | page 120 |
|     | 4.6.1.4 Discussion                 | page 121 |
|     | 4.6.2 Secondary Loss               | page 122 |
|     | 4.6.2.1 Kacker and Okapuu          | page 122 |
|     | 4.6.2.2 Craig and Cox              | page 122 |
|     | 4.6.2.3 Denton                     | page 123 |
|     | 4.6.2.4 Discussion                 | page 123 |
|     | 4.6.3 Trailing Edge Loss           | page 126 |
|     | 4.6.3.1 Kacker and Okapuu          | page 126 |
|     | 4.6.3.2 Craig and Cox              | page 126 |
|     | 4.6.3.3 Denton                     | page 126 |
|     | 4.6.3.4 Discussion                 | page 126 |
|     | 4.6.4 Tip Clearance Loss           | page 127 |
|     | 4.6.4.1 Kacker and Okapuu          | page 127 |

|          |  |                 |
|----------|--|-----------------|
|          | 4.6.4.2 Craig and Cox  | page 127        |
|          | 4.6.4.3 Denton   | page 127        |
|          | 4.6.4.4 Discussion   | page 128        |
| 4.7      | Results Summary  | page 128        |
| <b>5</b> | <b>Conclusions and Recommendations for Future Work</b>                                   | <b>page 133</b> |
| 5.1      | Implementation of selective loss correlation based on operating conditions and geometry. | page 133        |
| 5.2      | Conclusion   | page 134        |
| 5.3      | Recommendations for Future work  | page 135        |
| <b>6</b> | <b>Bibliography</b>  | <b>page 136</b> |
| <b>7</b> | <b>Appendices</b>  | <b>page 139</b> |
|          | Appendix A   | Page 140        |
|          | A.1 Sample MULTALL input file without blade geometry                                     | page 140        |
|          | Appendix B   | Page 141        |
|          | B.1 Denton profile loss bilinear interpolation   | page 141        |
|          | Appendix C   | Page 142        |
|          | C.1 Kacker and Okapuu VBA code for Loss Model  | page 142        |
|          | C.2 Denton VBA code for Loss Model   | page 148        |
|          | C.3 Craig and Cox VBA code for Loss Model  | page 152        |



## List of Tables

|   |          |
|---|----------|
| Table 1 Breakdown of losses in the Craig and Cox loss system (Craig and Cox 1971).                    | Page 53  |
| Table 2 Input parameters to mean line turbine performance prediction tool.                            | Page 75  |
| Table 3 MULTALL boundary conditions.  | Page 88  |
| Table 4 Important geometric ratios of the turbine stage geometries to be investigated.                | Page 89  |
| Table 5 Important geometric factors relating to the first turbine stage geometry to be investigated.  | Page 90  |
| Table 6 Important geometric factors relating to the second turbine stage geometry to be investigated. | Page 102 |
| Table 7 Important geometric factors relating to the third turbine stage geometry to be investigated.  | Page 113 |

## List of Figures

|   |         |
|---|---------|
| Fig. 1-1, Wartsila Goodman Energy Center in Kansas USA<br>( <a href="https://www.wartsila.com/media/news/16-12-2014-wartsila-supplies-extension-to-a-wind-balancing-power-plant-in-kansas-usa">https://www.wartsila.com/media/news/16-12-2014-wartsila-supplies-extension-to-a-wind-balancing-power-plant-in-kansas-usa</a> ) | Page 25 |
| Fig. 1-2a MV ETNE engine room (Napier Turbochargers).   | Page 25 |
| Fig. 1-2b MV ETNE<br>( <a href="https://www.marinetraffic.com/en/photos/of/ships/shipid:305467/ships">https://www.marinetraffic.com/en/photos/of/ships/shipid:305467/ships</a> )  | Page 25 |
| Fig. 2-1 Cutaway of a Napier NT1-10 turbocharger (Napier Turbochargers).  | Page 29 |
| Fig. 2-2 Axial flow turbine stage (Watson 1982).  | Page 30 |
| Fig. 2-3 Turbine performance map total to static efficiency (Napier Turbochargers).   | Page 31 |
| Fig. 2-4 Turbine performance map swallowing capacity (Napier Turbochargers).  | Page 31 |
| Fig. 2-5 Enthalpy entropy diagram (Watson 1982).  | Page 32 |
| Fig. 2-6 Velocity triangles (Watson 1982).  | Page 33 |
| Fig. 2-7 Smith chart (Smith 1965).  | Page 36 |
| Fig. 2-8 Turbine flow field (Denton 1994).  | Page 37 |
| Fig. 2-9a Secondary losses (Langston 2001).   | Page 38 |
| Fig. 2-9b Secondary losses (Klein 1966).  | Page 38 |
| Fig. 2-10 Secondary flow model (Sjolander1997).   | Page 38 |

|  |         |
|--|---------|
| Fig. 2-11 Flow over the tip gap for an unshrouded blade (Denton 1993).   | Page 39 |
| Fig. 2-12 Leading edge separation bubbles and their effect on blade surface static pressure distribution (Moustapha 2003).                                   | Page 39 |
| Fig. 2-13 Profile loss coefficients for conventional section blades at zero incidence (Ainley and Mathieson 1951).   | Page 42 |
| Fig. 2-14 Profile loss coefficients for conventional section blades at zero incidence (Ainley and Mathieson 1951).   | Page 43 |
| Fig. 2-15 Positive stalling incidences of cascades of turbine blades (Ainley and Mathieson 1951).  | Page 43 |
| Fig. 2-16 Positive stalling incidences of cascades of turbine blades (Ainley and Mathieson 1951).  | Page 44 |
| Fig. 2-17 Positive stalling incidences of cascades of turbine blades (Ainley and Mathieson 1951).  | Page 44 |
| Fig. 2-18 Profile loss incidence correction (Ainley and Mathieson 1951).   | Page 44 |
| Fig. 2-19 Secondary losses in turbine blade rows (Ainley and Mathieson 1951).  | Page 45 |
| Fig. 2-20 Effect of trailing edge thickness on blade loss coefficients (Ainley and Mathieson 1951).  | Page 46 |
| Fig. 2-21 Inlet Mach number ratio for nonfree-vortex turbine blades (Kacker and Okapuu 1982).  | Page 49 |
| Fig. 2-22 Combined effect of leading edge shock on inner end wall flow and the blade channel next to it (Kacker and Okapuu 1982).                            | Page 49 |
| Fig. 2-23 Mach number correction factor $K_1$ for the profile loss coefficient, for accelerating cascades of $M_1 \rightarrow M_2$ (Kacker and Okapuu 1982). | Page 50 |
| Fig. 2-24 Mach number correction factor $K_2$ for the profile loss coefficient (Kacker and Okapuu 1982).   | Page 50 |
| Fig. 2-25 Mach number correction factor $K_3$ for the secondary loss coefficient (Kacker and Okapuu 1982).   | Page 51 |
| Fig. 2-26 Trailing edge loss (energy) coefficient correlated against the ratio of trailing edge thickness to throat opening (Kacker and Okapuu 1982).        | Page 52 |
| Fig. 2-27 Profile loss ratio against Reynolds number effect (Craig and Cox 1971).  | Page 54 |
| Fig. 2-28 Lift parameter (Craig and Cox 1971).   | Page 54 |

|   |         |
|---|---------|
| Fig. 2-29 Basic profile loss (Craig and Cox 1971).  | Page 55 |
| Fig. 2-30 Contraction ratio for average profiles (Craig and Cox 1971).  | Page 55 |
| Fig. 2-31 Trailing edge thickness losses (Craig and Cox 1971).  | Page 56 |
| Fig. 2-32 Incidence losses (Craig and Cox 1971).  | Page 56 |
| Fig. 2-33 Basic positive stalling incidence (Craig and Cox 1971).   | Page 57 |
| Fig. 2-34 Incidence correction for positive stalling incidences (Craig and Cox 1971).                                       | Page 57 |
| Fig. 2-35 Incidence correction for positive stalling incidences (Craig and Cox 1971).                                       | Page 58 |
| Fig. 2-36 Basic negative stalling incidence (Craig and Cox 1971).   | Page 58 |
| Fig. 2-37 Incidence correction (Craig and Cox 1971).  | Page 59 |
| Fig. 2-38 Basic stalling incidences for blade angles greater than 90 (Craig and Cox 1971).                                  | Page 59 |
| Fig. 2-39 Minimum loss incidence-range ratio $F_i$ (Craig and Cox 1971).  | Page 60 |
| Fig. 2-40 Mach number loss for convergent blading (Craig and Cox 1971).   | Page 60 |
| Fig. 2-41 Blade back radius losses (Craig and Cox 1971).  | Page 61 |
| Fig. 2-42 Secondary loss – basic loss factor (Craig and Cox 1971).  | Page 62 |
| Fig. 2-43 Secondary loss – aspect ratio factor (Craig and Cox 1971).  | Page 62 |
| Fig. 2-44 Shrouded efficiency loss (Craig and Cox 1971).  | Page 63 |
| Fig. 2-45 Annulus wall loss (Craig and Cox 1971).   | Page 64 |
| Fig. 2-46 Cavity loss (Craig and Cox 1971).   | Page 64 |
| Fig. 2-47 Calculated dissipation coefficients for turbulent boundary layers (Denton 1993).                                  | Page 66 |
| Fig. 2-48 Dissipation coefficient for laminar and turbulent boundary layers (Denton 1993).                                  | Page 67 |
| Fig. 2-49 Comparison of design point efficiencies of 25 turbines (Dunham and Came 1970).                                    | Page 69 |
| Fig. 2-50 Turbine stage efficiency at zero tip leakage calculated by the Kacker and Okapuu method (Kacker and Okapuu 1982). | Page 70 |
| Fig. 2-51 Comparison of predicted efficiency with experimental efficiency of 33 turbines (Kacker and Okapuu 1982).          | Page 71 |
| Fig. 2-52 Comparison of predicted and measured test efficiencies (Craig and Cox 1971).                                      | Page 72 |

|   |         |
|---|---------|
| Fig. 3-1 Turbine blade nomenclature (Ainley and Mathieson 1951).  | Page 76 |
| Fig. 3-2 Turbine blade nomenclature (Ainley and Mathieson 1951)   | Page 76 |
| Fig. 3-3 Basic structure of the calculation process in the new mean line tool.  | Page 77 |
| Fig. 3-4 Screenshot of Chart digitization program developed by the author.  | Page 78 |
| Fig. 3-5 Parabola arc length ( <a href="https://www.vcalc.com/wiki/vCalc/Parabola+arc+length">https://www.vcalc.com/wiki/vCalc/Parabola+arc+length</a> ). | Page 79 |
| Fig. 3-6 Generic surface velocity distribution for a turbine (Denton 1990).   | Page 80 |
| Fig. 3-7 Predicted profile loss (%) of Turbine blades at optimum pitch to chord ratios (Denton 1993).   | Page 81 |
| Fig. 3-8 Tip leakage loss coefficient for unshrouded blades: contours in percent exist dynamic head per 1 percent clearance/height (Denton 1993).         | Page 82 |
| Fig. 4-1 Blade to blade view of grid on a streamwise surface from MULTALL.  | Page 85 |
| Fig. 4-2 Meridional view of grid from MULTALL   | Page 85 |
| Fig. 4-3 Mixing plane treatment (Denton 2017).  | Page 86 |
| Fig. 4-4 CFD mesh study.  | Page 87 |
| Fig. 4-5 Typical Napier Turbocharger axial turbine arrangement.   | Page 89 |
| Fig. 4-6 Normalised Efficiency curves predicted for Geometry 1 at a non-dimensional speed of $\frac{N}{\sqrt{T_{01}}} = 593 \text{ rpm}/\sqrt{K}$ .       | Page 90 |
| Fig. 4-7 Stator total loss coefficient $\frac{N}{\sqrt{T_{01}}} = 593 \text{ rpm}/\sqrt{K}$ geometry 1.   | Page 91 |
| Fig. 4-8 Turbine total loss coefficient $\frac{N}{\sqrt{T_{01}}} = 593 \text{ rpm}/\sqrt{K}$ geometry 1.  | Page 91 |
| Fig. 4-9 Breakdown of turbine losses Kacker and Okapuu $\frac{N}{\sqrt{T_{01}}} = 593 \text{ rpm}/\sqrt{K}$ geometry 1.                                   | Page 92 |
| Fig. 4-10 Breakdown of stator losses Craig and Cox $\frac{N}{\sqrt{T_{01}}} = 593 \text{ rpm}/\sqrt{K}$ geometry 1.                                       | Page 93 |
| Fig. 4-11 Breakdown of turbine losses Denton $\frac{N}{\sqrt{T_{01}}} = 593 \text{ rpm}/\sqrt{K}$ geometry 1.   | Page 94 |
| Fig. 4-12 Normalised Efficiency curves predicted for Geometry 1 at a non-dimensional speed of $\frac{N}{\sqrt{T_{01}}} = 989 \text{ rpm}/\sqrt{K}$ .      | Page 95 |
| Fig. 4-13 Stator total loss coefficient $\frac{N}{\sqrt{T_{01}}} = 989 \text{ rpm}/\sqrt{K}$ geometry 1.  | Page 95 |

Fig. 4-14 Turbine total loss coefficient  $\frac{N}{\sqrt{T_{01}}} = 989 \text{ rpm}/\sqrt{K}$  geometry 1. Page 96

Fig. 4-15 Breakdown of turbine losses Kacker and Okapuu  $\frac{N}{\sqrt{T_{01}}} = 989 \text{ rpm}/\sqrt{K}$  geometry 1. Page 96

Fig. 4-16 Breakdown of turbine losses Craig and Cox  $\frac{N}{\sqrt{T_{01}}} = 989 \text{ rpm}/\sqrt{K}$  geometry 1. Page 97

Fig. 4-17 Breakdown of turbine losses Denton  $\frac{N}{\sqrt{T_{01}}} = 989 \text{ rpm}/\sqrt{K}$  geometry 1. Page 98

Fig. 4-18 Normalised Efficiency curves predicted for Geometry 1 at a non-dimensional speed of  $\frac{N}{\sqrt{T_{01}}} = 1285 \text{ rpm}/\sqrt{K}$ . Page 99

Fig. 4-19 Stator total loss coefficient  $\frac{N}{\sqrt{T_{01}}} = 1285 \text{ rpm}/\sqrt{K}$  geometry 1. Page 99

Fig. 4-20 Turbine total loss coefficient  $\frac{N}{\sqrt{T_{01}}} = 1285 \text{ rpm}/\sqrt{K}$  geometry 1. Page 100

Fig. 4-21 Breakdown of turbine losses Kacker and Okapuu  $\frac{N}{\sqrt{T_{01}}} = 1285 \text{ rpm}/\sqrt{K}$  geometry 1. Page 100

Fig. 4-22 Breakdown of turbine losses Craig and Cox  $\frac{N}{\sqrt{T_{01}}} = 1285 \text{ rpm}/\sqrt{K}$  geometry 1. Page 101

Fig. 4-23 Breakdown of rotor losses Denton  $\frac{N}{\sqrt{T_{01}}} = 1285 \text{ rpm}/\sqrt{K}$  geometry 1. Page 101

Fig. 4-24 Normalised Efficiency curves predicted for Geometry 2 at a non-dimensional speed of  $\frac{N}{\sqrt{T_{01}}} = 635 \text{ rpm}/\sqrt{K}$ . Page 102

Fig. 4-25 Stator total loss coefficient  $\frac{N}{\sqrt{T_{01}}} = 635 \text{ rpm}/\sqrt{K}$  geometry 2. Page 103

Fig. 4-26 Turbine total loss coefficient  $\frac{N}{\sqrt{T_{01}}} = 635 \text{ rpm}/\sqrt{K}$  geometry 2. Page 103

Fig. 4-27 Breakdown of turbine losses Kacker and Okapuu  $\frac{N}{\sqrt{T_{01}}} = 635 \text{ rpm}/\sqrt{K}$  geometry 2. Page 104

Fig. 4-28 Breakdown of turbine losses Craig and Cox  $\frac{N}{\sqrt{T_{01}}} = 635 \text{ rpm}/\sqrt{K}$  geometry 2. Page 105

Fig. 4-29 Breakdown of turbine losses Denton  $\frac{N}{\sqrt{T_{01}}} = 635 \text{ rpm}/\sqrt{K}$  geometry 2. Page 106

Fig. 4-30 Normalised Efficiency curves predicted for Geometry 2 at a non-dimensional speed of  $\frac{N}{\sqrt{T_{01}}} = 1060 \text{ rpm}/\sqrt{K}$ . Page 106

Fig. 4-31 Stator total loss coefficient  $\frac{N}{\sqrt{T_{01}}} = 1060 \text{ rpm}/\sqrt{K}$  geometry 2. Page 107

Fig. 4-32 Turbine total loss coefficient  $\frac{N}{\sqrt{T_{01}}} = 1060 \text{ rpm}/\sqrt{K}$  geometry 2. Page 107

Fig. 4-33 Breakdown of turbine losses Kacker and Okapuu  $\frac{N}{\sqrt{T_{01}}} = 1060 \text{ rpm}/\sqrt{K}$  geometry 2. Page 108

Fig. 4-34 Breakdown of turbine losses Craig and Cox  $\frac{N}{\sqrt{T_{01}}} = 1060 \text{ rpm}/\sqrt{K}$  geometry 2. Page 108

Fig. 4-35 Breakdown of turbine losses Denton  $\frac{N}{\sqrt{T_{01}}} = 1060 \text{ rpm}/\sqrt{K}$  geometry 2. Page 109

Fig. 4-36 Normalised Efficiency curves predicted for Geometry 2 at a non-dimensional speed of  $\frac{N}{\sqrt{T_{01}}} = 1271 \text{ rpm}/\sqrt{K}$ . Page 110

Fig. 4-37 Stator total loss coefficient  $\frac{N}{\sqrt{T_{01}}} = 1271 \text{ rpm}/\sqrt{K}$  geometry 2. Page 110

Fig. 4-38 Turbine total loss coefficient  $\frac{N}{\sqrt{T_{01}}} = 1271 \text{ rpm}/\sqrt{K}$  geometry 2. Page 111

Fig. 4-39 Breakdown of turbine losses Kacker and Okapuu  $\frac{N}{\sqrt{T_{01}}} = 1271 \text{ rpm}/\sqrt{K}$  geometry 2. Page 111

Fig. 4-40 Breakdown of turbine losses Craig and Cox  $\frac{N}{\sqrt{T_{01}}} = 1271 \text{ rpm}/\sqrt{K}$  geometry 2. Page 112

Fig. 4-41 Breakdown of turbine losses Denton  $\frac{N}{\sqrt{T_{01}}} = 1271 \text{ rpm}/\sqrt{K}$  geometry 2. Page 112

Fig. 4-42 Normalised Efficiency curves predicted for Geometry 3 at a non-dimensional speed of  $\frac{N}{\sqrt{T_{01}}} = 745 \text{ rpm}/\sqrt{K}$ . Page 113

Fig. 4-43 Stator total loss coefficient  $\frac{N}{\sqrt{T_{01}}} = 745 \text{ rpm}/\sqrt{K}$  geometry 3. Page 114

Fig. 4-44 Turbine total loss coefficient  $\frac{N}{\sqrt{T_{01}}} = 745 \text{ rpm}/\sqrt{K}$  geometry 3. Page 114

Fig. 4-45 Breakdown of turbine losses Kacker and Okapuu  $\frac{N}{\sqrt{T_{01}}} = 745 \text{ rpm}/\sqrt{K}$  geometry 3. Page 115

Fig. 4-46 Breakdown of turbine losses Craig and Cox  $\frac{N}{\sqrt{T_{01}}} = 745 \text{ rpm}/\sqrt{K}$  geometry 3. Page 115

Fig. 4-47 Breakdown of turbine losses Denton  $\frac{N}{\sqrt{T_{01}}} = 745 \text{ rpm}/\sqrt{K}$  geometry 3. Page 116

Fig. 4-48 Normalised Efficiency curves predicted for Geometry 3 at a non-dimensional speed of  $\frac{N}{\sqrt{T_{01}}} = 1043 \text{ rpm}/\sqrt{K}$ . Page 116

Fig. 4-49 Stator total loss coefficient  $\frac{N}{\sqrt{T_{01}}} = 1043 \text{ rpm}/\sqrt{K}$  geometry 3. Page 117

Fig. 4-50 Turbine total loss coefficient  $\frac{N}{\sqrt{T_{01}}} = 1043 \text{ rpm}/\sqrt{K}$  geometry 3. Page 117

Fig. 4-51 Breakdown of turbine losses Kacker and Okapuu  $\frac{N}{\sqrt{T_{01}}} = 1043 \text{ rpm}/\sqrt{K}$  geometry 3. Page 118

Fig. 4-52 Breakdown of turbine losses Craig and Cox  $\frac{N}{\sqrt{T_{01}}} = 1043 \text{ rpm}/\sqrt{K}$  geometry 3. Page 118

Fig. 4-53 Breakdown of turbine losses Denton  $\frac{N}{T_{01}} = 1043 \text{ rpm}/\sqrt{K}$  geometry 3. Page 119

Fig. 4-54 Turbine profile losses at  $\frac{N}{T_{01}} = 989 \text{ rpm}/\sqrt{K}$  geometry 1. Page 121

Fig. 4-55 Turbine profile losses at  $\frac{N}{T_{01}} = 1060 \text{ rpm}/\sqrt{K}$  geometry 2. Page 121

Fig. 4-56 Turbine profile losses at  $\frac{N}{T_{01}} = 745 \text{ rpm}/\sqrt{K}$  geometry 3. Page 122

Fig. 4-57 Turbine secondary losses at  $\frac{N}{T_{01}} = 989 \text{ rpm}/\sqrt{K}$  geometry 1. Page 124

Fig. 4-58 Turbine secondary losses at  $\frac{N}{T_{01}} = 1060 \text{ rpm}/\sqrt{K}$  geometry 2. Page 124

Fig. 4-59 Turbine secondary losses at  $\frac{N}{T_{01}} = 745 \text{ rpm}/\sqrt{K}$  geometry 3. Page 125

Fig. 4-60 Comparison of the turbine secondary losses between geometry 1 and 2. Page 125

Fig. 4-61 Predicted turbine efficiency with CFD efficiency for geometry 1 at  $\frac{N}{\sqrt{T_{01}}} = 593 \text{ rpm}/\sqrt{K}$ . Page 128

Fig. 4-62 Predicted turbine efficiency with CFD efficiency for geometry 1 at  $\frac{N}{\sqrt{T_{01}}} = 989 \text{ rpm}/\sqrt{K}$ . Page 129

Fig. 4-63 Predicted turbine efficiency with CFD efficiency for geometry 1 at

$$\frac{N}{\sqrt{T_{01}}} = 1285 \text{ rpm}/\sqrt{K} \text{ N}/\sqrt{T}.$$

Page 129

Fig. 4-64 Predicted turbine efficiency with CFD efficiency for geometry 2 at

$$\frac{N}{\sqrt{T_{01}}} = 635 \text{ rpm}/\sqrt{K}.$$

Page 130

Fig. 4-65 Predicted turbine efficiency with CFD efficiency for geometry 2 at

$$\frac{N}{\sqrt{T_{01}}} = 1060 \text{ rpm}/\sqrt{K} \text{ N}/\sqrt{T}.$$

Page 130

Fig. 4-66 Predicted turbine efficiency with CFD efficiency for geometry 2 at

$$\frac{N}{\sqrt{T_{01}}} = 1271 \text{ rpm}/\sqrt{K}.$$

Page 131

Fig. 4-67 Predicted turbine efficiency with CFD efficiency for geometry 3 at

$$\frac{N}{\sqrt{T_{01}}} = 745 \text{ rpm}/\sqrt{K}.$$

Page 131

Fig. 4-68 Predicted turbine efficiency with CFD efficiency for geometry 3 at

$$\frac{N}{\sqrt{T_{01}}} = 1043 \text{ rpm}/\sqrt{K}.$$

Page 132



## Nomenclature

$A$  gas flow area; fluid relative inlet angle

$A_{n_0}$  annulus area at outlet to stator row

$A_{n_2}$  annulus area at outlet to rotor row

$B$  fluid relative outlet angle

$b$  backbone length

$b_x$  axial chord

$C$  absolute velocity

$C_L$  lift coefficient

$c$  true chord

$CR$  contraction ratio

$C_d$  dissipation coefficient

$C_f$  Friction factor

$C_s$  blade surface length

$C_{pb}$  base pressure coefficient

$C_p, C_v$  specific heat capacities

$e$  back surface radius of curvature

$f_{(AR)}$  aspect ratio function

$f_{Re}$  Reynolds number correction factor

$F_a$  Cavity Factor

$F_L$  lift parameter

$F_i$  minimum loss incidence-range ratio

$F_k$  efficiency debit factor

$g$  gravitational constant

$G$  mass flow through blades

$h$  enthalpy

$H$  height

$i$  incidence angle  
 $i_s$  stalling incidence  
 $i_{min}$  incidence for minimum loss  
 $i + stall$  positive stalling incidence  
 $i - stall$  negative stalling incidence  
 $(i + stall)_{basic}$  value for standard value of  $s/b$  and  $CR$   
 $(i - stall)_{basic}$  value for standard value of  $s/b$   
 $I. D.$  inside diameter of turbine annulus  
 $O. D.$  outside diameter of turbine annulus  
 $k$  radial tip clearance  
 $K_1, K_2, K_3, K_p, K_S$  correction factors  
 $M$  mach number  
 $m$  mass flow rate  
 $N$  loss ratio  
 $o$  throat opening  
 $P$  pressure  
 $Q$  heat transfer  
 $Re$  Reynolds number  
 $Re_o$  Reynolds number based on blade opening  
 $Re_\theta$  Reynolds number based on momentum thickness  
 $r$  radius  
 $s$  blade pitch  
 $\dot{S}$  total entropy  
 $\dot{S}_a$  entropy creation rate per unit surface area  
 $t$  time  
 $t_{max}$  maximum blade thickness  
 $te$  trailing edge thickness

$T$  temperature

$U$  blade speed

$U/C$  Velocity Ratio

$V$  volume

$W_x$  specific work transfer

$W$  velocity relative to blade

$W_1$  relative velocity at inlet to runner

$W_2$  relative velocity at outlet to runner

$x$  basic loss factor

$x, y, z$  cartesian coordinates

$X_{Te}$  trailing edge correction factor

$X_i$  incidence coefficient

$X$  total loss factor

$Y_p$  profile loss coefficient

$Y_p$  secondary loss coefficient

$Y_k$  clearance loss coefficient

$Y_{SHOCK}$  Shock loss

$Y_t$  Total loss coefficient

$Y_{TET}$  Trailing edge loss coefficient

## Greeks

$\alpha$  gas flow angle; blade inlet angle

$\alpha_m$  mean gas flow angle

$\beta$  blade angle

$\gamma$  ratio of specific heats

$\delta$

$\delta^*$  boundary layer displacement thickness

$\zeta_s, \zeta$  entropy and energy loss coefficient

$\eta$  efficiency

$\eta_b$  blading efficiency

$\Delta\eta$  efficiency debit

$\theta$  boundary layer momentum thickness

$\lambda$  empirical factor defining secondary loss

$\Lambda$  reaction

$\xi$  stagger angle

$\rho$  fluid density

$\phi$  flow coefficient

$\phi^2$  kinetic energy coefficient

$\Delta\phi_{TET}^2$  trailing edge K.E. loss coefficient

$\psi$  stage loading coefficient; runner blade velocity coefficient (Craig and Cox)

## Subscripts

0 stagnation

1,2,... stations define stations

$a$  annulus; axial

$b$  basic

$AMDC$  as per Ainley, Mathieson, Dunham and Came

$h$  hub

$h/b$  aspect ratio

$i$  incidence

$isen$  isentropic

$L$  leakage flow

$m$  mach number; mainstream flow

$p$  profile

$r$  Reynolds number

$s$  secondary

$s/e$  back curvature

$t$  tip

$T$  turbine

$ts$  total to static

$tt$  total to total

$\theta$  tangential

$\delta$  at the edge of the boundary layer

## Abbreviations

CFD Computational fluid dynamics

CFL The Courant–Friedrichs–Lewy condition

AM Ainley Mathieson loss model

AMDC Ainley Mathieson Dunham Came loss model

CC Craig and Cox loss model

KO Kacker and Okapuu loss model

*I, the author, confirm that the Thesis is my own work. I am aware of the University's Guidance on the Use of Unfair Means ([www.sheffield.ac.uk/ssid/unfair-means](http://www.sheffield.ac.uk/ssid/unfair-means)). This work has not been previously been presented for an award at this, or any other, university.*



# Chapter 1

## Introduction

### 1.1 Turbocharging and Performance

Turbocharging is an integral system of the internal combustion diesel engine. A turbocharger comprises of a compressor driven by a turbine which extracts energy from the engine exhaust gases. The compressor enables an increased amount of air to be delivered to the engine cylinder through compression of the intake air, this provides several benefits for engine performance including increased power output, fuel economy and reduced engine emissions. The compressor and turbine are matched to the engine to give optimum performance according to manufacturer requirements, this process involves the use of performance maps and simulation software.

Napier turbochargers supplies hardware for large and medium speed diesel engines for applications such as baseload power plant, pumping stations and nuclear back up engines in the energy sector and cruise ships, offshore vessels and merchant ships in the marine sector, as well as various traction applications for legacy turbochargers. Below are examples of turbocharger installations for a power plant application, Figure 1-1, and a marine application, Figure 1-2.





Fig. 1-1. Wärtsilä Goodman Energy Center in Kansas.

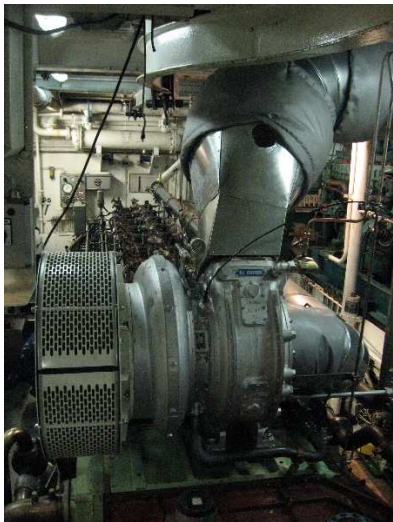


Fig. 1-2a



Fig. 1-2b

Fig. 1-2a MV Etne engine room, Fig. 1-2b MV Etne passenger ferry.

Depending on the type of application or where the application is located it is necessary to adhere to some form of emission legislation. Current emission legislations include IMO T3 (International Maritime Organisation ©2019), EPA T4 (United States Environmental Protection Agency ©2021) and TA-Luft (Bundesministerium für Umwelt, Naturschutz und nukleare Sicherheit ©2021) and ½ TA-Luft. The various emission legislations control the pollution of engines, regulating such pollutants as Nitrous Oxide, Carbon Dioxide, particulates, and the Sulphur content of fuels.

With the implementation of stricter emission legislation, engine manufacturers are demanding higher pressure ratio capabilities from turbochargers (Wik and Hallback 2007) and are developing alternative emission reduction technologies (Drews 2019). One of the advantages of increasing the inlet air density to the engine is the reduction of fuel consumption, this is permitted due to the higher cylinder pressures which enable the use of a leaner air/fuel mixture during combustion. There are a number of technologies that may be employed to satisfy the demand for lower emissions while

maintaining similar or improved fuel consumptions. One such technology is two stage turbocharging which compliments an engine strategy known as Miller timing which reduces combustion temperatures thus reducing NO<sub>x</sub> emissions. Other engine emission reduction technologies include selective catalytic reduction and exhaust gas recirculation which can also be used in combination with two stage or compound turbocharging (Mayr 2019) (Codan et al 2010).

To assess the performance of the diesel engine and such emission reducing technologies, engine simulation software is becoming more prevalent. This requires compressor and turbine characteristics to accurately predict system performance; thus, it is imperative the characteristics are of sufficient range and accuracy to ensure suitable interpretation in the simulation software and generation of realistic results.

Several computational tools are used to analyse turbine performance including CFD. This however can be time consuming and often demands a complete detailed model of the turbine blade and housing arrangement to produce accurate results. CFD code also requires a certain amount of calibration against experimental results in order to improve the accuracy of off design performance prediction. The one-dimensional mean line loss calculation method of turbine performance offers a less time consuming and more flexible tool, which can predict turbine performance over a wide range of operating conditions and is ideal for first design iterations, where the turbine blade geometry is not yet fixed, and performance map generation.

As a result of the demand for strict emission control at varying turbocharger operating conditions the accuracy of the turbine performance maps used in engine simulation software is paramount. This study investigates turbine efficiency prediction at a wide range of turbocharger operating conditions using typical turbocharger turbines where the previous studies researched of one-dimensional mean line performance prediction methods have tended to concentrate on design point efficiency performance.

## 1.2 Scope of Work

The software currently in use is based on the Ainley and Mathieson (Ainley and Mathieson 1951) mean line loss technique published in 1951 and updated by Dunham and Came in 1970 (Dunham and Came 1970). The program is written in Fortran without any standardisation or background text and contains many unorganised loops and unexplained factors which have been implemented as the code has undergone iterations to ensure correlation to the latest experimental test data is maintained, periodic iterations have also been necessary due to advancements in analytical capability, although the program still suffers from a number of limitations which impact the quality of the performance data produced. It is necessary to review suitable, more recent axial turbine loss mechanisms to update the current code to increase the accuracy of efficiency prediction over a wide range of operating conditions and families of turbine geometries.

The present work will be undertaken on a part time basis while the author continues to fulfil his post within Napier Turbochargers as Principal Performance Engineer. A literature review will be carried out to research turbine theory fundamentals and identify more modern common loss correlations. On completion of the literature review a programming language will be chosen for the one-

dimensional performance code. The basic performance calculations will be carried over from the original Fortran program, outlined by Ainley and Mathieson (1952), and the newly identified loss correlations will be built into the new program as selectable routines.

Due to the absence of a dedicated turbine test rig Napier does not possess sufficient complete turbine test data to adequately validate the turbine performance prediction method therefore the CFD based program MULTALL (Denton 2009) produced by Prof. J.D. Denton will be used to validate the performance code and assess the loss correlations. A number of productionised turbine geometries with differing features have been selected to test the suitability of each loss correlation. The results retrieved from each loss correlation will be compared based on accuracy over a wide range of operating conditions.

### 1.3 Thesis Outline and Synopses of Chapters

The thesis aims to improve the current mean line turbine performance prediction program by adopting a more accessible programming language and implementing more modern loss correlations. The performance results obtained from the new mean line loss program will be compared to CFD data to assess the accuracy of the loss models over a wide range of operating conditions and turbocharger turbine geometries. The results will also be examined, and opportunities identified where the loss models may be used selectively based on turbine operating condition or geometry. The thesis is divided into 5 Chapters, a synopsis of each is given in the following paragraphs:

Chapter 1 has introduced the turbocharger highlighting its advantages when applied to the internal combustion diesel engine and the requirement for further development. The requirement for accurate turbine performance prediction methods was also identified. A brief outline of the applications of Napier Turbochargers is also given.

Chapter 2 presents a review of the fundamentals of the turbocharger axial turbine as well as its main operating characteristics. The flow field of the axial turbine is examined and a classification of the relevant losses in a turbine stage are provided. Finally, more modern loss correlations are reviewed in detail.

Chapter 3 looks at the structure and design of the new mean line tool and explains how the chosen loss correlations have been translated into code.

Chapter 4 reviews the CFD program that will be used to validate the mean line tool and shows a comparison between CFD and predicted results. The individual loss mechanisms are also analysed and discussed. A summary of the results is also presented to assess the suitability of each loss model.

Chapter 5 concludes the results retrieved from the new mean line tool and CFD. Suggestions for further work are also presented.

# Chapter 2

## Literature Review

### 2.1 Introduction

This chapter aims to review the relevant literature on turbocharger axial turbine stages performance characteristics and loss mechanisms. A review of the fundamentals of turbocharger axial turbines will be covered where turbine efficiency, working cycle and velocity triangles of the turbocharger axial turbine are defined. The operating characteristics of an axial turbine will also be analysed including such parameters as the stage loading coefficient, flow coefficient and degree of reaction. The complex flow field of an axial turbine is broken down into its constituent parts where the major sources of loss are classified. Since the loss model the original code is based on was published there have been significant advancements not only in the research conducted on axial turbine loss mechanisms but also turbine design methodologies and analyses. There also exists a greater amount of turbine test data for a variety of turbine geometries. Kacker and Okapuu suggest that the loss system used in a mean line performance prediction program should be critically reviewed and updated at least once every decade (Kacker and Okapuu 1982). The loss correlations covered in the final section of this chapter are some of the more common and widely used methods which will be incorporated into the mean line performance prediction program.

## 2.2 Turbocharger Axial Turbine Fundamentals

The turbocharger comprises of three main components the compressor, turbine and a shaft linking the two. Fig. 2.1 shows a cutaway view of a Napier NT1-10 turbocharger revealing the rotor and showing the structure of the turbocharger. The compressor is a centrifugal type and the turbine can be of axial or radial construction. These components require a high level of design and engineering to ensure desirable performance at suitable service life. For a turbocharged engine to operate efficiently the turbocharger must be matched according to the target conditions set out by the engine manufacturer by selecting the correct aerodynamic components. The selection of these components is derived from various performance calculations based on an energy balance across the turbocharger.

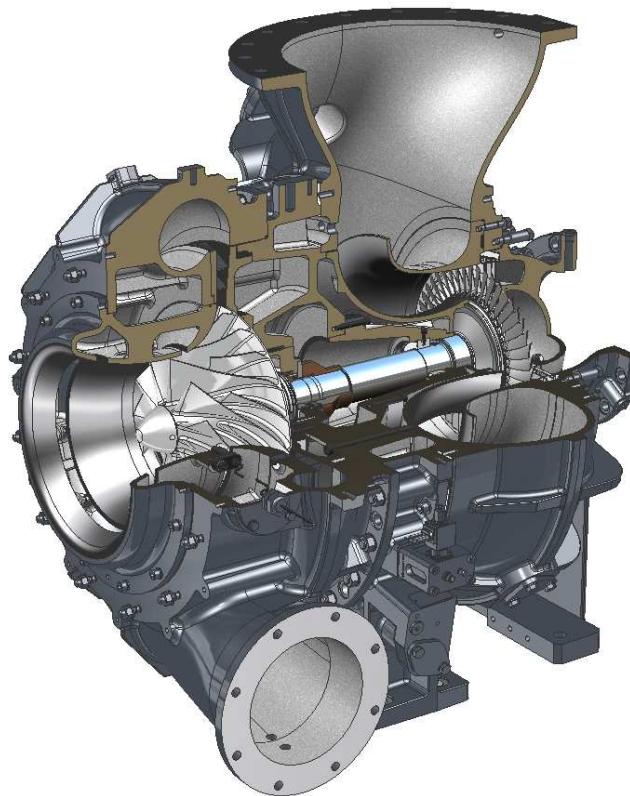


Fig. 2.1 NT1-10 Turbocharger Cutaway.

Figure 2-2 displays a typical arrangement of an axial turbine turbocharger. It can be seen a turbocharger axial turbine stage consists of a single row of nozzle (stator) blades and rotor (turbine) blades. Figure 2-2 also defines the station numbers used in the following calculations.

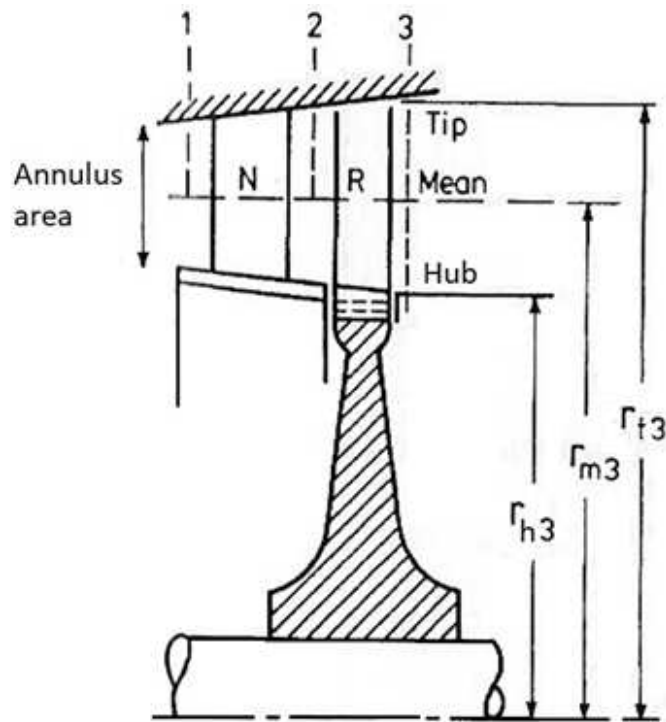


Fig. 2-2 Axial flow turbine stage (Watson 1982).

Component efficiency is critical in a turbocharger in order to deliver the best performance possible to optimise engine brake specification fuel consumption, emissions and thermal loading. The isentropic efficiency is used as an indicator for performance and is defined as the actual work divided by the isentropic work for a turbine.

$$\eta_{Ttt} = \frac{\text{actual work}}{\text{isentropic work}} = \frac{h_{01} - h_{03}}{h_{01} - h_{03\text{isen}}} \quad \text{Eq. 2-1}$$

There will be some residual kinetic energy that must be accounted for, typically turbochargers of the size considered in this paper include some kind of exhaust diffuser to recover some of this energy. Typically, it is industry standard to express the turbine efficiency as total-to-static. The total-to-static efficiency of the turbine is shown below.

$$\eta_{Tts} = \frac{1 - (T_{03}/T_{01})}{1 - (P_3/P_{01})^{(\gamma-1)/\gamma}} \quad \text{Eq. 2-2}$$

Examples of turbine performance maps used during the turbocharger matching process are shown below for an axial turbine, these maps are controlled by an SAE a standard (SAE International 1995).

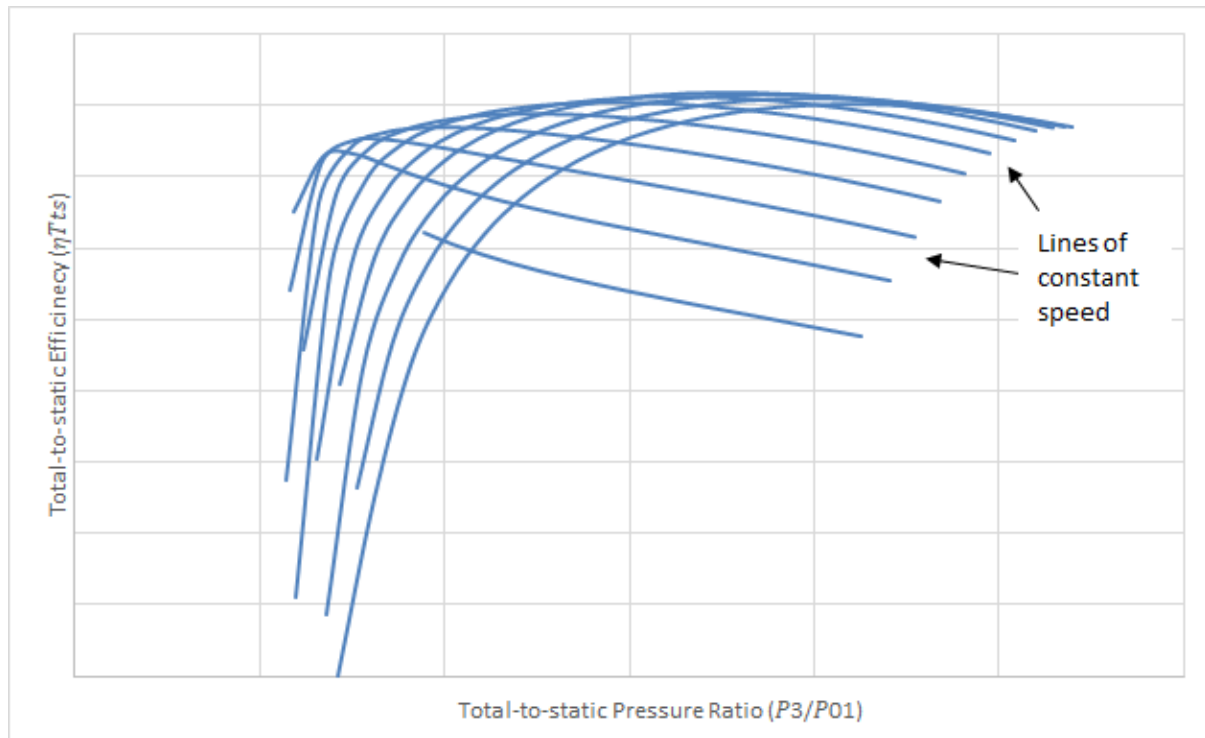


Fig. 2-3 Typical turbine efficiency characteristic of total to static efficiency plotted against turbine pressure ratio taken from a turbine map.

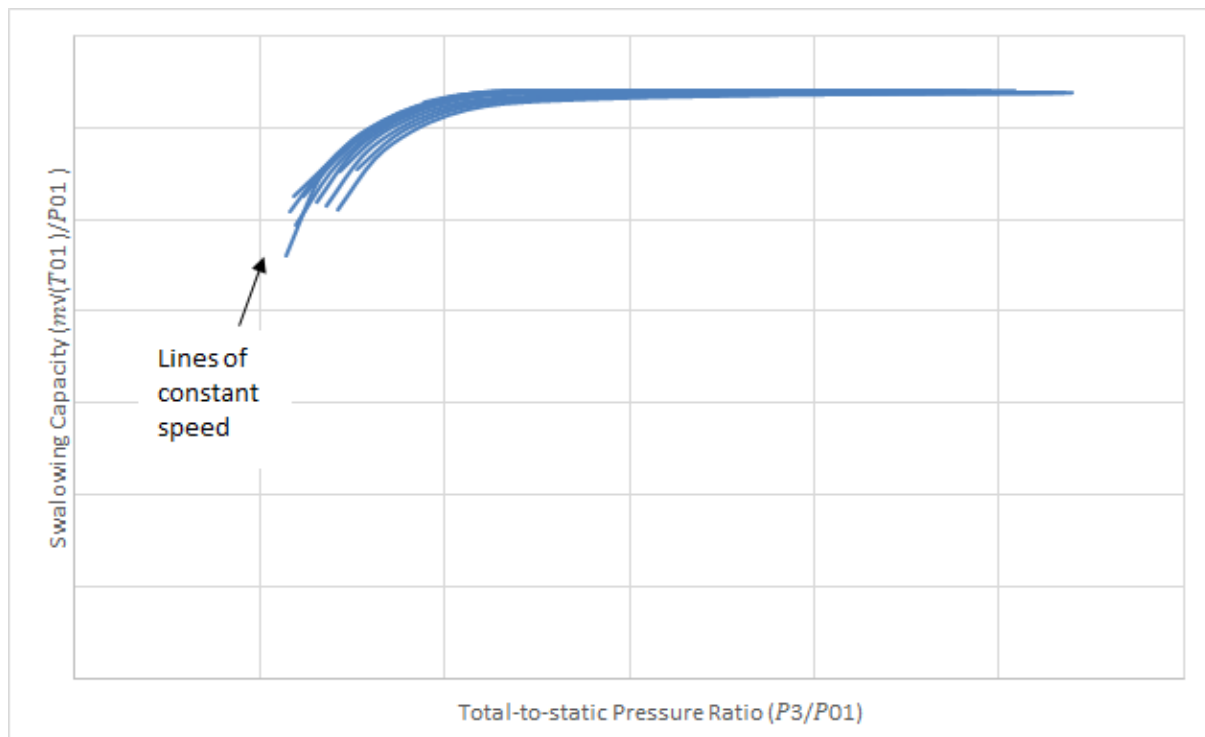


Fig. 2-4 Typical turbine swallowing capacity characteristic of turbine swallowing capacity plotted against turbine pressure ratio taken from a turbine map.

Both plots show characteristics (blue lines) at various turbocharger rotational speeds. The swallowing capacity used in the above chart is a quasi-nondimensional parameter which accounts for the turbine inlet conditions to facilitate data comparison and is defined below.

$$\text{Swallowing capacity} = \frac{m\sqrt{T_{01}}}{P_{01}} \quad \text{Eq.2-3}$$

Compressors and turbines used in turbochargers are rotordynamic machines in that the work transfer occurs by the interaction of moving blades and a fluid travelling through the machine. The operation of such machines is complex, the work transfer can be expressed in two distinct ways one is based on fluid mechanics, changes in fluid momentum, and the other on thermodynamics, changes in fluid enthalpy. Euler's turbomachine equation provides the connection between changes in work transfer and velocity. It is based on Newton's second law of motion equating the torque developed at the shaft to the rate of change of angular momentum. Where  $U$  is the blade speed and  $C_\theta$  the tangential velocity component.

$$W_x = U(C_{\theta 2} - C_{\theta 3}) \quad \text{Eq.2-3}$$

Using the first law of thermodynamics the work transfer can also be expressed in terms of the change of total enthalpy of the flow.

$$Q - W_x = h_{03} - h_{02} \quad \text{Eq.2-4}$$

So long as the heat transfer,  $Q$ , to the environment is small (i.e. the process is adiabatic) the specific work transfer relates directly to the total enthalpy change. The working cycle of the turbine can be expressed by a H-S diagram, this shows the changes of state through the stage during the expansion process.

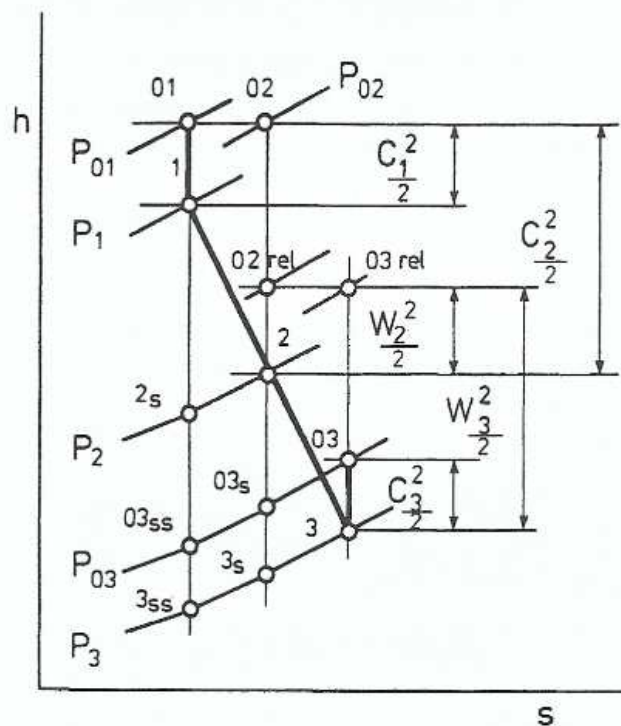


Fig 2-5 Enthalpy Entropy diagram for a turbine (Watson 1982).



Stations 1 to 2 show the change of state through the stator and stations 2 to 3 the rotor. From the H-S diagram it can be observed there is no stagnation enthalpy change in the stator therefore the total work done is equal to the work done only by the rotor. Also, it is shown how the stagnation enthalpy can be calculated by summing the kinetic energy and static enthalpy. Finally, it can be seen the static enthalpy drop is a function of the velocity components hence an expression for the work done as a function of the velocity components can be established.

$$\Delta W_x = \frac{1}{2} [(C_2^2 - C_3^2) + (W_3^2 - W_2^2)] \quad \text{Eq. 2-5}$$

The velocities in the relation above may be obtained by sketching the velocity diagrams for the turbine stage, an example is shown in Fig. 2-6. The relative velocities are denoted by a W and the absolute velocities by a C, the inlet and outlet angles are denoted using  $\alpha$  for absolute and  $\beta$  for relative, U denotes the rotor blade speed.

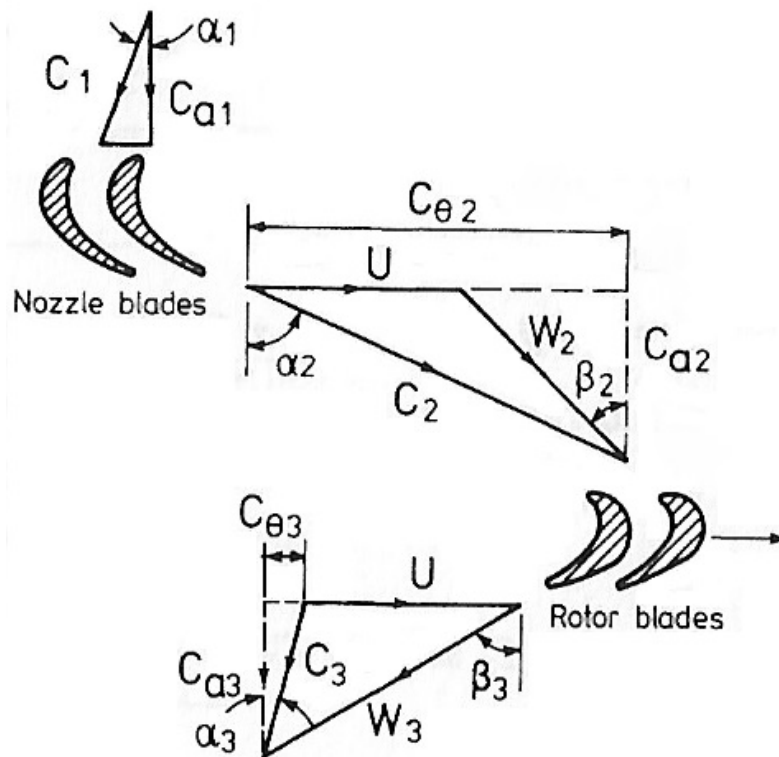


Fig. 2-6 Velocity diagram for axial flow turbine stage (Watson 1982).

## 2.3 Operating Characteristics

During the design of the turbine blade a number of dimensionless parameters are considered by the designer. These parameters include the stage loading coefficient, the flow coefficient, the velocity ratio and the degree of reaction. These parameters dictate the angles of the gas at the inlet and outlet of each blade row and with the addition of the blade speed set the gas velocities. These parameters will be briefly described as they will be used to compare the turbine designs selected to validate the one-dimensional mean line loss calculations and additional loss correlations, their implications on turbine performance will also be investigated.

### 2.3.1 Stage Loading Coefficient

The stage loading coefficient is defined as the change in total enthalpy across a stage divided by the blade speed squared. This is a measure of the work capacity of a stage, high stage loading coefficients are desirable but usually at the cost of efficiency.

$$\psi = \frac{\Delta h_0}{U^2} \quad \text{Eq. 2-6}$$

If the flow is adiabatic the total enthalpy change is equal to the specific work output and the above equation can be rewritten.

$$\psi = \frac{\Delta C_\theta}{U} \quad \text{Eq. 2-7}$$

Based on this it can be deduced a high stage loading coefficient signifies large flow turning. The stage loading coefficient can also be written.

$$\psi = \frac{C_P \Delta T_0}{\frac{1}{2}U^2} = \frac{2C_x}{U} (\tan\beta_2 + \tan\beta_3) \quad \text{Eq. 2-8}$$

### 2.3.2 Flow coefficient

The flow coefficient is the axial component of velocity divided by the blade speed.

$$\phi = \frac{C_x}{U} \quad \text{Eq. 2-9}$$

The value of the flow coefficient determines the relative flow angles in a stage velocity triangle. A stage with a low flow coefficient implies relative flow angles close to tangential whereas a high value for the flow coefficient implies low stagger and flow angles closer to axial line (Dixon and Hall, 2010). Larger flow coefficients require smaller areas, thus smaller blade heights at the cost of performance.

### 2.3.3 Velocity Ratio

The velocity ratio is another useful non-dimensional parameter. It is similar to the stage loading coefficient but in reverse. Where  $U$  is the blade speed which is divided by the isentropic enthalpy drop over the turbine stage. The velocity ratio is often used during the design stage of a turbocharger axial turbine where a velocity ratio is targeted to achieve maximum efficiency depending on the turbocharger application.

$$\frac{U}{c} = \frac{U}{\sqrt{2 \cdot c_p \cdot T_1 \cdot \left(1 - \left(\frac{P_3}{P_{01}}\right)^{\frac{\gamma-1}{\gamma}}\right)}} \quad \text{Eq. 2-10}$$

### 2.3.4 Degree of Reaction

The degree of reaction controls how the expansion through the turbine is divided between the stator and rotor. Typically, the reaction is expressed in terms of enthalpy, however it can also be expressed in terms of pressure.

$$\Lambda = \frac{h_2 - h_3}{h_{01} - h_{03}} \quad \text{Eq. 2-11}$$

The degree of reaction can be related to blade angles.

$$\Lambda = \frac{h_2 - h_3}{h_{01} - h_{03}} = \frac{c_x}{2U} (\tan\beta_3 + \tan\beta_2) \quad \text{Eq. 2-12}$$

The reaction is defined as the static enthalpy drop across the rotor divided by the total enthalpy change across the complete stage. The total enthalpy change across the stage is also used to define the stage loading coefficient, therefore it can be deduced that for a low reaction turbine most of the expansion occurs in the stator whereas for a high reaction turbine most of the expansion occurs across the rotor. In turbocharger turbines a neutral degree of reaction is preferable where the gas expansion is shared between the stator and rotor in order to preserve efficiency and limit gas velocities.

These non-dimensional parameters can be combined. The below equations can be used to obtain the gas and blade angles as a function of the dimensionless parameters.

$$\psi = 2\phi (\tan\beta_2 + \tan\beta_3) \quad \text{Eq. 2-13}$$

$$\Lambda = \frac{\phi}{2} (\tan\beta_3 - \tan\beta_2) \quad \text{Eq. 2-14}$$



## 2.4 Flow Field in Axial Turbines

The flow travelling through a turbine stage is very complex. It is understood the flow through an axial turbine is three dimensional, viscous and unsteady, comprising of many vortices and pressure gradients simultaneously (Wei 2000). There is also the possibility of compressible or incompressible flow, and subsonic, transonic or supersonic regimes that can be present at the same time in different regions throughout the field.

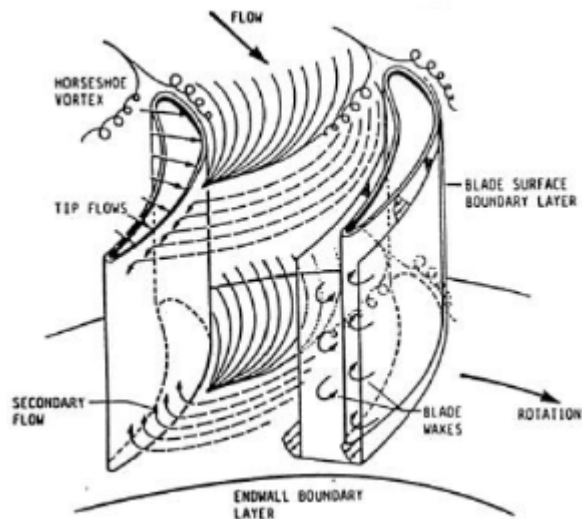


Fig. 2.8 Flow field in an axial turbine (Denton 1994)

As can be seen from Figure 2.8 there is a primary flow field through the blade row which describes the mean flow path, and an overlapping secondary flow. There is also a tip leakage flow over the blades from the pressure to the suction side for unshrouded blades which will disturb the primary flow. At the trailing edge blade wakes form which will interact with the next blade row. For transonic conditions there will also be shockwaves present at the blade suction surface.

The secondary flows in the turbine flow field are generated as the flow turns in the blade passage due to viscous effects at the endwall. In the endwall boundary layers fluid has a lower velocity compared to the mainstream and the cross-passage pressure gradient causes this low momentum boundary layer flow to migrate towards the suction side of the blade. This eventually causes the boundary layer to roll up into the passage vortices shown in Fig. 2.9. Horseshoe vortices are created in front of the blade at the saddle point forming a vortex which distributes itself about the pressure and suction sides of the blade. The secondary flow model presented by Klein (1966), Fig. 2.9b, shows the stagnation point vortex sweeping across the blade passage and rolling up into the passage vortex. Langston (2001) proposes a similar model based on three-dimensional cascade measurements and flow visualisations. Here it can be seen the pressure side leg of the vortex is drawn into the cascade passage forming the passage vortex and the suction side leg of the vortex is drawn into an adjacent passage with an opposite sense of rotation and possibly rotates around the axis of the passage vortex.

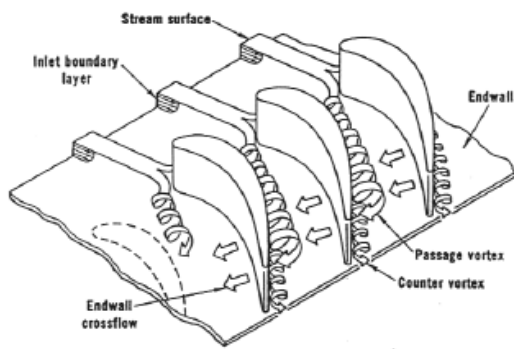


Fig. 2.9a

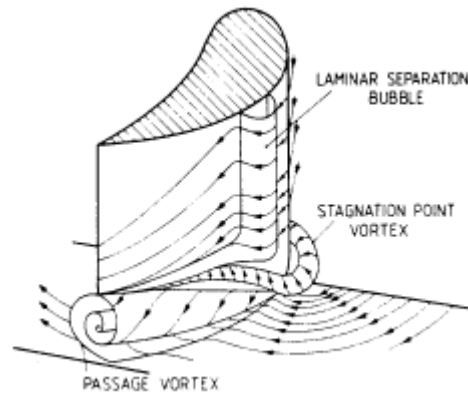


Fig. 2.9b

Fig 2.9 Endwall flow models (a) (Langston 2001), (b) (Klein 1966)

The tip clearance and associated loss have a significant impact on inefficiency in axial turbines. Flow that leaks through the tip clearance, driven by the pressure gradients between the pressure and suction sides, produces a loss in performance by bypassing the blade passage. The tip leakage flow also forms a vortex which interacts with the secondary flow. It has been shown that the effect of the tip clearance is not isolated to the tip gap itself and typically covers 50% of the blade height due to its intense and complex interaction with secondary flow (Moustapha 2003). The most influential parameters impacting the leakage flow are blade clearance and blade loading.

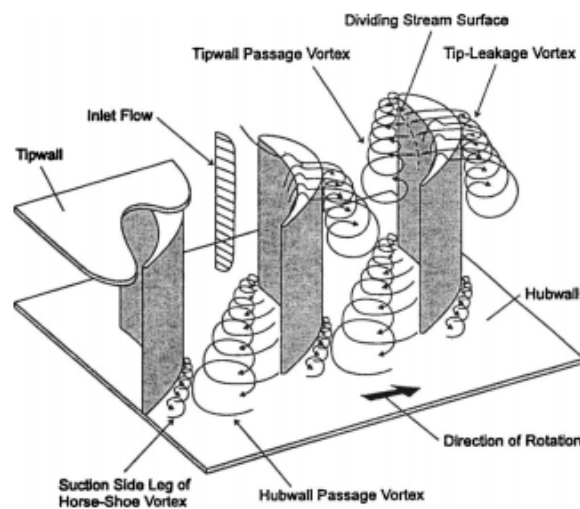


Fig. 2.10 Secondary flow model (Sjolander 1997)

For unshrouded blades, shown in Figure 2.11 from Denton (1993), the flow separates at the blade tip forming a jet and mixing with the mainstream flow on the suction side of the blade. The vortex formed by the leakage flow and its interaction with the main flow results in losses. It can also be seen how the jet mixes out over a thicker blade causing an increase in static pressure and entropy.

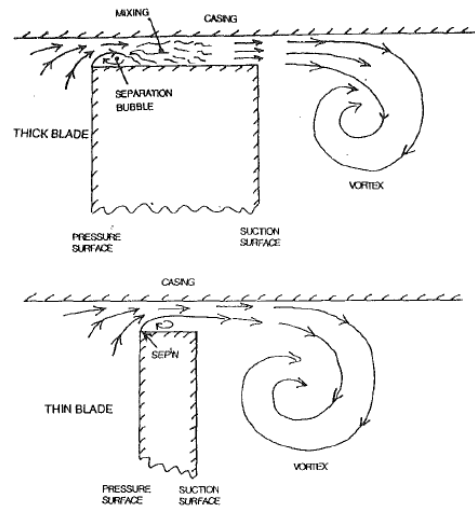


Fig. 2.11 Flow over the tip gap for an unshrouded blade (Denton 1993)

The flow conditions at the boundary layer effect blade heat transfer and aerodynamics therefore understanding boundary layer development and behaviour is important (Moustapha 2003). As illustrated in Figure 2.12, laminar flows can separate from the blade surface due to local adverse pressure gradients, caused by accelerating flows, forming a separation bubble. This separation bubble may reattach to the blade surface downstream initiating transitional flow which may result in turbulent flow increasing losses.

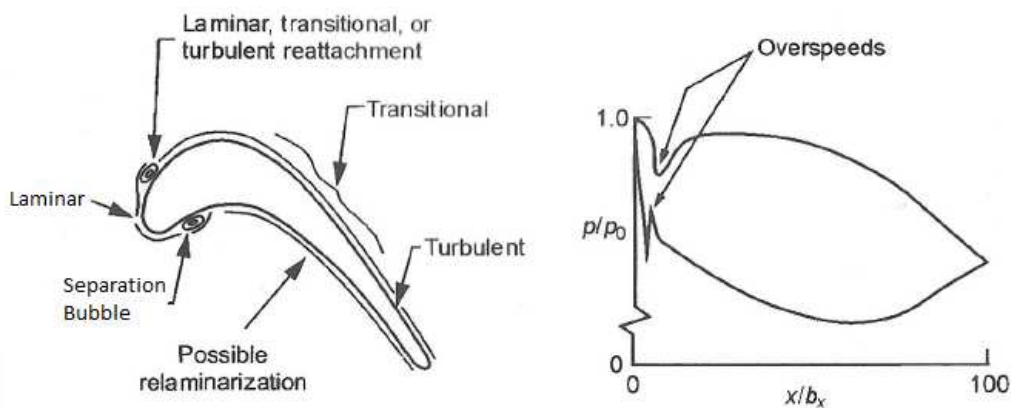


Fig. 2.12 Leading edge separation bubbles and their effect on blade surface static pressure distribution (Moustapha 2003).

## 2.5 Loss Classification

In order to predict the losses in a turbine it is common practice to divide the overall loss into the major sources of loss in the flow field. This is considered a simplification as each of the losses are interacting in some way and cannot be separated completely unambiguously. However, with an understanding of the physical processes which govern the blade passage flow a meaningful division is possible. The major sources of loss will now be described.

### 2.5.1 Profile Loss

The profile loss is the loss due to boundary layer growth over the blade itself and is influenced by such factors as Reynolds number, surface roughness, turbulence and the velocity distribution. Due to the complexity of the flow through the turbine it is almost impossible to isolate this loss hence the profile loss is typically estimated based on correlations derived from cascade data. Such profile loss correlations are described in the work of Ainley and Mathieson (1951) and Craig and Cox (1971). Kacker and Okapuu (1982) reviewed the Ainley and Mathieson (1951) method of profile loss prediction and proposed changes to account for shock losses, channel flow acceleration and supersonic drag rise. They also introduced a factor to account for Reynolds number. Craig and Cox (1971) define a basic profile loss parameter as a function of the modified lift parameter and blade contraction ratio. Craig and Cox (1971) also propose correction factors to account for higher Mach number conditions and Reynolds number. Denton states that the profile loss is equal to the entropy generated in the boundary layers and may be found by employing a typical blade velocity distribution (Denton 1993). To account for Reynolds number Denton includes a dissipation coefficient.

### 2.5.2 Trailing Edge Loss

Trailing edge loss is the loss associated with the separation of the pressure and suction surface boundary layers close to the trailing edge creating a recirculation zone. In this recirculation zone the dissipation of energy will be high as the blade wake mixes out downstream of the turbine blade. Ainley and Mathieson (1951) base their loss estimation method on a trailing edge thickness approximately equal to two percent of the blade pitch, for trailing-edge thickness to blade pitch ratios different to 0.02 they recommend the use of a correction factor. Craig and Cox (1971) account for the trailing edge thickness by applying a multiplication and additive loss factor to the profile losses. Denton states that the magnitude of the trailing edge loss has been seriously underestimated in the past (Denton 1993). In his work Denton proposes the trailing edge loss is a result of entropy generation in the mixing out of a wake behind the trailing edge and considers the surface boundary layers upstream of the trailing edge and base pressure acting on the trailing edge in his estimation. Sieverding (1980) provides a comprehensive summary of the importance of the base pressure term in the calculation of trailing edge loss in his work.



### 2.5.3 Annulus Loss

Annulus loss is the loss associated with the boundary layer drag on the turbine endwalls. This loss is dependent on such factors as the turbine blade geometry and in particular the blade chord length to height ratio (Watson 1982). The annulus loss is often accounted for with the secondary losses as they are difficult to separate in practice.

### 2.5.4 Secondary loss

Secondary losses are losses that occur as a result of the deflection of the boundary layers through the blade row, this is caused by lower endwall velocities and the cross-passage pressure gradient turning the flow creating vortices. These vortices mix with the main flow and can interact with the wall and blade boundary layer and wake causing additional losses. Denton states that the secondary loss component is the most difficult to understand and to predict and virtually all prediction methods are still based on correlations of empirical data (Denton 1993), most of these correlations were reviewed by Dunham (1970) and Sieverding (1985).

### 2.5.5 Tip clearance loss

Another main source of loss in a turbine is tip clearance loss which is the leakage of flow over the blade tip. Depending on the design of the blade this can be considered in two ways for either shrouded or unshrouded blades. Kacker and Okapuu (1982) estimate tip clearance loss using an iterative method to estimate an efficiency debit in unshrouded blades. Craig and Cox (1971) propose a method to calculate a tip clearance loss for shrouded blades and suggest applying a factor for unshrouded blades. Denton (1993) establishes a method for tip clearance loss for unshrouded blades based on the entropy generation of the leakage flow mixing with the main flow on the suction side of the blade. The total entropy production is dependent on the leakage flow rate and difference in streamwise velocity of the main flow and leakage flow.

## 2.6 Loss Correlations

Having established the fundamental flow physics involved in turbomachinery, the more common loss correlations used in turbine performance estimation will be examined. The loss correlation of the current original code will be described first.

### 2.6.1 Ainley and Mathieson Loss Model

The loss correlation of Ainley and Mathieson was first published in 1951, later it was refined by Dunham and Came. The original method of performance estimation calculated the efficiency of the subject turbines to within +/- 2% of the test efficiency.

#### 2.6.1.1 Total Loss

The total loss coefficient is a sum of the profile loss and secondary and tip clearance losses.

$$Y_t = (Y_p + Y_s + Y_k)X_{Te} \quad \text{Eq. 2-15}$$

#### 2.6.1.2 Profile Loss

In order to establish the profile loss, the loss at zero incidence is calculated first. This is based on charts showing cascade data of total pressure loss against pitch to chord ratio for nozzle and impulse blading.

$$Y_{p(i=0)} = \left\{ Y_{(\beta_1=0)} + \left( \frac{\beta_1}{\alpha_2} \right)^2 [Y_{(\beta_1=-\alpha_2)} - Y_{(\beta_1=0)}] \right\} \left( \frac{t/c}{0.2} \right)^{-\beta_1} \quad \text{Eq. 2-16}$$

It is stated the impulse blading is relevant for blade thickness to chord ratios between 0.15 to 0.25.

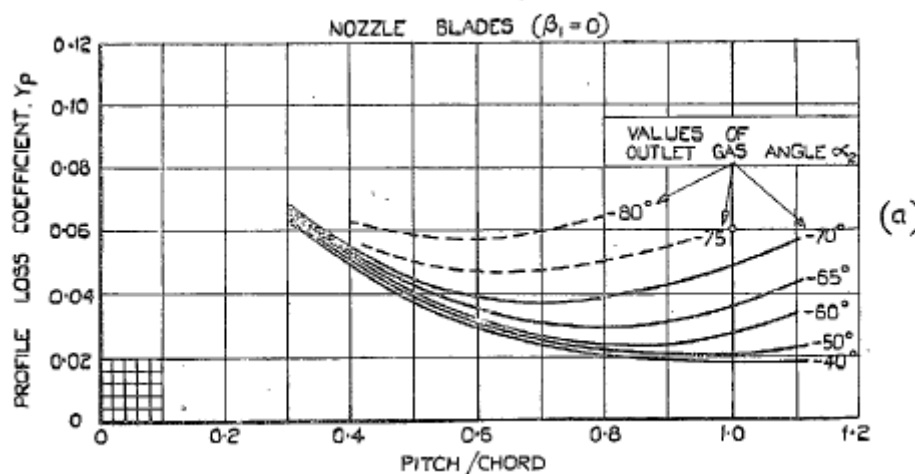


Fig. 2-13 Profile loss coefficients for conventional section blades at zero incidence (Ainley and Mathieson 1951)

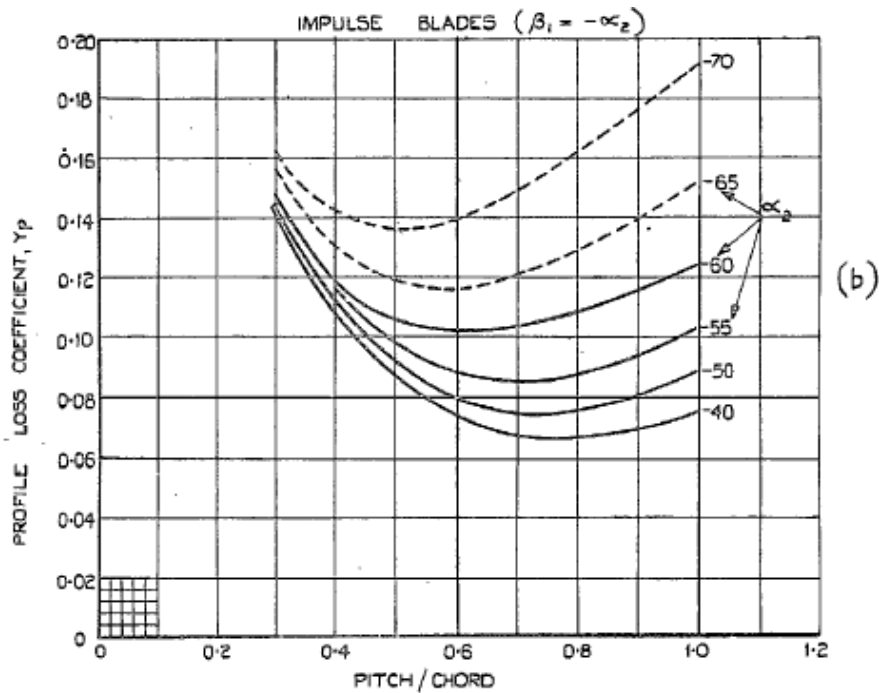


Fig. 2-14 Profile loss coefficients for conventional section blades at zero incidence (Ainley and Mathieson 1951)

To obtain the profile loss at incidences other than 0 the stalling incidence must be determined, Figure 2-15, Figure 2-16, Figure 2-17, then a correlation derived by Ainley and Mathieson relating the ratio of profile loss at any incidence to the profile loss at zero incidence and the ratio of incidence to stalling incidence, Figure 2-18, is used to correct the profile loss at zero incidence. The stalling incidence is approximately a function of gas outlet angle, the blade inlet angle to gas outlet angle ratio and the pitch to chord ratio. The stalling incidences for a wide range of blades having a pitch to chord ratio of 0.75 are established along with the variation of stalling incidence and gas outlet angle with pitch to chord ratio. The final expression for profile loss,

$$Y_p = X_i Y_{p(i=0)} \tag{Eq. 2-17}$$

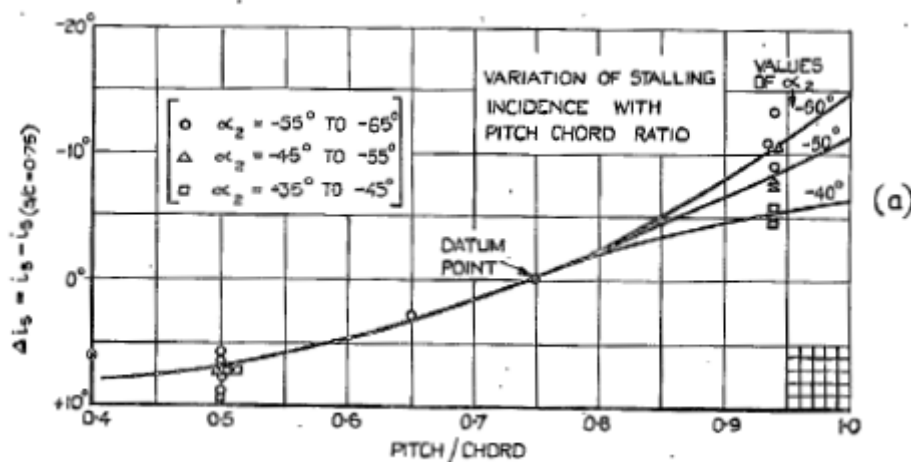


Fig.2-15 Positive stalling incidences of cascades of turbine blades (Ainley and Mathieson 1951)

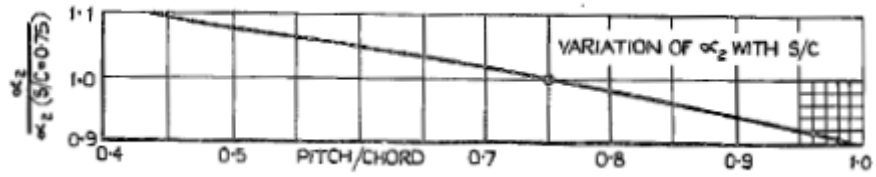


Fig.2-16 Positive stalling incidences of cascades of turbine blades (Ainley and Mathieson 1951)

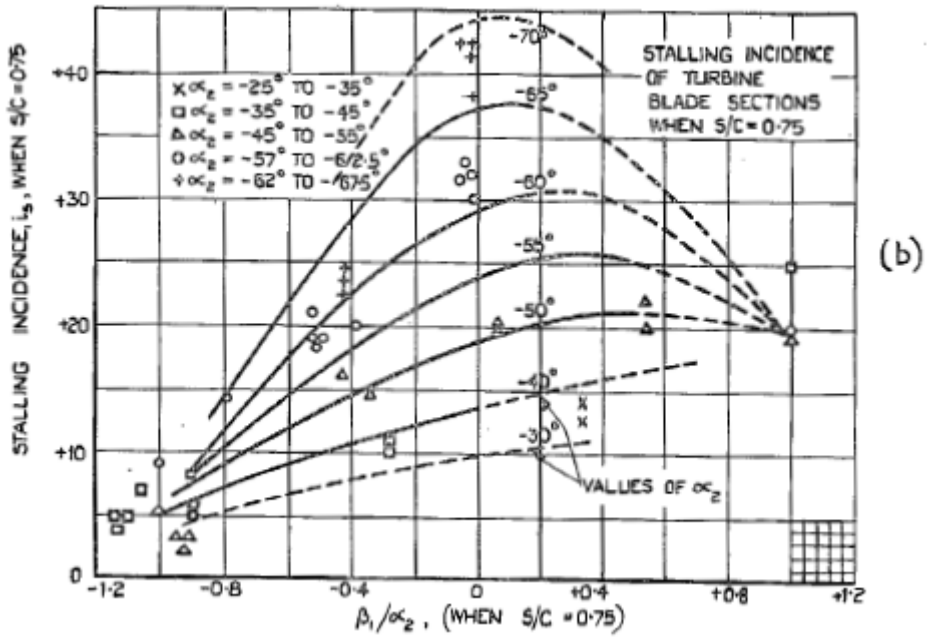


Fig.2-17 Positive stalling incidences of cascades of turbine blades (Ainley and Mathieson 1951)

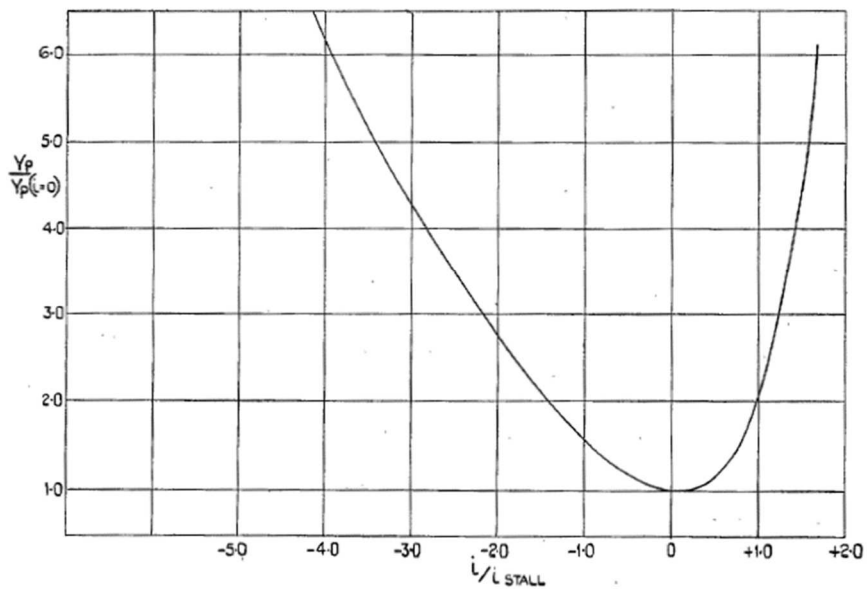


Fig. 2-18 Variation of profile loss with incidence for typical turbine blading (Ainley and Mathieson 1951)

### 2.6.1.3 Secondary and tip clearance loss

It was demonstrated by Ainley and Mathieson (1951) that secondary losses may be expressed by the following equation.

$$Y_s = \lambda \left[ \frac{C_L}{(s/c)} \right]^2 (\cos^2 \alpha_2 / \cos^3 \alpha_m) \quad \text{Eq. 2-18}$$

Where,

$\lambda$  is an empirical function which depends upon the degree of acceleration imparted on the gas as it flows through the blade row, Figure 2-19.

$$\lambda = f\{(A_2/A_1)^2 / (1 + I.D./O.D.)\} \quad \text{Eq. 2-19}$$

$$A_1 = A_{n_0} \cos \beta_1 \quad \text{Eq. 2-20}$$

$$A_2 = A_{n_2} \cos \alpha_1 \quad \text{Eq. 2-21}$$

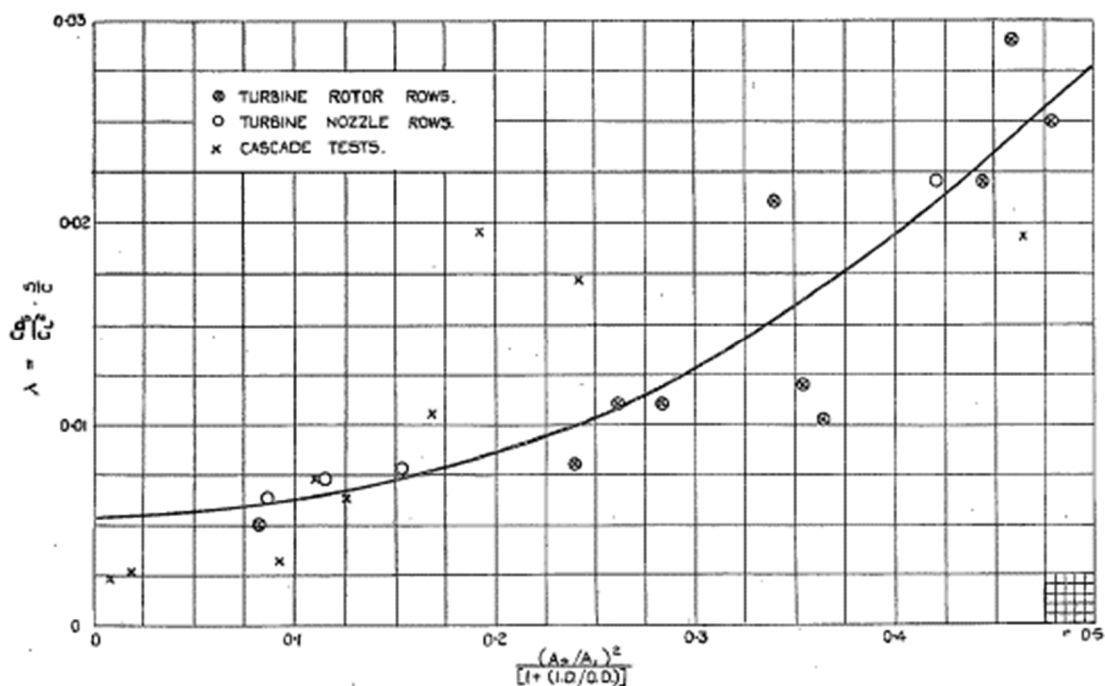


Fig. 2-19 Secondary losses in turbine blade rows (Ainley and Mathieson 1951)

$C_L$  is the lift coefficient thus  $C_L/(s/c)$  is defined as,

$$C_L/(s/c) = 2(\tan \alpha_1 - \tan \alpha_2) \cos \alpha_m \quad \text{Eq. 2-22}$$

$\alpha_m$  is the average flow angle in the cascade and is defined as,

$$\alpha_m = \tan^{-1}[(\tan \alpha_1 + \tan \alpha_2)/2] \quad \text{Eq. 2-23}$$

Thus, the secondary loss formula becomes,

$$Y_s = \lambda 4 (\tan\alpha_1 - \tan\alpha_2)^2 \left( \frac{\cos^2\alpha_2}{\cos\alpha_m} \right) \quad \text{Eq. 2-24}$$

#### 2.6.1.4 Tip Clearance loss

The tip clearance loss is defined similarly to the secondary loss, as a function of blade loading with the addition of the ratio of tip clearance to blade height.

$$Y_k = B \frac{k}{h} 4 (\tan\alpha_1 - \tan\alpha_2)^2 \left( \frac{\cos^2\alpha_2}{\cos\alpha_m} \right) \quad \text{Eq. 2-25}$$

In this instance B is a constant defined as 0.25 for shrouded blades or 0.5 for unshrouded blades.

#### 2.6.1.5 Trailing Edge Correction

The trailing edge correction factor presented by Ainley and Mathieson can be found from Figure 2-20. The method presented by Ainley and Mathieson was valid for turbine blades having a trailing edge thickness roughly equal to 2 percent of the blade pitch. Ainley and Mathieson identify trailing edge thickness can have a large impact on the total loss coefficient based on research of the time (Ainley and Mathieson 1951). Therefore, they introduce a correction factor when trailing edge thickness to blade pitch ratio,  $t_e/s$ , differs from 0.02.

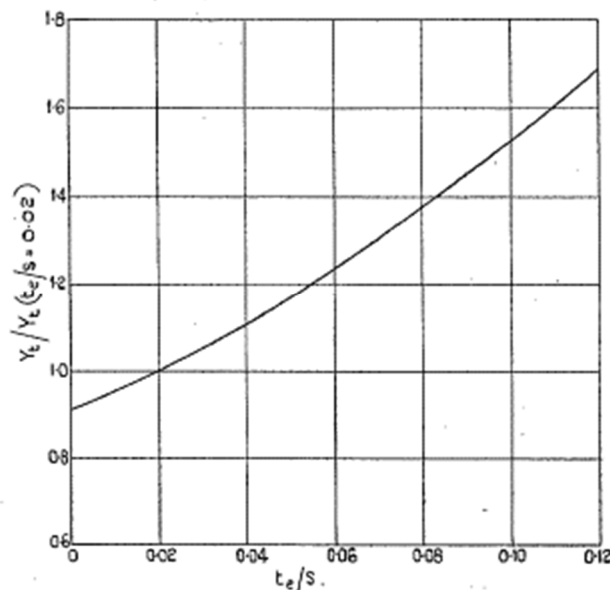


Fig. 2-20 Effect of trailing edge thickness on blade loss coefficients (Ainley and Mathieson 1951).

## 2.6.2 Dunham and Came Loss model

In 1970 Dunham and Came reviewed the Ainley and Mathieson (1951) turbine performance prediction method and proposed improvements based on experimental data from 25 turbine stages of the time. It was concluded the performance results for small turbines using the Ainley and Mathieson method were misleading, and a number of improvements were implemented.

### 2.6.2.1 Total loss

The total loss of the blade row now considers the influence of Reynolds number on the profile and secondary losses. The application of the Reynolds number correction accounts for conditions where  $Re < 2 \times 10^5$ .

$$Y_T = \left[ (Y_p + Y_s) \left( \frac{Re}{2 \times 10^5} \right)^{-0.2} + Y_K \right] X_{Te} \quad \text{Eq. 2-26}$$

Reynolds number is the measure which indicates whether a fluid is laminar or turbulent. Reynolds number may be defined as the ratio of the inertial forces and viscous forces and may be calculated using the formula below.

$$\text{Reynolds number} = \text{inertial force} / \text{friction force} = \rho V L / \mu$$

Where,

$\rho$  = density

$\mu$  = dynamic viscosity

$V$  = velocity

$L$  = characteristic length

### 2.6.2.2 Profile loss

The additional losses encountered when a blade row chokes due to the development of shockwaves is taken into account by using a correction factor incorporating the outlet Mach number in the profile loss calculation.

$$Y_p = [1 + 60(M_{out} - 1)^2] X_i Y_{p(i=0)} \quad \text{Eq. 2-27}$$

### 2.6.2.3 Secondary Loss

Dunham and Came (1970) proposed a new blade loading parameter based on cascade data which is a development of the loading parameter proposed by Ainley and Mathieson (1951). A single numerical constant was used in place of a function of wall boundary layer thickness and blade shape. The numerical constant was devised from comparisons with overall efficiency data.

$$Y_s = 0.0334 \left(\frac{c}{h}\right)^4 (\tan\alpha_1 - \tan\alpha_2)^2 \left(\frac{\cos^2\alpha_2}{\cos^3\alpha_m}\right) \left(\frac{\cos\alpha_2}{\cos\beta_1}\right) \quad \text{Eq. 2-28}$$

#### 2.6.2.4 Tip Clearance Loss

It was found that Ainley and Mathieson's blade loading parameter replicated the effect of blade loading satisfactorily (Dunham and Came 1970). Also, it was suggested by Dunham and Came that the usual linear dependence of loss on tip clearance should be replaced by the power law which showed greater correlation to experimental data.

$$Y_K = B \left(\frac{c}{h}\right) \left(\frac{k}{c}\right)^{0.78} 4 (\tan\alpha_1 - \tan\alpha_2)^2 \left(\frac{\cos^2\alpha_2}{\cos\alpha_m}\right) \quad \text{Eq. 2-29}$$

Where the constant  $B$  is modified to 0.47 for plain tip clearance and 0.37 for shrouded.

### 2.6.3 Kacker and Okapuu Loss Model

In 1982 Kacker and Okapuu reviewed the existing loss systems, specifically proposing modifications to the AMDC loss correlations based on analytical capability, which had seen major advancements in computer technology and aerodynamic analyses in the thirty years since Ainley and Mathieson published their loss method in 1951, and turbine data of the time. Their modifications were tested against design point efficiencies of 33 turbine stages.

#### 2.6.3.1 Total Loss

The total loss coefficient presented by Kacker and Okapuu (1982) is the sum of the profile, secondary, trailing edge and tip leakage losses where the profile losses are corrected for Reynolds number effects.

$$Y_T = Y_P f_{Re} + Y_s + Y_{TET} + Y_K \quad \text{Eq. 2-30}$$

Where  $f_{Re}$  is the Reynolds number correction factor.

$$f_{Re} = \begin{cases} \left(\frac{Re}{2 \times 10^5}\right)^{-0.4} & \text{for } Re \leq 2 \times 10^5 \\ 1 & \text{for } 2 \times 10^5 < Re < 10^6 \\ \left(\frac{Re}{10^6}\right)^{-0.2} & \text{for } Re > 10^6 \end{cases} \quad \text{Eq. 2-31}$$

#### 2.6.3.2 Profile Loss

Cascade testing following the publication of the Ainley and Mathieson (1951) method have shown profile loss is not independent of Mach number (Kacker and Okapuu 1982). The profile loss formulated by Kacker and Okapuu uses the relation proposed by AMDC but also takes into account turbine operation at higher Mach numbers and shock losses.

$$Y_P = 0.914 \left(\frac{2}{3} Y_{P,AMDC} K_p + Y_{SHOCK}\right) \quad \text{Eq. 2-32}$$



Shocks can occur at leading edges at relatively low inlet Mach numbers, due to acceleration of the flow adjacent to the highly curved leading edges. Kacker and Okapuu (1982) present a correction based on the inlet Mach number at the hub and the inlet and outlet mean line Mach numbers. The correlation to decipher the inlet Mach number at the blade hub is based on a sampling of known turbines.

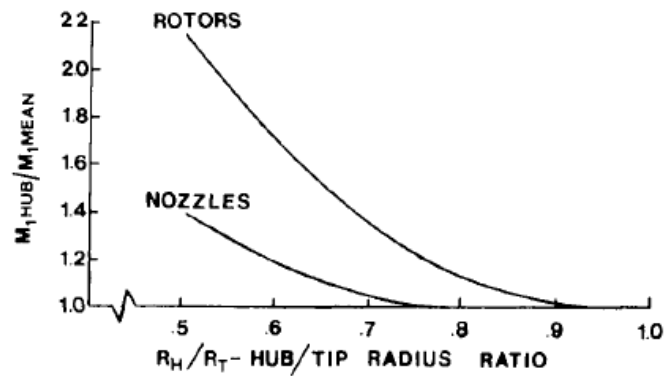


Fig. 2-21 Inlet Mach number ratio for nonfree-vortex turbine blades (Kacker and Okapuu 1982).

From Figure 2-21 the Mach number at the hub can be calculated when the midspan Mach number and the hub/tip radius ratio are known. The shock loss can then be found using Figure 2-22.

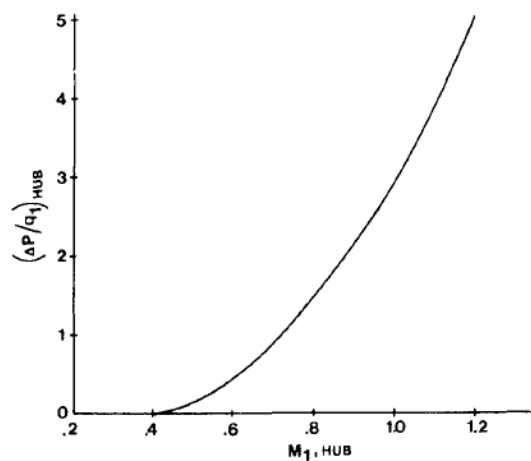


Fig. 2-22 Combined effect of leading edge shock on inner end wall flow and the blade channel next to it (Kacker and Okapuu 1982)

The final expression for shock loss is shown below which accounts for blade hub/tip ratio and is expressed in terms of blade exit dynamic head.

$$Y_{SHOCK} = 0.75(M_{1,HUB} - 0.4)^{1.75} \left(\frac{R_H}{R_T}\right) \left(\frac{P_1}{P_2}\right) \left(\frac{1 - \left(1 + \frac{\gamma-1}{2} M_1^2\right)^{\frac{\gamma}{\gamma-1}}}{1 - \left(1 + \frac{\gamma-1}{2} M_2^2\right)^{\frac{\gamma}{\gamma-1}}}\right) \quad \text{Eq. 2-33}$$

The Mach number correction factor  $K_p$  is based on correlations relating to the effects of exit Mach number and channel acceleration. The corrections for the effects of exit Mach number and channel acceleration are shown in Fig. 2-23 and Fig. 2-24, these are then combined to formulate  $K_p$ .

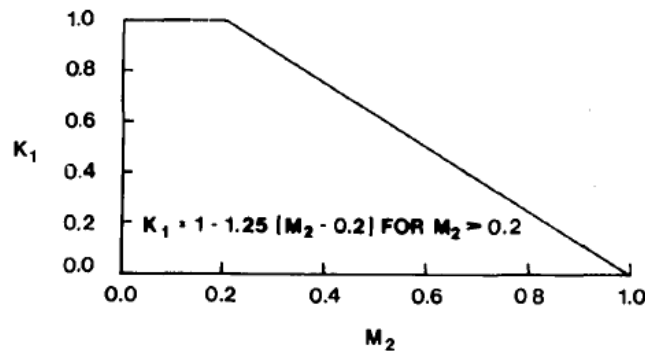


Fig. 2-23 Mach number correction factor  $K_1$  for the profile loss coefficient, for accelerating cascades of  $M_1 \rightarrow M_2$  (Kacker and Okapuu 1982)

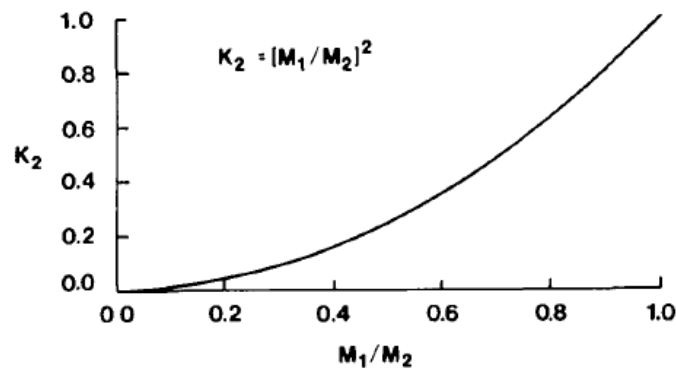


Fig. 2-24 Mach number correction factor  $K_2$  for the profile loss coefficient (Kacker and Okapuu 1982)

$$K_p = 1 - 1.25(M_2 - 0.2) \left(\frac{M_1}{M_2}\right)^2 \quad \text{Eq. 2-34}$$

In the final profile loss expression Kacker and Okapuu added two multiplying factors to make the AMDC loss system predict the correct shapes of the efficiency islands on the Smith chart.

### 2.6.3.3 Secondary Loss

The secondary loss calculation adopted by Kacker and Okapuu is similar to that of Dunham and Came (1970) apart from its dependency on aspect ratio. During their investigation Dunham and Came noted that the results of their method showed a rapid increase in losses as aspect ratio was decreased which when compared to experimental data exhibited poor correlation. Kacker and Okapuu (1982) confirmed this behaviour and identified that the increase in losses is less rapid for aspect ratios less than two. The following equations were established to predict secondary loss.

$$Y_{S\ AMDC} = 0.0334 f_{(AR)} \left(\frac{c}{h}\right) 4 (\tan\alpha_1 - \tan\alpha_2)^2 \left(\frac{\cos^2\alpha_2}{\cos^3\alpha_m}\right) \left(\frac{\cos\alpha_2}{\cos\beta_1}\right) \quad \text{Eq. 2-35}$$

Where,

$$f_{(AR)} = \begin{cases} \frac{1-0.25\sqrt{2-h/c}}{h/c} & \text{for } h/c \leq 2 \\ \frac{1}{h/c} & \text{for } h/c > 2 \end{cases} \quad \text{Eq. 2-36}$$

As with profile losses compressibility is also a factor when considering endwall losses. To account for this the correction factor is defined in terms of the factor for profile loss and aspect ratio.

$$K_s = 1 - K_3(1 - K_p) \quad \text{Eq. 2-37}$$

$K_3$  may be deduced from the following chart.

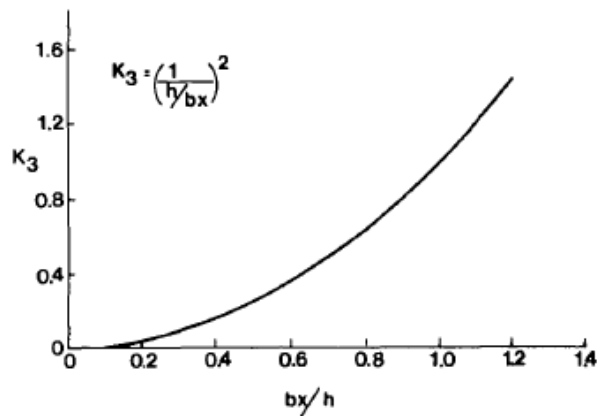


Fig. 2-25 Mach number correction factor  $K_3$  for the secondary loss coefficient (Kacker and Okapuu 1982)

The final expression for secondary loss is shown below.

$$Y_s = 1.2Y_{s\ AMDC}K_s \quad \text{Eq. 2-38}$$

#### 2.6.3.4 Trailing Edge Loss

Kacker and Okapuu also propose an expression for the trailing edge loss in terms of the trailing edge thickness and throat opening. The correlation shown in Figure 2-26 is based on a large quantity of published and in-house cascade data.

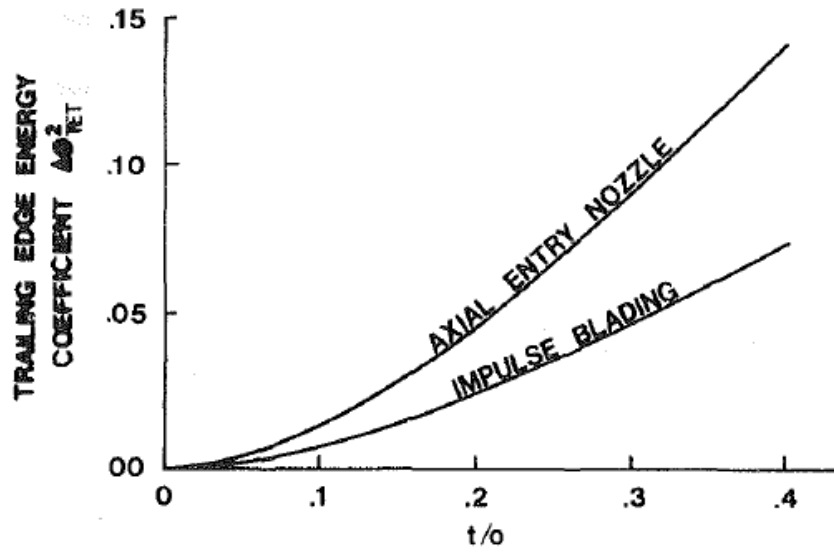


Fig. 2-26 Trailing edge loss (energy) coefficient correlated against the ratio of trailing edge thickness to throat opening (Kacker and Okapuu 1982)

Here the loss is expressed in terms of an energy loss coefficient. As is noticeable from Figure 2-26 two characteristics exist for axial entry nozzles and impulse blades. Kacker and Okapuu (1982) provide a method to interpolate between these curves for any combination of angles shown below, this is similar to the method used by Ainley and Mathieson (1951) for profile losses in equation 2-16.

$$\Delta\phi_{TET}^2 = \Delta\phi_{TET(\beta_1=0)}^2 + \left(\frac{\beta_1}{\alpha_2}\right)^2 \left[ \Delta\phi_{TET(\alpha_2=0)}^2 - \Delta\phi_{TET(\beta_1=0)}^2 \right] \quad \text{Eq. 2-39}$$

The trailing edge loss expressed as an energy coefficient may be converted to a pressure loss coefficient using the formula below.

$$Y_{TET} = \frac{\left[ 1 - \frac{\gamma-1}{2} M_2^2 \left( \frac{1}{1 - \Delta\phi_{TET}^2} - 1 \right) \right]^{\frac{\gamma}{\gamma-1}} - 1}{1 - \left( 1 + \frac{\gamma-1}{2} M_2^2 \right)^{\frac{\gamma}{\gamma-1}}} \quad \text{Eq. 2-40}$$

### 2.6.3.5 Tip Clearance Loss

Tip clearance losses are a major source of loss in a turbomachine, Kacker and Okapuu (1982) presented an iterative method to decipher the loss due to tip clearance for unshrouded blades. First the turbine efficiency is calculated with zero tip clearance then the efficiency loss due to tip clearance is estimated using the formula below and increasing the rotor loss coefficient until the process converges on efficiency, while recalculating the velocity triangles and other loss coefficients.

$$\Delta\eta = 0.93 \left( \frac{R_{TIP}}{R_{MEAN}} \right) \left( \frac{1}{h \cos \alpha_2} \right) \eta_{tt,0} \Delta k \quad \text{Eq. 2-41}$$

## 2.6.4 Craig and Cox Loss Model

In 1971 Craig and Cox presented a method for the prediction of losses in an axial turbine stage. The proposed method was expanded for use with steam and gas turbines accounting for the effects of aspect ratio and blade height which previous published methods of performance estimation neglected. The presented loss correlations are derived from linear cascade test data, the proposed method gave an accuracy of approximately +/- 1.25%. Craig and Cox categorised turbine stage losses into two groups shown below.

### 2.6.4.1 Total Loss

| Group 1               | Group 2                         |
|-----------------------|---------------------------------|
| Guide profile loss    | Guide gland leakage loss        |
| Runner profile loss   | Balance hole loss               |
| Guide secondary loss  | Rotor tip leakage loss          |
| Runner secondary loss | Lacing wire loss                |
| Guide annulus loss    | Wetness loss                    |
| Runner annulus loss   | Disc windage loss               |
|                       | Losses due to partial admission |

Table 1 Breakdown of losses in the Craig and Cox loss system (Craig and Cox 1971).

Craig and Cox (1971) evaluate the Group 1 losses as loss factors based on relative blade inlet and outlet velocities. Whereas the Group 2 losses are evaluated as efficiency debits this being the simplest way they are derived from test data. Thus, Craig and Cox (1971) give the following formula for stage efficiency.

$$\eta_t = \frac{\text{Work done in blading}}{\text{Work done in blading} + \text{Group 1 losses}} - \sum \text{Group 2 efficiency debits} \quad \text{Eq. 2-42}$$

Where the Group 1 losses may be written approximately as,

$$\text{Group 1 losses} = (X_p + X_s + X_a)_g \frac{C_1^2}{200gJ} + \left( X_p + X_s + X_a \frac{C_2^2}{W_2^2} \right)_r \frac{W_2^2}{200gJ} \quad \text{Eq. 2-43}$$

Based on over 100 cascade tests Craig and Cox (1971) established all losses are related on a basis of velocity coefficients and are dependent on Reynolds number, aspect ratio, blade angles and passage geometry, pitch to back bone length ratio, Mach number and incidence. The various loss correlations presented by Craig and Cox will now be examined.

### 2.6.4.2 Profile Loss

Craig and Cox (1971) proposed the following expression to calculate profile loss.

$$X_p = x_{pb} N_{pr} N_{pi} N_{pt} + (\Delta x_p)_t + (\Delta x_p)_{s/e} + (\Delta x_p)_m \quad \text{Eq. 2-44}$$

Craig and Cox (1971) account for the effect of Reynolds number using the correlation shown in Figure 2-27. The method used is based on the blade opening rather than the chord or axial width, the impact of surface roughness is also included.

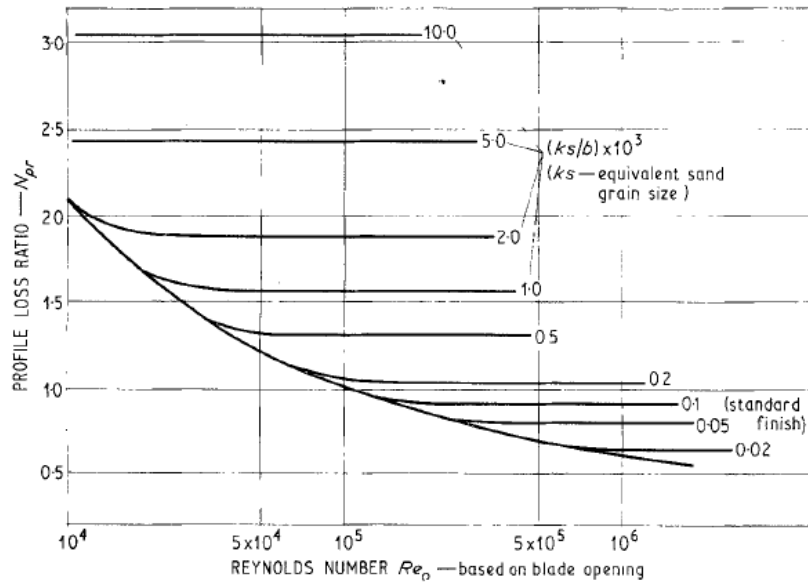


Fig. 2-27 Profile loss ratio against Reynolds number effect (Craig and Cox 1971)

Craig and Cox (1971) describe the basic profile loss, the loss at or near the incidence where loss is at a minimum, using Figure 2-28 and Figure 2-29. Figure 2-28 is a lift parameter and Figure 2-29 is the basic loss parameter as a function of the modified lift parameter and contraction ratio. The contract ratio shown in Figure 2-30 represents the internal blade passage width ratio and is a function of the pitch to backbone length and the inlet and outlet relative flow angles.

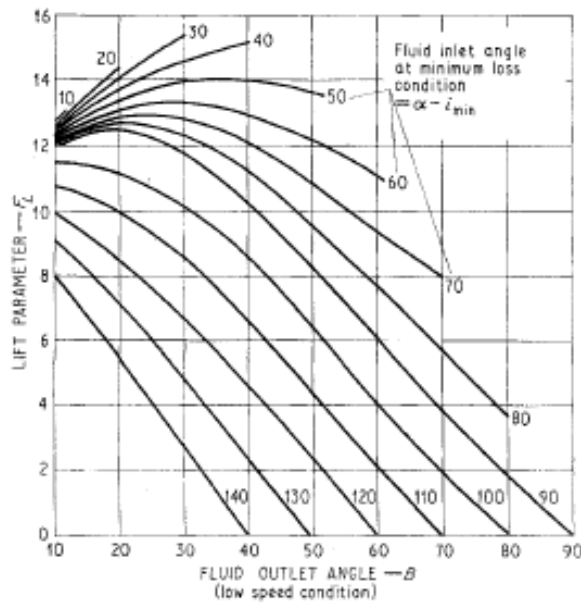


Fig. 2-28 Lift parameter (Craig and Cox 1971)

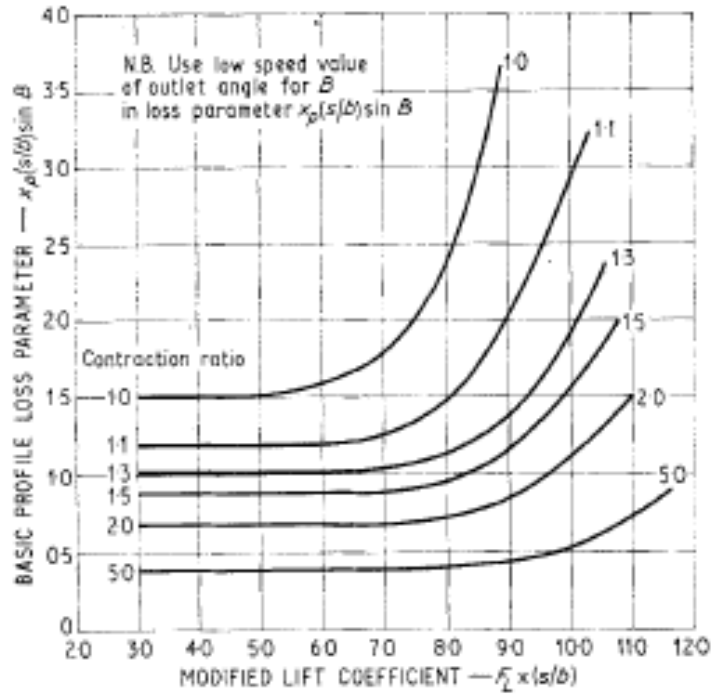


Fig. 5. Basic profile loss

Fig. 2-29 Basic Profile loss (Craig and Cox 1971)

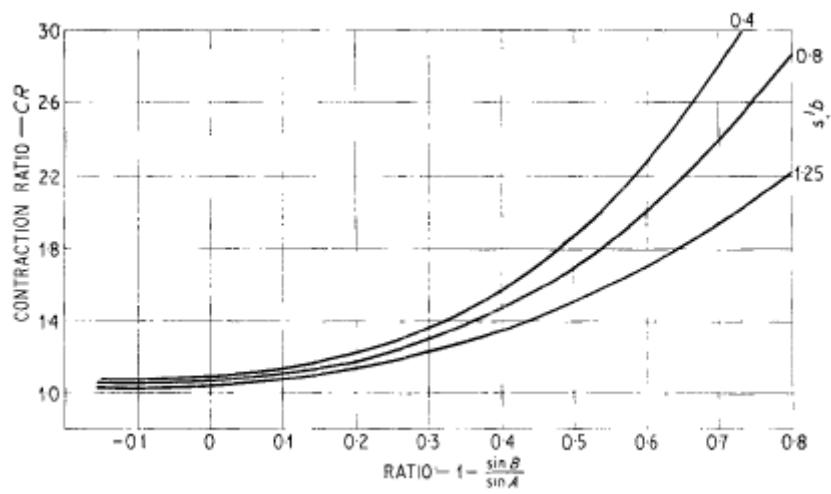


Fig. 2-30 Contraction ratio for average profiles (Craig and Cox 1971)

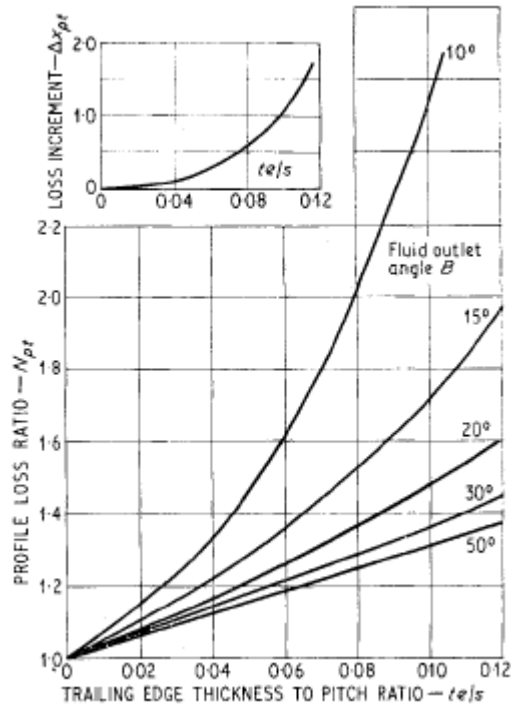


Fig. 2-31 Trailing edge thickness losses (Craig and Cox 1971)

The trailing edge loss parameter is described in Figure 2-31 and shows the loss parameter is a function of fluid outlet angle and trailing edge thickness to pitch ratio. The next parameter accounted for by Craig and Cox (1971) to estimate profile loss considers the impact of incidence loss at off design conditions. The incidence loss can become significant when incidences are not held at the optimum level. A correction for incidence is presented in Fig. 2-32.

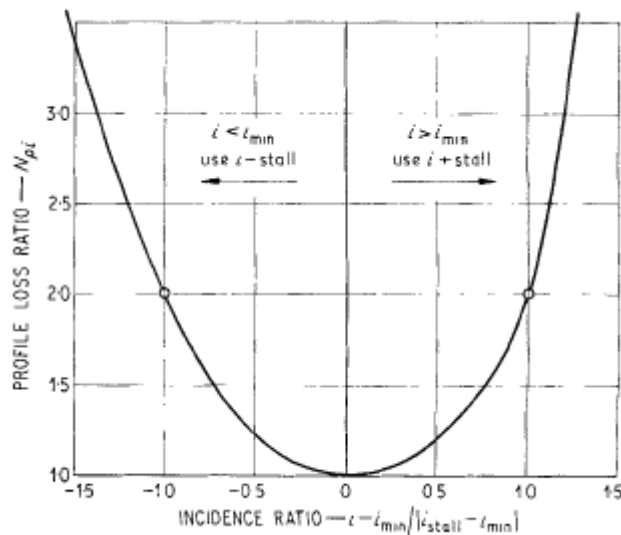


Fig. 2-32 Incidence losses (Craig and Cox 1971)



The correction given is similar to that given by Ainley and Mathieson (1951) however the negative stalling incidence and minimum loss incidence included in the incidence ratio are dealt with separately to the positive stalling incidence. The incidence parameters are determined from the following formulae. For the positive stalling incidence for  $\alpha \leq 90$ ,

$$i + stall = (i + stall)_{basic} + (\Delta i + stall)_{s/b} + (\Delta i + stall)_{CR} \quad \text{Eq. 2-45}$$

Where  $(i + stall)_{basic}$  is given by Fig. 2-32,  $(\Delta i + stall)_{s/b}$  by Fig. 2-33 and  $(\Delta i + stall)_{CR}$  by Fig. 2-34.

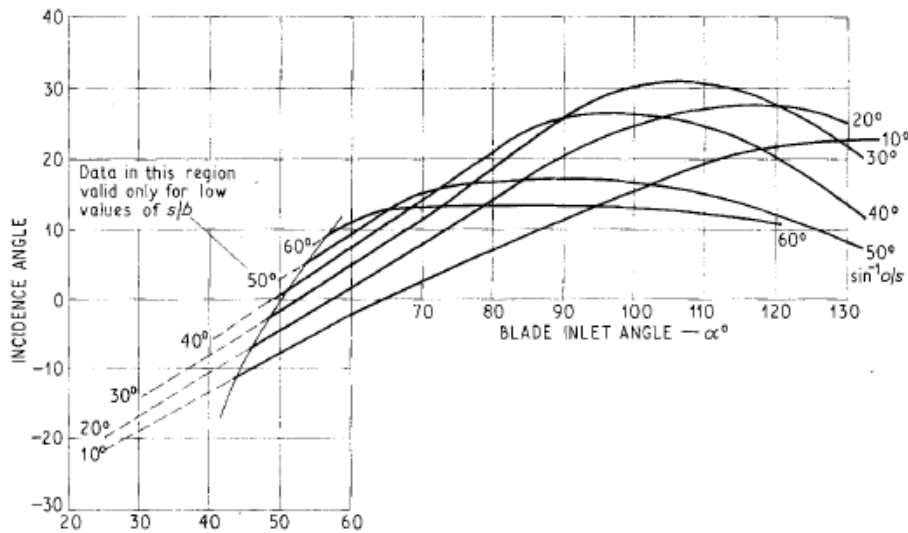


Fig. 2-33 Basic positive stalling incidence  $(i + stall)_{basic}$  (Craig and Cox 1971)

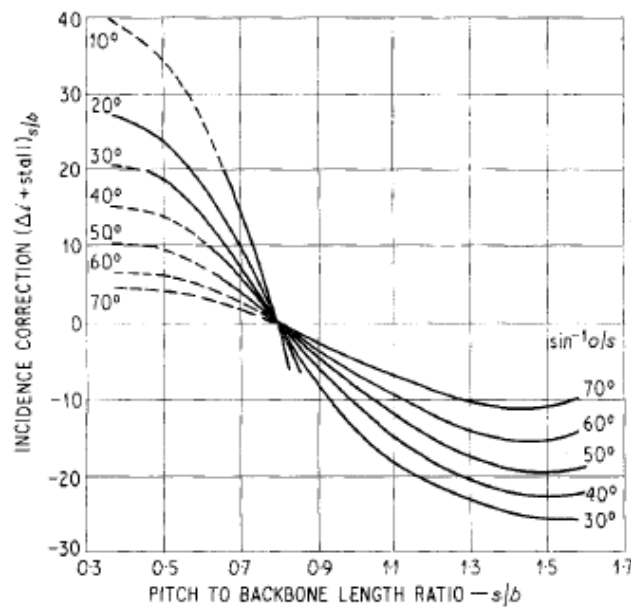


Fig. 2-34 Incidence correction for positive stalling incidences (Craig and Cox 1971)

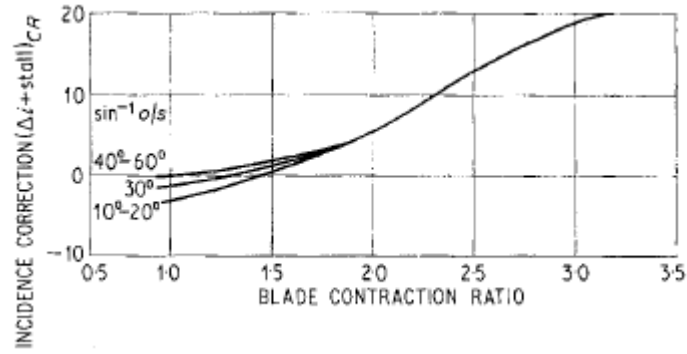


Fig. 2-35 Incidence correction for positive stalling incidences (Craig and Cox 1971)

Craig and Cox (1971) provided a correlation for the negative stalling incidence at  $\alpha \leq 90$  and a different correlation when  $\alpha > 90$  for positive stalling incidence.

$$i - stall = (i - stall)_{basic} + (\Delta i - stall)_{s/b} \tag{Eq. 2-46}$$

Where  $(i - stall)_{basic}$  is given by Fig. 2-35 and  $(\Delta i - stall)_{s/b}$  by Fig. 2-36.

$$i + stall = (i + stall)_{basic} + \left(1 - \frac{\alpha - 90}{90 - \sin^{-1} o/s}\right) \times [(\Delta i + stall)_{s/b} + (\Delta i + stall)_{CR}] \tag{Eq. 2-47}$$

Where  $(i + stall)_{basic}$  is given by Fig. 2-37 and for negative stalling incidence,

$$i - stall = (i - stall)_{basic} + \left(1 - \frac{\alpha - 90}{90 - \sin^{-1} o/s}\right) \times (\Delta i + stall)_{s/b} \tag{Eq. 2-48}$$

Where  $(i - stall)_{basic}$  may also be deciphered from Fig. 2-38.

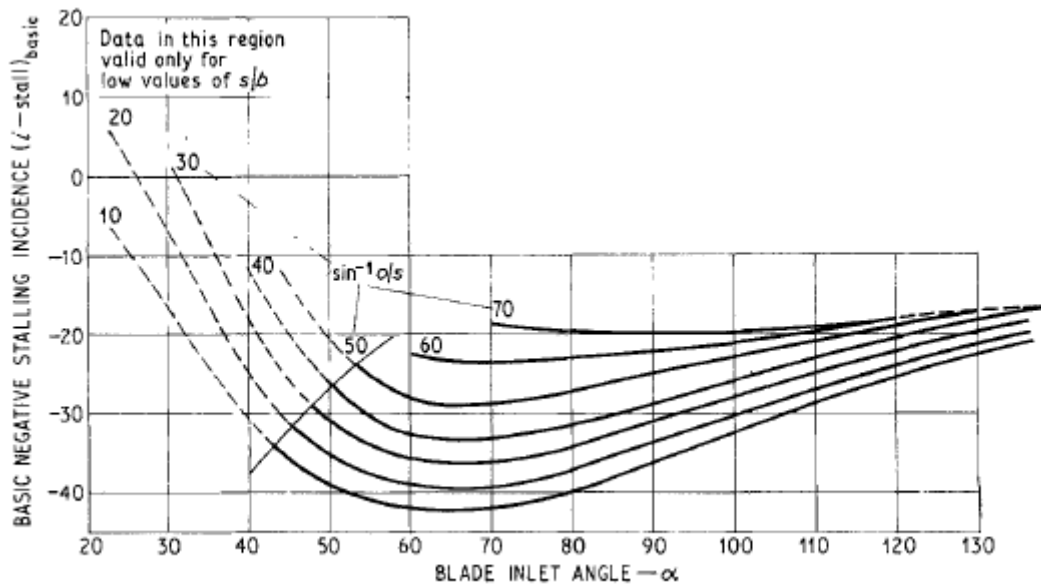


Fig. 2-36 Basic negative stalling incidence (Craig and Cox 1971)

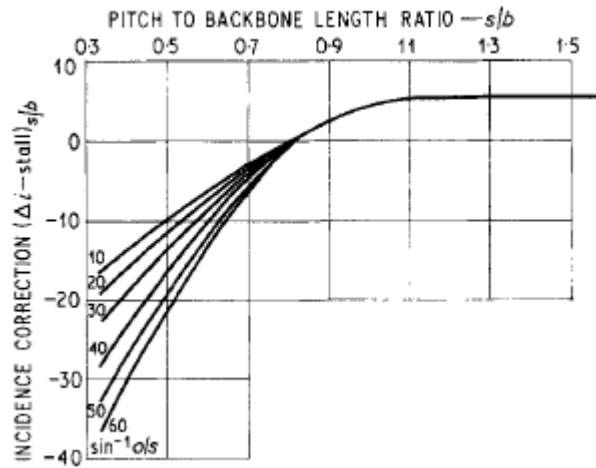


Fig. 2-37 Incidence correction (Craig and Cox 1971)

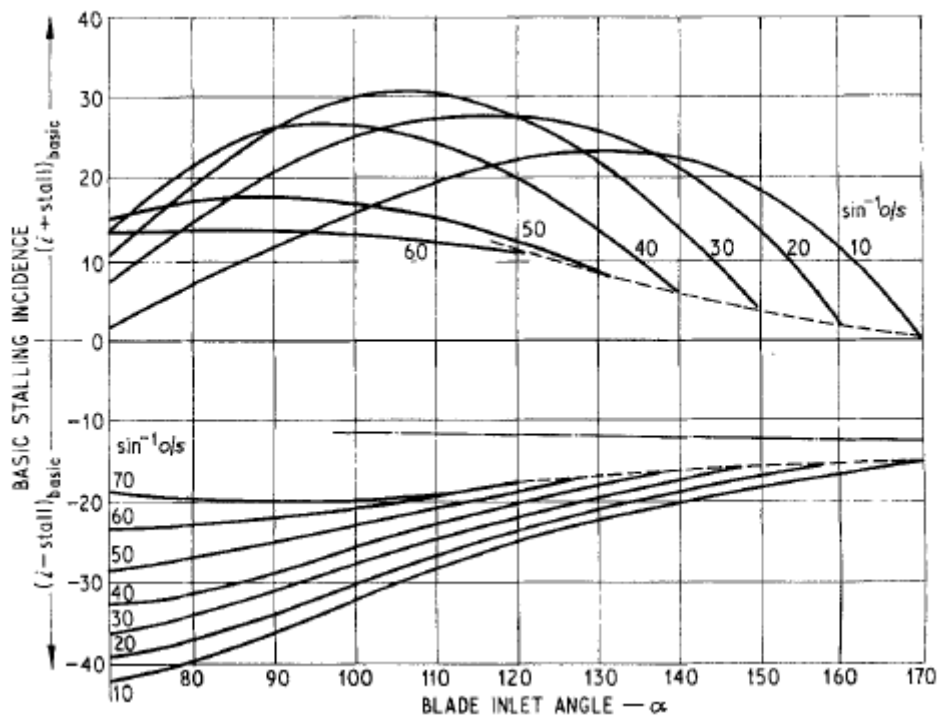


Fig. 2-38 Basic stalling incidences for blade angles greater than 90 (Craig and Cox 1971)

The minimum loss incidence may be established using the formula below.

$$i_{min} = \frac{(i+stall)+F_i(i-stall)}{1+F_i} \tag{Eq. 2-49}$$

Where  $F_i$  is given by Fig. 2-39.

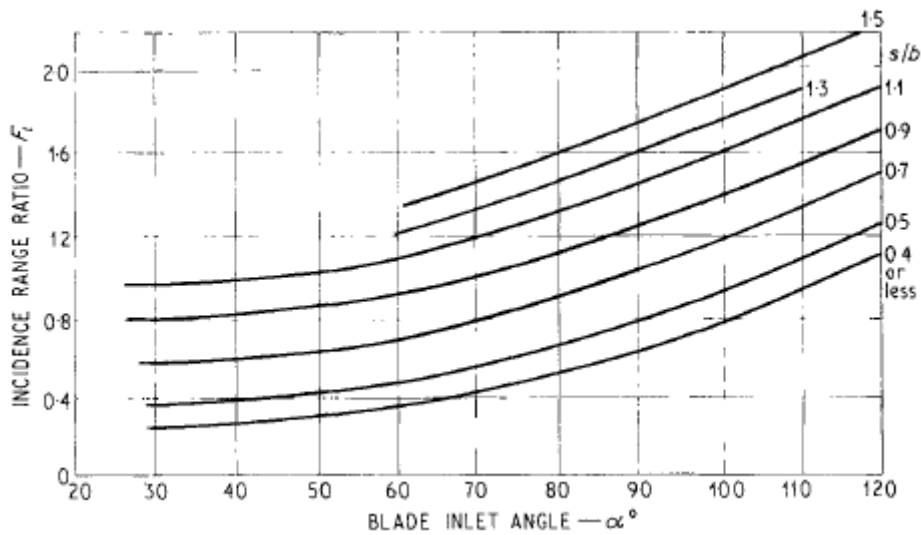


Fig. 2-39 Minimum loss incidence-range ratio  $F_i$  (Craig and Cox 1971)

The final expressions in the Craig and Cox (1971) profile loss estimation are additive losses relating to the trailing edge and high Mach numbers at the blade outlet. The increments relating to Mach number are to account for conditions above the subsonic regime which the loss mechanism was developed at. The trailing edge loss increment is shown in Figure 2-31. The first additive loss relating to high Mach numbers refers to convergent profiles designed with a straight suction surface downstream of the throat, shown in Fig. 2-40. The second additive loss relating to high Mach numbers accounts for profiles with a pronounced convex suction surface downstream of the throat, shown in Fig. 2-41.

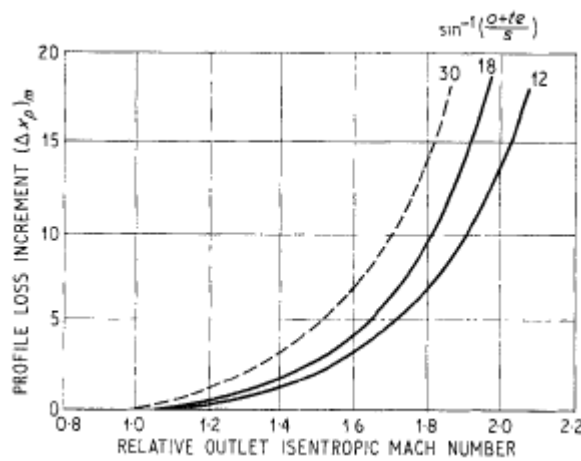


Fig. 2-40 Mach number loss for convergent blading (Craig and Cox 1971)

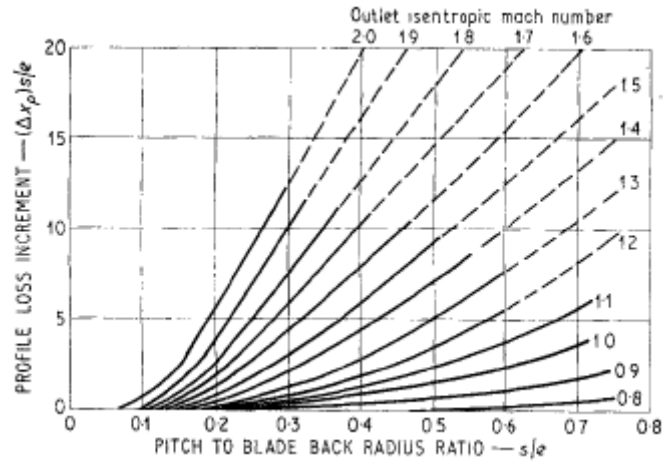


Fig. 2-41 Blade back radius losses (Craig and Cox 1971)

### 2.6.4.3 Secondary Loss

Craig and Cox (1971) describe the secondary loss as consisting of two sources of loss, partly from true aerodynamic secondary loss and partly also from wall friction. Both effects are difficult to predict accurately due to inconsistencies relating to wall shape and interaction with clearance flows. The correlation proposed assumes that the secondary loss is approximately inversely proportional to the aspect ratio of the blading and in addition shows a Reynolds number effect similar to that exhibited by the basic profile loss. The overall secondary loss factor may be calculated by,

$$X_s = (N_s)_r (N_s)_{h/b} (x_s)_b \tag{Eq. 2-50}$$

Where  $(x_s)_b$  is given by Figure 2-42 and  $(N_s)_{h/b}$  by Figure 2-43.

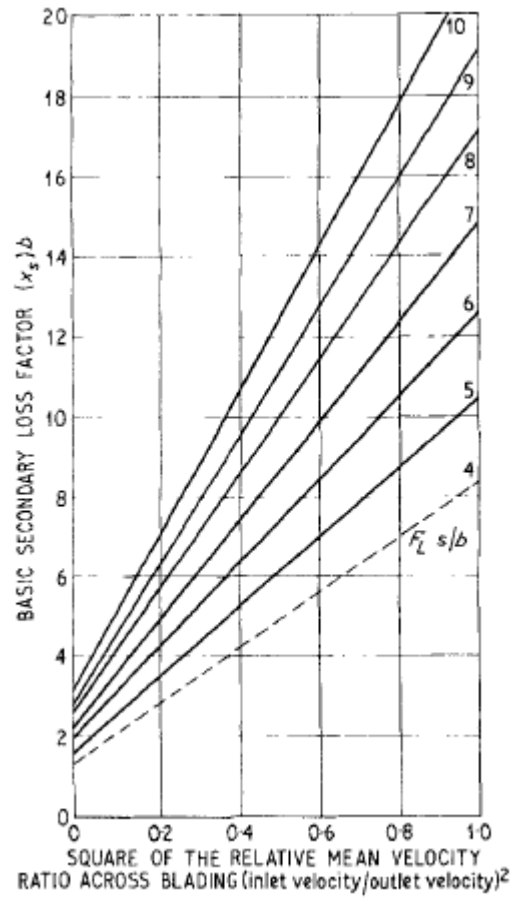


Fig. 2-42 Secondary loss – basic loss factor (Craig and Cox 1971)

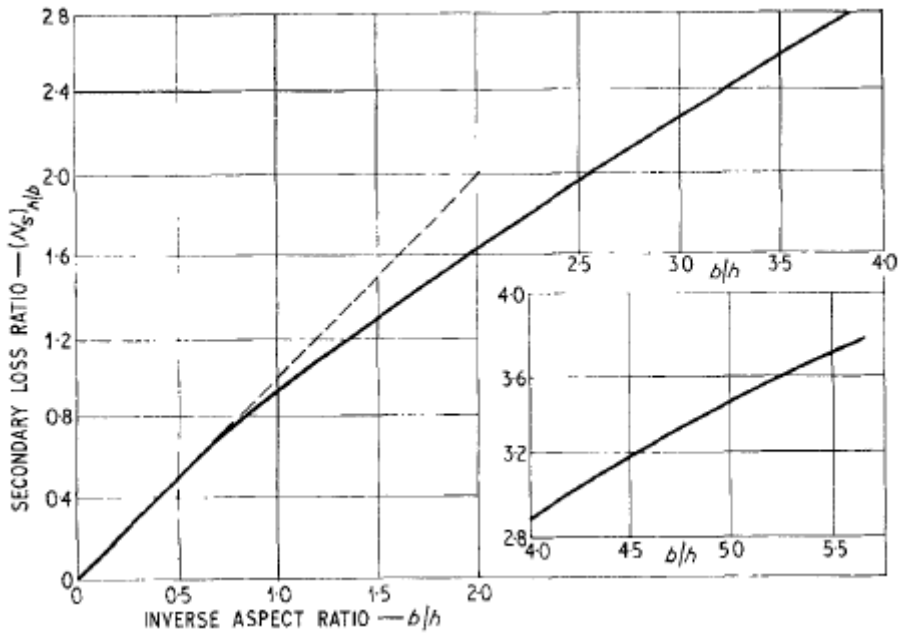


Fig. 2-43 Secondary loss – aspect ratio factor (Craig and Cox 1971)

### 2.6.4.4 Tip Clearance Loss

Craig and Cox (1971) account for tip clearance loss using an efficiency debit which is given by the following correlation for shrouded turbine blades, where  $F_k$  is given by Figure 2-44. Craig and Cox state for unshrouded blades the methodology presented by Ainley and Mathieson (1951) is representative when axial velocity remains approximately constant across the blade row and relative velocities are well below the sonic value.

$$\Delta\eta_k = F_k \frac{A_k}{A_t} \times \eta_{0,k} \tag{Eq. 2-51}$$

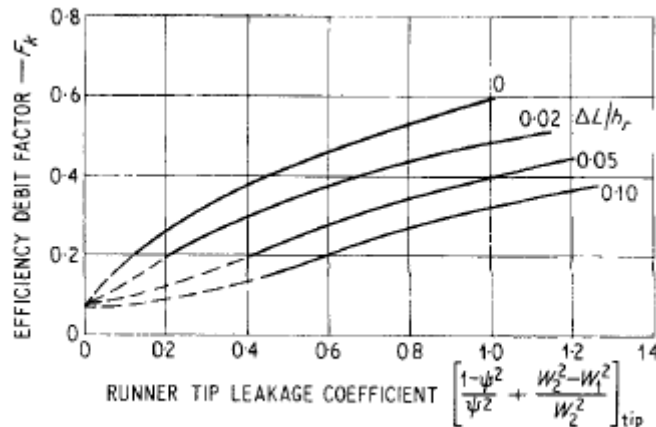


Fig. 2-44 Shrouded efficiency loss (Craig and Cox 1971)

### 2.6.4.5 Annulus loss

Craig and Cox (1971) also account for an annulus loss when there is an appreciable diffusion between two stages. The annulus wall loss may be obtained from Fig. 2-45 for controlled (solid lines) and uncontrolled expansion (dotted lines).

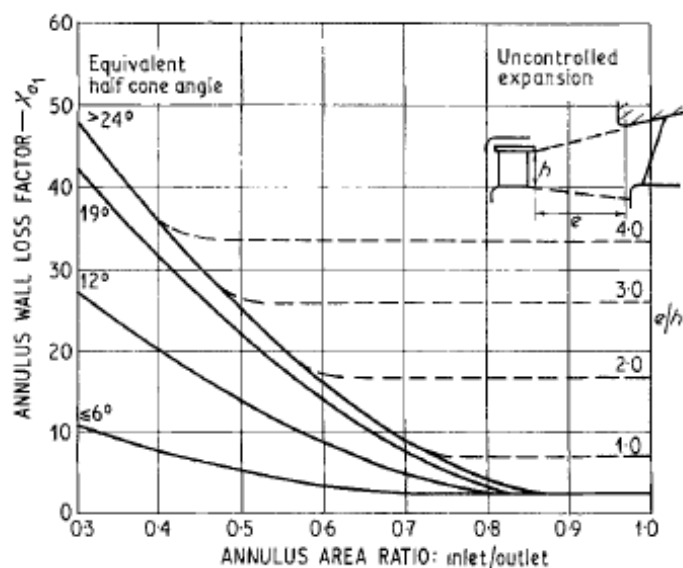


Fig. 2-45 Annulus wall loss (Craig and Cox 1971)

### 2.6.4.6 Cavity Loss

Craig and Cox (1971) include the cavity loss with the annulus loss coefficient. The cavity loss factor may be determined from Fig. 2-46 and is based on the geometry of the cavity.

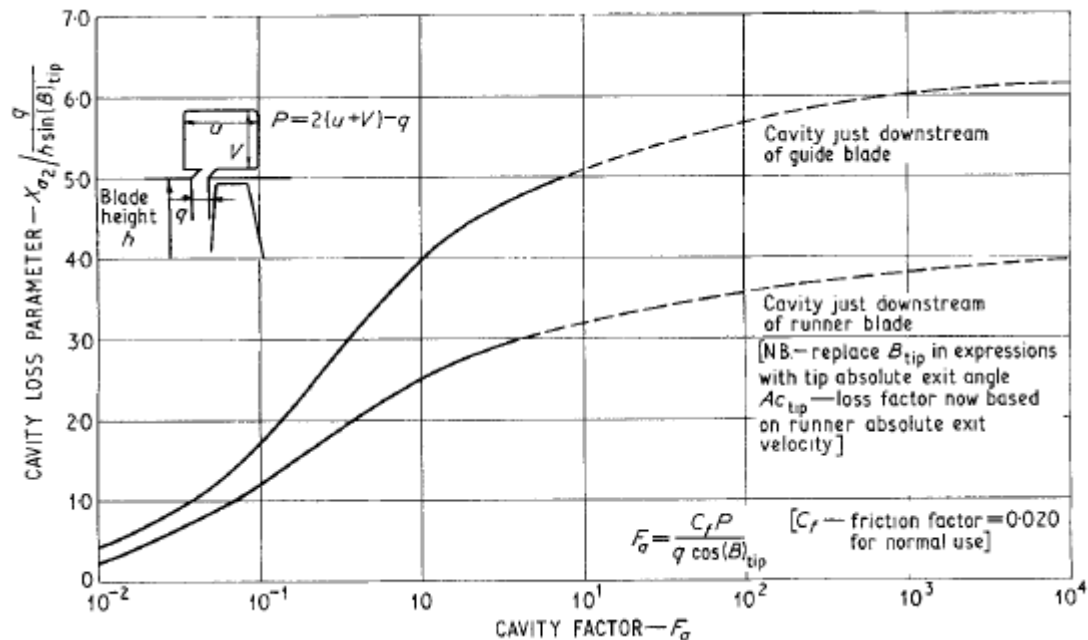


Fig. 2-46 Cavity loss (Craig and Cox 1971)

### 2.6.4.7 Leakage Flow Through Glands

Another contributor to loss in a turbine is as a result of leakage through glands. Craig and Cox (1971) give an approximation of the efficiency debit due to leakage flow through glands using the formula below,

$$\Delta \eta_{leakage} = \left( \frac{\Delta g}{G + \Delta g} \right) \eta_b \quad \text{Eq. 2-52}$$

Where  $\left( \frac{\Delta g}{G + \Delta g} \right)$  denotes the leakage fraction.

### 2.6.4.8 Other Losses

Other kinds of losses were also considered by Craig and Cox (1971) including lacing wire, wetness, disc windage and partial admission losses. These losses are considered as efficiency debits and are not taken into account in the overall cascade loss. These losses are also considered small when compared to the main sources of loss in a turbine.



## 2.6.5 Denton Loss Model

Denton promotes a greater understanding of the physics involved with performance loss in turbomachines in his work, rather than relying on correlations derived from empirical data. Denton ultimately attributes efficiency loss to entropy generation and using the basic principles of thermodynamics establishes a methodology for predicting the various losses in turbomachines.

There are many useful definitions of loss coefficient for individual blade rows (Brown 1972), for a turbine one of the more common definitions is in terms of stagnation pressure loss coefficient,

$$Y = (P_{01} - P_{02}) / (P_{02} - P_2) \quad \text{Eq. 2-53}$$

Another loss coefficient definition is the energy or enthalpy loss coefficient defined below for a turbine,

$$\zeta = \frac{h_2 - h_{2s}}{h_{02} - h_2} \quad \text{Eq. 2-54}$$

However, Denton states these definitions are not adequate for machines with a rotating blade row where the relative stagnation pressure and enthalpy can change as a result of changes in radius without any implied loss of efficiency. Changes to isentropic efficiency occur as a result of heat transfer or thermodynamic irreversibility. For adiabatic flow entropy creation due to irreversibility is the main contributing factor to loss of efficiency. Denton concludes the only rational measure of loss in an adiabatic machine is entropy creation (Denton 1993). Another advantage identified by Denton in the use of entropy as a measure of loss in a turbine stage is unlike stagnation pressure, stagnation enthalpy or kinetic energy it is not dependent on whether the blade row is stationary or rotating. The entropy loss coefficient for turbine blades is defined below,

$$\zeta_s = \frac{T_2 \Delta s}{h_{02} - h_2} \quad \text{Eq. 2-55}$$

### 2.6.5.1 Boundary Layer Loss

Denton (1993) attributes boundary layer entropy generation to viscous effects in the boundary layer and derives the following formula, from boundary layer theory, to calculate the total entropy creation in the boundary layer,

$$\dot{S} = \sum_S^P C_s \int_0^1 \frac{C_d \rho V^3}{T} d(x/C_s) \quad \text{Eq. 2-56}$$

For conveniency Denton recommends accounting for the entropy production rate by using a dissipation coefficient,  $C_d$ . Full knowledge of the state of the boundary layer is required to calculate the dissipation coefficient precisely. The dissipation coefficient is defined by the formula below,

$$C_d = \frac{T \dot{S}_a}{\rho V_\delta^3} \quad \text{Eq. 2-57}$$

Based on much experimental data some general results have been established relating to the magnitude of the dissipation coefficient for varying boundary layers (Schlichting 1966). It has been found for turbulent boundary layers the dissipation coefficient is much less dependent on the shape

of the boundary layer. Schlichting gives the following relationship for turbulent boundary layers with  $1.2 < \text{Shape Factor} < 2.0$  and with  $10^3 < Re_\theta < 10^5$ ,

$$C_d = 0.0056Re_\theta^{-1/6} \quad \text{Eq. 2-58}$$

On comparison of the formula above (Equation 15) with the results of the Cebeci calculation (Denton 1993), Figure 2-47, Denton recommends employing a dissipation coefficient of 0.002 for turbulent boundary layers.

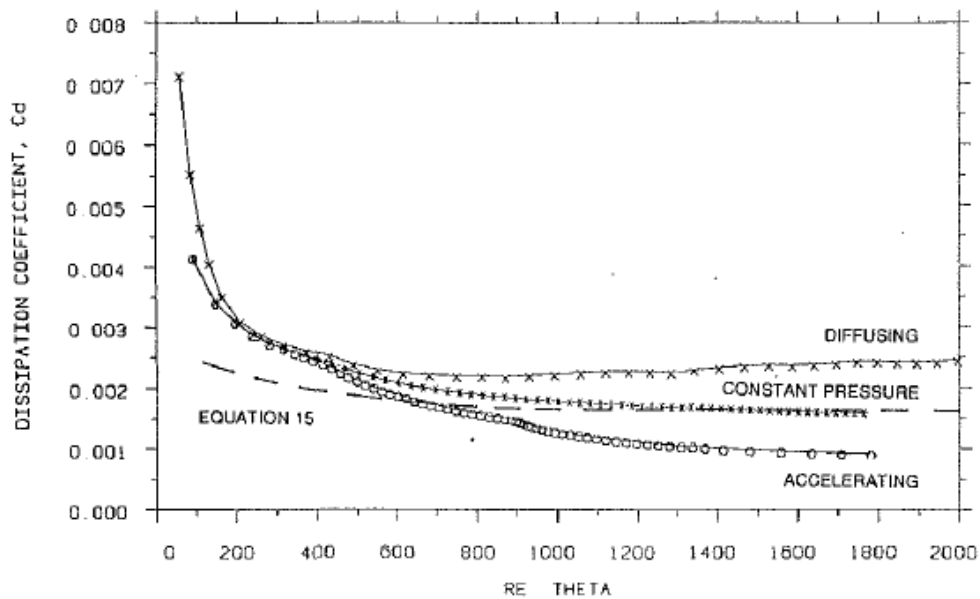


Fig. 2-47 Calculated dissipation coefficients for turbulent boundary layers (Denton 1993).

Denton also stresses the importance of predicting the boundary layer transition due to the large difference in dissipation coefficient between laminar and turbulent boundary layers around this point (Denton 1993), shown in Figure 2-48.

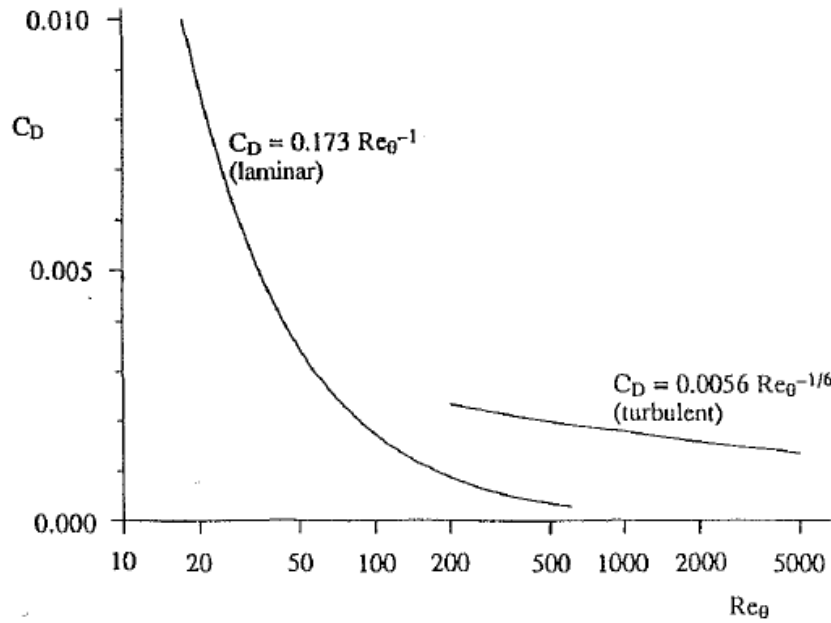


Fig. 2-48 Dissipation coefficient for laminar and turbulent boundary layers (Denton 1993).

It can also be discerned from equation 2-56 that the boundary layer loss is proportional to the cube of the velocity. The total entropy generation is then converted to an entropy loss coefficient by dividing the total entropy produced by the mass flow rate and a reference dynamic head using the formula below,

$$\zeta = \frac{T\dot{S}}{\dot{m} 0.5 V_{ref}^2} \quad \text{Eq. 2-59}$$

The formulae above are applicable for both stator and turbine where in the case of the stator the absolute velocity is used and for the turbine the relative velocity is used.

### 2.6.5.2 Trailing Edge Loss

Denton (1993) also attributes the losses at the trailing edge to viscous dissipation in the mixing out of the wake behind the trailing edge. Here the overall entropy generation can be calculated applying the equations of conservation of mass, energy and momentum to a control volume between the blade throat and some point downstream where the flow has returned to uniformity. The base pressure acting on the trailing edge is also included in the relationship.

Denton adopts the following formula to estimate the trailing edge loss,

$$\zeta = \frac{\Delta P_0}{0.5 \rho V_{te}^2} = \frac{C_{pbte}}{o \cos \alpha_2} + \frac{2 \theta}{o \cos \alpha_2} + \left( \frac{\delta^* + te}{o \cos \alpha_2} \right)^2 \quad \text{Eq. 2-60}$$

Denton (1993) gives the following correlation for the base pressure, typical values of  $C_{pb}$  are in the range -0.1 to -0.2 according to the relationship below,

$$C_{pb} = (P_b - P_{ref}) / (0.5 \rho V_{ref}^2) \quad \text{Eq. 2-61}$$

### 2.6.5.3 Tip Leakage Loss

Denton (1993) provides separate correlations for tip leakage losses depending on whether the blade row is shrouded or unshrouded. Entropy creation in tip leakage flows is mainly associated with the mixing of the leakage flow with the mainstream flow.

For shrouded turbines the entropy creation is calculated using,

$$\zeta = 2 \frac{m_L}{m_m} \left( 1 - \frac{\tan \alpha_1}{\tan \alpha_2} \sin^2 \alpha_2 \right) \quad \text{Eq. 2-62}$$

For unshrouded turbines the condition is more complex involving the formation of a jet interacting with the mainstream flow. To simplify the calculation process Denton suggests using the same velocity distribution as utilised to calculate the boundary layer loss,

$$\zeta = \frac{2C_d k C}{h p \cos \alpha_2} \int_0^1 \left( \frac{V_s}{V_2} \right)^3 \left( 1 - \frac{V_p}{V_s} \right) \sqrt{\left( 1 - \left( \frac{V_p}{V_s} \right)^2 \right)} \frac{dz}{c} \quad \text{Eq. 2-63}$$

### 2.6.5.4 Endwall Loss

Endwall loss also referred to as secondary loss is a major contributor to overall efficiency loss in turbines. Denton states endwall loss is difficult to understand and predict with virtually all previous prediction methods based on correlations of empirical data (Denton 1993). However, by adopting endwall boundary layer calculations, similar to those used to predict profile losses, Denton (1993) established the formula below to predict endwall entropy generation.

$$\dot{S} = 0.25 \int_0^{C_x} \frac{C_d}{T} \frac{(V_s^4 - V_p^4)}{(V_s - V_p)} \rho w dx \quad \text{Eq. 2-64}$$

### 2.6.5.5 Shock Loss

Denton (1993) also considers shock waves in turbines and their potential associated losses in transonic conditions. The formula below may be used to calculate the entropy creation due to shock. From this it can be seen that entropy creation roughly varies with the cube of  $(M^2 - 1)$ .

$$\Delta s \approx C_v \frac{2\gamma(\gamma-1)}{3(\gamma+1)^2} (M^2 - 1)^3 \quad \text{Eq. 2-65}$$

## 2.7 Loss Model Accuracy

Now the formulation of the more common methods of loss prediction in axial turbines has been established where available their correlation to experimental data of the time period will be summarised. Each author verifies their method against typical experimental turbine test data of the time period the method was presented, this gives an indication of the accuracy of the method and its suitability to predict design point turbine efficiency.

### 2.7.1 Ainley Mathieson Loss Model

The Ainley Mathieson turbine performance prediction method was compared to a variety of single and two stage turbines. All of the comparisons made were within  $\pm 2$  percent in turbine efficiency at the turbine design point. Turbine capacity variance in turbine capacity compared to test data was  $\pm 3$  percent.

### 2.7.2 Dunham Came Loss Model

The Dunham and Came loss model was verified against twenty five single stage gas turbines, these covered a wide range of designs and sizes. With cold air rig performance data available for each stage. The original Ainley Mathieson method predicted design point efficiencies to within  $\pm 3$  percent, the revised method proposed by Dunham and Came improved the correlation with test data bringing the majority of the examples to within  $\pm 2$  percent (Dunham and Came 1970).

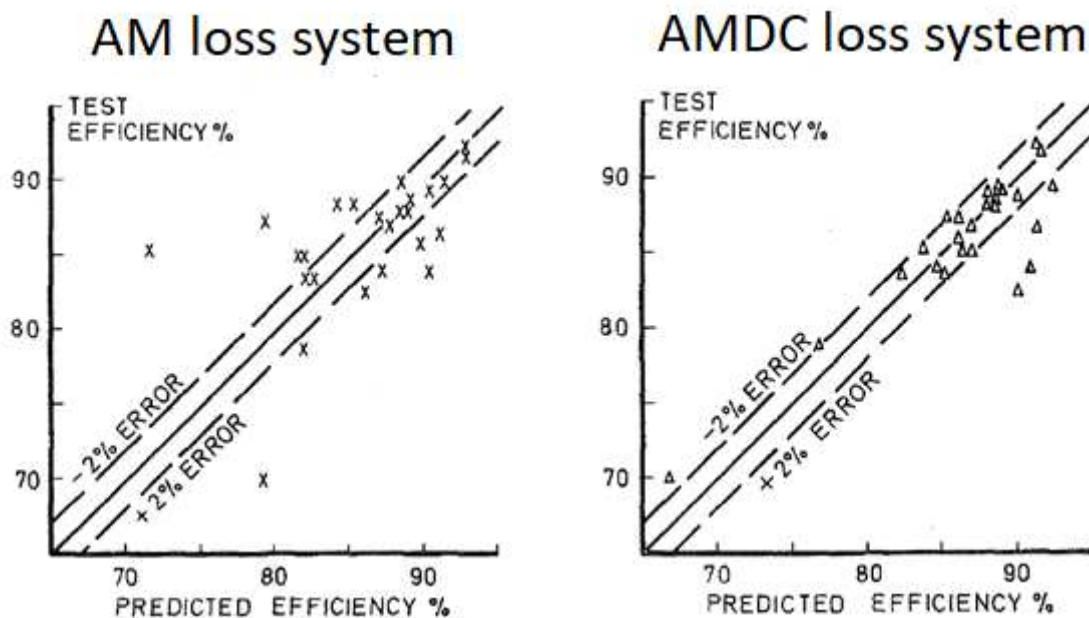


Fig. 2-49 Comparison of design point efficiencies of 25 turbines (Dunham and Came 1970).

Dunham and Came (1970) also found their method improved efficiency prediction at choke conditions when compared to experimental data from a typical aircraft engine. However, the main improvement was found when considering low aspect ratio turbines and low reaction turbines where previously the prediction of secondary losses was inadequate. When comparing their calculated efficiencies to a turbine with mean aspect ratio of about unity efficiency prediction is improved significantly at design speed and 50 percent design speed.

### 2.7.3 Kacker Okapuu Loss Model

Kacker and Okapuu (1982) validated their loss model against the Smith chart, Figure 2-7, and 33 turbines which included gas generator, automobile and thrust turbofan turbines. Kacker and Okapuu found that when comparing the Ainley and Mathieson loss system to the Smith chart while satisfying the change in efficiency with stage loading it struggled to replicate accurately the change with stage flow factor at values higher than 0.6. Kacker and Okapuu concluded that only compressibility and shock loss corrections to the profile loss and secondary loss can accurately replicate the Smith chart, with the shock loss correction mainly impacting turbine operation at higher stage flow factors and the acceleration correction influencing the overall efficiency level (Kacker and Okapuu 1982). As such Figures 2-21, 2-22, 2-23, 2-24 and 2-25 were determined iteratively to achieve correlation with the efficiency contours in Smith's chart. Kacker and Okapuu (1982) produced a chart similar to that of Smith using their new loss system, Figure 2-50. The contours estimated using the Kacker and Okapuu method seem to display satisfactory correlation to the Smith chart. Quantitatively, the efficiency contours predicted by Kacker and Okapuu (1982) peak at a lower stage loading factor and extend to a higher stage flow factor. Nonetheless, the quantitative agreement was considered satisfactory by Kacker and Okapuu (1982) despite the unavoidable scatter of the data.

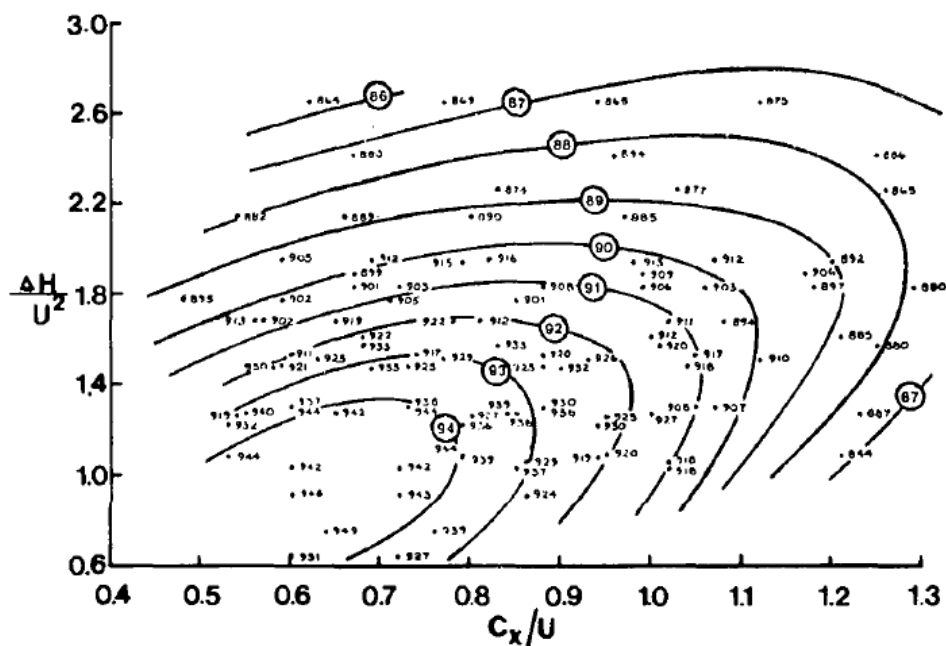


Fig. 2-50 Turbine stage efficiency at zero tip leakage calculated by the Kacker and Okapuu method (Kacker and Okapuu 1982).

Kacker and Okapuu (1982) also tested their loss system against design point efficiencies from 33 state of the art turbines of the time period. These ranged from a gas generator turbine of a small automobile to a low-pressure turbine of a thrust turbofan turbine. As can be seen from the charts depicted in Figure 2-51 the correlation between experimental and calculated data using the method developed by Kacker and Okapuu is within +/- 1.5 percent whereas the correlation using the AMDC loss system is not desirable (Kacker and Okapuu 1982).

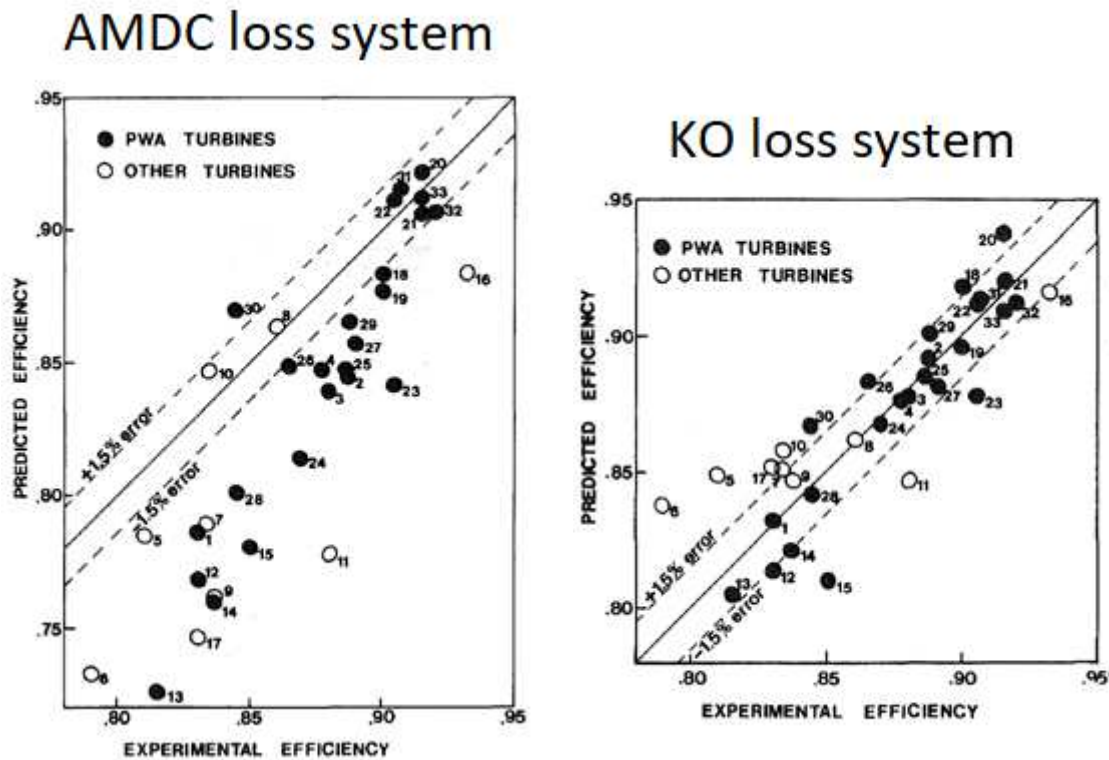


Fig. 2-51 Comparison of predicted efficiency with experimental efficiency of 33 turbines (Kacker and Okapuu 1982).

### 2.7.4 Craig and Cox Loss Model

Craig and Cox (1971) validated their loss system against a large number of turbines for which suitable experimental data was available. During their investigation Craig and Cox found no systematic or major discrepancies during comparison with over fifty machines with most calculated values of turbine efficiency being significantly within +/- 1.4 percent. Figure 2-52 presents their findings of the efficiency difference between measured and calculated values plotted against the output of each machine.

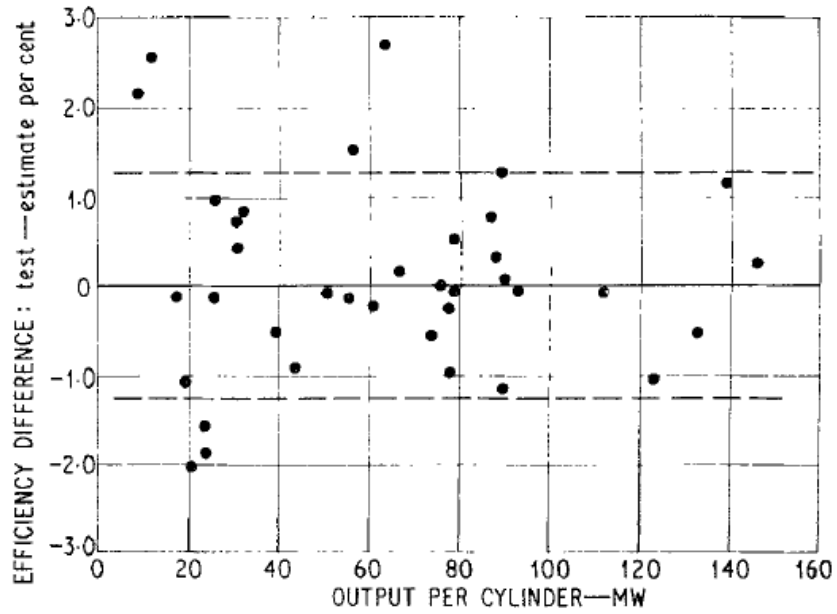


Fig. 2-52 Comparison of predicted and measured test efficiencies (Craig and Cox 1971).

### 2.7.5 Discussion

Reviewing each authors validation of their loss model it is clear when compared to design point efficiencies each loss system seems to perform relatively well. Only Dunham and Came (1970) present a comparison at half and 85 percent turbine design speed with a favourable result. Turbocharger turbines are required to run at off design conditions for prolonged periods depending on the turbocharger application. Whether it be a marine application where low load operation is expected for manoeuvring in port or a peaking power plant application which continuously cycles load. Therefore, accurate efficiency prediction over a wide range of operating conditions is required.



## Chapter 3

# Mean Line Performance Prediction Tool

### 3.1 Introduction

In this chapter the mean line performance prediction program will be examined in more detail. The program chosen to construct the mean line tool was Microsoft Excel where the inbuilt programming language, Excel VBA, was used to create the mathematical model. The author has extensive programming experience in Excel VBA having written a number of programmes related to turbocharger test data analysis, engine data analysis and also a chart digitiser program which was used to extract the data for the loss correlations described in the previous chapter. Microsoft Excel was also chosen due to its accessibility and well-known interface; Excel also provides a significant number of inbuilt tools for data analysis and manipulation which may prove useful in the development of the program in the future.

## 3.2 Mean Line Tool Structure

To begin structuring the mean line tool in Excel VBA it was first necessary to decode the original Fortran program. Most of the calculation steps were identifiable by following the performance prediction method described by Ainley and Mathieson (1951) which the original code was based on. However, no informative text existed on the structure of the program and there were no details on some of the differences between the method described by Ainley and Mathieson and the code used by Napier Turbochargers. As the code has undergone various modifications by past employees of Napier Turbochargers without any documentation some of the modifications to the code have been interpreted as improvements to maintain the accuracy of the efficiency prediction compared to modern blade designs as such they have been carried over and applied to the chosen loss correlations. For example, one of the main limitations of the original code is it uses correlations which are based on turbine designs from when the method was first conceived. The Ainley and Mathieson method was first conceived in 1951 since then turbine blade design has evolved including blade leading edge design, with modern designs employing a more elliptical shape. To account for this change in the original code the leading-edge blade angle is multiplied by a factor of 0.3. Other unexplained modifications include the limiting of the range of incidence to stalling incidence ratio when calculating the profile loss incidence correction factor, Figure 2-18, and the blade outlet angle is divided by a factor of 100 when deciphering the profile loss coefficient, Figure 2-13 and 2-14. Eventually most of the code was unravelled and translated into Excel VBA, Figure 3-3 shows the basic structure of the calculation process in the new mean line tool.

The tool begins by importing the input data and initiating the speed increment at the lowest speed outlined in the input file. The turbine mass flow is then imposed, the first flow step to be computed is the design flow, the program then increments the stage row number calculating the loss coefficients and operating conditions for the stator and turbine. The loss coefficient is modified based on the outlet conditions from each row, the loss coefficient and outlet condition calculations are iterated until the loss coefficient converges. Once converged the choking mass flow is established and imposed and the row increment is repeated calculating the loss coefficient and operating conditions for the stator and turbine. Thereafter the flow is incremented using a correlation from the original code based on the choking mass flow and minimum mass flow. Once all of the speeds have been processed a .txt file is output containing the turbine map parameters, non-dimensional speed, swallowing capacity, turbine pressure ratio and total to static efficiency as outlined by the standard SAE International (1995).

### 3.3 Mean line Tool Inputs

Each set of geometry or input file is extracted from blade profile data and includes parameters for both blade rows of the turbocharger. The parameters required for each blade row are shown below.

| Symbol    | Code Input File  |
|-----------|--|
| -         | Number of cases  |
| -         | Title  |
| -         | Number of blade rows   |
| $o$       | Throat width   |
| $e$       | Back surface radius of curvature   |
| $k$       | Tip clearance  |
| -         | Tip clearance turbine factor   |
| -         | Unshrouded turbine factor  |
| -         | Throat area  |
| $s$       | Pitch  |
| $\beta_1$ | Leading Edge blade angle   |
| $c$       | True chord   |
| $t$       | Max. thickness   |
| $te$      | Trailing edge thickness  |
| $r_h$     | Hub radii  |
| $r_t$     | Tip radii  |
| -         | $C_p(\text{gas})$ , $N/rtT(\text{design})$ , $MrtT/P(\text{design})$ , $T01$ |
| -         | $MrtT/P(\text{min})$ , Max. Mach   |
| -         | Pressure recovery of TOC, Efficiency debit                                   |
| -         | Number of $N/rtT$ curves required  |

Table 2 Input parameters for mean line tool.

The inputs for the program include parameters relating to the geometry of the turbine stage and the stator and rotor arrangement as well as a number of parameters defining design conditions and stage constants. The following section describes the non-geometric parameters. The number of blade rows for a turbocharger will typically be two. The tip clearance factor is defined in section 2.6.1.4 and depends on whether the stage is shrouded or unshrouded, there is also a factor included in the Ainley and Mathieson (1951) method to account for radial tip clearance when calculating blade flow outlet angle, for unshrouded turbines this figure is 1.35 (Ainley and Mathieson 1951). The following boundary conditions are included in the input file, the specific heat capacity,  $C_p$ , of the gas entering the stage is 1115.3 J/kg C° and the stage total inlet temperature,  $T01$ , is 763 Kelvin. The following non dimensional parameters are used to describe the design speed  $N/vT(\text{design})$ , swallowing capacity  $MVT/P(\text{design})$ , and minimum swallowing capacity  $MVT/P(\text{min})$  these parameters are dictated by the particular application the turbine is intended for in order to achieve optimum performance. The maximum Mach number is also included in the input and is typically set at 1.6. In order to account for the pressure recovery which occurs in the exhaust diffuser a factor is included which has been derived from CFD and test data. There is also a constant efficiency debit to account for lacing wire loss and non-swirl related losses which for simplicity is subtracted from the

turbine efficiency. Finally, the number of speed lines required is declared. The following sketches provide a definition of the geometric parameters included in the input file.

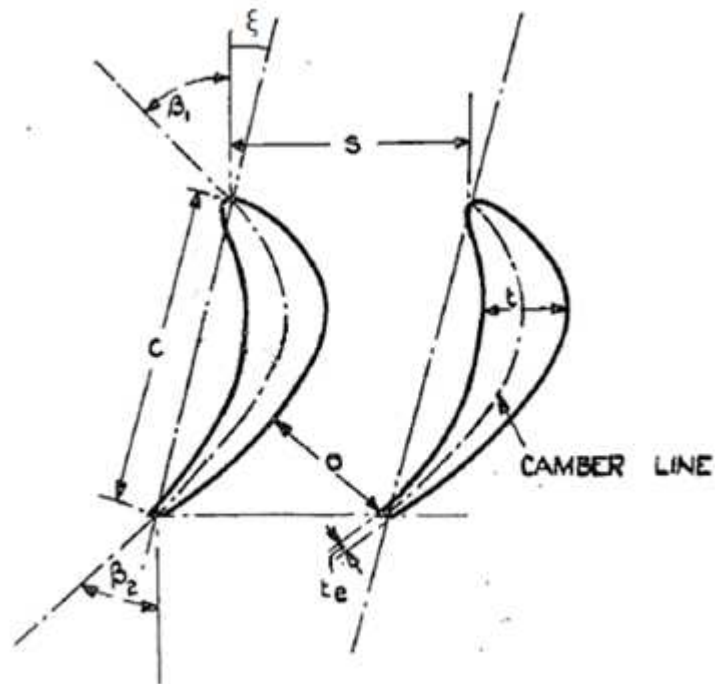


Fig. 3-1 Turbine blade nomenclature (Ainley and Mathieson 1951)

The throat area of the stator and turbine blade is calculated at the throat opening. The calculation of the back-surface radius of curvature for each blade row is derived below.

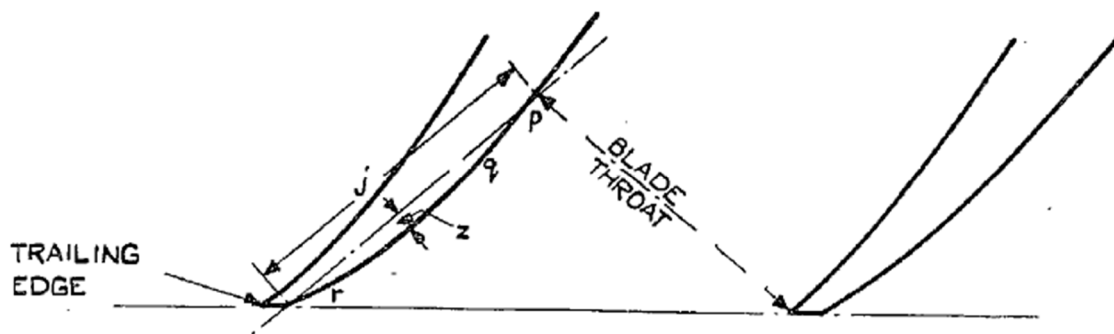
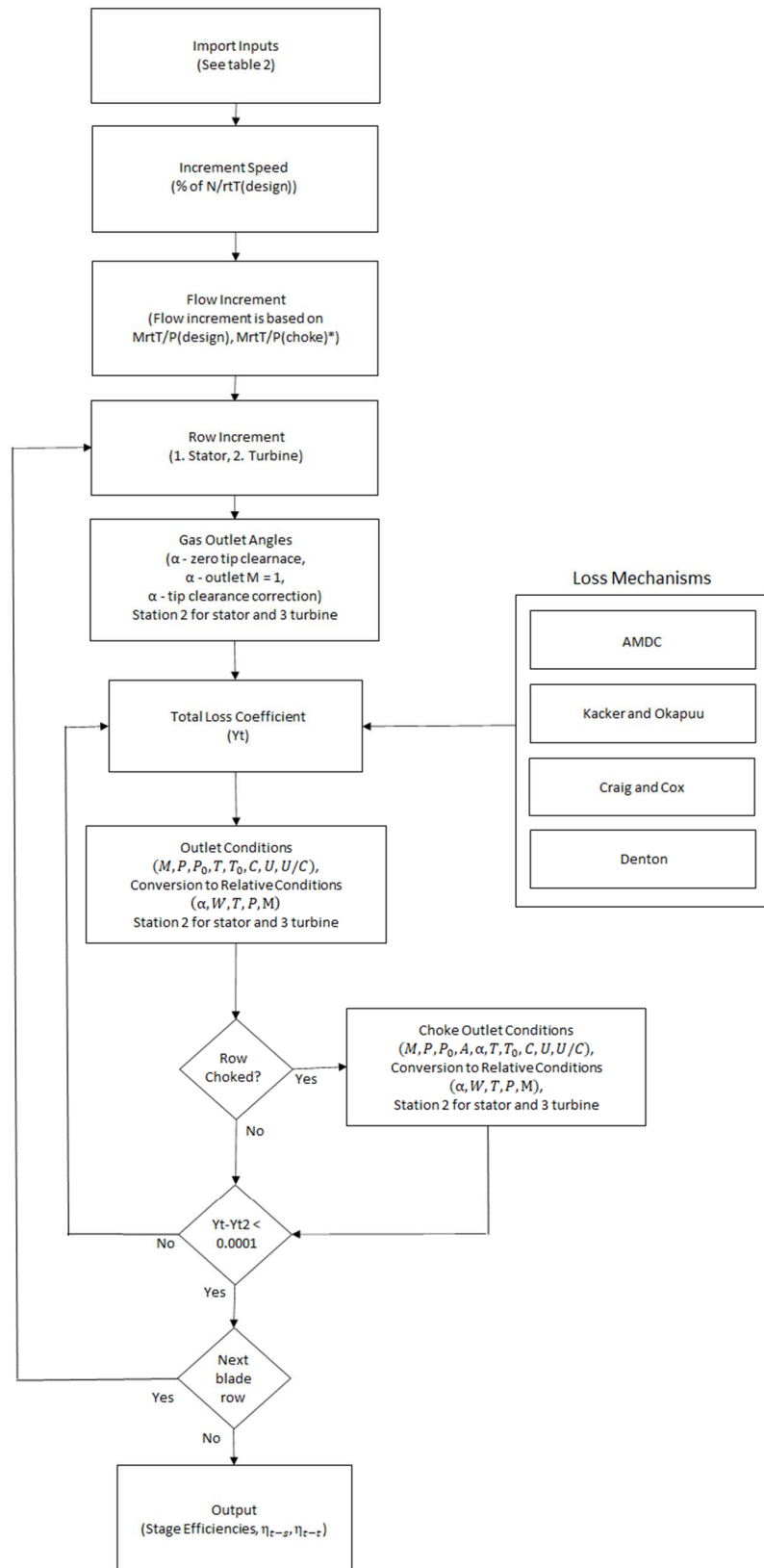


Fig. 3-2 Turbine blade nomenclature (Ainley and Mathieson 1951)

$$pqr = e = j^2/8z \quad \text{Eq. 3-1}$$



\*This is the swallowing capacity where the turbine stage reaches choke conditions.

Fig. 3-3 Basic structure of the calculation process in the new mean line tool.

### 3.3 Loss Correlation Implementation

In this section the implementation of the loss models to the chosen program are described. As the chosen loss mechanisms include various correlations the translation of these into a digital format and integration into the math code will be covered first.

In order to retrieve the raw data from the correlations a digitization tool developed in Excel VBA code using Microsoft Excel by the author during his employment at Napier Turbochargers was used. The program allows you to import a picture file, set the axis and extract the required data, a screenshot of the program is shown in Figure 3-4.

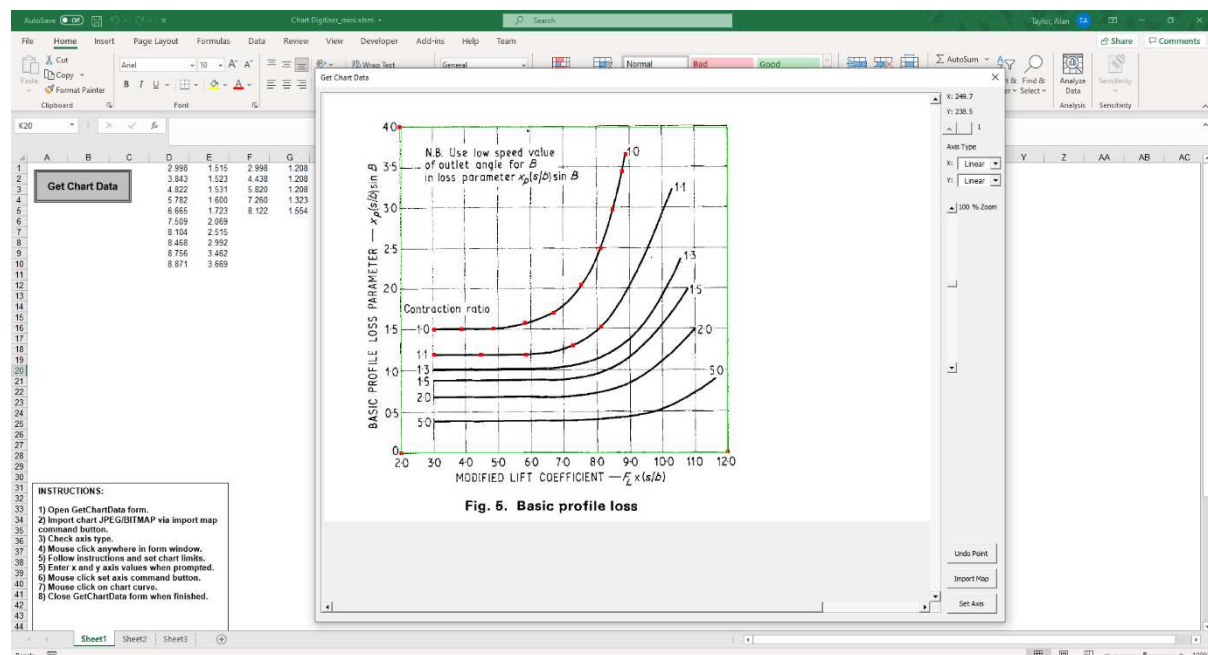


Fig. 3-4 Screenshot of Chart digitization program developed by the author.

This tool has been tested extensively in the Napier Turbochargers Engineering department and is regularly utilised for tasks such as the construction of compressor characteristics from rig data and the retrieval of data from published material. Once the raw data has been retrieved it is tabulated and stored in Microsoft Excel where necessary the data is referenced by the code using double interpolation.

Where double interpolation was not appropriate, for example the correlations used by Denton for profile loss and tip clearance loss (Denton 1993) where there are three variables  $x$ ,  $y$ ,  $z$ , and  $x$ ,  $y$  are independent variables and  $z$  is dependent on both, bi-linear interpolation was employed. The data presented by Denton (1993) was digitised using the digitization tool and used to construct a matrix of data which can be stored in Microsoft Excel, bi-linear interpolation was then used to interpolate within this grid to find the desired value of  $z$  at the given  $x$  and  $y$  values. The formula for bi-linear interpolation is shown in Eq. 3-2, the grid of values and corresponding contour chart used in the code for Denton's correlation relating to profile loss is shown in Appendix B.

$$f(x, y) \approx \frac{1}{(x_2 - x_1)(y_2 - y_1)} (z_{11}(x_2 - x)(y_2 - y) + z_{21}(x - x_1)(y_2 - y) + z_{12}(x_2 - x)(y - y_1) + z_{22}(x - x_1)(y - y_1)) \quad \text{Eq. 3-2}$$

### 3.3.1 Kacker and Okapuu

The loss models proposed by Kacker and Okapuu have been translated into code with minimal modification. As the Kacker and Okapu loss model is a development of the Ainley and Mathieson technique the modifications included in the original code have been carried over to the Kacker and Okapuu model. The Kacker and Okapuu routine does include an extra iteration in order to decipher the tip clearance efficiency debit as described in section 2.6.3.5. The VBA code relating to the Kacker and Okapuu loss model is included in Appendix C.

### 3.3.2 Craig and Cox

For the Craig and Cox method the losses relating to annulus, cavity and gland leakage loss have been left out as they do not apply to an axial turbine in a turbocharger. Also, as there are no productionised shrouded turbines in the Napier product range only the calculations relating to unshrouded turbines have been considered. The Craig and Cox method also requires the blade camber line length or backbone length, the following parabola arc length formula will be adopted to give an estimate of this length.

$$L = \frac{1}{2} \sqrt{b^2 + 16 \cdot a^2} + \frac{b^2}{8 \cdot a} \ln \left( \frac{4 \cdot a + \sqrt{b^2 + 16 \cdot a^2}}{b} \right) \quad \text{Eq. 3-3}$$

Where,

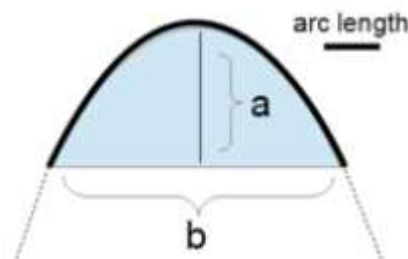


Fig.3-5 Parabola arc length

The correlations used by the Craig and Cox (1971) method were digitised using the digitization tool and are stored in the mean line program for reference when calculating the loss coefficients. The VBA code relating to the Craig and Cox loss model is included in Appendix C.

### 3.3.3 Denton

The Denton loss mechanism has been simplified for implementation to the mathematical model. The equations set out previously relating to Denton's method require complete knowledge of the velocity distribution at both suction and pressure sides of the turbine stage. As this knowledge is often not always available Denton proposed a simplified method to estimate turbine performance. This method concentrates on the profile, trailing edge, secondary and tip clearance losses. The VBA code relating to the Denton loss model is included in Appendix C.

#### 3.3.3.1 Profile Loss

Denton adapts the semi-analytical method presented by Balje and Binsley (1968). Which is based on an approximate blade surface velocity distribution and a simple turbulent boundary layer calculation to estimate the trailing edge momentum thicknesses. This method is not dependent on experimental conditions, only the mean level is adjusted to agree with a range of test data. Denton uses a similar method applying the theories of entropy generation in boundary layers to calculate profile loss coefficients at optimum pitch-to-chord ratios.

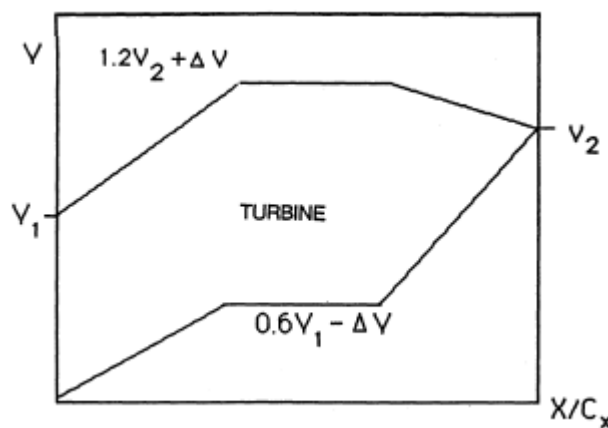


Fig. 3-6 Generic surface velocity distribution for a turbine (Denton 1990).

A typical surface velocity distribution used by Denton in his work is shown in Fig 3-6. By equating the blade load to the momentum change it is possible to predict the entropy creation and energy loss coefficients from equation 2-56. The chart in Fig. 3-7 is generated by systematically varying the blade load. As described initially this is translated into the mathematical model as a matrix deciphering the profile loss at given inlet and outlet angles using bi-linear interpolation.



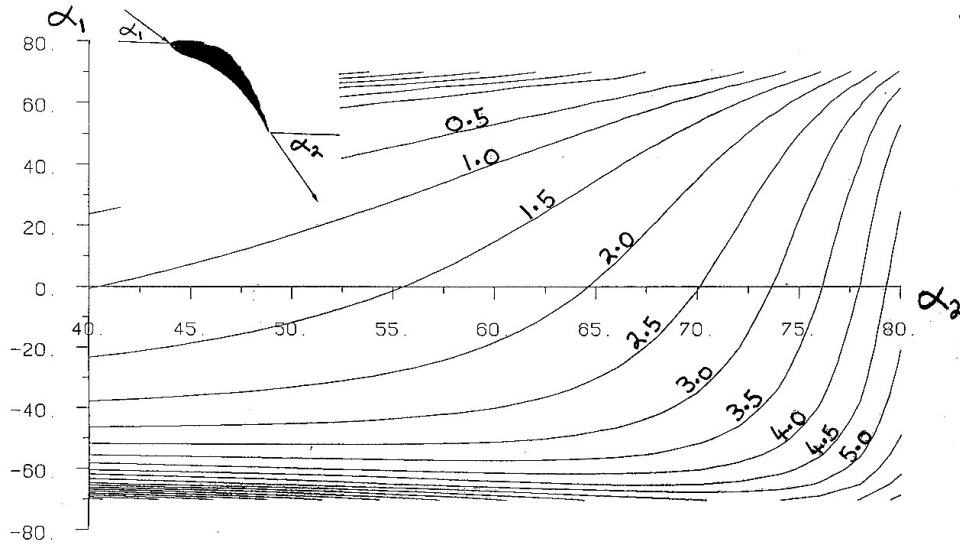


Fig. 3-7 Predicted profile loss (%) of Turbine blades at optimum pitch to chord ratios (Denton 1993).

### 3.3.3.2 Trailing Edge Loss

The calculation of the entropy generation due to mixing losses at the trailing edge requires the formulation of the momentum and displacement thicknesses of the boundary layer. For the purposes of this investigation, it was deemed acceptable to simplify the calculation of these parameters by considering the momentum and displacement thicknesses of a flat plate at turbulent conditions. Firstly, the Reynolds number was established.

$$\text{Reynolds number} = \text{inertia force} / \text{friction force} = \rho VL / \mu \quad \text{Eq. 3-4}$$

The relationships for a flat plate at turbulent conditions were used to calculate the displacement and momentum thicknesses.

### 3.3.3.3 Secondary Loss

It is suggested by Denton that the Dunham and Came (1970) method of calculating endwall losses remains the most satisfactory. This is an extension of the method developed by Ainley and Mathieson (1951) enabling different users to apply correction factors to suit their own needs based on test data. Based on a large number of comparisons with test data Denton uses a modification of this applying a factor of 0.375.

$$Y_s = 0.375 * 0.0334 \left(\frac{c}{h}\right)^4 (\tan\alpha_1 - \tan\alpha_2)^2 \left(\frac{\cos^2\alpha_2}{\cos^3\alpha_m}\right) \left(\frac{\cos\alpha_2}{\cos\beta_1}\right) \quad \text{Eq. 3-5}$$

### 3.3.3.4 Tip clearance loss

Tip leakage loss provides one of the main sources of loss in turbines. Denton (1993) provides two correlations for shrouded and unshrouded blades. For unshrouded blades Denton (1993) uses simple theoretical methods to produce the correlation shown in Fig 4-6 assuming a tip clearance of 1% on height ratio.

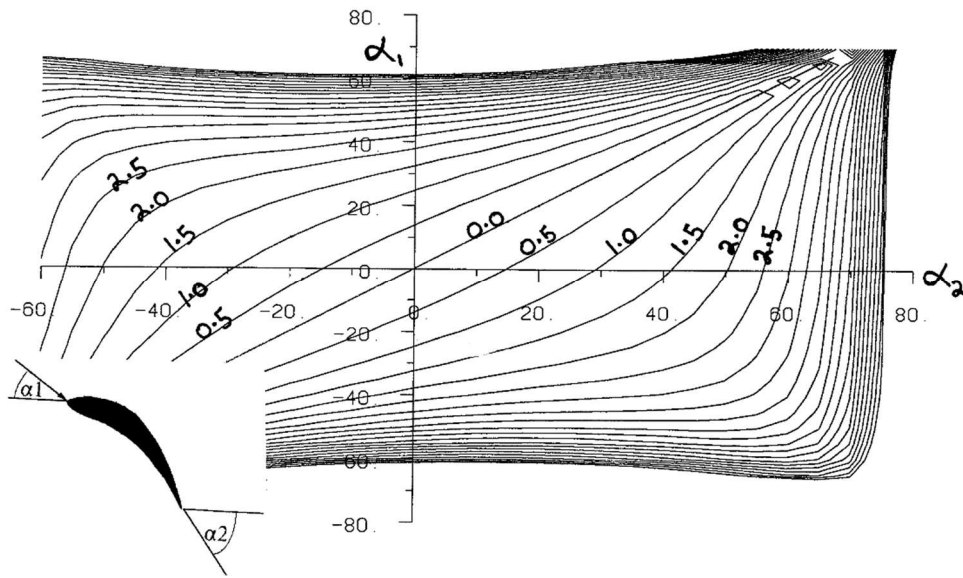


Fig. 3-8 Tip leakage loss coefficient for unshrouded blades: contours in percent exist dynamic head per 1 percent clearance/height (Denton 1993).

# Chapter 4

## CFD and Results Comparison

### 4.1 Introduction

In order to assess the suitability of the chosen loss correlations the results gained from the mean line performance prediction method and loss mechanisms will be compared to CFD data. In this chapter an overview of the chosen CFD program will be outlined including descriptions of the main aspects of the CFD code and diagrams of a representative mesh used to simulate the selected turbine geometries. Then the comparison and analysis of the results obtained using the mean line prediction method and the CFD data for the selected turbine geometries will be presented. Each geometry will be simulated at various turbine speeds and mass flows to gain an understanding of how the loss mechanisms perform over a wide range of operating conditions. Typically, a turbine map is produced by computing a range of speeds however, rather than analysing the entire map at once the following analysis will concentrate on low speed, design speed and high speed conditions. The geometries selected for the test analysis are taken from the current Napier product range and represent the current standard and design philosophy of turbine blade. As Napier Turbochargers would rather not publicise the performance and geometries of their turbines all turbine efficiencies will be normalised using the maximum efficiency and only some of the important geometric ratios will be detailed. The individual loss mechanisms of each loss model will also be analysed and discussed. Finally, a summary of the results and comparisons will be included at the end of this chapter to assess each loss models suitability regarding efficiency prediction.

## 4.2 MULTALL CFD Code

Due to the lack of availability of turbine test data at the required operating conditions it was decided a CFD program will be used to validate the chosen loss mechanisms. This is mainly a result of Napier Turbochargers not having access to a dedicated turbine test rig to enable the testing of a given turbine at the full range of velocity ratio. The chosen CFD program is MULTALL, which was developed by Prof. John Denton at the Whittle Lab, Cambridge UK. Napier Turbochargers have accumulated extensive experience with MULTALL which has been used in the Aerodynamics department for turbine analysis for a number of years. A computer of suitable performance based on campus at The University of Sheffield was enlisted to run MULTALL remotely, the computer includes a Zenon processor, with 12 cores and was built in 2014. As a number of constant turbine speed lines were required with a suitable number of points to achieve a meaningful efficiency characteristic it was imperative the chosen computer was able to run uninterrupted.

MULTALL is a 3D multistage turbomachinery flow calculation for steady flows. The version of MULTALL used by Napier Turbochargers and for this investigation, MULTALL-09, uses the SCREE solution algorithm. The SCREE algorithm is a second order method which is extremely simple and very fast. The code is based on an explicit time marching finite method for solving the N-S equations (Denton 2017). Each computed time derivative is stored and utilised in the next time step. The primary flow variables integrated over a time step for a finite volume cell can be written,

$$\Delta F = \frac{\Delta t}{Vol} \sum_{Cellfaces} Fluxes \quad \text{Eq. 4-1}$$

Where F is any one of the conserved variables ( $F = \rho, \rho E, \rho V_x, \rho V_r$  or  $\rho r V_t$ ).  $\Delta F$  is calculated for every conserved variable on every time step. The value of  $dF/dt$  from the previous time step is combined with the current value in order to extrapolate the value of  $dF/dt$  to the end of the time step, and we use the extrapolated values to update the time step,

$$F_{n+1} = F_n + \Delta F, \text{ where } \Delta F = \left( 2 \left( \frac{\partial F}{\partial t} \right)^n - \left( \frac{\partial F}{\partial t} \right)^{n-1} \right) \Delta t \quad \text{Eq. 4-2}$$

This method was found to be stable and very robust for CFL numbers up to approximately 0.5 (Denton 2017). The SCREE algorithm only requires a single computation of the fluxes and update of the variables for each time step and is therefore very simplistic. Also, the method works at extremely low Mach numbers so incompressible flow can be computed (Denton 2002).

The mesh in MULTALL is defined using pitchwise, streamwise and quasi-orthogonal grid lines. This type of grid simplifies generation, the application of boundary conditions and modelling of mixing planes. The grid lines should be closely spaced around the leading edge where fluid properties are changing rapidly. A body force field and a fine grid may be applied to the trailing edge to force the flow to separate (Denton 2009). Figure 4-1 shows a blade to blade view of a representative mesh used in MULTALL to simulate the chosen blade geometries. Figure 4-2 shows the meridional view of the same mesh.

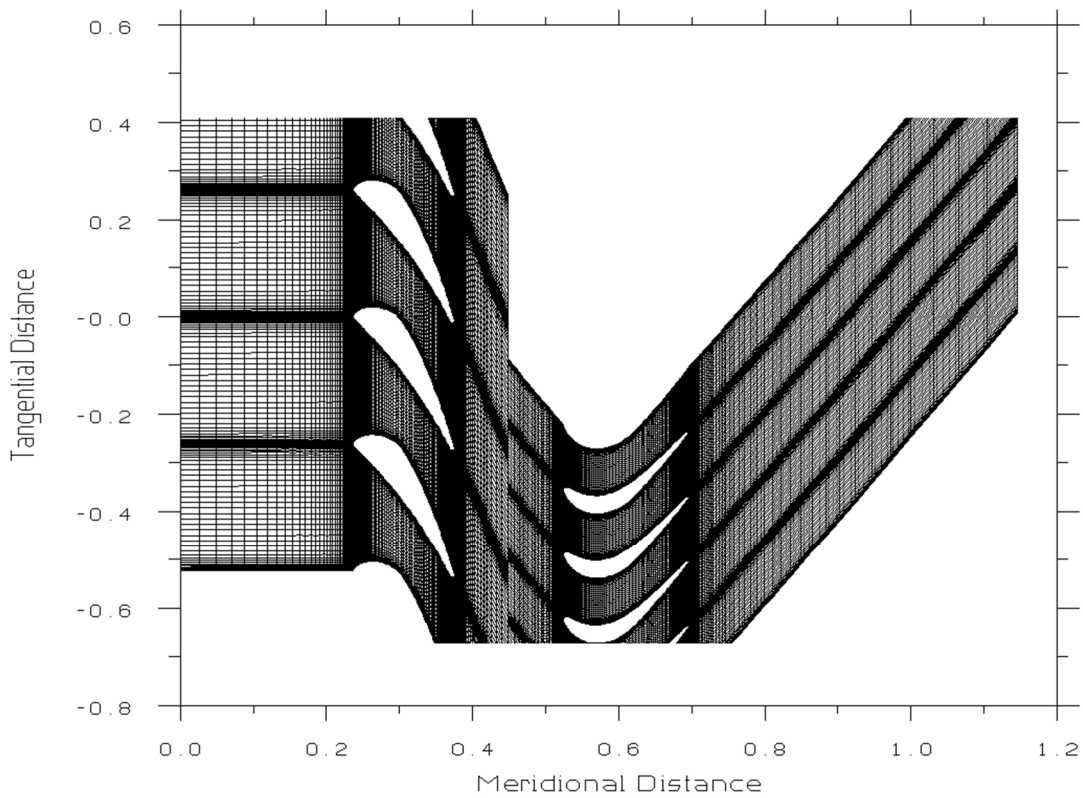


Fig. 4-1 Blade to blade view of grid on a streamwise surface from MULTALL

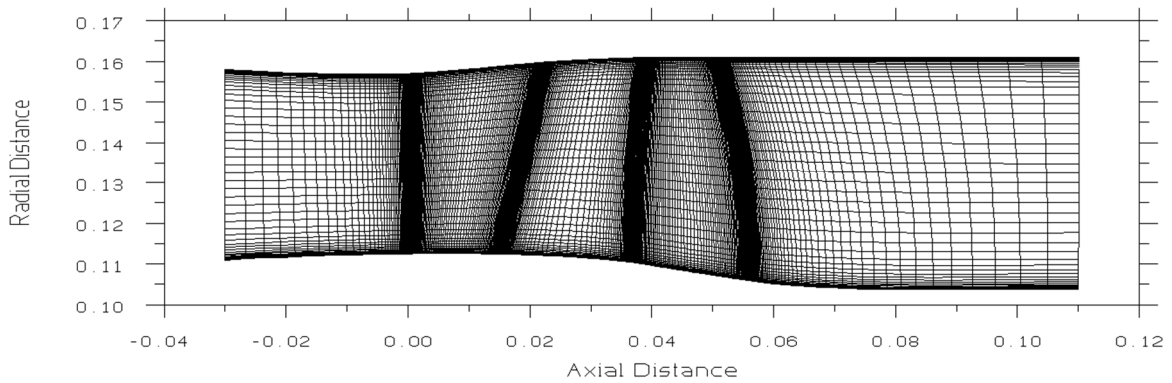


Fig. 4-2 Meridional view of grid from MULTALL

The mixing plane model used in MULTALL-09 has been developed over a number of years (Denton 2017). The aim of the mixing plane model is to allow instantaneous mixing out at a plane rather than downstream of the blade row. Static pressure and entropy will increase across the mixing plane to replicate a real mixing process. An improved version of the “flux extrapolation” model is used in the present code (Denton 1990). Figure 4-3 gives a visual representation of the method.

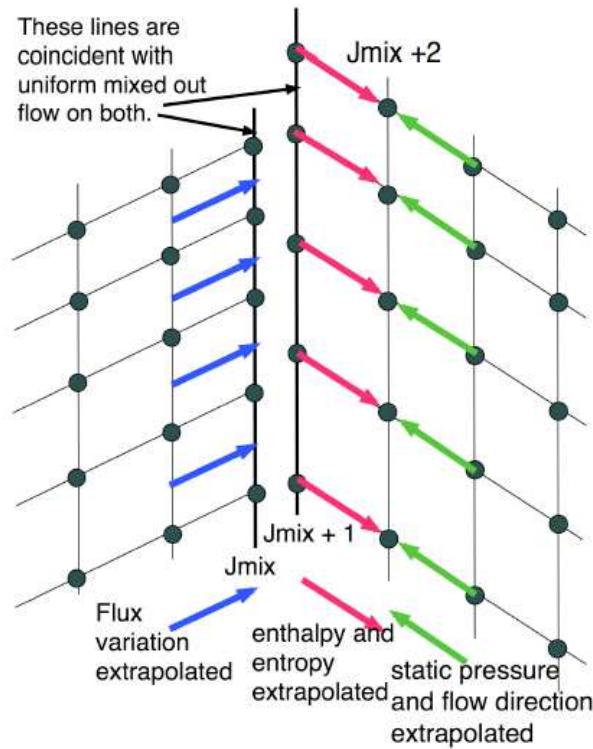


Fig. 4-3 Mixing plane treatment (Denton 2017).

At all spanwise points there are two equivalent pitchwise gridlines, labelled  $J_{mix}$  and  $J_{mix}+1$ , the flow on both these lines is pitchwise uniform. A one-dimensional time marching method is used to pass information between  $J_{mix}$  and  $J_{mix}+1$  to update the pitchwise uniform variables. This guarantees the flow on the two equivalent lines match when the solution is converged, and the flow is mixed out (Denton 1990). The treatment of the upstream face may be summarized by the following equation,

$$FLUX_{J_{mix}} = FLUX_{avg,J_{mix}} + F_{ext}(FLUX_{J_{mix}-1} - FLUX_{avg,J_{mix}-1}) \quad \text{Eq. 4-3}$$

The total flux across the mixing plane is not affected by the average value of the extrapolated flux however it causes only a gradual decay of pitchwise non uniformity in the cells adjacent to the mixing plane rather than a sudden removal which would cause an upstream disturbance in the flow. The downstream of the mixing plane will have pitchwise uniform relative stagnation enthalpy and entropy but the flow direction and static pressure must not be pitchwise uniform. The mixed out entropy and relative stagnation temperature from the mixing plane with the calculated static pressure is used to calculate an isentropic velocity and density at  $J_{mix}+2$ . The flow direction at  $J_{mix}+2$  is extrapolated and combined with the isentropic velocity to give the velocity components, deviations in these are reduced to ensure pitchwise uniformity of the entropy and relative stagnation enthalpy entering the downstream row.

The viscous model in MULTALL-09 is a body force model, where body forces are used to solve the Navier-Stokes equations. The body forces are obtained from a thin shear layer approximation to the Navier stokes equations, the model assumes that viscous normal stresses and viscous stresses on the quasi-orthogonal faces of the elements can be neglected (Denton 2009). CPU time is greatly reduced using the body force method as the viscous terms are calculated every five time steps. The wall

shear stresses are calculated using wall functions which use curve fit to the log law for equilibrium boundary layers.

Denton (2009) strongly recommends that a cusp is used at the trailing edge of the blade and as such a cusp generation method is included in MULTALL-09. The simulations carried out using MULTALL-09 use the default cusp at the trailing edge.

Tip leakage flows are accounted for in MULTALL-09 using the pinched tip model where the blade is thinned towards the tip and periodicity is applied across the tip gap.

#### 4.2.1 CFD Mesh Study

A mesh study was performed to check the optimum mesh was being used in MULTALL. The current mesh size adopted by Napier Turbochargers for MULTALL was tested at -50%, -25%, +25% and +50% mesh density. The chart in Figure 4-3 shows the findings. The turbine efficiency has been removed from the y axis however the increment on the y axis is 0.2% efficiency. The findings show a very small variance in turbine efficiency between the mesh densities tested.

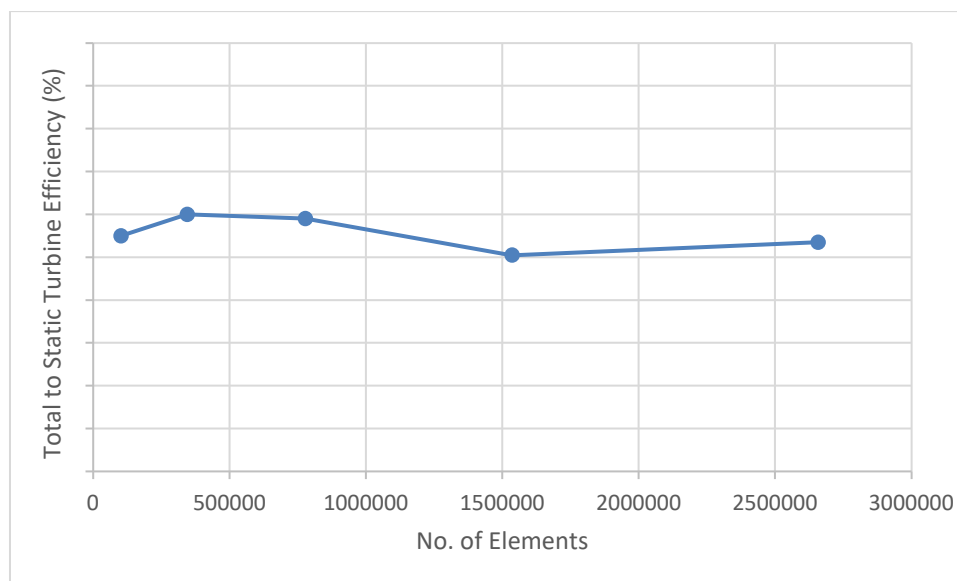


Fig. 4-4 CFD mesh study carried out at -50%, -25%, +25% and +50% mesh density using geometry one.

#### 4.3 MULTALL CFD Validation

The MULTALL CFD code has been validated internally by Napier Turbochargers using the MT1 turbine DERA experimental data. The MT1 turbine stage has undergone extensive investigation at the Isentropic Light Piston Facility at DERA, Pyestock, Hilditch et al (1994) reports the installation of the facility. Napier Turbochargers had access to this data while they were owned by Siemens who were partners in the turbine performance investigations carried out using the MT1 turbine. Napier Turbochargers became a limited company in 2008, and therefore were no longer under ownership

by Siemens. Unfortunately, this meant Napier Turbochargers no longer had access to the reports detailing summaries of the measurements gained at the DERA facility. As these reports are not in the public domain and are under restricted access the results of the validation cannot be included here. However, the investigations carried out by Napier Turbochargers revealed MULTALL showed good agreement to the MT1 data and also highlighted some weaknesses in the CFD code which required attention. Further work was carried out using MULTALL in order to calibrate the CFD code against the MT1 data including investigations relating to mesh density and trailing edge body forces.

#### 4.4 MULTALL Boundary Conditions

In order to achieve a complete speed line with an appropriate distribution of efficiency, the following boundary conditions were used to simulate the selected turbine geometries in MULTALL at the rotational speeds corresponding to the mean line tool input files. An example of the MULTALL input file used during the CFD simulations, without the blade geometry, is included in Appendix A, detailing the additional parameters that were used for the simulations. An overview of the input file can be found in the MULTALL manual Denton (2009).

| P01 | T01 | Pexit |
|-----|-----|-------|
| bar | K   | bar   |
| 1.5 | 763 | 1.0   |
| 2.0 | 763 | 1.0   |
| 2.5 | 763 | 1.0   |
| 3.0 | 763 | 1.0   |
| 4.0 | 763 | 1.0   |
| 4.5 | 763 | 1.0   |

Table 3 MULTALL boundary conditions

#### 4.5 Results Comparison and Analysis

The following section concentrates on the comparison of the turbine efficiency gained from the mean line method of turbine efficiency prediction combined with the chosen loss methods described previously and CFD MULTALL data. The losses are analysed separating the stator and rotor total loss coefficients initially and then the total losses are broken down further into individual losses where the characteristics of each loss are analysed. Only the rotor losses will be analysed in detail however if the individual stator losses are of interest they will be included also. The analysis of the first geometry will be examined in greater detail and will be referenced for the second and third geometry where appropriate in order to avoid repetition. The analysis of the third geometry will comprise of a summary as the trends are expected to be close to that of the second geometry.

The overall turbine efficiency of a turbocharger should include the pressure recovery which takes place in the turbine exhaust diffuser, a typical axial turbine turbocharger arrangement is pictured in Figure 4-5 showing the exhaust diffuser. A casing recovery factor is included in the original code which accounts for this pressure recovery however, in order to gain a direct comparison when



comparing the model results to the proposed CFD performance data the pressure recovery factor has been set to zero.

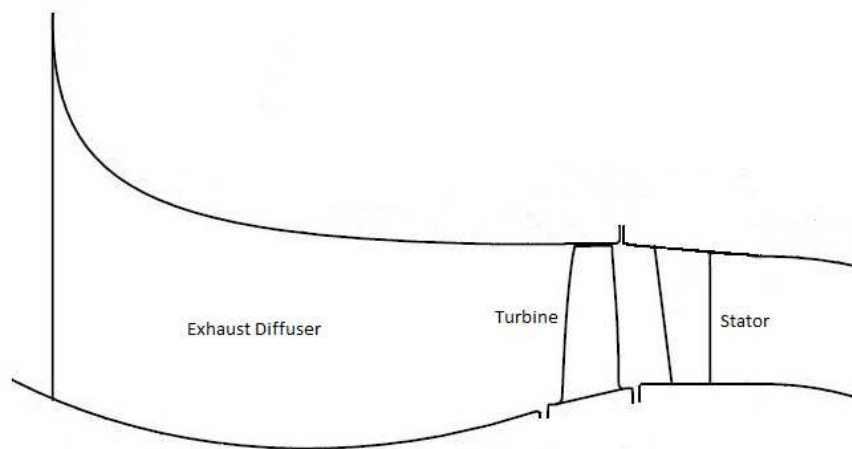


Fig. 4-5 Typical Napier Turbocharger axial turbine arrangement.

Another factor which is often accounted for in the turbine efficiency, which is included in the SAE turbine map standard (SAE International 1995), are mechanical losses. Again, in order to achieve a direct comparison between performance data the mechanical losses will be omitted from any analysis. The lacing wire loss and non-swirl related losses are accounted for by a constant efficiency debit for simplicity which will be subtracted from both sets of performance results.

#### 4.5.1 Geometry for Simulation

The important geometric ratios of the chosen turbines stages to be analysed are shown in Table 4. The chosen stages are taken from the existing Napier turbochargers turbocharger portfolio. Geometry 2 and 3 are taken from one of the latest turbochargers and have a higher aspect ratio compared to Geometry 1. The blade design philosophy applied to these turbines was intended to maximise efficiency by increasing the trailing edge area by lengthening the turbine blade, this reduces the absolute-frame outlet velocity reducing outlet Mach numbers and in turn minimising losses. Geometry 3 is the largest of the turbines in terms of swallowing capacity and has the highest number of blades.

| Geometric Ratio                    | Geometry 1     |         | Geometry 2     |         | Geometry 3     |         |
|------------------------------------|----------------|---------|----------------|---------|----------------|---------|
|                                    | Stator         | Turbine | Stator         | Turbine | Stator         | Turbine |
| Pitch to Chord Ratio ( $s/c$ )     | 0.84           | 0.72    | 0.73           | 0.78    | 0.76           | 0.64    |
| Aspect Ratio ( $H/c$ )             | 1.09           | 2.05    | 0.74           | 2.38    | 1.03           | 2.26    |
| Trailing Edge to Throat Area Ratio | 0.08           | 0.03    | 0.10           | 0.04    | 0.05           | 0.03    |
| Reynolds number range              | 25000 - 190000 |         | 25000 - 190000 |         | 30000 - 320000 |         |

Table 4 Important geometric ratios of the turbine stage geometries to be investigated.

## 4.5.2 Geometry 1

The first turbine stage to be analysed is taken from a current productionised Napier turbocharger. The following table shows the important geometric ratios.

| Geometric Ratio                    | Stator | Turbine |
|------------------------------------|--------|---------|
| Pitch to Chord Ratio ( $s/c$ )     | 0.84   | 0.72    |
| Aspect Ratio ( $H/c$ )             | 1.09   | 2.05    |
| Trailing Edge to Throat Area Ratio | 0.08   | 0.03    |

Table 5 Important geometric factors relating to the second turbine stage geometry to be investigated.

Figure 4-6 shows the normalised total to static efficiency at the low-speed condition retrieved using the chosen loss models compared to MULTALL data at the non-dimensional speed  $593 \text{ rpm}/\sqrt{K}$ . It is clear to see that the Kacker and Okapuu method shows good correlation to the MULTALL data, with the Craig and Cox and AMDC efficiency characteristics showing optimistic efficiency characteristics compared to MULTALL. The Denton efficiency characteristic however appears to underestimate the loss coefficients resulting in an overestimated efficiency characteristic.

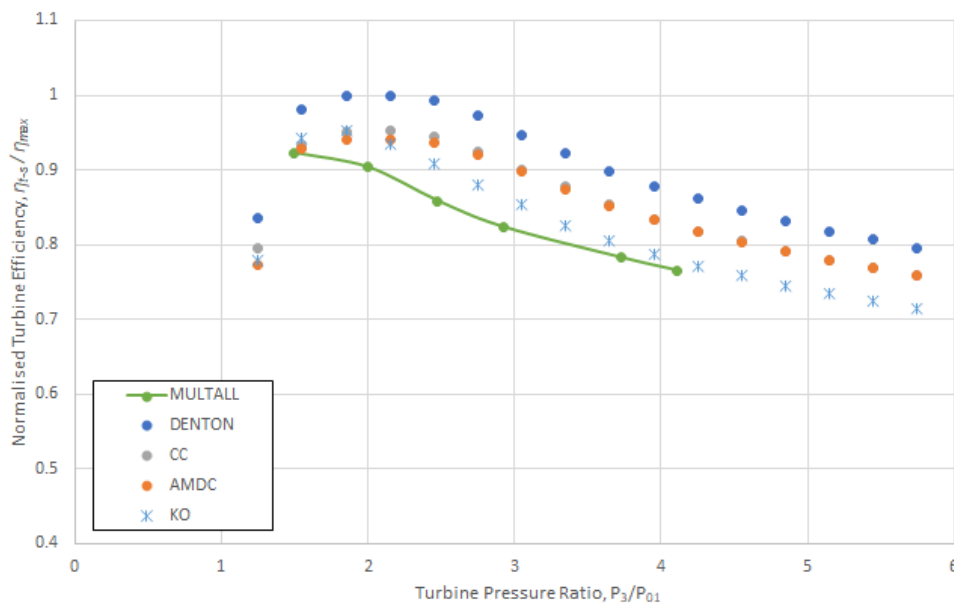


Fig. 4-6 Normalised Efficiency curves predicted for Geometry 1 at a non-dimensional speed of  $\frac{N}{\sqrt{T_{01}}} = 593 \text{ rpm}/\sqrt{K}$ .

As anticipated observing Figure 4-7 and Figure 4-8 it is clear that the Denton loss mechanism predicts the lowest losses which results in the highest efficiency. Also, as anticipated the stator loss coefficient is reasonably constant for all the loss mechanisms.

Looking at the loss coefficients in more detail it appears the profile losses in the Denton method for the stator and the turbine are grossly under predicted compared to the other loss mechanisms at this rotor speed.

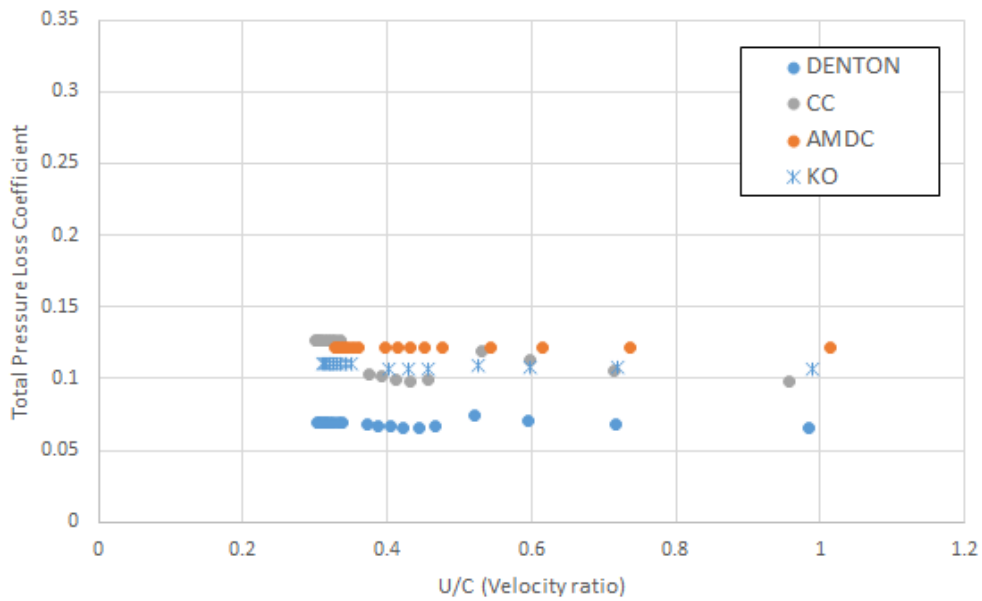


Fig. 4-7 Stator total loss coefficient  $\frac{N}{\sqrt{T_{01}}} = 593 \text{ rpm}/\sqrt{K}$  geometry 1.

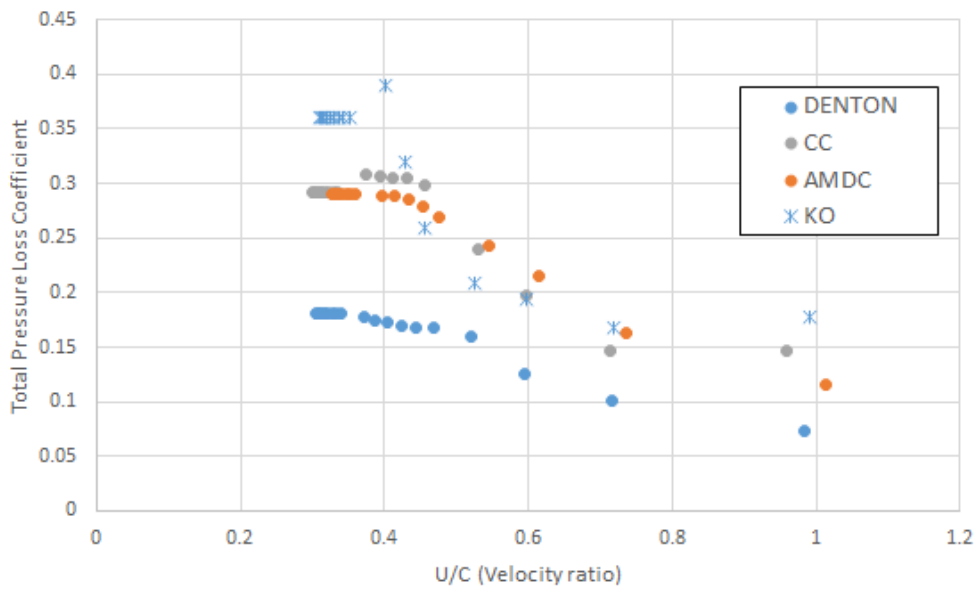


Fig. 4-8 Turbine total loss coefficient  $\frac{N}{\sqrt{T_{01}}} = 593 \text{ rpm}/\sqrt{K}$  geometry 1.

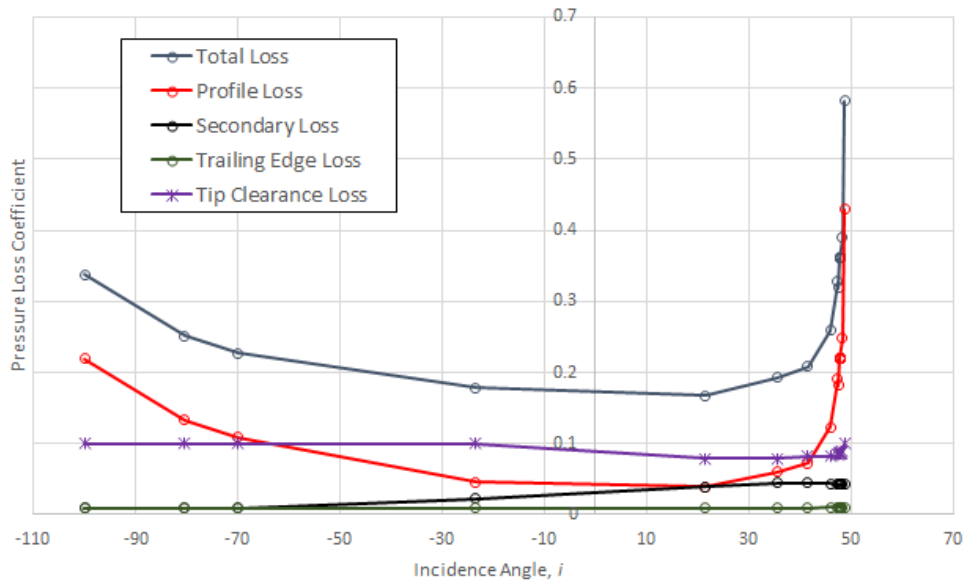


Fig. 4-9 Breakdown of turbine losses Kacker and Okapuu  $\frac{N}{\sqrt{T_{01}}} = 593 \text{ rpm}/\sqrt{K}$  geometry 1.

Figure 4-9 shows a breakdown of the losses for the Kacker and Okapuu loss model in the turbine plotted against blade incidence. Profile loss is lowest close to zero incidence, as incidence loss deviates from zero profile loss will increase. This is due to the correlation in the loss mechanism used to correct for off-design conditions. The off-design correlation for varying incidence in the Kacker and Okapuu method is taken from the Ainley and Mathieson method and is based on the ratio of incidence and stalling incidence. The stalling incidence is based on pitch to chord ratio and the ratio of blade inlet and outlet flow angles. The high incidence angle and large absolute ratio of blade inlet and outlet flow angle indicates possible separation of the flow on the blade surfaces and results in a small stalling incidence producing high profile losses at off-design conditions. The Kacker and Okapuu profile loss is lower compared to the original Ainley and Mathieson loss due to the application of a factor reducing the profile loss by a third.

As already outlined secondary losses arise as a result of the boundary layers on the blade endwalls interacting with the main flow stream. Secondary losses also increase as incidence rises, in the Kacker and Okapuu mechanism secondary loss is mainly influenced by blade turning defined by the inlet and outlet flow angles, as incidence rises the difference between the inlet and outlet flow angles increases implying high turning of the flow in the blade passage and high blade loading. A subsonic Mach number correction factor is also included in the Kacker and Okapuu secondary loss term to account for compressibility which impacts the acceleration of flow next to the endwalls, the Mach number correction factor is based on outlet Mach number and the ratio of inlet and outlet Mach number. This would explain why the secondary loss reduces slightly at high incidence, as the turbine is operating with a negative degree of reaction under choke conditions where flow is decelerating through the turbine which decreases the Mach number correction factor reducing the secondary losses.

The tip clearance losses are mainly a function of the tip clearance and blade loading. For unshrouded turbines the tip clearance losses are calculated iteratively using an efficiency debit which is

subtracted from the total-to-total efficiency as suggested by Kacker and Okapuu. Fig. 4-9 shows the trailing edge losses at this low-speed condition are very minimal.

It can be seen the total loss increases more severely at positive incidence due to the increase in profile loss.

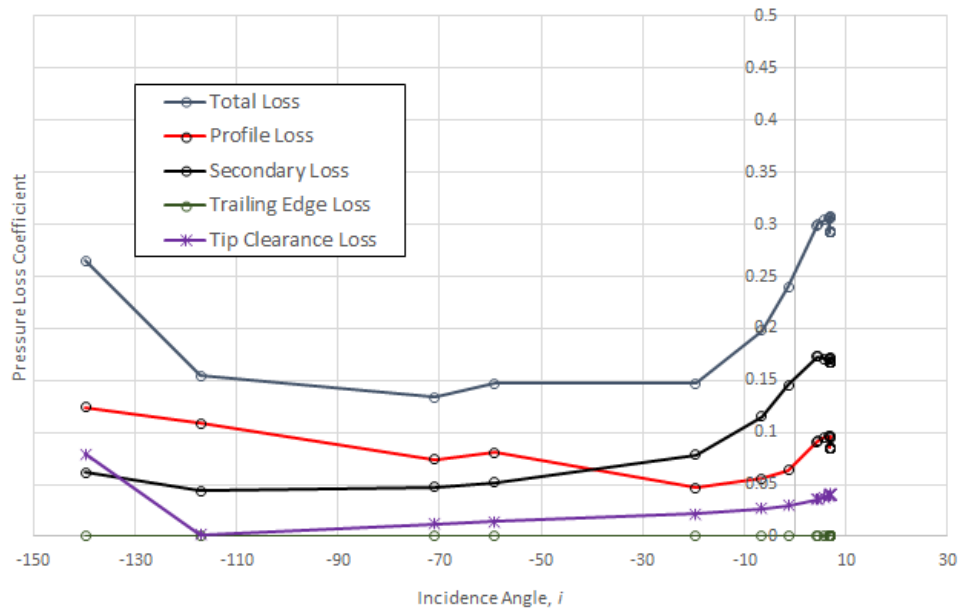


Fig. 4-10 Breakdown of stator losses Craig and Cox  $\frac{N}{\sqrt{T_{01}}} = 593 \text{ rpm}/\sqrt{K}$  geometry 1.

A breakdown of the turbine losses calculated in the Craig and Cox method are shown in Fig. 4-10. The basic profile loss is derived from the pitch to backbone length, contraction ratio and lift parameter which are a function of the inlet and outlet flow angle. The profile loss will increase at the off-design points where incidence angle and stalling incidence angle deviate from the optimum values. Craig and Cox provide a correlation based on an incidence ratio where negative stalling incidence and minimum loss incidence are correlated independently of positive stalling incidence. The incidence correlations are based on blade inlet angle, outlet angle, ratio of pitch to backbone length and the contraction ratio describing the blade passage. If the difference in blade inlet and outlet angle is large, the ratio of pitch to backbone length is large and contraction ratio is low the flow passing through the blade passage will increase causing flow separation at the blade surfaces leading to increased off-design profile losses.

For this speed condition the Craig and Cox model predicts the secondary losses are higher than the profile losses at high incidences. Craig and Cox use a blade loading parameter, Reynolds number factor and a basic secondary loss factor to predict secondary losses. The basic secondary loss factor is a function of the relative mean velocity and lift parameter. Therefore, a high lift parameter, mean velocity and aspect ratio means increased losses at high incidences. As incidence rises the difference between the inlet and outlet flow angles increases implying high turning of the flow in blade passage and high blade loading which lead to high losses.

The tip clearance losses for unshrouded blades in the Craig and Cox model is taken from the Ainley and Mathieson method as recommended by the authors. As such the tip clearance loss is a function

of the tip clearance and blade loading, therefore as the difference between blade inlet and outlet flow angles increases blade loading will increase which will give rise to tip clearance losses. Again, the trailing edge losses are minimal at this low-speed condition.

Comparing the total turbine loss coefficient to the other methods shows the Craig and Cox model predicts similar losses to Kacker and Okapuu and Ainley and Mathieson.

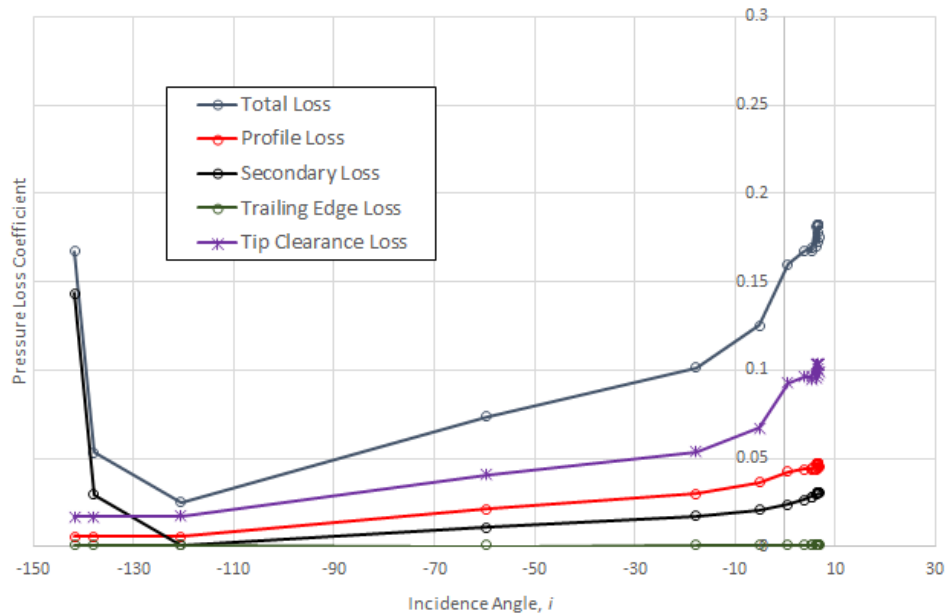


Fig. 4-11 Breakdown of turbine losses Denton  $\frac{N}{\sqrt{T_{01}}} = 593 \text{ rpm}/\sqrt{K}$  geometry 1.

On analysing the Denton losses in greater detail, it is apparent they are a lot lower when compared to the other loss models at the low-speed condition. Figure 4-11 shows the tip clearance loss is the most significant and is higher than both the profile and secondary losses. Checking the inlet and outlet flow angles show that the inlet flow angle is outside the range of applicability for the Denton profile loss correlation, which ranges from -60 to 60. Thus, the inlet flow angle has been limited to the corresponding maximum value for the purposes of profile loss prediction in the loss mechanism.

The tip clearance loss provides one of the main sources of loss in a turbine. The difference in pressure between the blade pressure and suction surfaces dictates the magnitude of tip leakage flow for an unshrouded blade. The correlation employed by Denton assumes a tip gap of 1% of the blade height ratio, this seems to give comparable results compared to the other loss mechanisms.

Figure 4-12 shows the results at the design speed condition at a non-dimensional speed of  $989 \text{ rpm}/\sqrt{K}$ . Here the efficiency characteristics of the Kacker and Okapuu and AMDC show good correlation to the MULTALL data whereas the Craig and Cox data appears to correlate at low pressure ratios and diverge at higher pressure ratios, again the Denton loss mechanism appears to overestimate the efficiency. It must be noted in this instance the efficiency prediction using Denton's loss mechanism is substantially closer to the MULTALL reference when compared with the low-speed data and the correlation at low turbine pressure ratios is improved.

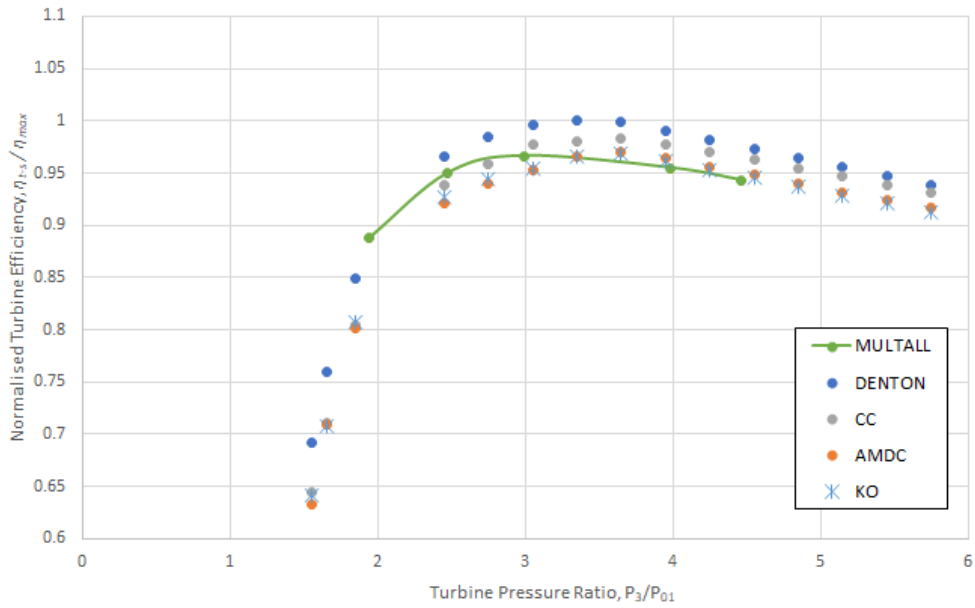


Fig 4-12. Normalised Efficiency curves predicted for Geometry 1 at a non-dimensional speed of  $\frac{N}{\sqrt{T_{01}}} = 989 \text{ rpm}/\sqrt{K}$ .

A similar trend may be identified in the design speed data as for the low-speed data when analysing the loss coefficients. Plotting the stator and rotor loss coefficients separately enables the identification of the underestimated Denton loss coefficients

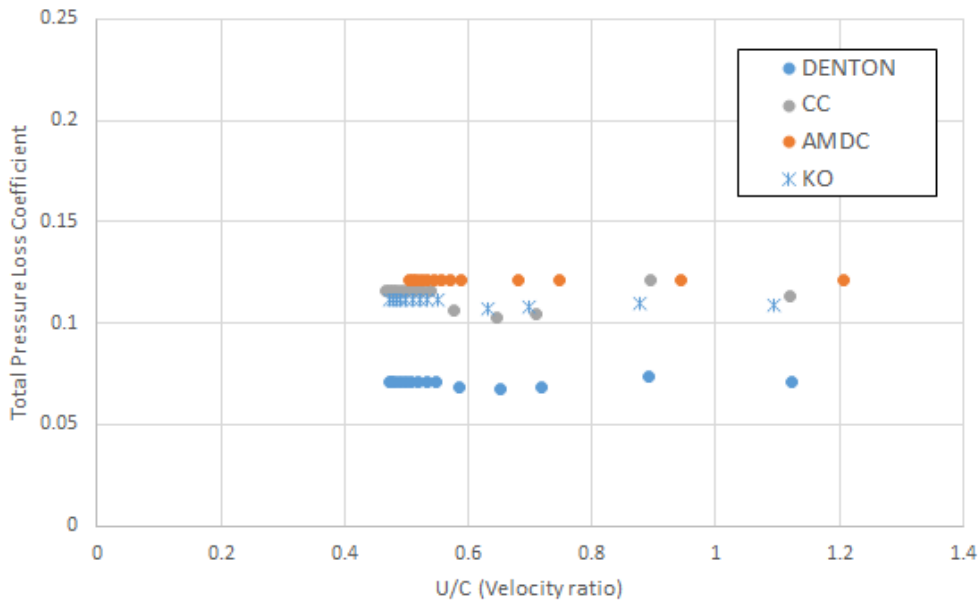


Fig. 4-13 Stator total loss coefficient  $\frac{N}{\sqrt{T_{01}}} = 989 \text{ rpm}/\sqrt{K}$  geometry 1.

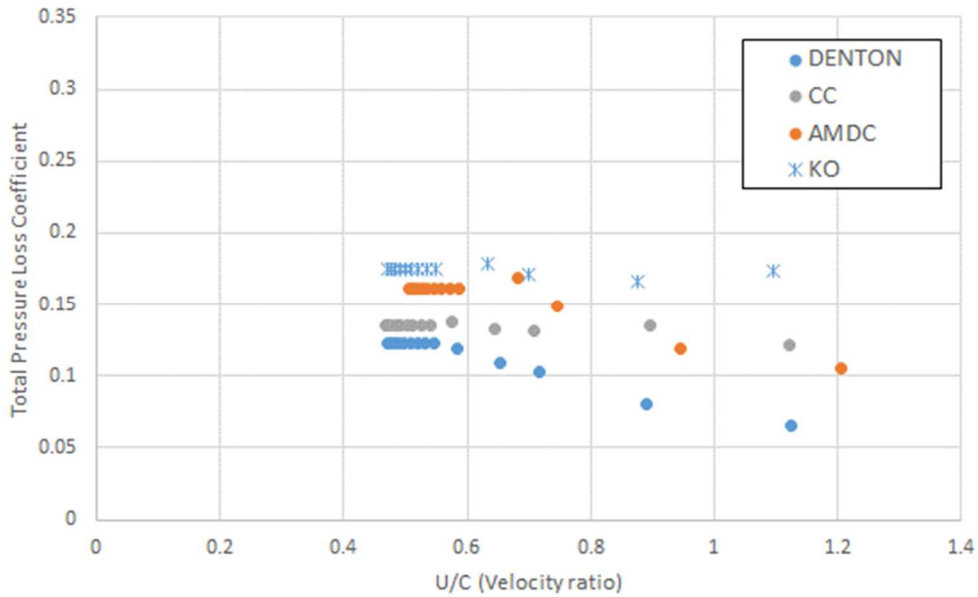


Fig. 4-14 Turbine total loss coefficient  $\frac{N}{\sqrt{T_{01}}} = 989 \text{ rpm}/\sqrt{K}$  geometry 1.

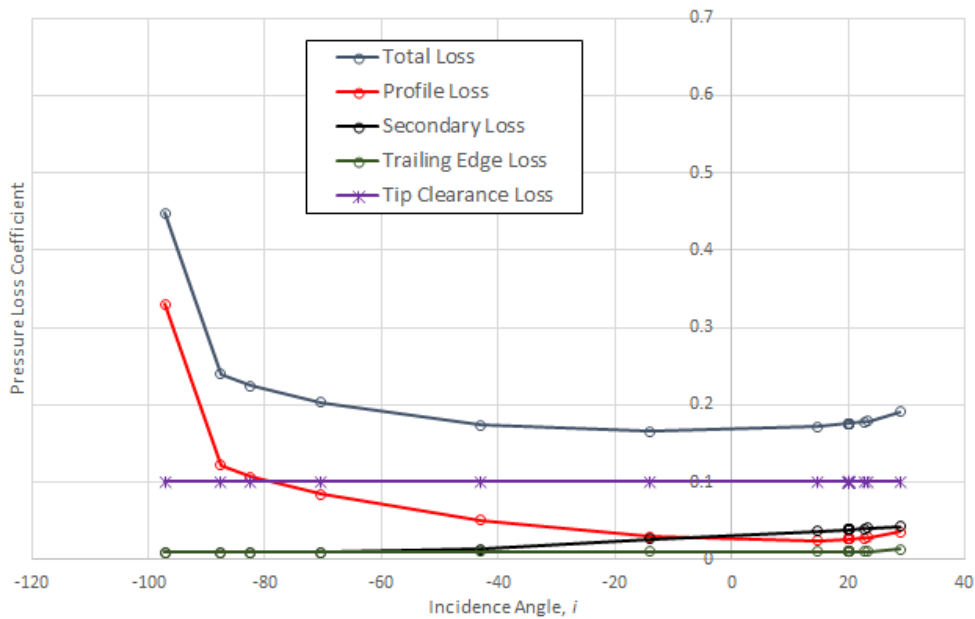


Fig. 4-15 Breakdown of turbine losses Kacker and Okapuu  $\frac{N}{\sqrt{T_{01}}} = 989 \text{ rpm}/\sqrt{K}$  geometry 1.

Figure 4-15 shows a breakdown of the turbine losses from the Kacker and Okapuu loss model. It is noticeable that the levels of loss have reduced and now the dominating loss in the rotor is the tip clearance loss. The profile loss has a similar trend to the loss from the low-speed condition in that the minimum loss occurs around zero incidence. As rotor speed increases the incidence angle reduces, the absolute ratio of blade inlet and outlet flow angle also reduces which lessens the possibility of flow separation on the blade surfaces. The variation in loss with incidence is also not as pronounced as the low-speed condition which is another result of the blade incidence reducing.



The secondary losses have also reduced in magnitude and increase steadily towards higher incidences as shown at the low-speed condition.

From Figure 4-15 it is noticeable the tip clearance loss is constant; this is due to the efficiency debit iteration reaching its upper limit. Typically for the efficiency penalty due to tip clearance losses Napier would expect no more than approximately 1.5% this roughly corresponds to a tip clearance pressure loss of approximately 0.1. Concerning the trailing edge loss predictions have increased slightly compared to the low-speed condition.

The total loss has reduced compared to the low-speed condition as a result of the profile and secondary losses decreasing.

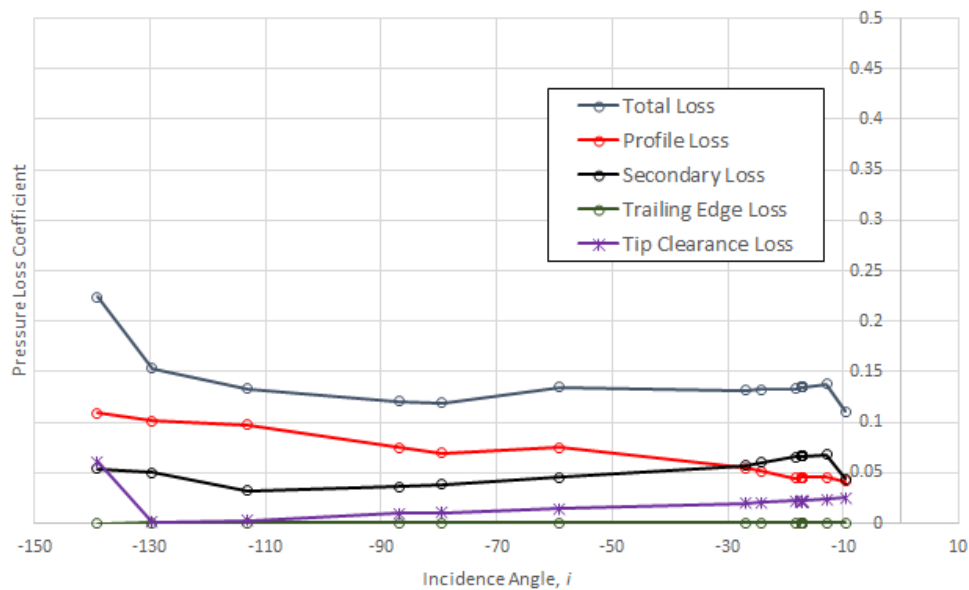


Fig. 4-16 Breakdown of turbine losses Craig and Cox  $\frac{N}{\sqrt{T_{01}}} = 989 \text{ rpm}/\sqrt{K}$  geometry 1.

A summary of the losses predicted by the Craig and Cox model are shown in Figure 4-16. The profile losses have decreased compared to the low-speed condition due to the reduction in incidence angle. The profile losses for the design speed condition resemble part of the trend from the low-speed condition with the indicated lowest profile loss occurring at a higher incidence angle thus the profile losses are still reducing above zero incidence.

The secondary losses have reduced compared to the low-speed condition. As previously discussed, this is as a result of the increase in rotor speed reducing the blade inlet and outlet angle ratio resulting in less flow turning in the blade passage and lower blade loading.

The tip clearance loss steadily increases towards higher incidence angles as it is mainly a function of tip clearance and blade load. As incidence increases, the inlet to outlet flow angle ratio increases which results in higher tip clearance loss. Regarding trailing edge loss there is a slight increase compared to the low-speed condition.

The total loss has reduced for a given mass flow compared to the low-speed condition resulting in a higher efficiency characteristic.

The losses computed using the Denton loss prediction method are shown in Figure 4-17. As for the lower speed conditions the losses predicted using Denton’s methodology are low by comparison to the other methods.

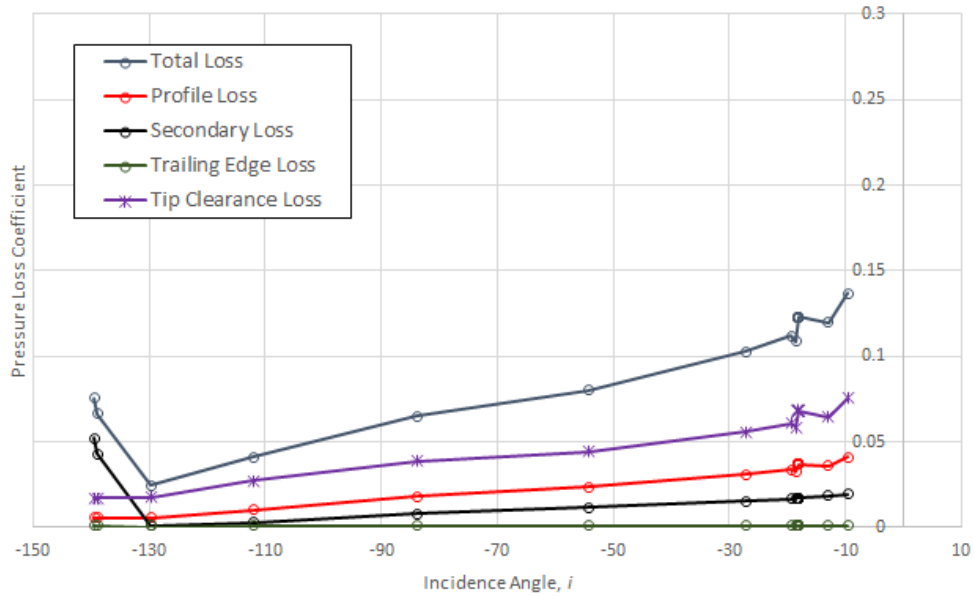


Fig. 4-17 Breakdown of turbine losses Denton  $\frac{N}{\sqrt{T_{01}}} = 989 \text{ rpm}/\sqrt{K}$  geometry 1.

Figure 4-18 shows the final high-speed condition for geometry 1 at a non-dimensional speed of  $1285 \text{ rpm}/\sqrt{K}$ . Kacker and Okapuu efficiency characteristic seems to show the best correlation to MULTALL data. With a similar trend seen for the Denton and Craig and Cox efficiency characteristics as previous turbine speeds.

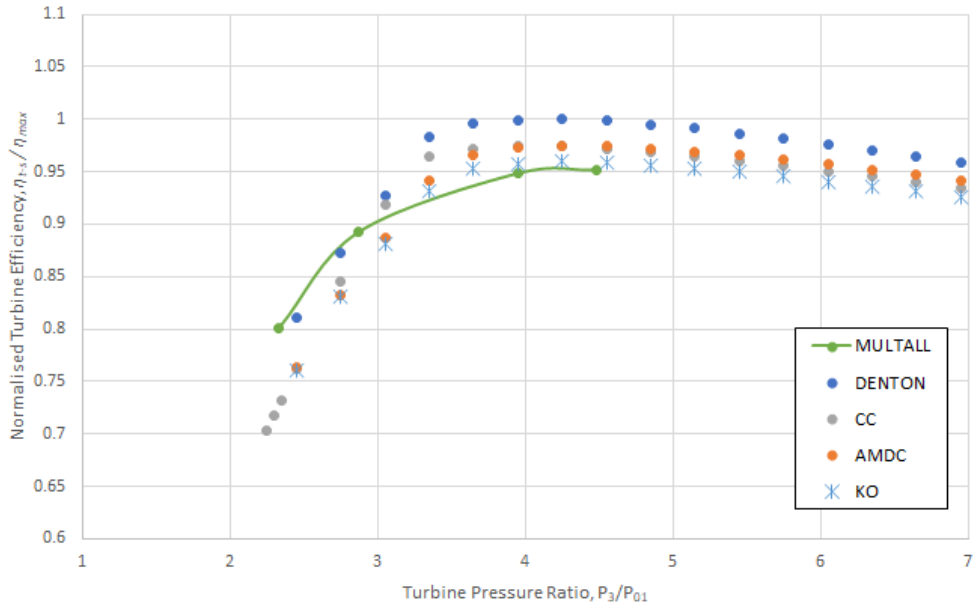


Fig. 4-18. Normalised Efficiency curves predicted for Geometry 1 at a non-dimensional speed of  $\frac{N}{\sqrt{T_{01}}} = 1285 \text{ rpm}/\sqrt{K}$ .

Plotting the loss coefficients for the stator and rotor reveals a similar state to the previous speed conditions. Similarly, to the lower and design speed conditions Denton predicts the lowest total loss coefficients.

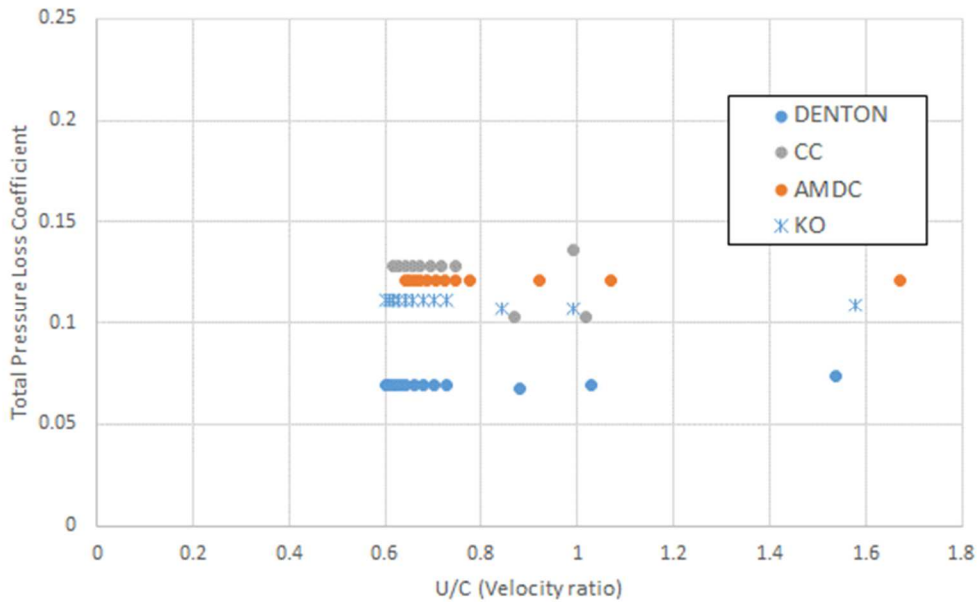


Fig. 4-19 Stator total loss coefficient  $\frac{N}{\sqrt{T_{01}}} = 1285 \text{ rpm}/\sqrt{K}$  geometry 1.

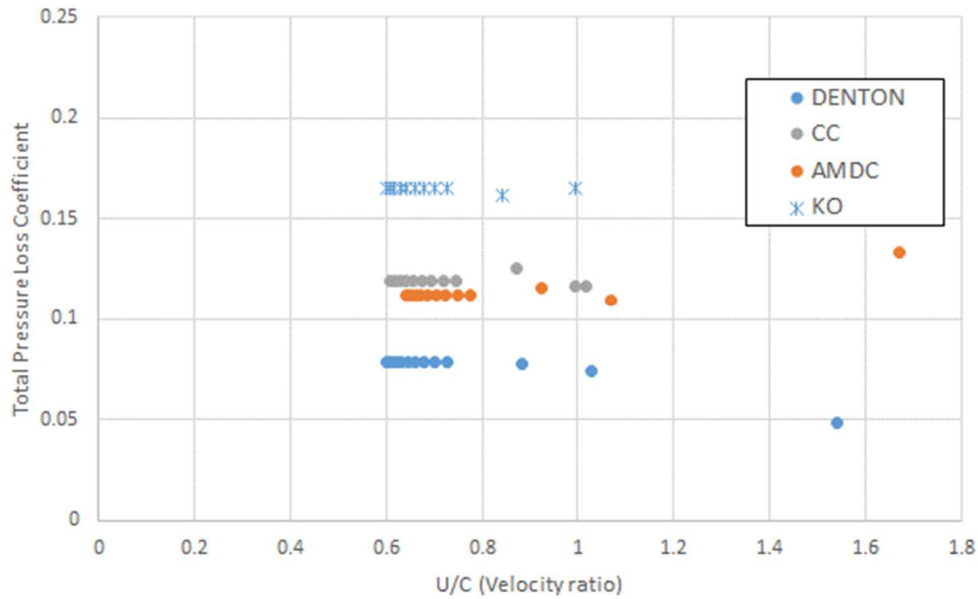


Fig. 4-20 Turbine total loss coefficient  $\frac{N}{\sqrt{T_{01}}} = 1285 \text{ rpm}/\sqrt{K}$  geometry 1.

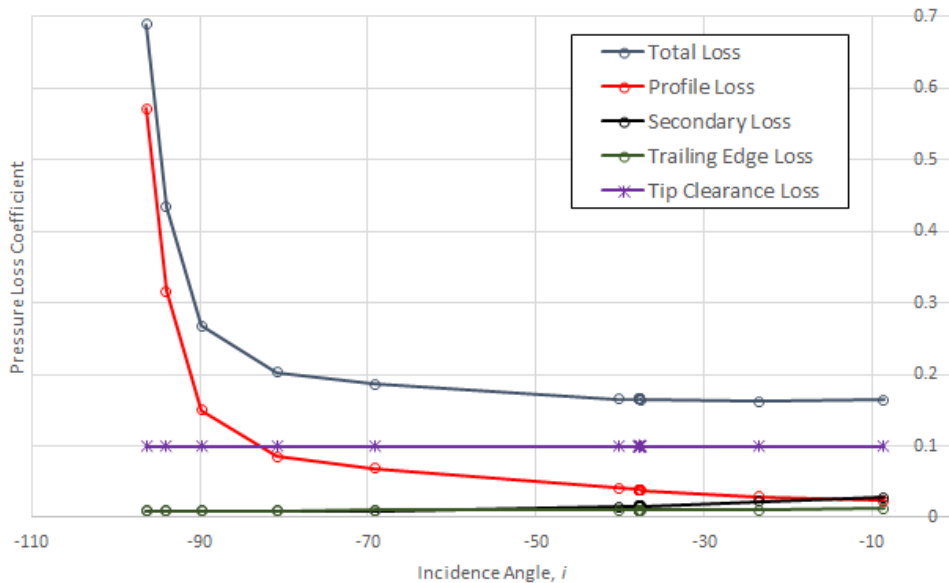


Fig. 4-21 Breakdown of turbine losses Kacker and Okapuu  $\frac{N}{\sqrt{T_{01}}} = 1285 \text{ rpm}/\sqrt{K}$  geometry 1.

Looking at the losses predicted by Kacker and Okapuu in more detail shows a similar trend to the design speed condition. Profile losses show the same trend as the design speed condition with losses beginning to increase at very low incidence angles due to the off-design incidence correction discussed previously. Blade inlet angle reduces, minimising blade incidence angles thus lowering the profile and secondary loss coefficients. Tip clearance remains at the maximum specified value of 0.1 and trailing edge losses increase slightly.

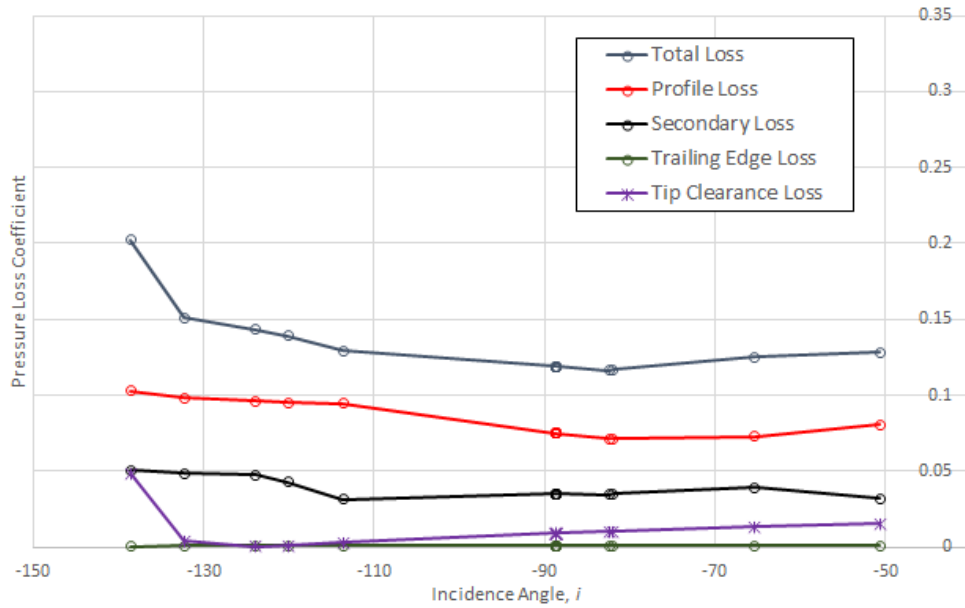


Fig. 4-22 Breakdown of turbine losses Craig and Cox  $\frac{N}{\sqrt{T_{01}}} = 1285 \text{ rpm}/\sqrt{K}$  geometry 1.

Viewing Figure 4-22 showing the turbine losses predicted by the Craig and Cox method for the high-speed condition it is apparent the losses seem to be following the correct trends. Profile loss is increasing as it deviates from the optimum incidence range, secondary loss has reduced again due to the increase in turbine speed reducing the blade inlet and outlet angle ratio and blade loading. Tip clearance has reduced slightly due the reduction in blade loading but increases at low incidences. Trailing edge loss has remained roughly constant compared to the lower and design speed conditions. Total loss has increased as the profile loss has begun to increase.

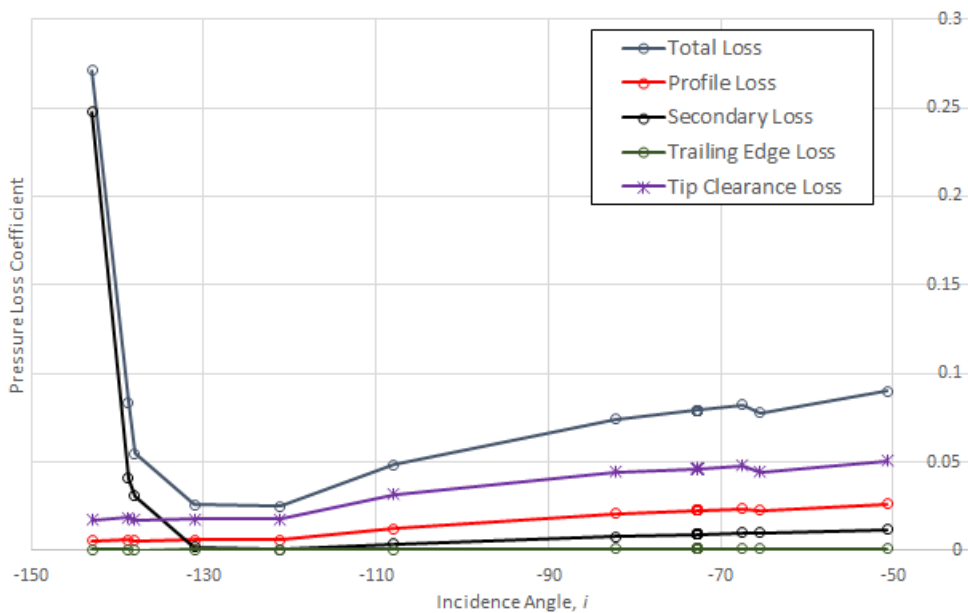


Fig. 4-23 Breakdown of rotor losses Denton  $\frac{N}{\sqrt{T_{01}}} = 1285 \text{ rpm}/\sqrt{K}$  geometry 1.

The losses calculated by the Denton loss model for the high-speed condition are shown in Figure 4-23. Profile and secondary losses have reduced compared to the previous speed condition as expected. Tip clearance losses have also reduced as the pressure gradient between the pressure and suction surfaces reduces reducing the leakage flow over the turbine blade. Trailing edge loss has also remained roughly constant compared to the design speed condition.

### 4.5.3 Geometry 2

The second turbine stage to be analysed is also from a productionised turbocharger and has a longer turbine blade compared to the first geometry investigated. The table below shows the geometric ratios of the second turbine stage to be investigated.

| Geometric Ratio                    | Stator | Turbine |
|------------------------------------|--------|---------|
| Pitch to Chord Ratio ( $s/c$ )     | 0.73   | 0.78    |
| Aspect Ratio ( $H/c$ )             | 0.74   | 2.38    |
| Trailing Edge to Throat Area Ratio | 0.10   | 0.04    |

Table 6 Important geometric factors relating to the second turbine stage geometry to be investigated.

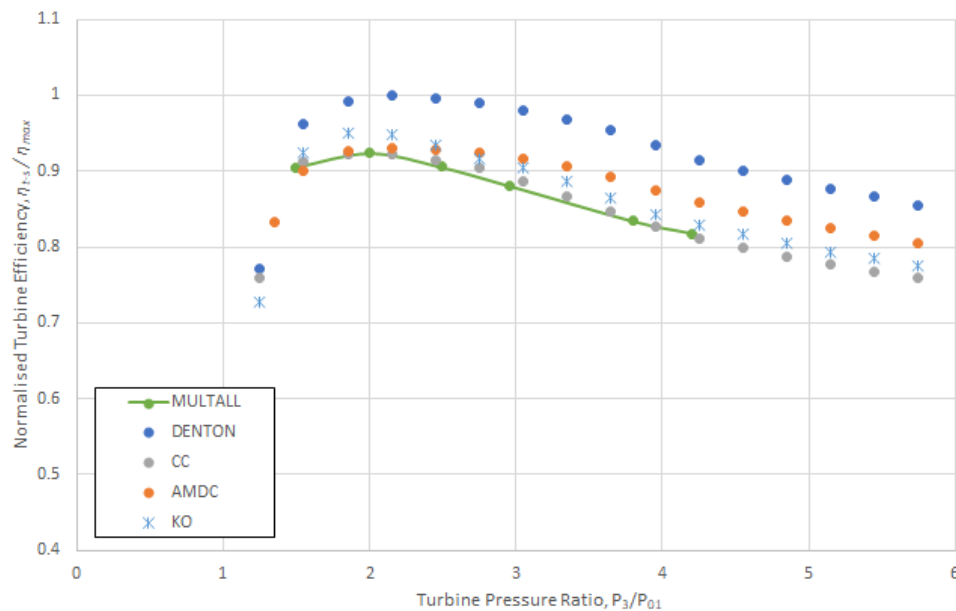


Fig. 4-24 Normalised Efficiency curves predicted for Geometry 2 at a non-dimensional speed of  $\frac{N}{\sqrt{T_{01}}} = 635 \text{ rpm}/\sqrt{K}$ .

The efficiency characteristics predicted by the selected loss models are shown in Fig. 4-24 for the second geometry at the low-speed condition. Kacker and Okapuu and AMDC seem to show good correlation to the MULTALL data while Craig and Cox displays very good correlation and again Denton overestimates the efficiency.

Plotting the pressure loss coefficients of the stator and turbine enables the detection of the low loss coefficients for both the stator and rotor produced by the Denton Method.

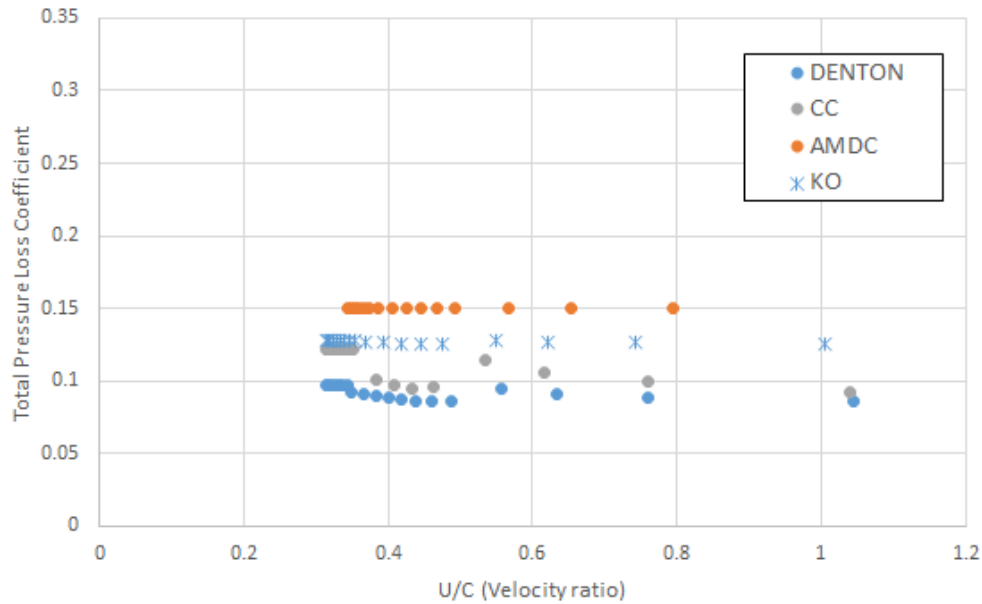


Fig. 4-25 Stator total loss coefficient  $\frac{N}{\sqrt{T_{01}}} = 635 \text{ rpm}/\sqrt{K}$  geometry 2.

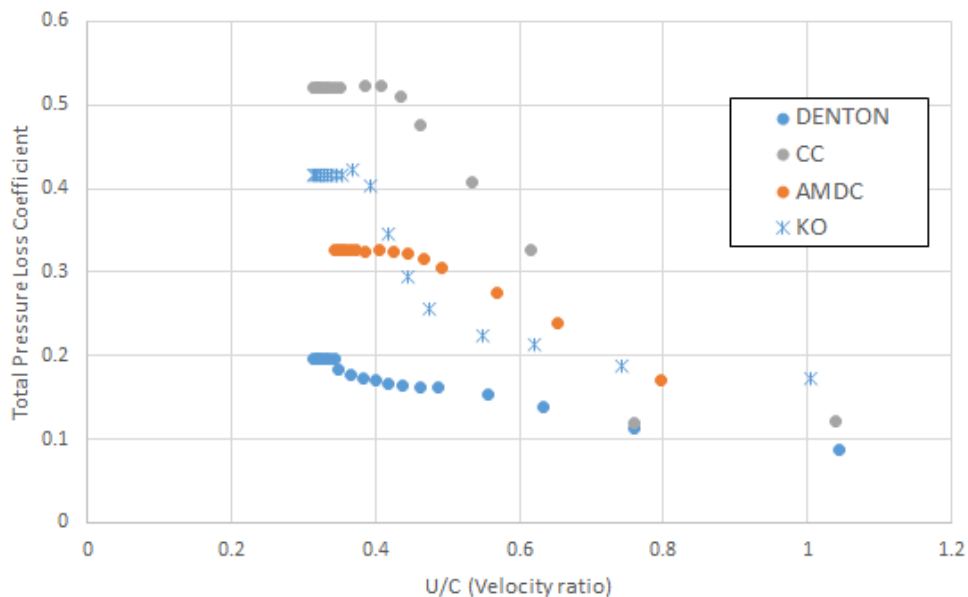


Fig 4-26 Turbine total loss coefficient  $\frac{N}{\sqrt{T_{01}}} = 635 \text{ rpm}/\sqrt{K}$  geometry 2.

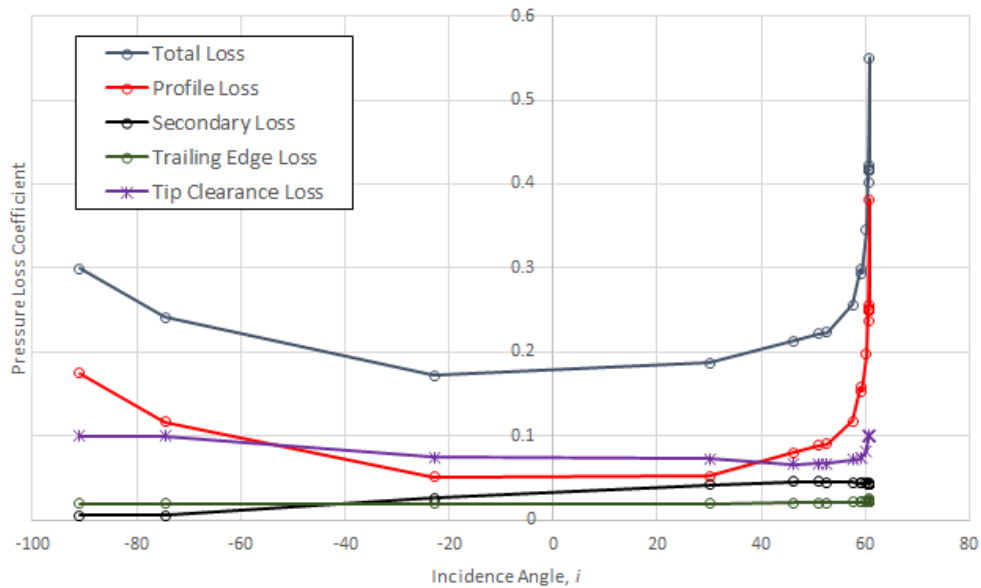


Fig. 4-27 Breakdown of turbine losses Kacker and Okapuu  $\frac{N}{\sqrt{T_{01}}} = 635 \text{ rpm}/\sqrt{K}$  geometry 2.

Analysing the loss coefficients produced by the Kacker and Okapuu method in greater detail for the low-speed condition shows the profile losses are the main contributing factor at high incidences as expected. As incidence increases the turbine operates away from the optimum incidence and the off-design correction factor increases. Profile losses are not affected by the increase in aspect ratio as this parameter is not included in the profile loss correlation.

The secondary losses appear to have reduced compared to the low-speed condition of the first geometry. This is caused by the increase in blade height which reduces the possibility of interaction between the passage vortices on the endwalls reducing losses. Secondary losses also reduce slightly at high incidences this is due to the Mach number correction factor and the turbine operating with negative reaction while choking as seen with the first geometry.

Tip leakage losses have also reduced slightly compared to the findings of the first geometry analysis. This is due to the increase in aspect ratio and the efficiency debit in the Kacker and Okapuu method reducing due to the increase in blade height. There is also an increase in trailing edge loss compared to the first geometry due to increase in the trailing edge thickness to throat opening ratio with the second geometry.

There is a reduction in the total loss compared to the first geometry as anticipated which is due to the increase in aspect ratio.



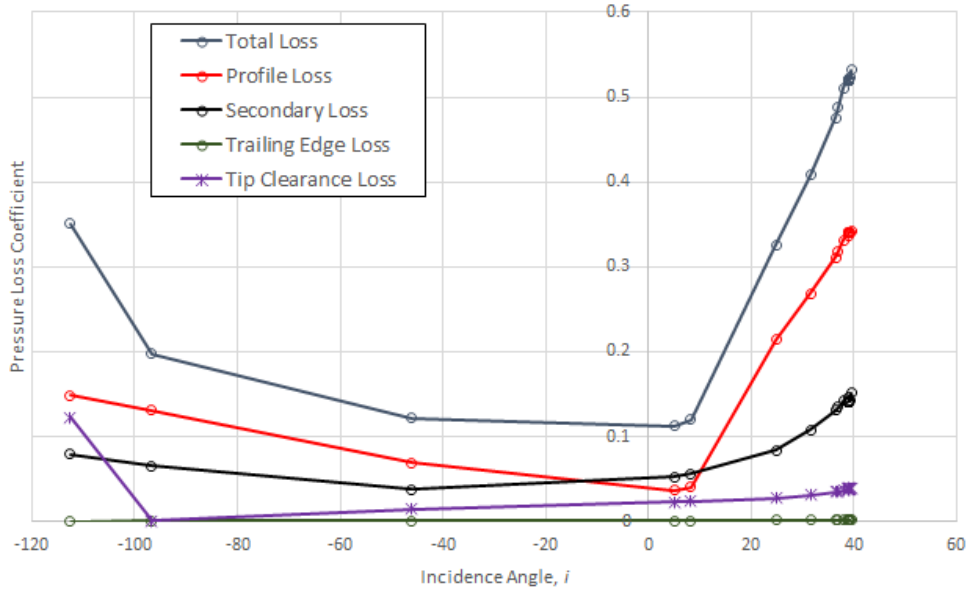


Fig. 4-28 Breakdown of turbine losses Craig and Cox  $\frac{N}{\sqrt{T_{01}}} = 635 \text{ rpm}/\sqrt{K}$  geometry 2.

The breakdown of losses shown in Figure 4-28 were calculated using the Craig and Cox method. Similarly, to the first geometry investigated profile loss increases at high incidences due to off-design conditions. The incidence is also higher with the second geometry due to the reduction of the blade inlet angle by almost half. Secondary loss has reduced compared to the first geometry due to the increase in blade aspect ratio as seen with the Kacker and Okapuu secondary loss coefficient. Tip clearance losses have also reduced due to the increase in blade height. Trailing edge loss is still very low compared to the other loss coefficients and has reduced slightly compared to the first geometry. Total loss is higher than the first geometry at high incidences due to the sharp increase in profile losses at high incidences.

The losses shown in Figure 4-29 are formulated using the Denton loss model and show a similar trend to those retrieved while analysing the first geometry at the low-speed condition. Tip clearance loss is the highest loss while the profile and secondary losses are predicted low compared with the other loss methods which results in a low total loss coefficient. As theorised previously it is possible the adopted Denton profile loss correlation is not suited for turbocharger turbine operation at such a low speed. Concerning the secondary loss, it is also possible the factor of 0.375 is too severe for this operating condition.

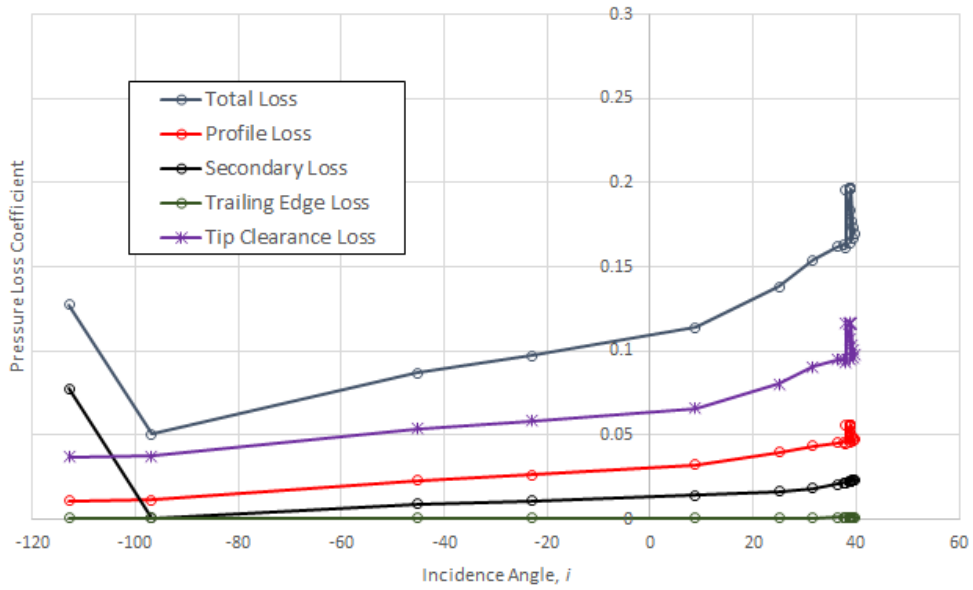


Fig. 4-29 Breakdown of turbine losses Denton  $\frac{N}{\sqrt{T_{01}}} = 635 \text{ rpm}/\sqrt{K}$  geometry 2.

Figure 4-30 shows the results retrieved at the design speed condition at a non-dimensional speed of  $1060 \text{ rpm}/\sqrt{K}$  for the second geometry. Kacker/Opkauu and AMDC show reasonable correlation to the MULTALL data. The Denton and Craig and Cox methods seem to correlate at mid turbine pressure ratios but are slightly higher at low and high turbine pressure ratios.

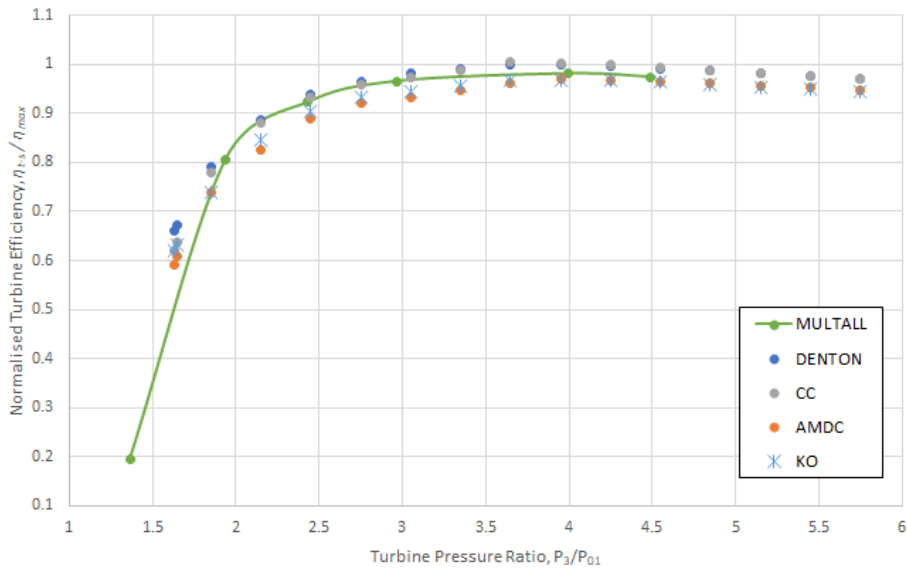


Fig. 4-30 Normalised Efficiency curves predicted for Geometry 2 at a non-dimensional speed of  $\frac{N}{\sqrt{T_{01}}} = 1060 \text{ rpm}/\sqrt{K}$ .

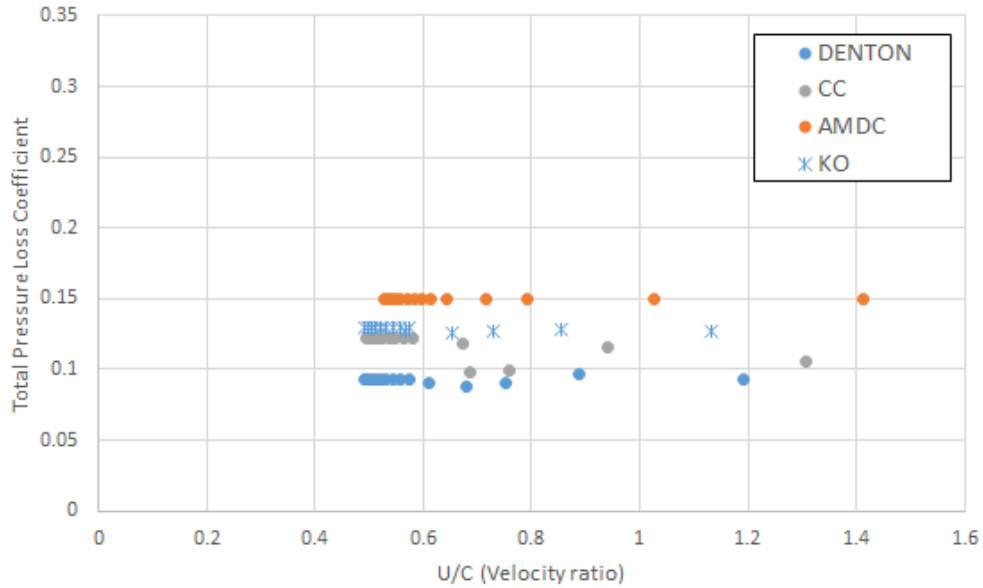


Fig. 4-31 Stator total loss coefficient  $\frac{N}{\sqrt{T_{01}}} = 1060 \text{ rpm}/\sqrt{K}$  geometry 2.

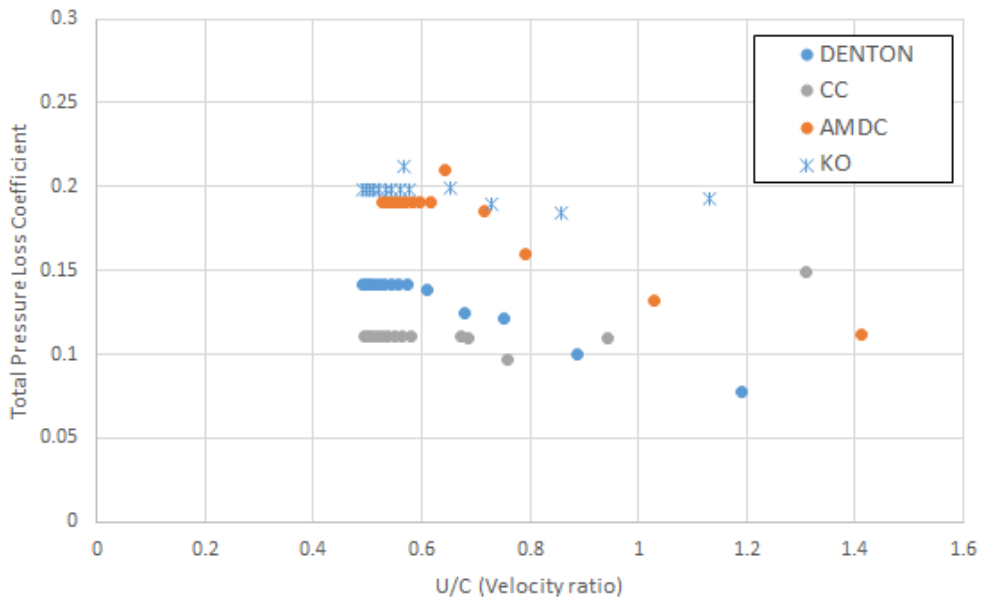


Fig. 4-32 Turbine total loss coefficient  $\frac{N}{\sqrt{T_{01}}} = 1060 \text{ rpm}/\sqrt{K}$  geometry 2.

The breakdown of losses shown in Figure 4-33 were formulated using the Kacker and Okapuu method at the design speed for geometry 2. They follow a similar trend to the losses obtained in the first investigation at a higher speed compared to the low-speed condition. As with the low-speed condition secondary losses have reduced slightly compared to the first investigation due to the increase in blade height. Tip clearance losses are limited to the maximum value stated previously. Trailing edge losses remain roughly constant. Total loss has reduced at a higher speed compared to the low-speed condition due to the profile and secondary losses reducing.

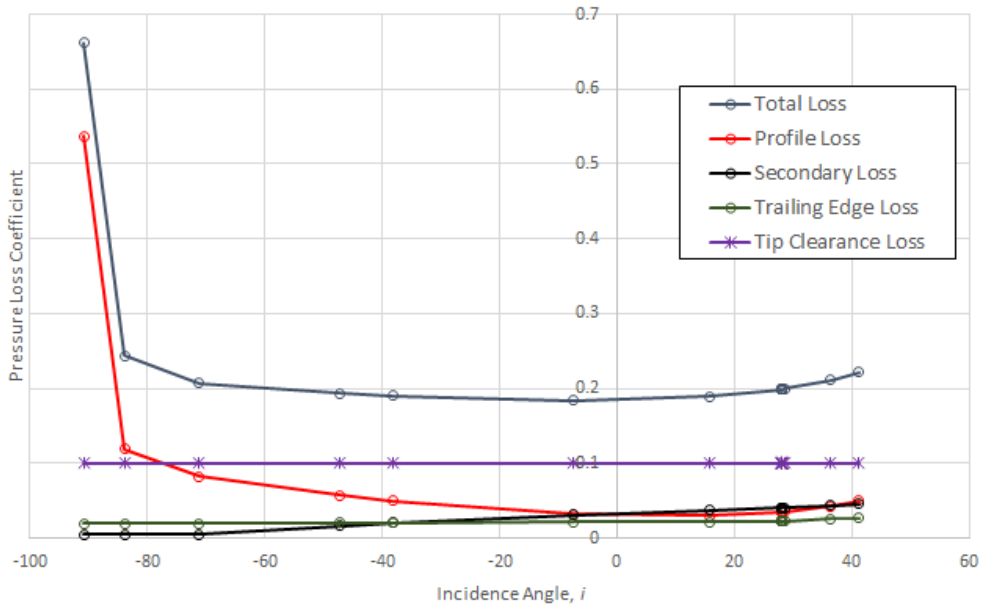


Fig. 4-33 Breakdown of turbine losses Kacker and Okapuu  $\frac{N}{\sqrt{T_{01}}} = 1060 \text{ rpm}/\sqrt{K}$  geometry 2.

Figure 4-34 shows the loss coefficients gained using the Craig and Cox loss model. The losses show a similar trend to the losses investigated with the first geometry. Profile loss has remained at a similar level compared to the first investigation and secondary losses have reduced slightly due to the increase in blade height. Tip clearance losses have reduced compared to the lower speed condition due to reduced blade loading. Trailing edge losses have remained roughly constant. Total loss has reduced compared to the low-speed condition due to the turbine operating around optimum conditions.

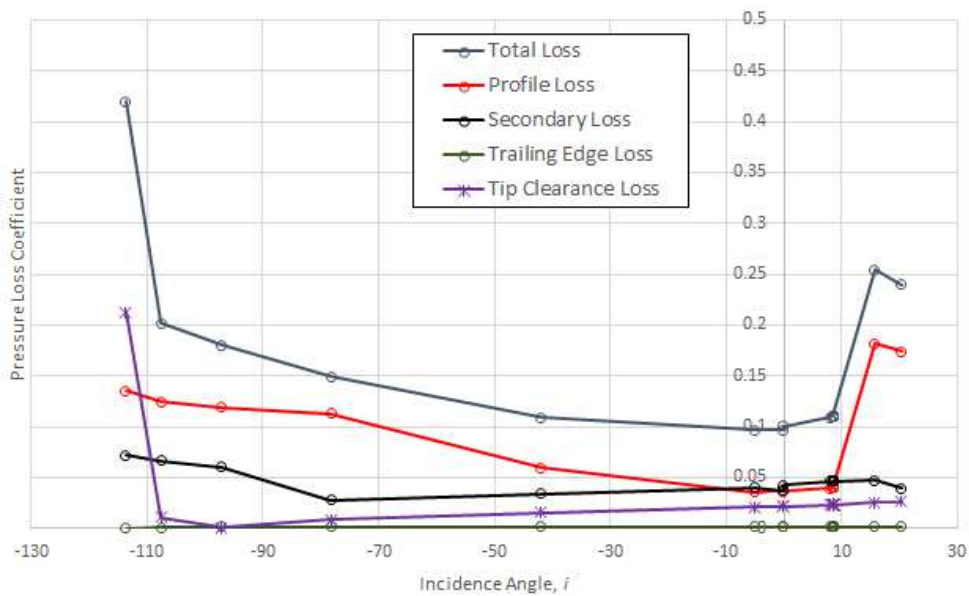


Fig. 4-34 Breakdown of turbine losses Craig and Cox  $\frac{N}{\sqrt{T_{01}}} = 1060 \text{ rpm}/\sqrt{K}$  geometry 2.

The losses shown in Figure 4-35 are taken from the Denton loss method and show similar behaviour to the losses predicted in the first investigation. Profile and secondary losses have reduced, tip clearance losses have also reduced, and trailing edge losses have remained roughly constant. Total loss has reduced as turbine operation nears the optimum operating range.

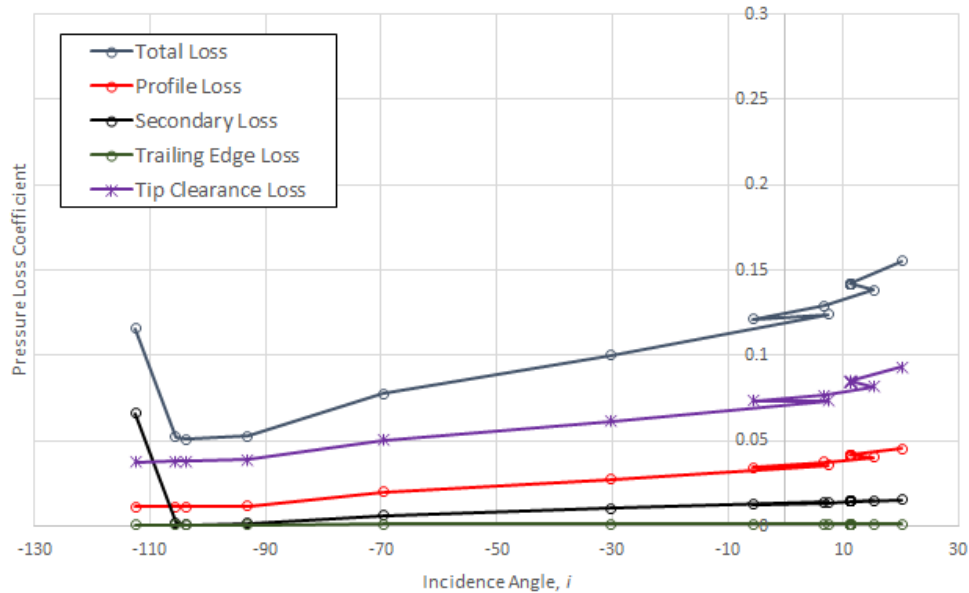


Fig. 4-35 Breakdown of turbine losses Denton  $\frac{N}{\sqrt{T_{01}}} = 1060 \text{ rpm}/\sqrt{K}$  geometry 2.

The final speed to be examined for the second geometry is the high-speed condition at a non-dimensional speed of  $1271 \text{ rpm}/\sqrt{K}$ , the results are shown in Figure 4-36. It can be seen the Kacker and Okapuu and AMDC loss methods predict an efficiency characteristic close to the MULTALL data throughout the turbine pressure ratio range, while Denton's predictions are close at low turbine pressure ratios but diverge at higher pressure ratios and the Craig and Cox predictions show very good correlation up to a turbine pressure ratio of 3 where at higher pressure ratios the efficiency deviates from the MULTALL data.

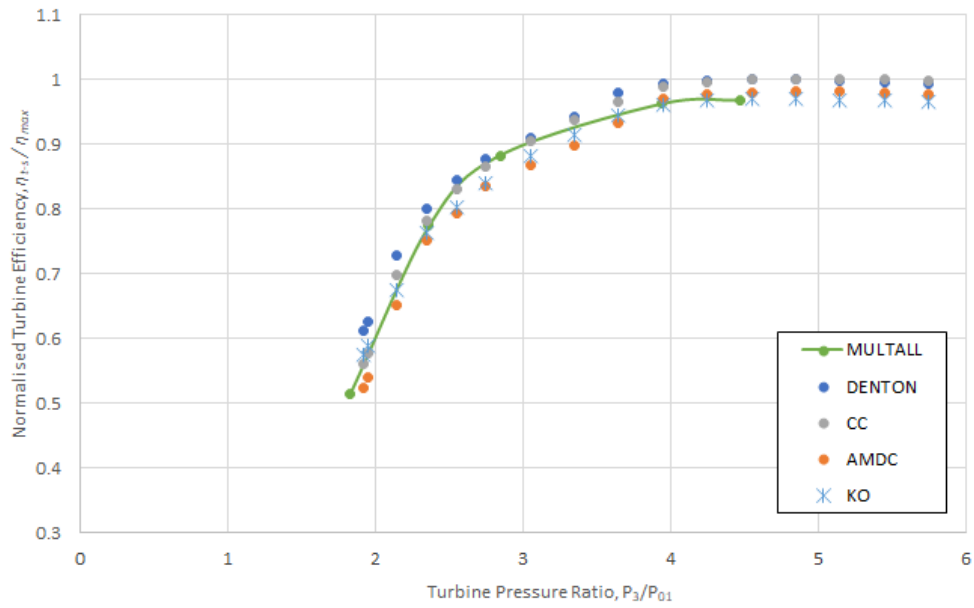


Fig. 4-36 Normalised Efficiency curves predicted for Geometry 2 at a non-dimensional speed of  $\frac{N}{\sqrt{T_{01}}} = 1271 \text{ rpm}/\sqrt{K}$ .

The stator and rotor total loss coefficients are shown in Figures 4-37 and 4-38.

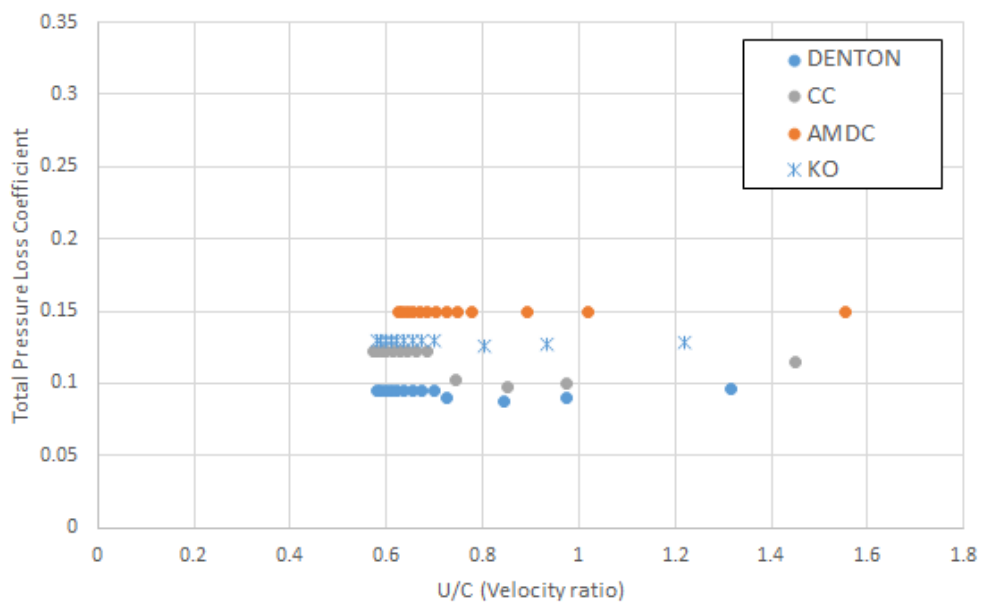


Fig. 4-37 Stator total loss coefficient  $\frac{N}{\sqrt{T_{01}}} = 1271 \text{ rpm}/\sqrt{K}$  geometry 2.

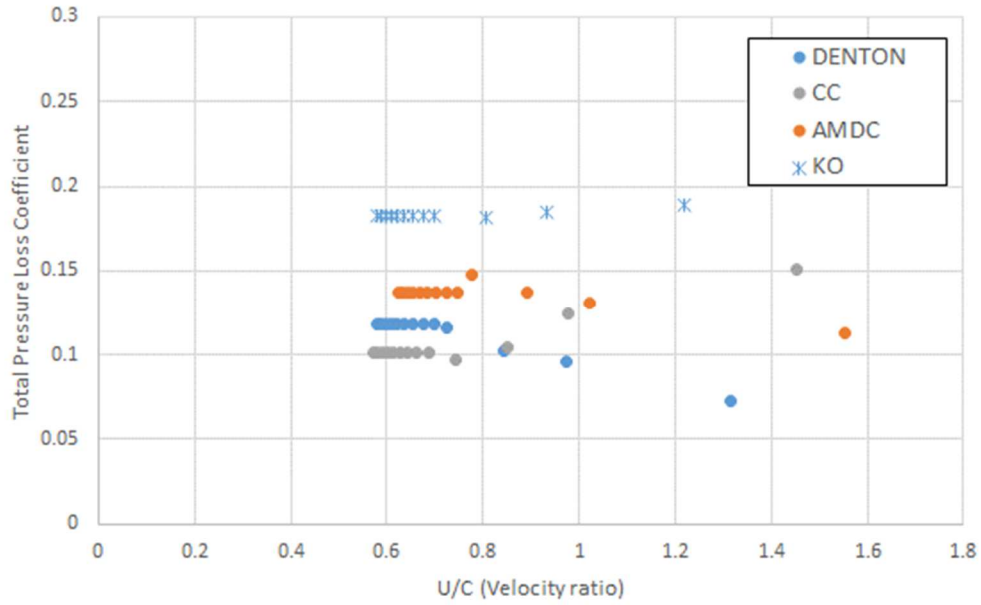


Fig. 4-38 Turbine total loss coefficient  $\frac{N}{\sqrt{T_{01}}} = 1271 \text{ rpm}/\sqrt{K}$  geometry 2.

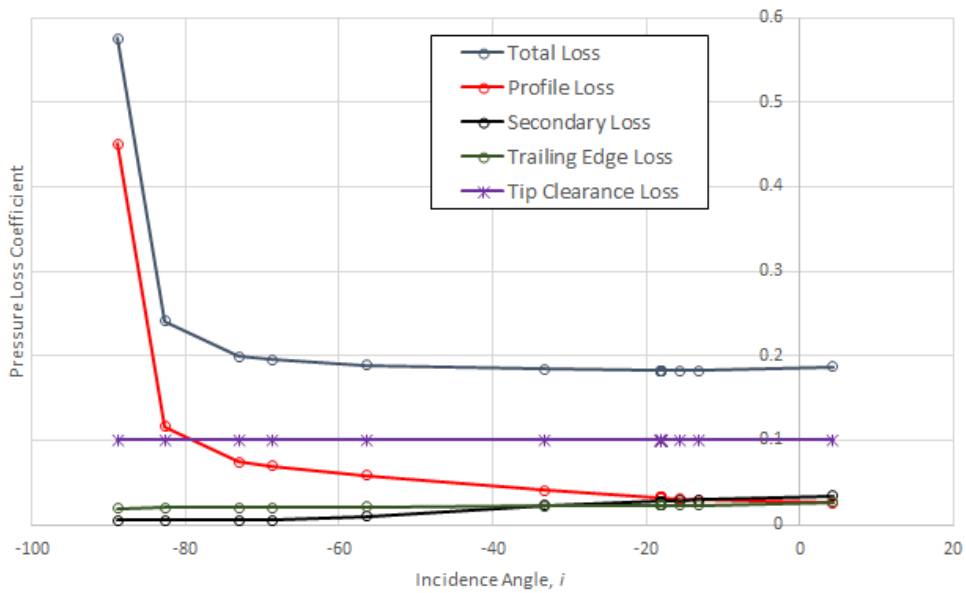


Fig. 4-39 Breakdown of turbine losses Kacker and Okapuu  $\frac{N}{\sqrt{T_{01}}} = 1271 \text{ rpm}/\sqrt{K}$  geometry 2.

The Kacker and Okapuu losses are shown in Figure 4-39 for the high-speed condition of geometry 2. The results follow a similar trend to the data analysed in the first investigation at the high-speed condition.

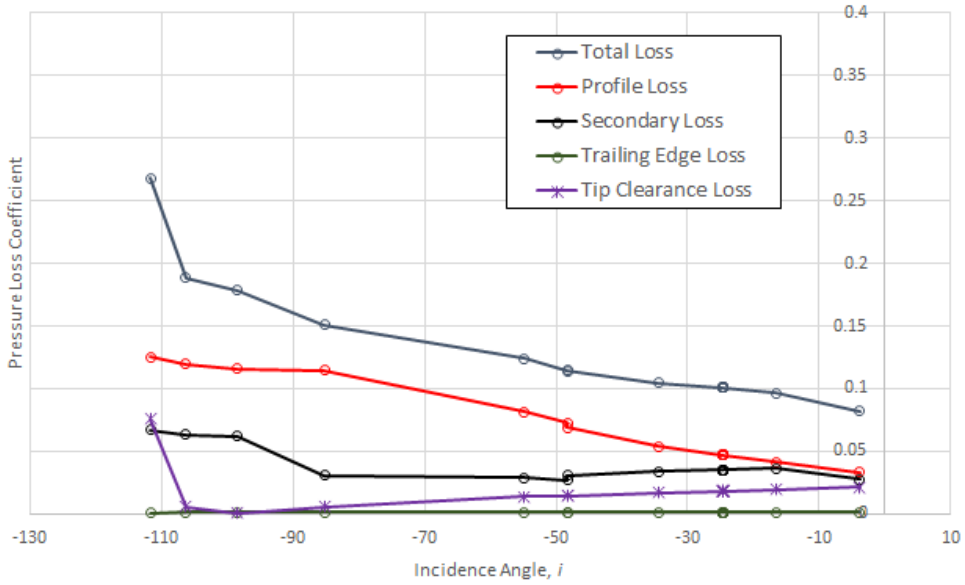


Fig. 4-40 Breakdown of turbine losses Craig and Cox  $\frac{N}{\sqrt{T_{01}}} = 1271 \text{ rpm}/\sqrt{K}$  geometry 2.

A breakdown of the losses from the Craig and Cox model at the high-speed condition for geometry 2 are shown in Figure 4-40. The results display similar trends to the previous geometry and behave as expected.

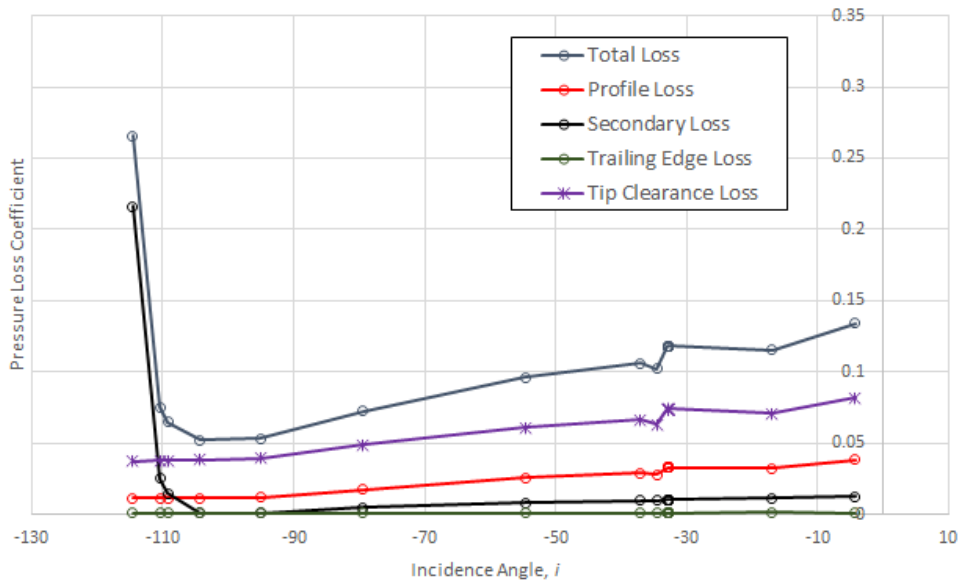


Fig. 4-41 Breakdown of turbine losses Denton  $\frac{N}{\sqrt{T_{01}}} = 1271 \text{ rpm}/\sqrt{K}$  geometry 2.

A breakdown of the losses from the Denton model at the high-speed condition for geometry 2 are shown in Figure 4-41. The results display similar trends to the previous geometry and behave as anticipated.



#### 4.5.4 Geometry 3

The third geometry to be analysed has similar attributes to the second geometry, which are shown below, but has a higher swallowing capacity. The third geometry turbine will be simulated at design and a high-speed conditions.

| Geometric Ratio                    | Stator | Turbine |
|------------------------------------|--------|---------|
| Pitch to Chord Ratio ( $s/c$ )     | 0.76   | 0.64    |
| Aspect Ratio ( $H/c$ )             | 1.03   | 2.26    |
| Trailing Edge to Throat Area Ratio | 0.05   | 0.03    |

Table 7 Important geometric factors relating to the second turbine stage geometry to be investigated.

It can be seen from Figure 4-42 that the loss models of Kacker and Okpauu and AMDC show reasonable correlation to the MULTALL data with Craig and Cox showing very good alignment to the CFD data. The efficiency characteristic from the Denton loss model is higher compared to the CFD data.

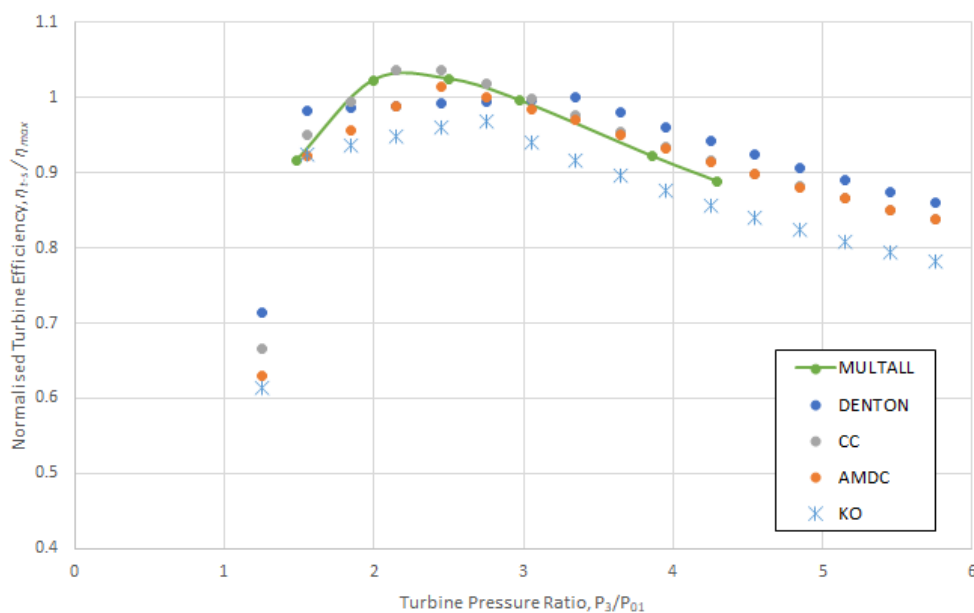


Fig. 4-42 Normalised Efficiency curves predicted for Geometry 3 at a non-dimensional speed of  $\frac{N}{\sqrt{T_{01}}} = 745 \text{ rpm}/\sqrt{K}$ .

The total loss coefficients from the stator and rotor are shown in Figures 4-43 and 4-44. For this turbine speed Kacker and Okapuu, Craig and Cox and AMDC predict the similar stator total loss coefficients. As seen previously the Denton loss model predicts the lowest losses.

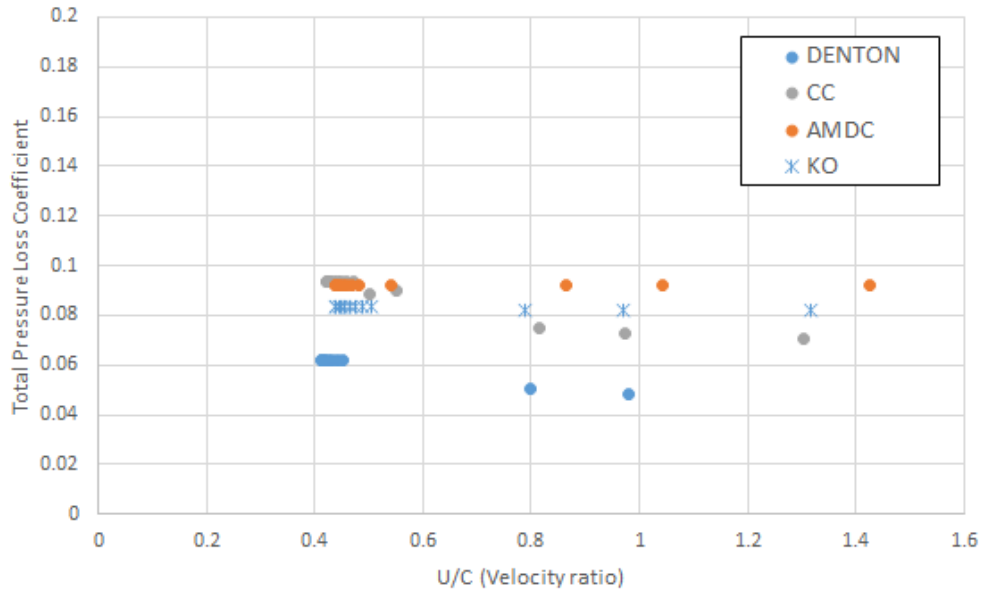


Fig. 4-43 Stator total loss coefficient  $\frac{N}{\sqrt{T_{01}}} = 745 \text{ rpm}/\sqrt{K}$  geometry 3.

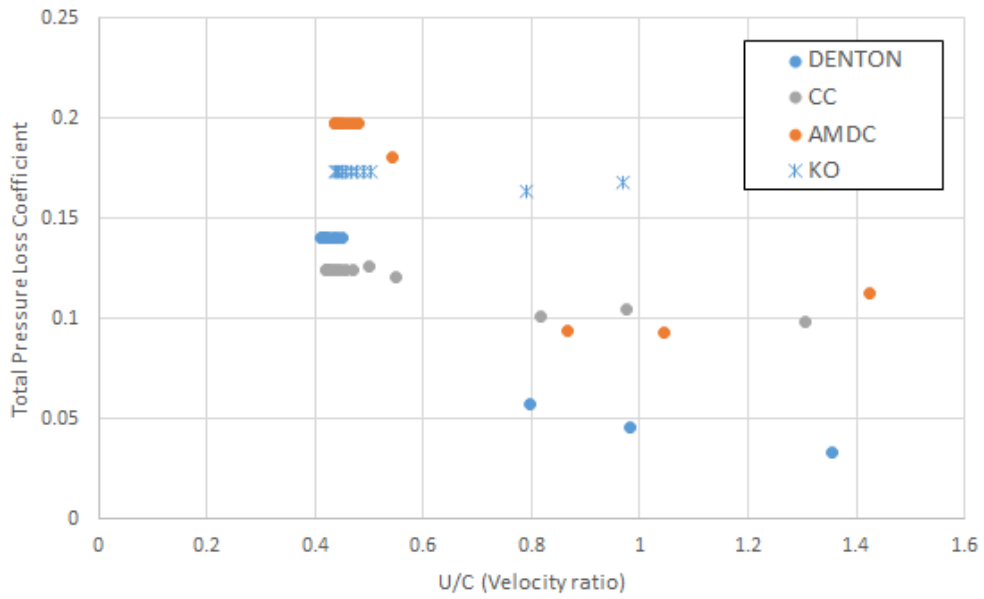


Fig. 4-44 Turbine total loss coefficient  $\frac{N}{\sqrt{T_{01}}} = 745 \text{ rpm}/\sqrt{K}$  geometry 3.

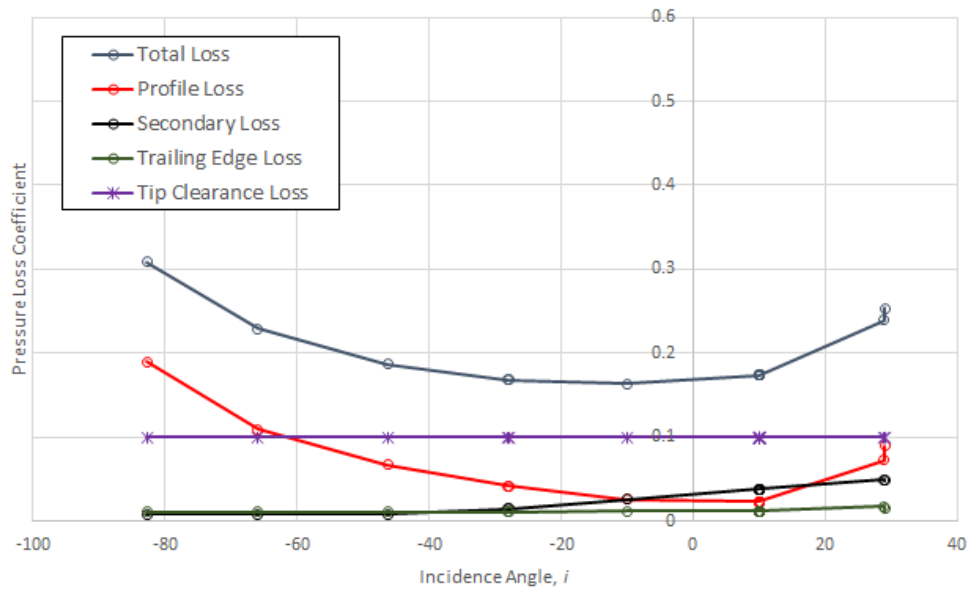


Fig. 4-45 Breakdown of turbine losses Kacker and Okapuu  $\frac{N}{\sqrt{T_{01}}} = 745 \text{ rpm}/\sqrt{K}$  geometry 3.

The breakdown of losses shown in Figure 4-45 for the Kacker and Okapuu loss model behave as expected and follow trends similar to the previous investigations.

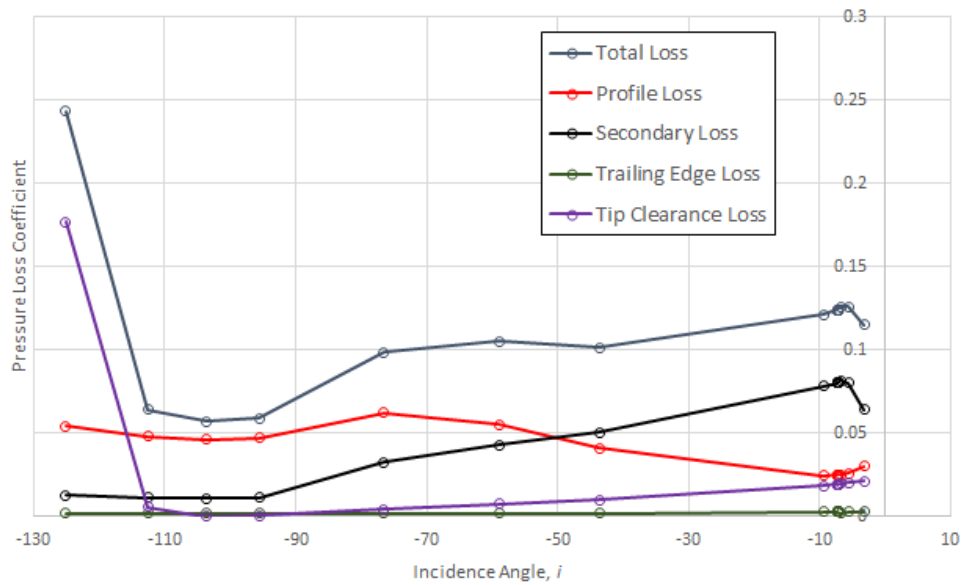


Fig. 4-46 Breakdown of turbine losses Craig and Cox  $\frac{N}{\sqrt{T_{01}}} = 745 \text{ rpm}/\sqrt{K}$  geometry 3.

The breakdown of losses shown in figure 4-46 for the Craig and Cox prediction method follow a similar trend to the previous investigations.

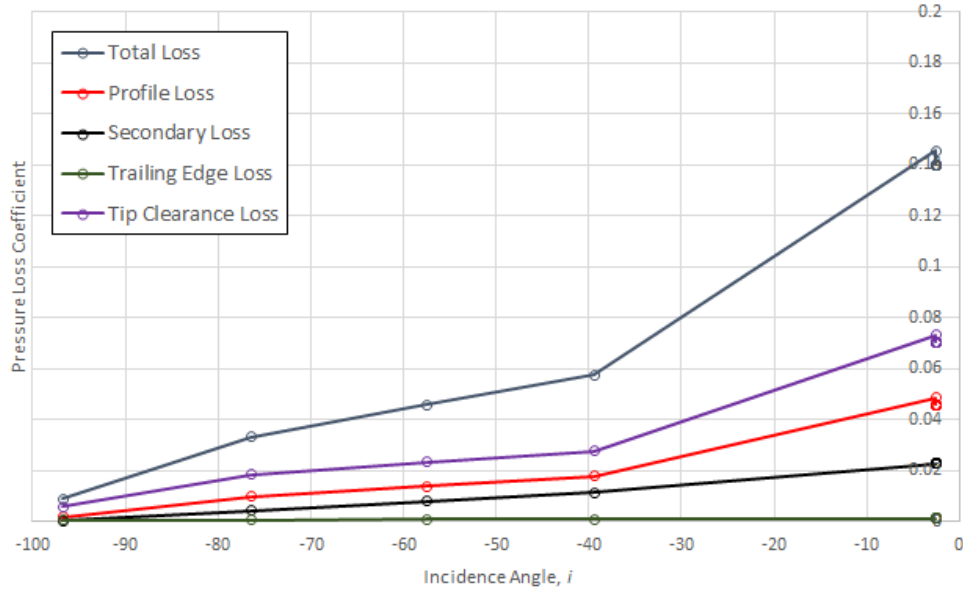


Fig. 4-47 Breakdown of turbine losses Denton  $\frac{N}{\sqrt{T_{01}}} = 745 \text{ rpm}/\sqrt{K}$  geometry 3.

As with the other loss models the losses predicted by Denton replicate the trends shown in previous investigations.

The efficiency plot in Figure 4-48 shows the turbine efficiency characteristics simulated at the non-dimensional speed  $1043 \text{ rpm}/\sqrt{K}$ . The Craig and Cox loss model displays close correlation to the MULTALL data. While the remaining efficiency characteristics diverge from the CFD data at certain turbine pressure ratios.

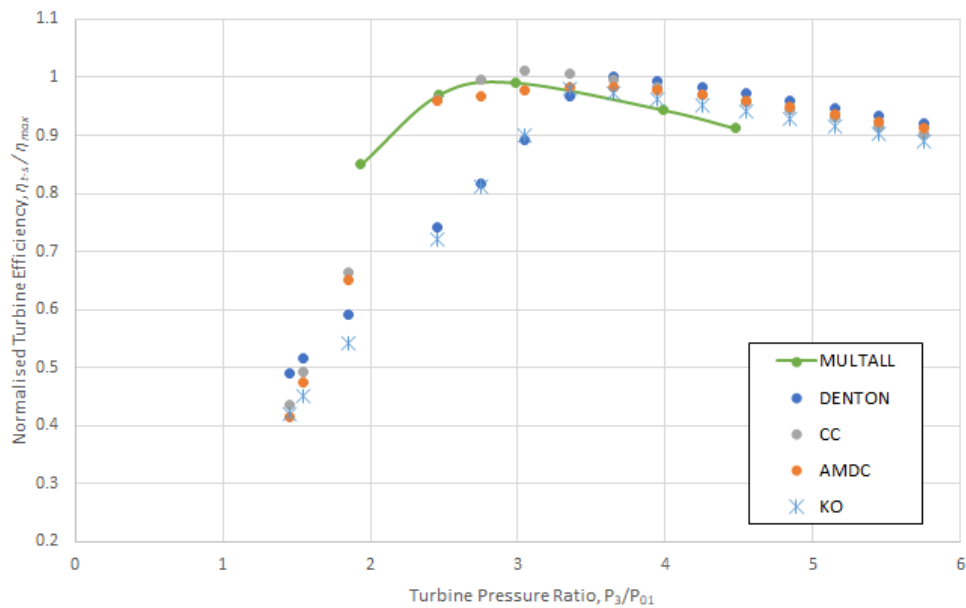


Fig. 4-48 Normalised Efficiency curves predicted for Geometry 3 at a non-dimensional speed of  $\frac{N}{\sqrt{T_{01}}} = 1043 \text{ rpm}/\sqrt{K}$ .

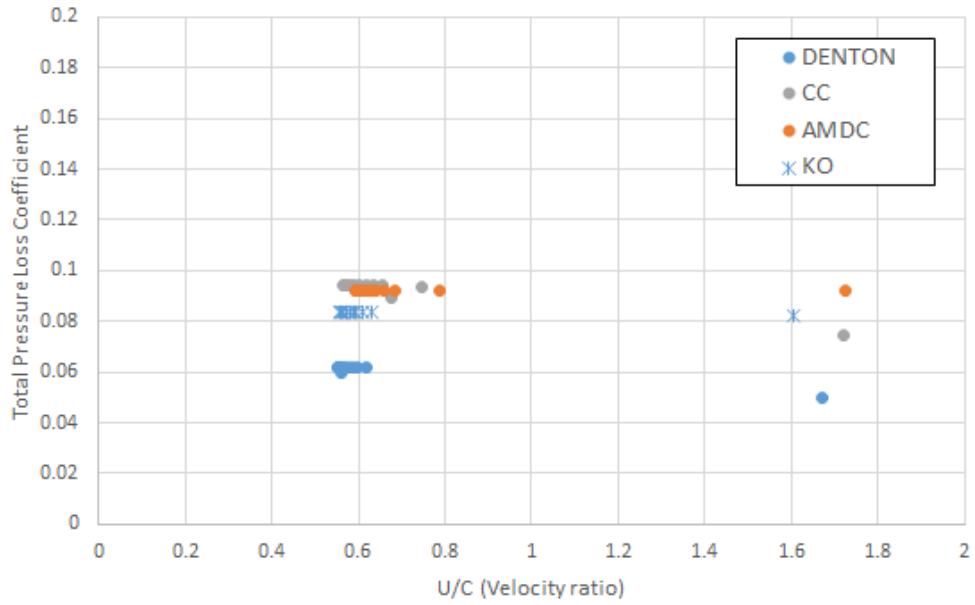


Fig. 4-49 Stator total loss coefficient  $\frac{N}{\sqrt{T_{01}}} = 1043 \text{ rpm}/\sqrt{K}$  geometry 3.

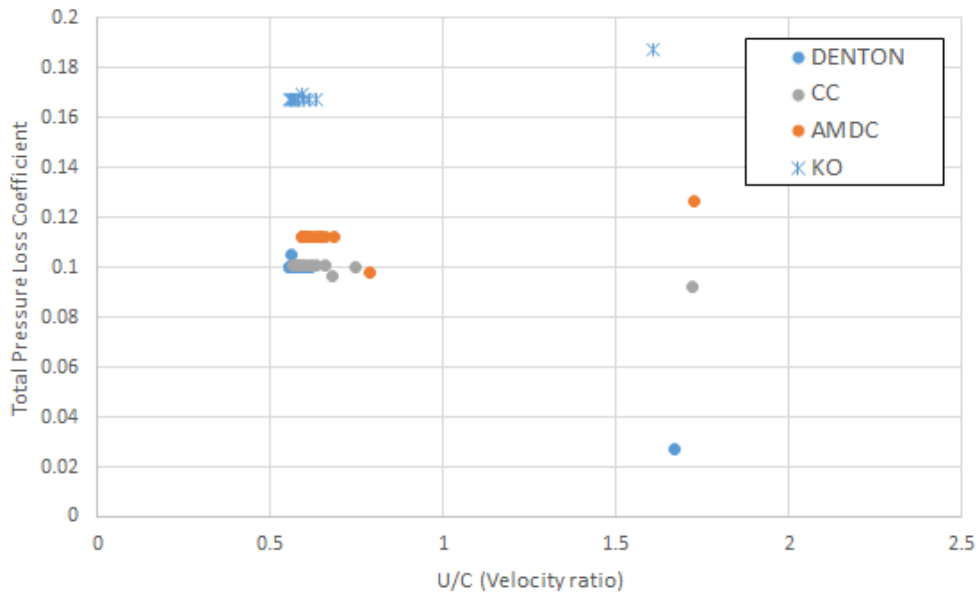


Fig. 4-50 Turbine total loss coefficient  $\frac{N}{\sqrt{T_{01}}} = 1043 \text{ rpm}/\sqrt{K}$  geometry 3.

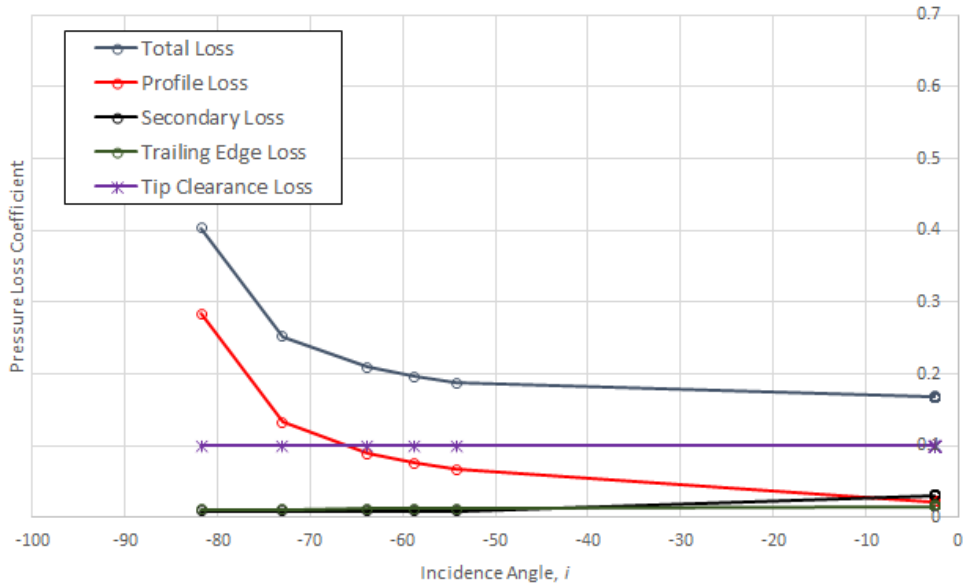


Fig. 4-51 Breakdown of turbine losses Kacker and Okapuu  $\frac{N}{\sqrt{T_{01}}} = 1043 \text{ rpm}/\sqrt{K}$  geometry 3.

The breakdown of losses shown in Figure 4-51 for the Kacker and Okapuu loss model shows similar trends to previous analyses.

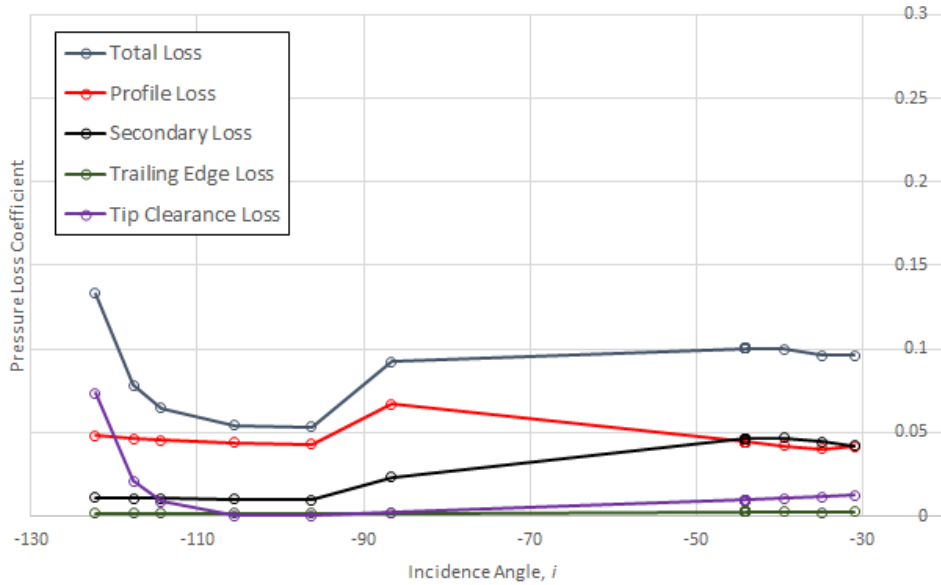


Fig. 4-52 Breakdown of turbine losses Craig and Cox  $\frac{N}{\sqrt{T_{01}}} = 1043 \text{ rpm}/\sqrt{K}$  geometry 3.

The breakdown of losses shown in Figure 4-52 for the Craig and Cox displays comparable trends to previous analyses.

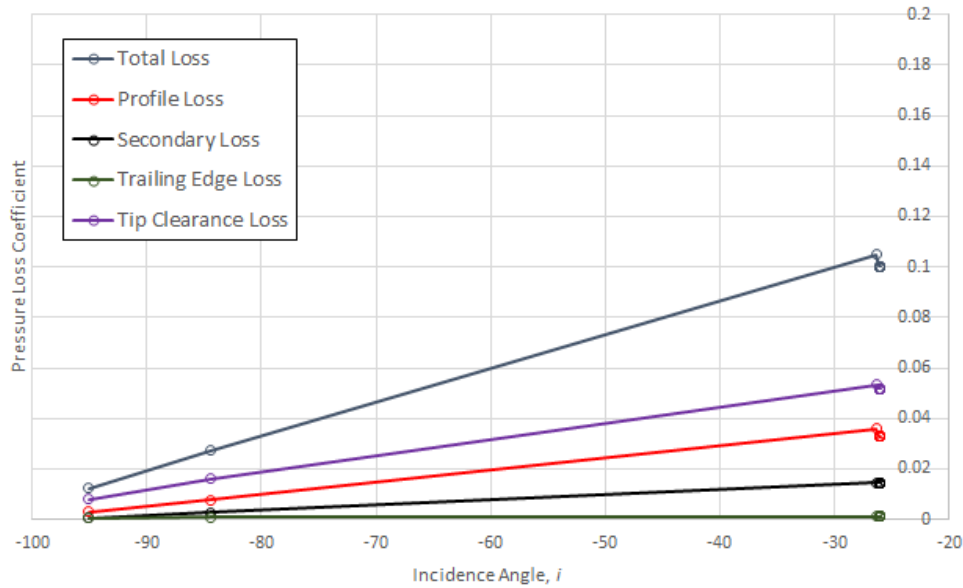


Fig. 4-53 Breakdown of turbine losses Denton  $\frac{N}{T_{01}} = 1043 \text{ rpm}/\sqrt{K}$  geometry 3.

The breakdown of losses shown in Figure 4-53 for the Denton displays comparable trends to previous analyses.

## 4.6 Individual loss mechanism analysis

Now the chosen loss models have been simulated and have provided plausible results compared to CFD performance data the various individual loss mechanisms will be reviewed outlining their constituent parts.

### 4.6.1 Profile Loss

#### 4.6.1.1 Kacker and Okapuu

The profile loss correlation proposed by Kacker and Okapuu (1982) is based on the work of Ainley and Mathieson (1951) which was later improved by Dunham and Came (1970). The correlation is based on experimental data of turbines of the time when the method was proposed. Kacker and Okapuu identified that since the method had been proposed turbine technology and aerodynamic analysis had evolved and suggested the Ainley and Mathieson approach overestimated the profile loss and as such they recommended applying a reduction factor of two thirds to the loss. Kacker and Okapuu also identified that the Ainley and Mathieson profile loss was based on cascade test data with subsonic velocities and did not account for operation at high Mach numbers. A correction factor was introduced to account for high Mach numbers based on the outlet Mach number and ratio of inlet and outlet Mach numbers. Kacker and Okapuu also suggested shock losses should be accounted for in the profile loss. They introduced a shock loss which is correlated to the Mach

number at the hub of the blade and hub to tip radius ratio. Finally, Kacker and Okapuu also include a factor to account for the effect of Reynolds number. They assume the profile loss coefficient is calculated at a reference Reynolds number based on true chord and cascade exit conditions. From the investigations performed it is clear inlet and exit flow angles have an impact on profile loss. This can be seen in Figures 2-13 and 2-14 where a higher outlet flow angle results in a higher profile loss. These figures also show the range of applicability and are valid for outlet angles ranging from 40° to 70° for turbine blades and 40° to 80° for nozzle blades, for outlet angles outside of these values the profile loss is extrapolated which could lead to unreliable profile loss estimation.

#### 4.6.1.2 Craig and Cox

The method of predicting profile loss proposed by Craig and Cox (1971) for subsonic flow uses a lift parameter and contraction ratio to establish a basic profile loss parameter which is near the incidence at which loss is at a minimum. The lift parameter and contraction ratio are functions of inlet and outlet flow angles and pitch to backbone length ratio. The contraction ratio describes the internal blade passage width ratio. The other factors considered by Craig and Cox relate to high Mach number conditions and a Reynolds number correction factor. Craig and Cox give two correlations for Mach numbers exceeding unity to account for different styles of blading including convergent profiles designed with straight suction surface downstream of the throat and profiles designed with pronounced convex suction surfaces. The Reynolds number correction is based on the blade opening to give better correlation. Craig and Cox also introduced Reynolds number values with varying surface roughness as it is believed to control the boundary layer thickness. Similarly, to the correlation of Ainley and Mathieson (1951) the Craig and Cox profile loss has a range of applicability extrapolation outside of these values can lead to unreliable results. The outlet flow angle should be in the range 10° to 90° and the inlet flow angle should be within 10° to 140°.

#### 4.6.1.3 Denton

The profile loss estimation used by Denton (1993) is based on the theories of entropy generation in the boundary layers due to friction on the blade surfaces. To accurately predict profile loss Denton states full knowledge of the state of the boundary layer is required (Denton 1993). His correlation depends on a dissipation coefficient and the velocity distribution over the blade surface. Denton provides generic surface velocity distributions which can be used to estimate profile loss. He also provides a simplified correlation to obtain minimum loss coefficients at optimum pitch to chord ratios. As described in previously in the implementation of the loss correlation section this simplified correlation was obtained by systematically varying the blade load. The correlation provided by Denton is a function of inlet and outlet blade angle and also has a range of applicability, inlet angles range from -60° to 60° and out angles from 40° to 80°. Denton also reviews the impact of shock losses in his work however concludes without an accurate measurement of the average pressure at the blade surface reliable prediction is difficult.



#### 4.6.1.4 Discussion

The profile loss mechanisms reviewed agree that flow turning is an important factor dictating profile loss. Large absolute ratios of blade inlet and outlet flow angle indicate high flow turning and blade loading which can result in possible flow separation on the blade surfaces causing a large increase in loss. This is shown in Figures 4.54, 4.55 and 4.57. Analysing the plotted data, it can be seen the Craig and Cox method predicts the highest profile losses at  $\frac{N}{T_{01}} = 989 \text{ rpm}/\sqrt{K}$  for geometry 1. For geometry 2 all methods produce roughly the same loss below  $80^\circ$  flow turning at  $\frac{N}{T_{01}} = 1060 \text{ rpm}/\sqrt{K}$ . For geometry 3 the Denton loss mechanism produces the highest profile losses below  $75^\circ$  flow turning at  $\frac{N}{T_{01}} = 745 \text{ rpm}/\sqrt{K}$ . It can also be seen the useful range of data appears less with Denton's method compared to the other loss mechanisms which may indicate the Kacker and Okapuu and Craig and Cox mechanisms are more proficient at off design conditions.

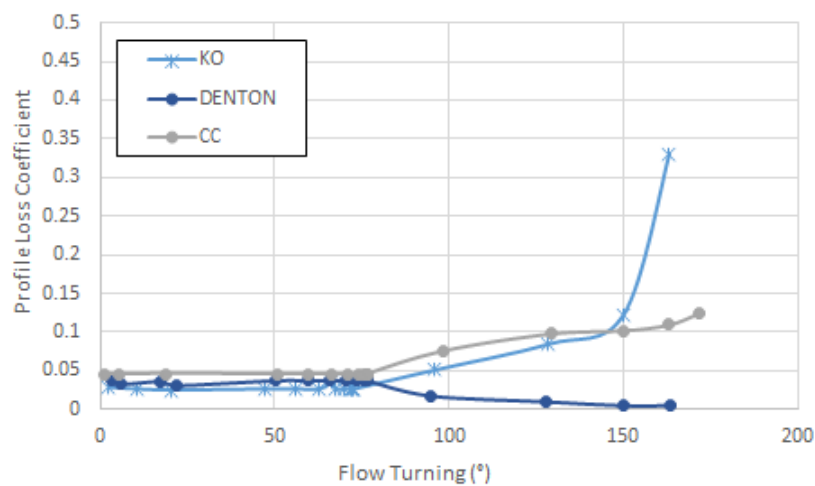


Fig. 4-54 Turbine profile losses at  $\frac{N}{T_{01}} = 989 \text{ rpm}/\sqrt{K}$  geometry 1.

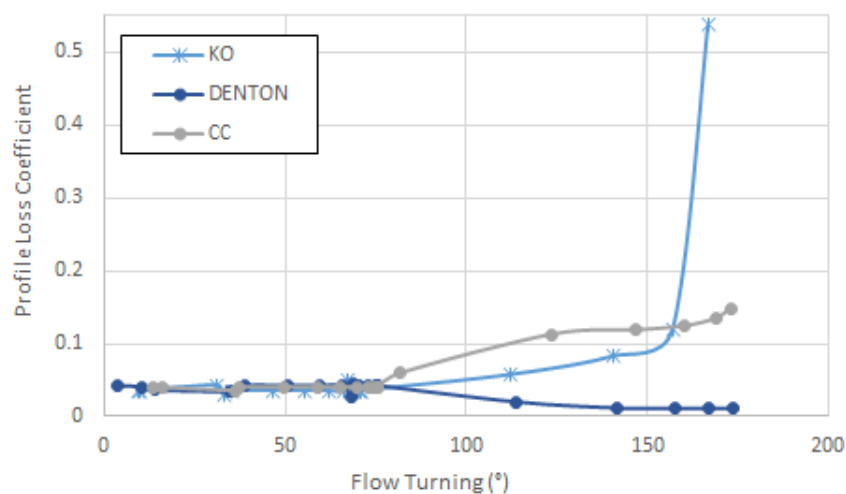


Fig. 4-55 Turbine profile losses at  $\frac{N}{T_{01}} = 1060 \text{ rpm}/\sqrt{K}$  geometry 2.

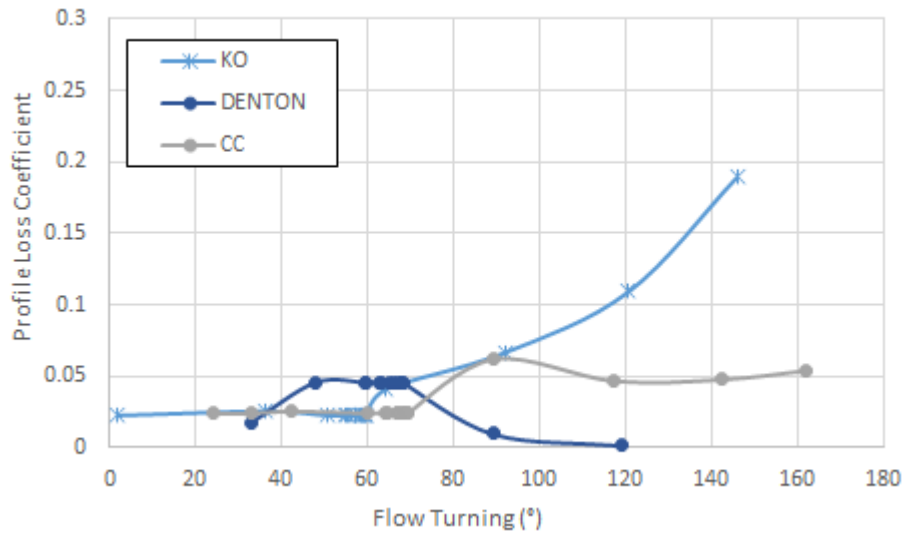


Fig. 4-56 Turbine profile losses at  $\frac{N}{T_{01}} = 745 \text{ rpm}/\sqrt{K}$  geometry 3.

Another important factor considered by all of the correlations when predicting profile loss is pitch to chord ratio. This implies there is an optimum value where blade surface friction and diffusion losses are minimal. All the correlations agree Reynolds number is also an important factor in estimating profile loss as is compressibility at high Mach number conditions.

## 4.6.2 Secondary Loss

### 4.6.2.1 Kacker and Okapuu

Kacker and Okapuu (1982) base their secondary loss correlation on the work of Dunham and Came (1970). Based on experimental data they applied a factor to correct the correlation of Dunham and Came below aspect ratios of two in order to replicate the more significant increase in loss as aspect ratio is decreased. Kacker and Okapuu also separated the secondary and trailing edge losses, which were replaced by a multiplying factor of 1.2 in their final loss system. As with profile losses Kacker and Okapuu account for the effect of compressibility on acceleration of flow next to the endwalls by applying a subsonic Mach number correction factor. The factor for the secondary losses is a function of the profile loss factor and aspect ratio. Regarding range of applicability Kacker and Okapuu state the rise in secondary loss in their loss system is less rapid below aspect ratios of two. Regarding the inlet and outlet flow angles although no limits are specified it would be sensible to apply the same range as considered for the profile loss.

### 4.6.2.2 Craig and Cox

Craig and Cox (1971) estimate secondary losses in their loss system using a basic loss factor which is a function of the blade loading parameter or lift parameter and the velocity ratio. They also apply a factor to accommodate for the impact of aspect ratio which they consider to be approximately inversely proportional to the secondary losses. Craig and Cox also consider the effects of Reynolds number on secondary losses. They apply a factor similar to the method used for profile losses.

#### 4.6.2.3 Denton

In his work Denton (1993) identifies that the secondary losses as the most complex and hardest to comprehend of the loss mechanisms with virtually all current correlations based on empirical data. Denton suggests the entropy generation per unit surface area of the endwalls may be estimated in a similar way to that of the blade surfaces with an approximation of the dissipation coefficient. However, this would require knowledge of the velocity distribution and boundary layer transition from laminar to a turbulent state for reliable predictions. Denton also states the entropy generation in the endwalls only accounts for two thirds of the loss coefficient and the remaining losses are associated with inlet boundary layer mixing and an increase in secondary kinetic energy due to vortices formation (Denton 1993). In order to simplify the secondary loss calculation process Denton recommends using the correlation provided by Dunham and Came (1970) which he promotes as being one of the best methods for secondary loss prediction with the inclusion of an additional factor (Denton 2012). Denton also considers the total entropy production near the endwalls is inversely proportional to aspect ratio if independent of blade height which is in agreement with other loss models.

#### 4.6.2.4 Discussion

All of the correlations regarding secondary loss agree blade loading and aspect ratio are the main factors impacting loss prediction. All of the correlations are based on empirical data, and until the physics governing secondary losses are better understood secondary loss prediction will be reliant on empirical correlations. It is also noticeable from Figures 4-57, 4-58 and 4-59 that the secondary losses of the Denton mechanism are under predicted compared to the other loss prediction methods. Where the losses predicted by the Kacker and Okapuu method are approximately 2.2 times greater compared to Denton method and the losses gained using the Craig and Cox method are approximately 3.8 times higher for geometry 1 at  $\frac{N}{T_{01}} = 989 \text{ rpm}/\sqrt{K}$ . For geometry 2 both the Kacker and Okapuu and Craig and Cox methods predicted secondary losses roughly 3 times higher than Denton at  $\frac{N}{T_{01}} = 1060 \text{ rpm}/\sqrt{K}$ . Finally, for geometry 3 the secondary losses predicted by Kacker and Okapuu are similar, and the losses calculated by Craig and Cox are 3.1 times higher. This may be due to Denton recommending using the secondary loss calculation proposed by Dunham and Came which is a modification of the Ainley and Mathieson method. However, Denton uses a factor of 0.375, based on a large number of comparisons, which dramatically decreases the secondary losses.

The results also show how blade turning and loading effect secondary losses as incidence angle increases and the difference between the inlet and outlet flow angle increases secondary losses increase. The greater the blade load and turning the sooner the endwall boundary layer migrates to the suction surface which leads to increased losses. The only correlation to consider Reynolds number effect is Craig and Cox, by applying a Reynolds number correction factor to the secondary loss in a similar manner to the profile loss.

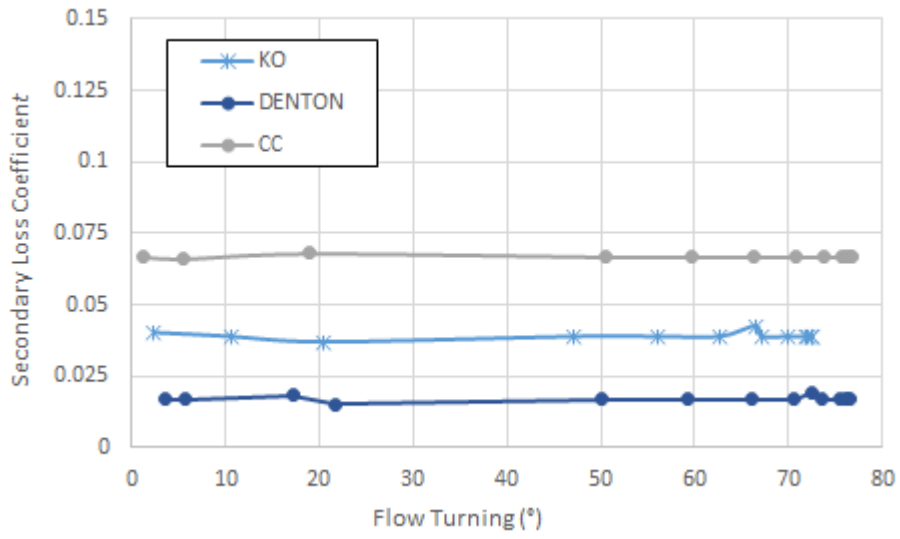


Fig. 4-57 Turbine secondary losses at  $\frac{N}{T_{01}} = 989 \text{ rpm}/\sqrt{K}$  geometry 1.

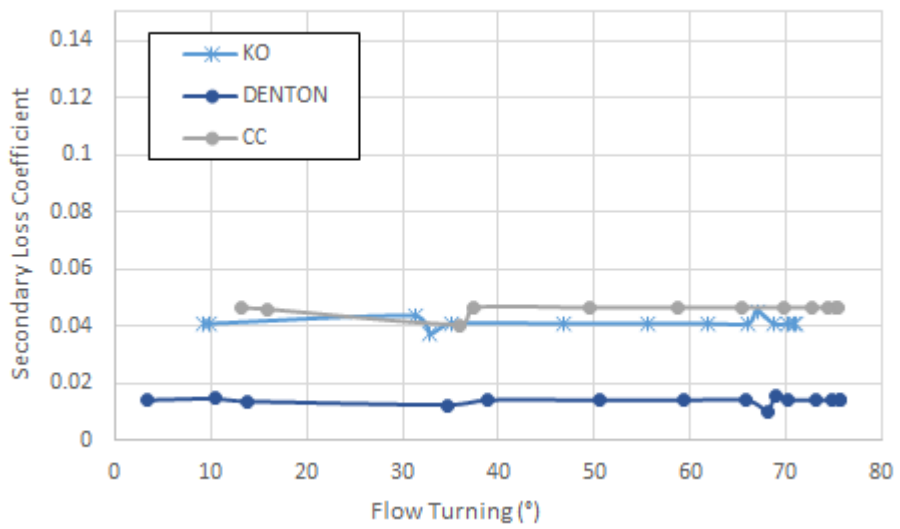


Fig. 4-58 Turbine secondary losses at  $\frac{N}{T_{01}} = 1060 \text{ rpm}/\sqrt{K}$  geometry 2.

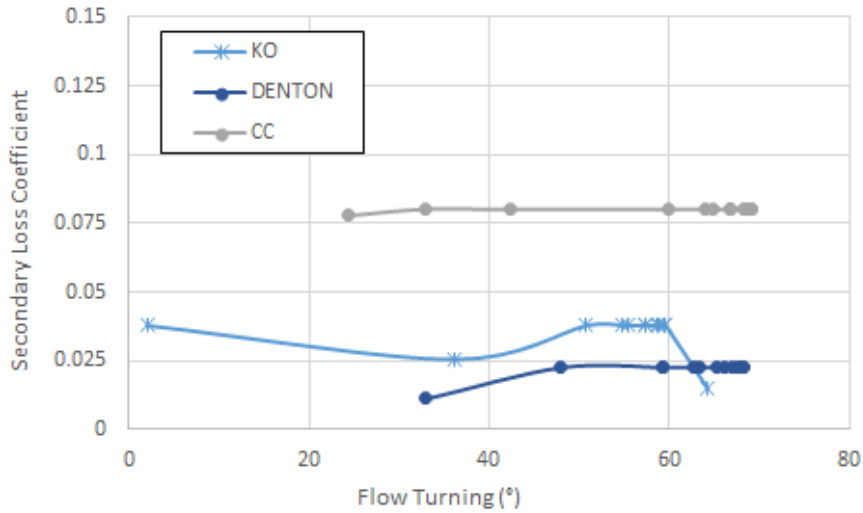


Fig. 4-59 Turbine secondary losses at  $\frac{N}{T_{01}} = 745 \text{ rpm}/\sqrt{K}$  geometry 3.

The results gained for geometry 2 with a higher aspect ratio when compared to geometry 1 show a decrease in secondary losses for the Craig and Cox and Denton methods shown in Figure 4-60. Increasing blade height reduces the possibility of interaction between the passage vortices on the endwalls reducing losses.

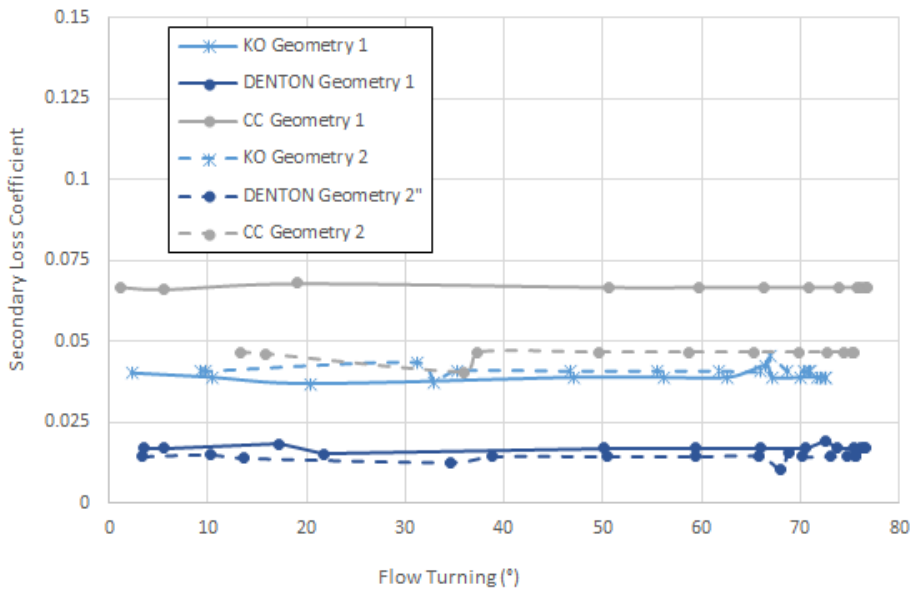


Fig. 4-60 Comparison of the turbine secondary losses between geometry 1 and 2.

## 4.6.3 Trailing Edge Loss

### 4.6.3.1 Kacker and Okapuu

The trailing edge loss coefficient adopted by Kacker and Okapuu (1982) is in terms of trailing edge blockage. Based on experimental data Kacker and Okapuu produce a relationship of trailing edge energy loss coefficient and trailing edge blockage. Figure 2-26 shows two different curves for axial entry nozzles and impulse blades. The difference between the curves relates to profile boundary layer thicknesses at the trailing edges, impulse blades have thick boundary layers and low base pressure coefficients resulting in lower losses. Kacker and Okapuu provide a means of interpolating the trailing edge energy loss coefficient for blades other than the types mentioned. The experimental data shown by Kacker and Okapuu ranges from 0 to 0.4 trailing edge to throat opening ratios.

### 4.6.3.2 Craig and Cox

The estimation of the trailing edge loss coefficient provided by Craig and Cox (1971) is a function of the flow outlet angle and trailing edge thickness to pitch ratio. The applicability range for the outlet angle ranges from  $10^\circ$  to  $50^\circ$ .

### 4.6.3.3 Denton

Denton (1993) relates trailing edge loss to the mixing out of a wake behind the trailing edge. The wake will experience high shear rates and turbulent flow will induce high entropy generation. The entropy produced by this process can be equated to a balance of the mass, momentum, and energy at an upstream boundary where the flow is known and a downstream boundary where the flow has returned to uniformity. The formula includes the base pressure term acting on the trailing edge. For accurate prediction of the trailing edge loss complete details of the boundary layer state are also required.

### 4.6.3.4 Discussion

Trailing edge loss is treated in the same way in all of the chosen methodologies. The main factors impacting the trailing edge losses are flow acceleration and trailing edge to throat opening ratios. Also, trailing edge thickness effects the base pressure at the trailing edge and strongly influences the drag of highly accelerating cascades. Trailing edge to pitch ratio intuitively has an impact on trailing edge losses as pitch increases the number of blades decreases reducing trailing edge losses. The final characteristic effecting trailing edge loss is the mixing process behind the trailing edge where suction and pressure side boundary layers propagate from either side of the blade. Certain simplifications are necessary when considering the boundary layers as the exact state of the boundary layer is not known.

## 4.6.4 Tip clearance loss

### 4.6.4.1 Kacker and Okapuu

Tip clearance losses are calculated in the Kacker and Okapuu (1982) loss model for unshrouded blades using an efficiency debit which is computed iteratively and is based on tip clearance to blade height ratio and the outlet flow angle from the rotor. As the tip clearance to blade height ratio increases leakage flow will increase causing more mixing to take place between the main flow and leakage flow on the suction side of the blade thus increasing losses. As seen in the comparison between mean line performance data and CFD data as flow turning increases mixing loss will also increase.

### 4.6.4.2 Craig and Cox

Craig and Cox (1971) recommend using the tip clearance loss correlation of Ainley and Mathieson (1951) which is a function of tip clearance to height ratio and blade loading.

### 4.6.4.3 Denton

The tip clearance loss correlation provided by Denton (1993) for unshrouded blades is mainly influenced by the ratio of leakage to main flow, the inlet and outlet blade velocities and the outlet flow angle. Higher losses are experienced at conditions of higher leakage flow and higher velocities and small outlet flow angles. In a similar manner to the profile loss mechanism Denton provides a simplified version of the tip clearance losses which assume a tip gap of 1% of the blade span. Denton also demonstrates how blade thickness effects leakage flow, shown in Figure 2-11, where the jet formed as the leakage flow passes over the blade tip mixes out causing an increase in static pressure and entropy.

### 4.6.4.4 Discussion

The chosen loss models conclusively agree that any increase in blade tip gap increases tip clearance losses. An increased tip gap would allow more leakage flow which would in turn increase mixing with the main flow. Changes to velocities and outlet angles are well documented to increase mixing.

## 4.7 Results Summary

The charts in this section show the efficiencies calculated using each loss mechanism how they compare to those simulated in the CFD program MULTALL for each geometry at each speed condition. For example, the data depicted in Figure 4-61 shows the normalised predicted and normalised MULTALL turbine stage efficiencies from Figure 4-6 presented in a similar manner to Figure 2-49 from Dunham and Came (1970) and Figure 2-51 from Kacker and Okapuu (1982) but for the entire constant speed line.

It can be seen from the charts in Figures 4-61, 4-62 and 4-63 that the correlation at the low-speed condition is very poor for all of the loss models tested. For the higher speeds the correlation is improved with all but the Denton method predicting turbine efficiencies relatively close to a variance of +/- 1.5%. Kacker and Okpauu state their loss model can predict design point efficiencies to within +/-1.5%, viewing the design speed plot at a non-dimensional speed of 989 most of the operating points are within or close to the target of +/- 1.5% variance. The loss system of Craig and Cox was also validated against experimental data predicting losses to within +/- 1.25% however it seems Craig and Cox shows good correlation to the corresponding MULTALL data at the design speed but shows poor alignment at the low and high-speed conditions. Similarly, for the first geometry investigated, the Denton loss system seems to predict efficiencies closest to the CFD data at the design speed conditions.

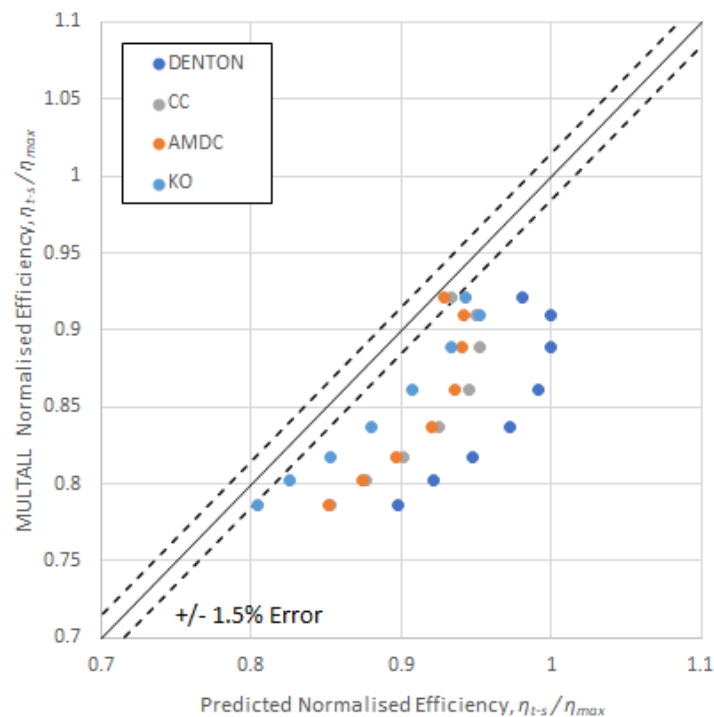


Fig. 4-61 Predicted turbine efficiency with CFD efficiency for geometry 1 at  $\frac{N}{\sqrt{T_{01}}} = 593 \text{ rpm}/\sqrt{K}$ .



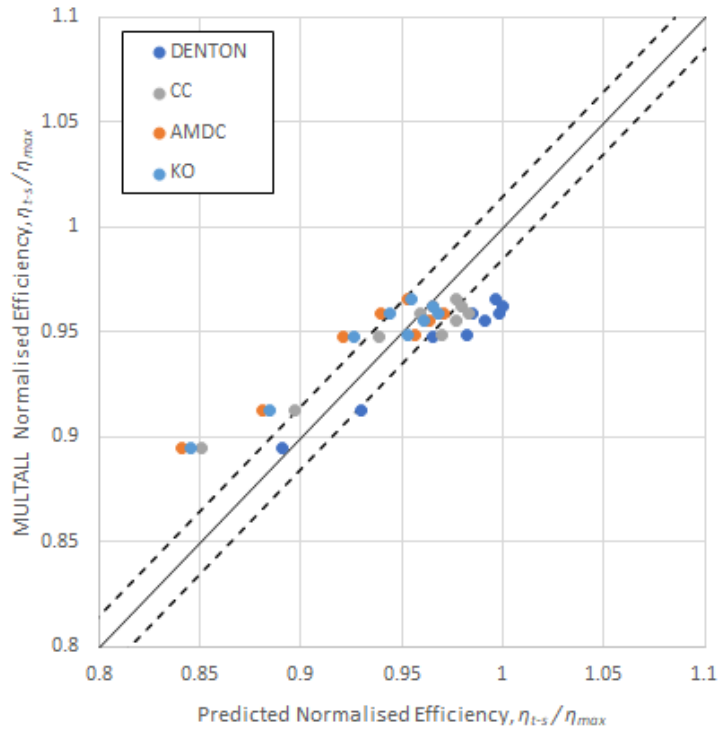


Fig. 4-62 Predicted turbine efficiency with CFD efficiency for geometry 1 at  $\frac{N}{\sqrt{T_{01}}} = 989 \text{ rpm}/\sqrt{K}$ .

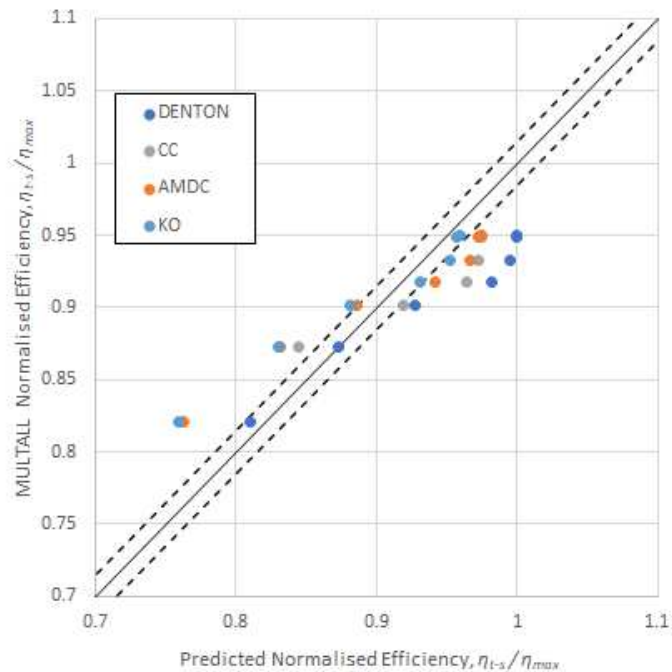


Fig. 4-63 Predicted turbine efficiency with CFD efficiency for geometry 1 at  $\frac{N}{\sqrt{T_{01}}} = 1285 \text{ rpm}/\sqrt{K}$   
N/VT.

The efficiencies gained from the second geometry, Figures 4-64, 4-65 and 4-66 show improved correlation to CFD data at the design and high-speed conditions for all loss correlations. The Craig

and Cox method shows good correlation throughout the speed range for the second geometry investigated predicting efficiencies within a +/-1.5% variance. As can be seen from the following charts the efficiencies predicted by the Denton loss correlation are optimistic at the low-speed condition however show improved alignment at the design speed and high-speed conditions.

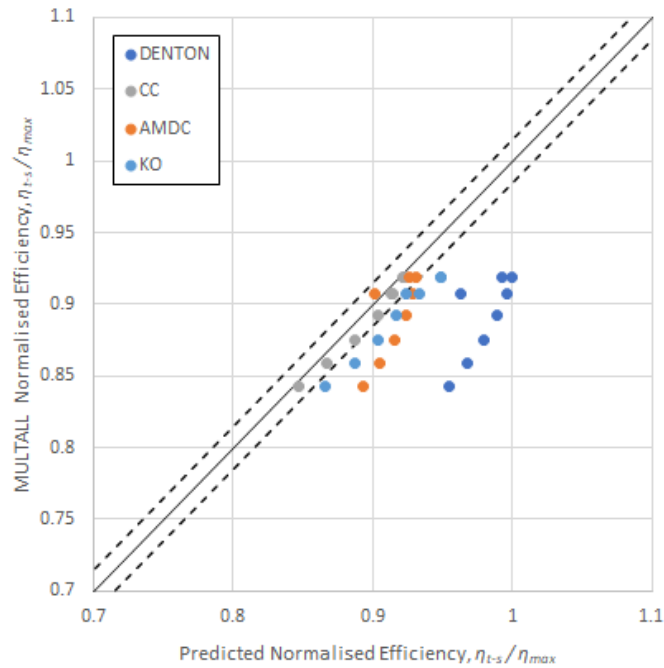


Fig. 4-64 Predicted turbine efficiency with CFD efficiency for geometry 2 at  $\frac{N}{\sqrt{T_{01}}} = 635 \text{ rpm}/\sqrt{K}$ .

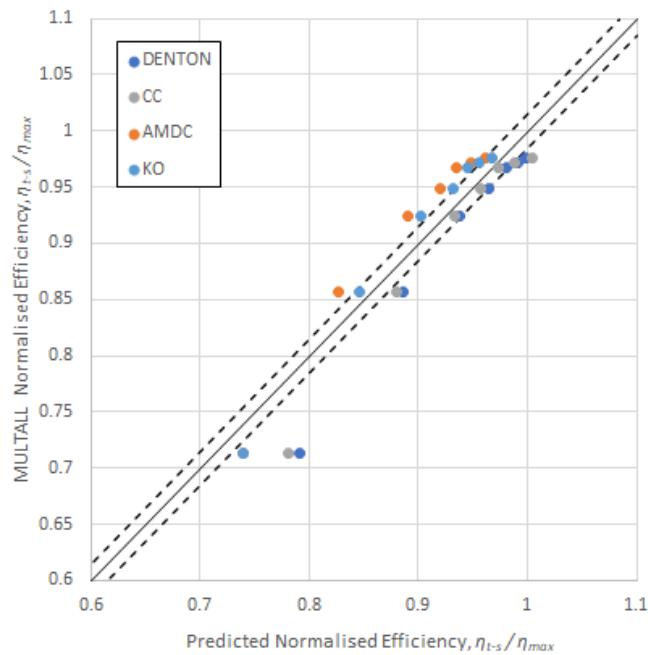


Fig. 4-65 Predicted turbine efficiency with CFD efficiency for geometry 2 at  $\frac{N}{\sqrt{T_{01}}} = 1060 \text{ rpm}/\sqrt{K}$   
N/VT.

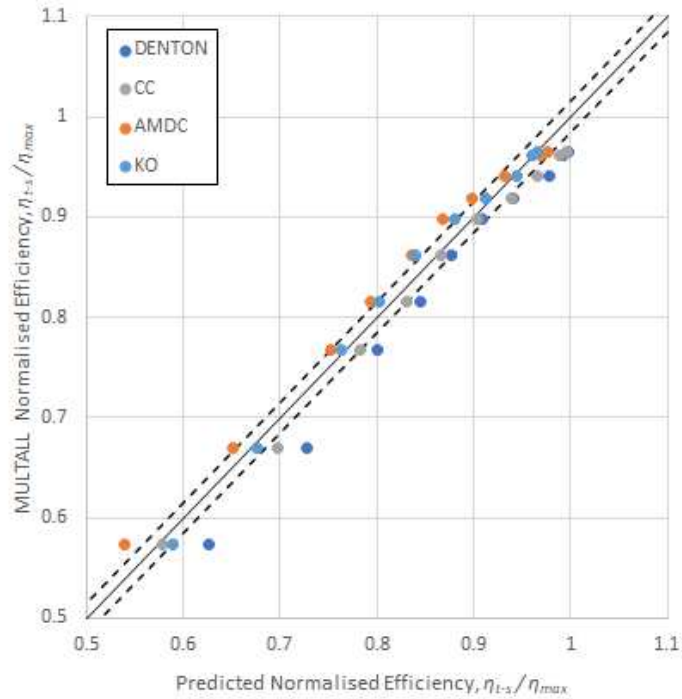


Fig. 4-66 Predicted turbine efficiency with CFD efficiency for geometry 2 at  $\frac{N}{\sqrt{T_{01}}} = 1271 \text{ rpm}/\sqrt{K}$ .

The chart in Figure 4-67 shows the Craig and Cox loss model gave the most accurate results at the low-speed condition for the third turbine geometry. The data in Figure 4-68 is skewed due to large gaps encountered in the data between standard operating conditions and choke conditions.

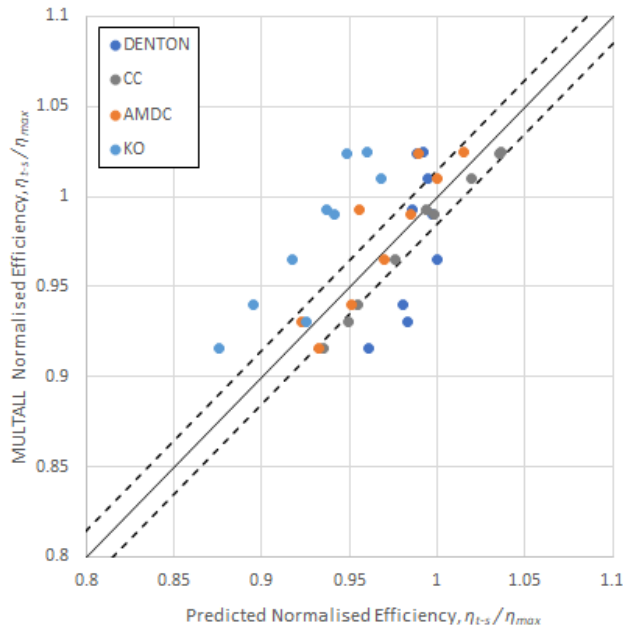


Fig. 4-67 Predicted turbine efficiency with CFD efficiency for geometry 3 at  $\frac{N}{\sqrt{T_{01}}} = 745 \text{ rpm}/\sqrt{K}$ .

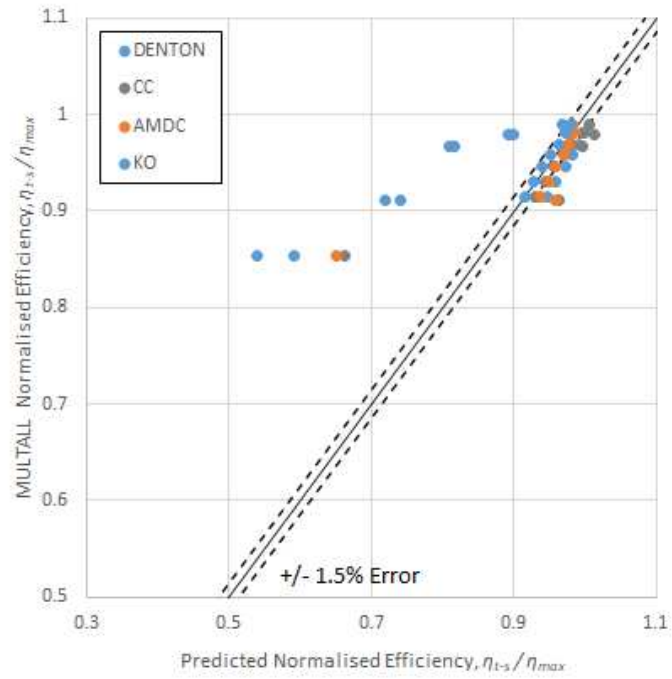


Fig. 4-68 Predicted turbine efficiency with CFD efficiency for geometry 3 at  $\frac{N}{\sqrt{T_{01}}} = 1043 \text{ rpm}/\sqrt{K}$ .

## Chapter 5

# Conclusions and Recommendations for Future work

### 5.1 Implementation of selective loss correlation based on operating conditions and geometry.

One of the aims of this work was to identify whether the chosen loss correlations could be used in conjunction with each other to better predict a significant range of operating conditions which make up a turbine map. Based on the data collected the Kacker and Okapuu method seems to show the best correlation to the MULTALL data for the first geometry investigated which has a standard blade height. For the turbine geometries with higher aspect ratios the Craig and Cox method shows the most accurate correlation to the MULTALL data especially at the low-speed conditions. At higher speed conditions all of the loss correlations predicted turbine efficiency satisfactorily. Based on these three investigations it would be possible to implement a selective algorithm to the current code to choose a loss correlation based on turbine geometry and operating condition however, to further solidify the findings of this investigation a much larger number of turbine geometries would require simulation.

## 5.2 Conclusions

The main aim of this work was to investigate, recode and expand the current mean line turbine efficiency prediction method used by Napier Turbochargers. Implementing additional loss correlations and proposing a selective tool which chooses a loss correlation based on operating condition and blade geometry.

The original code has been rewritten into a more accessible language with extensive notes and clear highlighting of calculation steps to enable future development as aerodynamic analysis progresses. The availability of three loss prediction methods at the turbine design point should facilitate design iterations and enhance knowledge of limiting design features.

Common loss systems were identified, studied and implemented to the code. A number of current turbine geometries were selected, and the chosen loss systems were used to predict turbine performance. The results were then compared to CFD data to ascertain the chosen loss systems accuracy and relevance to a typical turbocharger axial turbine.

The various loss mechanisms were investigated and compared. The profile losses were found to depend principally on flow turning and pitch to chord ratio. The secondary losses are the most complex of the loss mechanisms in a turbomachine, still with many unknowns thus most loss correlations in use are based on empirical data. It has been established that the main factors governing secondary losses are blade aspect ratio and loading. Trailing edge losses are dictated by flow acceleration and trailing edge thickness ratios and tip clearance loss is mainly a function of blade tip gap.

The results obtained via the new mean line turbine efficiency prediction tool and chosen loss systems also show desirable correlation to similar works Wei (2000), Guedez (2011), Sieverding (1985). With each individual loss mechanism behaving as expected and aligning with other detailed theoretical studies.

One of the main limitations of the loss correlations reviewed relates to the design of the blades used in the experimental data which the loss correlations have been based on. For example, the correlation of Ainley and Mathieson is based on blade profiles designed prior to 1950 where designs were comprised of circular arcs and straight lines with circular or parabolic camber lines. Hence the requirement for review every decade, as recommended by Kacker and Okapuu (1982), to ensure a high level of accuracy is maintained to turbine blade designs of the current time period. Based on the results retrieved and comparison to CFD data the more recent loss correlations seem to show an acceptable level of applicability to Napier Turbocharger axial turbine stages but may require some additional refinement to further improve correlation.

Based on the results of the investigation of the chosen three loss prediction methods the methods of Kacker and Okapuu and Craig and Cox showed the most promising results across the turbine geometries and speed conditions simulated. The method proposed by Denton showed poor correlation at off design conditions compared to the MULTALL data but displayed improved alignment at design conditions. This was primarily illustrated by the data presented in Chapter 4 although, the investigation did not result in a decisive strategy for selecting a loss correlation based

on turbine blade geometry and speed condition the Kacker and Okpauu and Craig and Cox methods showed improvements compared to the current loss prediction method in most cases.

Although the method proposed by Denton showed the worst correlation at off design conditions there are a number of aspects which require verification in the Denton loss model. One in particular is the appropriateness of using a correlation which is based on optimum pitch to chord ratio, this requires an assessment on how realistic its application to a Napier Turbocharger turbine stage is.

The efficiency characteristics of the final geometry tested are not complete and the interpolation method used on the raw data has skewed the efficiency trend due to large gaps in the data between normal operating conditions and choke conditions. The gap in the data only became apparent on the third turbine investigated and was not detected previously. In the mean line performance prediction program of the present work the choking mass flow is kept constant when choking of a stage is detected and this was thought to be the method used in the original program however recent developments have shown that there is a difference between the original code which is kept on a Linux system and the converted code suitable for a Windows system which the present work was calibrated against. After going through the original Linux code, it was found the mass flow at choking conditions is reduced which aids population of the gap in the efficiency characteristic on the same trend. Although there is a gap in the data the efficiency trends of the original and new mean line tools either side of the gap are identical. This is the reason some of the data in the charts in Figure 4-60 are so far away from the CFD data.

### 5.3 Recommendations for Future work

The turbine geometries examined represent current production intent however, further investigation of the chosen loss correlations is required in order to confirm the variance of performance prediction with an extensive range of turbine geometries over a wide range of operating conditions. Testing more geometries can only facilitate the goal of establishing a selective tool to choose a loss correlation based on operating condition or turbine design.

The availability and range of actual in-house turbine test data is a concern. Napier Turbochargers current in-house test rig setup only permits the acquisition of turbine performance data for a narrow band of velocity ratio. It would be very advantageous for Napier Turbochargers to commission a series of tests, using current production turbine geometries, on a dedicated turbine test rig to fully map turbine performance across a wide range of velocity ratio to enable validation of current CFD and mean line performance prediction methods.

Now the new mean line performance prediction program has been established in the near future it may be developed further, potential modifications may include adding Excel plots to give a preview of the output data, updating the user interface based on feedback from users and adjustment of the mass flow iterations in the code to give better results at all operating conditions. The large gaps encountered in the performance data during the analysis of the third turbine geometry may be attributed to the stages of the turbine transitioning into choke conditions. Further investigation is required to confirm how the choke flow is reduced in the original code. This must be addressed as high swallowing capacity turbines are part of the Napier portfolio thus prediction of reliable and complete performance data is essential.

## Bibliography

- Ainley, D.G., Mathieson, G.C.R., (1951), A Method of Performance Estimation for Axial-Flow Turbines, R. and M. No. 2974, ARC Technical Report.
- Balje, O.E., Binsley, R.L., (1968), Axial Turbine Performance Evaluation. Part A – Loss-Geomertry Relationships, ASME Journal of Engineering for Gas Turbines and Power, Oct 1968, 90(4): pp 341-348.
- Baines, N.C., (2005), Fundamentals of Turbocharging, Concepts NREC.
- Brown, L.E., (1972), Axial Flow Compressor and Turbine Loss Coefficients: A Comparison of Several Parameters, ASME Journal Eng Power Trans, Jul 1972, 94(3): pp 193-201.
- Bundesministerium für Umwelt, Naturschutz und nukleare Sicherheit (Federal Environment Ministry), (@2021), Bundesministerium für Umwelt, Naturschutz und nukleare Sicherheit (Federal Environment Ministry), Available from: <https://www.bmu.de/>.
- Codan, E., Bernasconi, S., Born, H., (2010), IMO III Emission Regulation: Impact on the Turbocharging System, CIMAC World Congress on Combustion Engine, 2010, Paper No. 139, Bergen, Norway.
- Cohen, H., Rogers, G.F.C., Saravanamuttoo, H.I.H., (1996), Gas Turbine Theory, Addison Wesley Longman Limited.
- Craig, H.R.M., Cox, H.J.A., (1971), Performance Estimation of Axial Flow Turbines, Vol 185 32/71, Thermodynamics and Fluid Mechanics Group.
- Dahlquist, A., (2008), Investigation of Losses Prediction Methods in 1D for Axial Gas Turbines. MSc Thesis, Lund University, Department of Energy Sciences, Lund, Sweden.
- Denton, J.D. (1990), The calculation of three-dimensional viscous flow through multistage turbomachines, ASME International Gas Turbine and Aeroengine Congress and Exposition, Jun 1990, paper 90, Brussels.
- Denton, J.D., (1990), Entropy Generation in Turbomachinery Flows, 902011 SAE International.
- Denton, J.D., (1993), Loss Mechanisms in Turbomachines, ASME Journal of Turbomachinery, Oct 1993, 115(4): pp 621-656.
- Denton, J.D., Xu, L., (2002), The effects of lean and sweep on transonic fan performance, ASME, International Gas Turbine Institute, Turbo Expo (Publication) IGTI 5 A, Jun 2002, 5 pp. 23-32.
- Denton, J.D., (2009), Multistage Turbomachinery Flow Calculation Program – MULTALL, Available from: <https://www.dropbox.com/sh/8i0jyxzjb57q4j4/AABD9GQ1MUFwUm5hM>.
- Denton, J.D., (2012), Axial Turbines Design, lecture notes from Cambridge turbomachinery course.
- Denton, J.D., (2017), MULTALL- an open source, CFD based, turbomachinery design system, ASME Journal of Turbomachinery, Dec 2017, 139(12) Article number 121001.



Dixon, S.L., Hall, C., (2010), Fluid Mechanics and Thermodynamics of Turbomachinery, Butterworth-Heinemann, Elsevier.

Douglas, J.F., Gasiorek, J. M., Swaffield, J.A., Jack, L.B., (2005), Fluid Mechanics, Pearson Education Limited.

Drews, M., (2019), Marine Application: Meeting IMO III / EPA Tier 4 Regulations Challenges and Solutions From The View Of A Solution Provider, CIMAC World Congress on Combustion Engine, 2019, Paper 401, Vancouver.

Dunham, J., Came, P.M., (1970), Improvements to the Ainley-Mathieson Method of turbine Performance Prediction, ASME Journal of Engineering for Gas Turbines and Power, Jul 1970, 92(3): pp 252-256.

Dunham, J., (1970), A Review of Cascade Data on Secondary Losses in Turbines, Journal of Mechanical Engineering Science, Feb 1970, 12(1): pp48-59.

Greitzer, E.M., Tan, C.S., Graf, M.B., (2004), Internal Flow – Concepts and Applications, Cambridge University Press.

Guedez, R., (2011), Implementation and Validation of Loss Prediction Methods to An Existing One-Dimensional Axial Turbine Design Program. MSc Thesis, KTH School of Industrial Engineering and Management Energy Technology, Division of Heat and Power Technology, Stockholm, Sweden.

Hilditch, M. A., Fowler, A., Jones, T. V., Chana, K. S., Oldfield, M. L. G., Ainsworth, R. W., Hogg, S. I., Anderson, S. J., and Smith, G.S., 1994, Installation of a turbine stage in the Pyestock Isentropic Light Piston Facility, ASME 1994 International Gas Turbine and Aeroengine Congress and Exposition, paper 94-GT-277.

International Maritime Organization, (©2019), International Maritime Organization. Available from: <https://www.imo.org/en/>.

Kacker, S.C., Okapuu, U. (1982), A Mean Line Prediction Method for Axial Flow Turbine Efficiency, ASME Journal of Engineering for Gas Turbines and Power, Jan 1982, 104(1): pp111-119.

Klein, A., (1966), Untersuchungen über die Einfluss Der Zustromgrenzschicht auf die Sekundärströmung in den Beschaufelungen von Axialturbinen, Fotsch. Ing., Ba 32, Nr. 6.

Langston, L., (2001), Secondary Flows in Axial Turbines - A Review, University of Connecticut.

Lozza, G., (1982), A Comparison Between the Craig-Cox and the Kacker-Okapuu Methods of Turbine Performance Prediction, 17, 211-221 La Meccanica.

Mayr, S., (2019), Turbocharger Innovations for Compliance with Tier III Emission Limits, CIMAC World Congress on Combustion Engine, 2019, Paper 123, Vancouver.

Moustapha, S., Kacker, S.C., Tremblay, B., (1990), An Improved Incidence Losses Prediction Method for Turbine Airfoils, Journal of Turbomachinery, Apr. 112(2): pp 267-276.

Moustapha, H., Zelesky, M.F., Baines, N.C., Japikse, D., (2003), Axial and Radial Turbines, Concepts NREC.

SAE International, (1995), Surface Vehicle Recommended Practice, Turbocharger Gas Stand Test Code, J1826 199503, SAE International.

Schlichting, H., (1987), Boundary-Layer Theory, McGraw Hill.

Sieverding, C.H., (1985), Recent Progress in the Understanding of Basic Aspects of Secondary Flows in Turbine Blade Passages, ASME Journal of Engineering for Gas Turbines and Power, Apr 1985, 107(2): pp248-257.

Sieverding, C.H., (1985), Axial Turbine Performance Prediction Methods, Thermodynamics and Fluid Mechanics of Turbomachinery Volume 2, NATO ASI Series.

Sieverding, C.H., Stanisias, M., Snoeck, J., (1980), The Base Pressure problem in Transonic Turbine Cascades, ASME Journal of Engineering for Gas Turbines and Power, Jul 1980, 102(3): pp 711-718.

Sjolander, S. A., (1997), Overview of Tip-Clearance Effects in Axial Turbines, Secondary and Tip Clearance Flows in Axial Turbines VKI Lecture Series 1997-01, Von Karman Institute for Fluid Dynamics, Rhode-St-Genèse, Belgium.

Smith, S.F., (1965), A Simple Correlation of Turbine Efficiency, Journal of the Royal Aeronautical Society.

The International Council of Combustion Engines, (2007), Turbocharging Efficiencies – Definitions and Guidelines for Measurement and Calculation, No. 27.

United States Environmental Protection Agency, (©2021), United States Environmental Protection Agency, Available from: <https://www.epa.gov/>.

Watson, N., Janota, M.S., (1982), Turbocharging the Internal Combustion Engine, Palgrave Macmillan.

Wei, N., (2000), Significance of Loss Models in Aerothermodynamics Simulation for Axial Turbines. Doctoral Thesis, Royal Institute of Technology - KTH, Department of Energy Technology, Stockholm, Sweden.

Wik, C., Hallback, B., (2007), Utilisation of 2-stage turbo charging as an emission reduction mean on a Wartsila 4-stroke medium-speed diesel engine, Paper 101, CIMAC Congress 2007, Vienna.

Wilson, D.G., (1991), The Design of High-Efficiency Turbomachinery and Gas Turbines, pp 487-492, published by the MIT Press, Cambridge, Massachusetts, 1984, 5th printing 1991.

# Appendices

# Appendix A

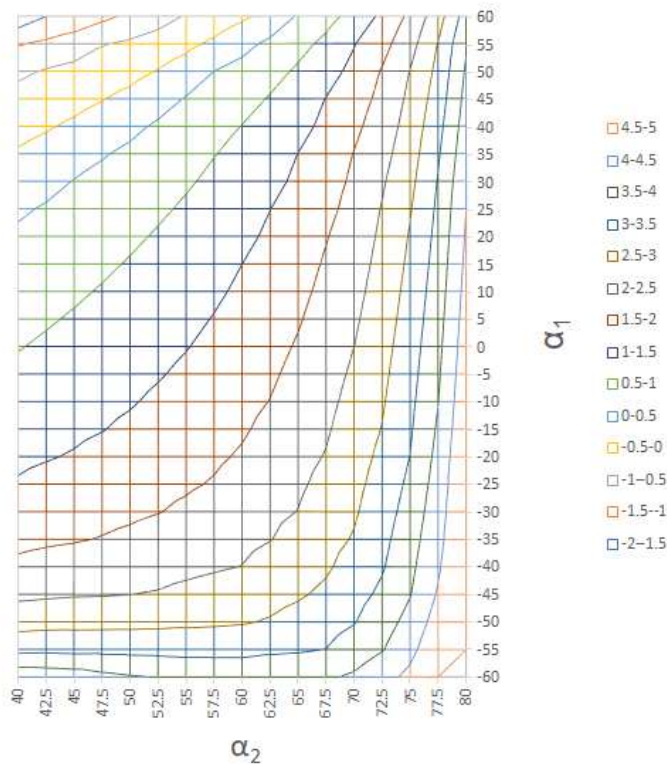
## A.1 Sample MULTALL input file without blade geometry

```
Bladerows: 01 + 03
 39 292 39 0 6000 0 0 3 2 1 2 3 20 20 0
 0 2 3 3 0 0 0 9 5 0 0 0
 3 3 3 9 9 9
#####NOZZLE#####
142 34 117 24 0 0 998 999 998 999 0 1 1 1 1 1
 0 0 0
 0.0 155925.0 154365.8 131780.3 130462.5 0.0 0.0
0.00100
>>>> GEOMETRY HERE <<<<
#####TURBINE#####
150 26 109 53 0 0 22 113 998 999 0 1 1 1 1 1
 0 0 0
-10293.0 130462.5 129157.9 106060.6 105000.0 0.0 -10293.0
0.00100
>>>> GEOMETRY HERE <<<<
1126.57361 1.34200 0.40000 0.01250 0.01250 0.00000 0.00000 0.00000
10.00000 0.00000 0.40000 0.20000 0.10000 0.00000 0.00001 0.10000
155925.0 155925.0 105000.0 105000.0 0.0 0.0 0.0 0.1
157500.0 157500.0 157500.0
 763.0 763.0 763.0
 0.0 0.0 0.0
 27.1 27.1 27.1
 0.0 0.0 0.0
 10.2 -2.8 -15.8
 1.0 1.0 1.0
 1.29361 25.00000 0.00000 0.00000 0.00000 0.00000 0.00000 0.00000
0.00000 0.00000 0.00000 0.00000 0.00000 0.00000 0.00000 0.00000
0.00000 0.00000 0.00000 0.00000 0.00000 0.00000 0.00000 0.00000
0.00000 0.00000 0.00000 0.00000 0.00000 0.00000 0.00000 0.00000
0.00000 0.00000 0.00000 0.00000 0.00000 0.00000
9000090000900009000090000
0 0 0 0 0 0 0 0 0 0 0 0 0 0 0
0 0 0 0 0 0 0 0 0 0 0 0 0 0 0 0 0 0 0 0 0 0 0 0 0 0 0 0 0 0 0
-1.80000 0.50000 15.00000 0.80000 0.00000 1.00000 0.00000
0.02000 0.80000 1.00000
1.29361 25.00000 0.00000 0.00000 0.00000 0.00000 0.00000 0.00000
0.00000 0.00000 0.00000 0.00000 0.00000 0.00000 0.00000 0.00000
0.00000 0.00000 0.00000 0.00000 0.00000 0.00000 0.00000 0.00000
0.00000 0.00000 0.00000 0.00000 0.00000 0.00000 0.00000 0.00000
0.00000 0.00000 0.00000 0.00000 0.00000 0.00000 0.00000 0.00000
0.03000 0.03000 0.03000 0.03000 0.03000 0.03000
0.03000 0.03000 0.03000 0.03000 0.03000 0.03000
2.0 1
```

# Appendix B

## B.1 Denton predicted profile loss (percent) at optimum pitch to chord ratio correlation for bilinear interpolation

|            |          | $\alpha_2$ |          |          |          |          |          |          |          |          |          |          |          |          |          |          |          |         |
|------------|----------|------------|----------|----------|----------|----------|----------|----------|----------|----------|----------|----------|----------|----------|----------|----------|----------|---------|
|            |          | 40         | 42.5     | 45       | 47.5     | 50       | 52.5     | 55       | 57.5     | 60       | 62.5     | 65       | 67.5     | 70       | 72.5     | 75       | 77.5     | 80      |
| $\alpha_1$ | -60      | 4.353932   | 4.303301 | 4.252098 | 4.126159 | 4.042921 | 3.978788 | 3.95     | 3.909091 | 3.887878 | 3.908416 | 3.911904 | 3.941176 | 4.06566  | 4.316235 | 4.624542 | 5        | 5       |
|            | -55      | 3.359738   | 3.38609  | 3.35639  | 3.37163  | 3.35639  | 3.34998  | 3.32081  | 3.32659  | 3.33211  | 3.40665  | 3.44073  | 3.50783  | 3.74532  | 3.97178  | 4.360019 | 4.893446 | 5       |
|            | -50      | 2.797328   | 2.83411  | 2.84763  | 2.85148  | 2.86286  | 2.88209  | 2.90858  | 2.93058  | 2.9618   | 3.03786  | 3.16755  | 3.29617  | 3.47537  | 3.78266  | 4.157723 | 4.720336 | 5       |
|            | -45      | 2.395258   | 2.43141  | 2.46071  | 2.47279  | 2.49666  | 2.53087  | 2.60794  | 2.67148  | 2.73509  | 2.83671  | 2.94408  | 3.0886   | 3.32922  | 3.59354  | 3.97925  | 4.547046 | 5       |
|            | -40      | 2.100228   | 2.15824  | 2.20161  | 2.24608  | 2.2887   | 2.33591  | 2.39602  | 2.45252  | 2.50837  | 2.65475  | 2.79946  | 2.94045  | 3.18307  | 3.45562  | 3.88469  | 4.444196 | 5       |
|            | -35      | 1.885498   | 1.93321  | 1.96761  | 2.01936  | 2.08073  | 2.15602  | 2.238    | 2.31212  | 2.38901  | 2.48575  | 2.65483  | 2.83657  | 3.03692  | 3.36781  | 3.79013  | 4.367596 | 5       |
|            | -30      | 1.711991   | 1.77448  | 1.82165  | 1.87853  | 1.92784  | 1.9861   | 2.07157  | 2.17172  | 2.27376  | 2.39054  | 2.51021  | 2.73269  | 2.94435  | 3.28001  | 3.69556  | 4.290996 | 5       |
|            | -25      | 1.538678   | 1.61575  | 1.67569  | 1.74571  | 1.80989  | 1.88143  | 1.94783  | 2.03132  | 2.15852  | 2.29533  | 2.42779  | 2.6288   | 2.8699   | 3.1922   | 3.601    | 4.214396 | 5       |
|            | -20      | 1.415058   | 1.47208  | 1.52974  | 1.61289  | 1.69194  | 1.77676  | 1.85446  | 1.93522  | 2.04327  | 2.20012  | 2.3501   | 2.52492  | 2.79545  | 3.1044   | 3.50644  | 4.137806 | 4.99081 |
|            | -15      | 1.305738   | 1.36897  | 1.42373  | 1.48634  | 1.57399  | 1.67209  | 1.7611   | 1.85185  | 1.95274  | 2.10491  | 2.2724   | 2.44925  | 2.721    | 3.01659  | 3.44545  | 4.061206 | 4.93586 |
|            | -10      | 1.196408   | 1.26586  | 1.32794  | 1.39528  | 1.46748  | 1.56742  | 1.66774  | 1.76847  | 1.87706  | 2.0097   | 2.19471  | 2.38248  | 2.64654  | 2.95075  | 3.38691  | 3.98842  | 4.88092 |
|            | -5       | 1.087088   | 1.16275  | 1.23215  | 1.30422  | 1.38023  | 1.46948  | 1.57437  | 1.6851   | 1.80139  | 1.93441  | 2.11701  | 2.31571  | 2.57209  | 2.89003  | 3.32837  | 3.9308   | 4.82597 |
|            | 0        | 0.979166   | 1.059645 | 1.136363 | 1.213168 | 1.292981 | 1.383721 | 1.482652 | 1.601727 | 1.725718 | 1.861386 | 2.039318 | 2.248944 | 2.497819 | 2.829308 | 3.269841 | 3.873177 | 4.77103 |
|            | 5        | 0.876738   | 0.95618  | 1.04059  | 1.12212  | 1.20574  | 1.29797  | 1.39736  | 1.51837  | 1.65005  | 1.78837  | 1.96228  | 2.18218  | 2.4289   | 2.76859  | 3.21131  | 3.81556  | 4.71609 |
|            | 10       | 0.774318   | 0.85222  | 0.93884  | 1.03108  | 1.11851  | 1.21222  | 1.31208  | 1.43156  | 1.57439  | 1.71536  | 1.88589  | 2.11543  | 2.35998  | 2.70788  | 3.15278  | 3.75795  | 4.66116 |
|            | 15       | 0.671898   | 0.74826  | 0.83268  | 0.92744  | 1.03127  | 1.12647  | 1.22679  | 1.34377  | 1.49837  | 1.64234  | 1.8095   | 2.04867  | 2.29106  | 2.64717  | 3.09426  | 3.70034  | 4.60622 |
|            | 20       | 0.569478   | 0.6443   | 0.72652  | 0.81727  | 0.92546  | 1.04073  | 1.14151  | 1.25598  | 1.40074  | 1.56933  | 1.73311  | 1.97489  | 2.22214  | 2.58646  | 3.03573  | 3.64273  | 4.55129 |
|            | 25       | 0.437148   | 0.54034  | 0.62037  | 0.7071   | 0.80927  | 0.93386  | 1.05622  | 1.16819  | 1.30311  | 1.49419  | 1.65671  | 1.88217  | 2.15322  | 2.52575  | 2.96475  | 3.58511  | 4.49426 |
|            | 30       | 0.241718   | 0.37205  | 0.51421  | 0.59692  | 0.69308  | 0.80787  | 0.95174  | 1.0804   | 1.20548  | 1.37897  | 1.58032  | 1.78945  | 2.0843   | 2.44103  | 2.87423  | 3.5275   | 4.40774 |
| 35         | 0.046288 | 0.16295    | 0.30349  | 0.47048  | 0.57689  | 0.68189  | 0.81011  | 0.98636  | 1.10785  | 1.26375  | 1.50393  | 1.69673  | 2.01539  | 2.33861  | 2.78371  | 3.4441   | 4.32122  |         |
| 40         | -0.14914 | -0.04615   | 0.07659  | 0.22494  | 0.40588  | 0.5559   | 0.66848  | 0.82417  | 1.01022  | 1.14852  | 1.36159  | 1.60401  | 1.89484  | 2.23619  | 2.69319  | 3.33712  | 4.23471  |         |
| 45         | -0.34457 | -0.25525   | -0.15031 | -0.02059 | 0.1276   | 0.32909  | 0.52685  | 0.66198  | 0.82837  | 1.0333   | 1.21566  | 1.51129  | 1.75945  | 2.13377  | 2.60267  | 3.23014  | 4.14819  |         |
| 50         | -0.58844 | -0.46435   | -0.37721 | -0.26613 | -0.15067 | 0.02183  | 0.22204  | 0.49948  | 0.63667  | 0.83088  | 1.06973  | 1.32011  | 1.62406  | 2.03135  | 2.51216  | 3.12317  | 4.06168  |         |
| 55         | -1.03526 | -0.9078    | -0.73282 | -0.52601 | -0.42894 | -0.28543 | -0.12095 | 0.09056  | 0.36769  | 0.593    | 0.84263  | 1.11527  | 1.47429  | 1.83493  | 2.31761  | 3.01619  | 3.93951  |         |
| 60         | -1.84473 | -1.49927   | -1.36879 | -1.1239  | -0.90776 | -0.70223 | -0.46393 | -0.31837 | -0.0932  | 0.17297  | 0.54123  | 0.83029  | 1.16703  | 1.59705  | 2.10691  | 2.7847   | 3.72882  |         |



## Appendix C

### Mean Line Tool Program Constants

|                       |  |
|-----------------------|--|
| Rowdata(bladerow, 0)  | Throat opening                               |
| Rowdata(bladerow, 1)  | BS radius of curvature                       |
| Rowdata(bladerow, 2)  | Tip clearance                                |
| Rowdata(bladerow, 3)  | Tip clearance turbine factor                 |
| Rowdata(bladerow, 4)  | Unshrouded turbine factor                    |
| Rowdata(bladerow, 5)  | Throat area                                  |
| Rowdata(bladerow, 6)  | Pitch  |
| Rowdata(bladerow, 7)  | Blade inlet angle                            |
| Rowdata(bladerow, 8)  | Chord  |
| Rowdata(bladerow, 9)  | Max thickness                                |
| Rowdata(bladerow, 10) | Trailing edge thickness                      |
| Rowgeom(0, 0)         | Nozzle inlet hub diameter                    |
| Rowgeom(0, 1)         | Turbine inlet hub diameter                   |
| Rowgeom(0, 2)         | Turbine outlet hub diameter                  |
| Rowgeom(1, 0)         | Nozzle inlet tip diameter                    |
| Rowgeom(1, 1)         | Turbine inlet tip diameter                   |
| Rowgeom(1, 2)         | Turbine outlet tip diameter                  |
| nozzleout(0, 0)       | Stator gas outlet angle                      |
| nozzleout(1, 0)       | Stator Outlet velocity                       |
| nozzleout(2, 0)       | Stator Outlet temperature                    |
| nozzleout(3, 0)       | Stator Outlet pressure                       |
| nozzleout(4, 0)       | Stator Outlet Mach number                    |
| turbineout(0, 0)      | Turbine gas outlet angle                     |
| turbineout(1, 0)      | Turbine Outlet velocity                      |
| turbineout(2, 0)      | Turbine Outlet temperature                   |
| turbineout(3, 0)      | Turbine Outlet pressure                      |
| turbineout(4, 0)      | Turbine Outlet Mach number                   |
| alpha2                | Gas outlet angle corrected for tip clearance |
| alpha3                | Gas outlet angle at M = 1                    |
| alpha4                | Gas outlet angle at zero tip clearance       |

### C.1 Kacker and Okapuu VBA code Loss Model

|                      |   |
|----------------------|---|
| Dim sc As Double     | pitch to chord ratio                            |
| Dim tc As Double     | max thickness to chord ratio                    |
| Dim a9 As Double     | Gas flow angle with zero tip clearance          |
| Dim am As Double     | Intermediate secondary loss term                |
| Dim p As Double      | Gas outlet angle radians                        |
| Dim p2 As Double     | Intermediate term                               |
| Dim p3 As Double     | Intermediate term                               |
| Dim tecorr As Double | Trailing edge correction                        |
| Dim a75 As Double    | Incidence angle term at $s/c = 0.75$ (Fig 2-16) |
| Dim sc2 As Double    | pitch to chord ratio correction                 |
| Dim i75 As Double    | Incidence angle term at $s/c = 0.75$ (Fig 2-17) |
| Dim dis As Double    | incidence intermediate term                     |
| Dim dis1 As Double   | incidence intermediate term                     |
| Dim dis2 As Double   | incidence intermediate term                     |
| Dim ai As Double     | Inlet gas flow angle                            |
| Dim CLsc As Double   | Intermediate secondary loss term                |
| Dim d1 As Double     | Ratio of incidence and stalling incidence       |

Dim LossCoeff As Collection  
Dim Loss As Variant  
Set LossCoeff = New Collection

Reference diameter

LossCoeff.Add "" & 0.25 \* (rowgeom(i1 + 1, 1) + rowgeom(i1, 1) - rowgeom(i1 + 1, 0) - rowgeom(i1, 0)) & "", "bldhgt" & i1 & ""

Profile loss coefficient (Yp)

sc = rowdata(i1, 6) / rowdata(i1, 8)  
tc = rowdata(i1, 9) / rowdata(i1, 8)  
a9 = Application.WorksheetFunction.Degrees(alpha4(i1, 0))  
p = Application.WorksheetFunction.Radians(a9) \* 0.57296  
p2 = p \* p  
p3 = p2 \* p

If Abs(Application.WorksheetFunction.Radians(a9)) > 0.01 Then  
r = (rowdata(i1, 7) \* 0.3) / a9  
Else  
r = 0  
End If

TC upper and lower limits

If tc < 0.15 Then  
tc = 0.15  
End If

If tc > 0.25 Then  
tc = 0.25  
End If

tecorr = 0.914 + 3.86 \* rowdata(i1, 10) / rowdata(i1, 6) + 21.6 \* (rowdata(i1, 10) / rowdata(i1, 6)) ^ 2

LossCoeff.Add "" & 0.120684 - 0.159513 \* p - 0.518933 \* p2 - 0.457871 \* p3 + (-0.113447 + 1.88405 \* p + 5.26857 \* p2 + 4.21486 \* p3) \*  
sc - (0.501061 + 6.27734 \* p + 15.6447 \* p2 + 11.7592 \* p3) \* sc ^ 2 + (0.434537 + 4.01075 \* p + 9.61499 \* p2 + 6.96877 \* p3) \* sc ^ 3 & "",  
"ypbi0" & i1 & "" Trailing edge thickness correction Fig. 9

LossCoeff.Add "" & 0.376147 + 0.411941 \* p + 1.01691 \* p2 + 0.640577 \* p3 - (1.35419 + 3.41232 \* p + 7.4935 \* p2 + 4.54488 \* p3) \* sc +  
(1.81574 + 5.63873 \* p + 10.499 \* p2 + 4.27037 \* p3) \* sc ^ 2 - (0.948148 + 3.88398 \* p + 7.04043 \* p2 + 3.00627 \* p3) \* sc ^ 3 & "",  
"ypbia2" & i1 & ""

LossCoeff.Add "" & (((LossCoeff.Item("ypbi0" & i1 & "")) + r \* r \* (LossCoeff.Item("ypbia2" & i1 & "")) - LossCoeff.Item("ypbi0" & i1 & ""))) \*  
(tc \* 5) ^ -r) \* tecorr & "", "Yp" & i1 & ""

If LossCoeff.Item("Yp" & i1 & "") < 0.02 Then  
LossCoeff.Remove ("Yp" & i1 & "")  
LossCoeff.Add "" & 0.02 \* tecorr & "", "Yp" & i1 & ""  
End If

Stalling incidence

a75 = 57.296 \* Application.WorksheetFunction.Radians(a9) / (1.3 - 0.4 \* sc)

If Abs(a75) > 0.01 Then  
sc2 = (rowdata(i1, 7) \* 0.3) / a75  
Else  
sc2 = 0  
End If

i75 = 0.174819 + 0.865909 \* p + 1.71529 \* p2 + 0.501105 \* p3 + (-0.0128059 - 0.057039 \* p + 0.305076 \* p2 + 0.354952 \* p3) \* sc2 -  
(0.495033 + 3.11324 \* p + 5.91235 \* p2 + 3.0187 \* p3) \* sc2 ^ 2 - (0.180332 + 1.2849 \* p + 2.80671 \* p2 + 1.83452 \* p3) \* sc2 ^ 3  
i75 = 180 \* i75  
dis = -37.47 \* sc ^ 2 + 20.15 \* sc + 6  
dis1 = dis  
If (sc - 0.75) > 0 Then

```

If (a9 + 50) >= 0 Then
dis2 = 41.75 * sc ^ 2 - 98.1 * sc + 50.15
dis = dis1 - (a9 + 50) * (dis1 - dis2) / 10
Else
dis2 = -40 * sc ^ 2 + 11 * sc + 14.2
dis = dis1 - (a9 + 50) * (dis1 - dis2) / 10
End If
End If
istall = (dis + i75) / 57.296
If i1 = 0 Then
ai = 0
Else
ai = nozzleout(0, 0)
End If
ince = ai - Application.WorksheetFunction.Radians(rowdata(i1, 7) * 0.3)
d1 = ince / istall

Profile loss change with incidence (Xi)

If d1 < 0 Then
Ypt = ((((((0.023643 * d1) + 0.351157) * d1) - 0.265154) * d1) + 0.977649) * LossCoeff.Item("Yp" & i1 & ""))
Else
Ypt = ((((((0.993138 * d1) + 0.030551) * d1) + 0.022075) * d1) + 0.996574) * LossCoeff.Item("Yp" & i1 & ""))
End If

Secondary Loss (Ysk)

Dim a10 As Double

If d1 < -1.5 Then
d1 = -1.5
End If

If d1 > 1 Then
d1 = 1
End If

If i1 = 0 Then
a10 = 0
Else
a10 = d1 * istall
End If

Dim ang_m As Double
ang_m = Atn(0.5 * (Tan(a10) + Tan(alpha4(i1, 0))))

CLsc = 2 * (Tan(a10) - Tan(alpha4(i1, 0))) * Cos(ang_m)

Ysk = 0.0334 * ((rowdata(i1, 8) * 0.0254) / (LossCoeff.Item("bldhgt" & i1 & "") * 0.0254)) * (Cos(alpha4(i1, 0)) /
Cos(Application.WorksheetFunction.Radians(rowdata(i1, 7) * 0.3))) * CLsc ^ 2 * (Cos(alpha4(i1, 0)) ^ 2 / (Cos(ang_m) ^ 3))

Yt = Ypt + Ysk

Kp

Find Inlet Mach number

If i1 = 0 Then

Dim a1 As Double
a1 = Application.WorksheetFunction.Pi() * ((rowgeom(0, 0) * 0.0254) ^ 2) / 4

```



```

Dim a2 As Double
a2 = Application.WorksheetFunction.Pi() * ((rowgeom(0, 1) * 0.0254) ^ 2) / 4

Dim Annulus As Double
Annulus = a2 - a1

Dim rho As Double
rho = (Pi * 6.89 * 1000) / (ti * 287.04)

Dim v7 As Double
v7 = w / (rho * Annulus)

Dim Min1 As Double
Min1 = v7 / Sqr(g1 * 3088.6 * ti)

End If

Dim Min As Double
Dim Mout As Double
If i1 = 0 Then
Min = Min1
Mout = m
Else
Min = nozzleout(4, 0)
Mout = m
End If

Evaluate Kp

Dim Kp As Double

If m > 0.2 Then
Kp = 1 - 1.25 * (Mout - 0.2) * (Min / Mout) ^ 2
Else
Kp = 1
End If

Dim RhRt As Double

RhRt = rowgeom(i1, 0) / rowgeom(i1, 1)

M1Hub

Dim M1Hub As Double

If i1 = 0 Then
M1Hub = Min * (((4.09223572657754 * RhRt) - 6.69433665602768) * RhRt) + 3.72628470188226)
Else
M1Hub = Min * (((6.20462437817264 * RhRt) - 11.6399297569545) * RhRt) + 6.46172992099636)
End If

YShock

Dim Pin As Double
Dim Pout As Double

If i1 = 0 Then
Pin = Pi
Pout = nozzleout(3, 0)
Else
Pin = nozzleout(3, 0)
Pout = turbineout(3, 0)

```

End If

Dim Ysh As Double

$$Ysh = 0.75 * (If(M1Hub < 0.4, 0.4, M1Hub) - 0.4) ^ 1.75 * (rowgeom(i1, 0) / rowgeom(i1, 1)) * (Pin / Pout) * ((1 - (1 + ((g1 - 1) / 2) * Min ^ 2) ^ (g1 / (g1 - 1))) / (1 - (1 + ((g1 - 1) / 2) * Mout ^ 2) ^ (g1 / (g1 - 1))))$$

Calculate new Profile loss

Dim YpKO

$$YpKO = 0.914 * (2 / 3 * Ypt * Kp + Ysh)$$

K3

Dim Axc As Double

If i1 = 0 Then

Axc = Worksheets("Input").Range("B29").Value

Else

Axc = Worksheets("Input").Range("C29").Value

End If

Dim K3 As Double

$$K3 = 1 - (Axc / (LossCoeff.Item("bldhgt" & i1 & "") * 0.0254)) ^ 2 * (1 - Kp)$$

Dim Xar As Double

If ((rowgeom(i1, 1) - rowgeom(i1, 0)) / 2) / rowdata(i1, 8) <= 2 Then

$$Xar = 1 - 0.25 * Sqr(2 - ((rowgeom(i1, 1) - rowgeom(i1, 0)) / 2) / rowdata(i1, 8))$$

Else

Xar = 1

End If

Calculate new Secondary loss

Dim YsKO As Double

$$YsKO = 1.2 * K3 * Xar * Ysk$$

Calculate Trailing Edge Loss

Dim tou As Double

$$tou = rowdata(i1, 10) / rowdata(i1, 0)$$

Trailing edge Beta=0

Dim DtetB0 As Double

$$DtetB0 = ((((-1.01708866742956 * tou) + 1.17997684231952) * tou) + 4.00468287252138E-02) * tou - 1.89626026330796E-04$$

Trailing edge Beta=alpha2

Dim DtetBa As Double

$$DtetBa = ((((-0.643405817332678 * tou) + 0.696695855185969) * tou) + 7.27785820593739E-03) * tou + 5.08558021152712E-04$$

Trailing edge loss

Dim Dtet As Double

$$Dtet = DtetB0 + r ^ 2 * (DtetBa - DtetB0)$$

Dim YteKO As Double

$$YteKO = ((1 - ((g1 - 1) / 2) * m ^ 2 * ((1 / (1 - Dtet)) - 1)) ^ -(g1 / (g1 - 1)) - 1) / (1 - (1 + ((g1 - 1) / 2) * m ^ 2) ^ -(g1 / (g1 - 1)))$$

Reynolds Number

Dynamic viscosity

Dim mu As Double

```

If i1 = 0 Then
mu = ((((((((-6.0671918E-12 * (nozzleout(2, 0) - 273.15)) + 2.212997838519E-08) * (nozzleout(2, 0) - 273.15)) - 3.46909333623785E-05) *
(nozzleout(2, 0) - 273.15)) + 4.95001977743888E-02) * (nozzleout(2, 0) - 273.15)) + 16.9760680267161) * 10 ^ -6
Else
mu = ((((((((-6.0671918E-12 * (turbineout(2, 0) - 273.15)) + 2.212997838519E-08) * (turbineout(2, 0) - 273.15)) - 3.46909333623785E-05) *
(turbineout(2, 0) - 273.15)) + 4.95001977743888E-02) * (turbineout(2, 0) - 273.15)) + 16.9760680267161) * 10 ^ -6
End If

Density

Dim rho2 As Double

If i1 = 0 Then
rho2 = (nozzleout(3, 0) * 6.89 * 1000 + 100000) / (nozzleout(2, 0) * 287)
Else
rho2 = (turbineout(3, 0) * 6.89 * 1000 + 100000) / (turbineout(2, 0) * 287)
End If

Dim Re2 As Double
Re2 = (rho2 * (vo * 0.3048 * (rowdata(i1, 8) * 0.0254)) / mu)

Dim Xre As Double
Xre = IIf(Re2 <= 2 * 10 ^ 5, (Re2 / (2 * 10 ^ 5)) ^ -0.4, IIf(Re2 > 10 ^ 6, (Re2 / (10 ^ 6)) ^ -0.2, 1))

Tip Clearance Loss

Dim deff As Double
Dim efftt3 As Double

deff = 0.93 * (rowgeom(1, i1) / refdia) * (1 / (LossCoeff.Item("bldhgt" & i1 & "") * Cos(alpha2(i1, 0)))) * efftt1 * rowdata(i1, 2)

efftt3 = efftt1 - Abs(deff)

Yt2clr = Yt

Do
countclr = countclr + 1
Yt2clr = Yt2clr + 0.0001
If countclr > 1000 Then
Ytclr = 0.1
Exit Sub
End If

If efftt1 < 0 > 150 Then
Ytclr = 0.1
Exit Sub
End If

Loop Until Abs(efftt1 - efftt3) < 0.01

Ytclr = Yt2clr - Yt

Yt = Xre * YpKO + YsKO + YteKO + Ytclr

End Sub

```

## C.2 Denton VBA code for Loss Model

```
Dim YpDc As Double
Dim YtcDc As Double
Dim YteDc As Double
Dim YsD As Double
Dim convert As Double

convert = (1 + 0.5 * (g1 - 1) * m ^ 2) ^ (1 / (g1 - 1))

Dim LossCoeff As Collection
Dim Loss As Variant
Set LossCoeff = New Collection
Reference Diameter
LossCoeff.Add "" & 0.25 * (rowgeom(i1 + 1, 1) + rowgeom(i1, 1) - rowgeom(i1 + 1, 0) - rowgeom(i1, 0)) & "", "bldhgt" & i1 & ""

Profile Loss (YpD)

Input

Dim x7 As Double
Dim y7 As Double

x7 = -alpha2(i1, 0)

If i1 = 0 Then
y7 = 0
Else
y7 = -Application.WorksheetFunction.Degrees(nozzleout(0, 0))
End If

If y7 > 60 Then
y7 = 60
End If

If y7 < -60 Then
y7 = -60
End If

Dim x1 As Double
Dim x2 As Double
Dim y1 As Double
Dim y2 As Double
Dim q11 As Double
Dim q12 As Double
Dim q21 As Double
Dim q22 As Double

If y7 = 60 Then

x1 = Application.WorksheetFunction.Index(Worksheets("Denton Contour Plots").Range("C4:S4"),
Application.WorksheetFunction.Match(x7, Worksheets("Denton Contour Plots").Range("C4:S4"), 1))
x2 = Application.WorksheetFunction.Index(Worksheets("Denton Contour Plots").Range("C4:S4"),
Application.WorksheetFunction.Match(x7, Worksheets("Denton Contour Plots").Range("C4:S4"), 1) + 1)
y1 = Application.WorksheetFunction.Index(Worksheets("Denton Contour Plots").Range("B5:B29"),
Application.WorksheetFunction.Match(y7, Worksheets("Denton Contour Plots").Range("B5:B29"), 1) - 1)
y2 = Application.WorksheetFunction.Index(Worksheets("Denton Contour Plots").Range("B5:B29"),
Application.WorksheetFunction.Match(y7, Worksheets("Denton Contour Plots").Range("B5:B29"), 1))

Else
```

```

x1 = Application.WorksheetFunction.Index(Worksheets("Denton Contour Plots").Range("C4:S4"),
Application.WorksheetFunction.Match(x7, Worksheets("Denton Contour Plots").Range("C4:S4"), 1))
x2 = Application.WorksheetFunction.Index(Worksheets("Denton Contour Plots").Range("C4:S4"),
Application.WorksheetFunction.Match(x7, Worksheets("Denton Contour Plots").Range("C4:S4"), 1) + 1)
y1 = Application.WorksheetFunction.Index(Worksheets("Denton Contour Plots").Range("B5:B29"),
Application.WorksheetFunction.Match(y7, Worksheets("Denton Contour Plots").Range("B5:B29"), 1))
y2 = Application.WorksheetFunction.Index(Worksheets("Denton Contour Plots").Range("B5:B29"),
Application.WorksheetFunction.Match(y7, Worksheets("Denton Contour Plots").Range("B5:B29"), 1) + 1)

```

End If

```

q11 = Application.WorksheetFunction.Index(Worksheets("Denton Contour Plots").Range("C5:S29"),
Application.WorksheetFunction.Match(y1, Worksheets("Denton Contour Plots").Range("B5:B29"), 0),
Application.WorksheetFunction.Match(x1, Worksheets("Denton Contour Plots").Range("C4:S4"), 0))
q12 = Application.WorksheetFunction.Index(Worksheets("Denton Contour Plots").Range("C5:S29"),
Application.WorksheetFunction.Match(y2, Worksheets("Denton Contour Plots").Range("B5:B29"), 0),
Application.WorksheetFunction.Match(x1, Worksheets("Denton Contour Plots").Range("C4:S4"), 0))
q21 = Application.WorksheetFunction.Index(Worksheets("Denton Contour Plots").Range("C5:S29"),
Application.WorksheetFunction.Match(y1, Worksheets("Denton Contour Plots").Range("B5:B29"), 0),
Application.WorksheetFunction.Match(x2, Worksheets("Denton Contour Plots").Range("C4:S4"), 0))
q22 = Application.WorksheetFunction.Index(Worksheets("Denton Contour Plots").Range("C5:S29"),
Application.WorksheetFunction.Match(y2, Worksheets("Denton Contour Plots").Range("B5:B29"), 0),
Application.WorksheetFunction.Match(x2, Worksheets("Denton Contour Plots").Range("C4:S4"), 0))

```

Dim YpD As Double

If x7 < 40 Or x7 > 80 Then

YpD = 0.02

Else

YpD = (1 / ((x2 - x1) \* (y2 - y1)) \* (q11 \* (x2 - x7) \* (y2 - y7) + q21 \* (x7 - x1) \* (y2 - y7) + q12 \* (x2 - x7) \* (y7 - y1) + q22 \* (x7 - x1) \* (y7 - y1))) / 100

End If

Tip Clearance Loss (YtcD)

Input

If i1 = 0 Then

Else

Dim x8 As Double

Dim y8 As Double

x8 = -alpha2(i1, 0)

y8 = -Application.WorksheetFunction.Degrees(nozzleout(0, 0))

If y8 > 60 Then

y8 = 60

End If

If y8 < -60 Then

y8 = -60

End If

Dim x81 As Double

Dim x82 As Double

Dim y81 As Double

Dim y82 As Double

Dim q811 As Double

Dim q812 As Double

Dim q821 As Double  
Dim q822 As Double

If y7 = 60 Then

```
x81 = Application.WorksheetFunction.Index(Worksheets("Denton Contour Plots").Range("C33:AF33"),  
Application.WorksheetFunction.Match(x8, Worksheets("Denton Contour Plots").Range("C33:AF33"), 1))  
x82 = Application.WorksheetFunction.Index(Worksheets("Denton Contour Plots").Range("C33:AF33"),  
Application.WorksheetFunction.Match(x8, Worksheets("Denton Contour Plots").Range("C33:AF33"), 1) + 1)  
y81 = Application.WorksheetFunction.Index(Worksheets("Denton Contour Plots").Range("B34:B58"),  
Application.WorksheetFunction.Match(y8, Worksheets("Denton Contour Plots").Range("B34:B58"), 1) - 1)  
y82 = Application.WorksheetFunction.Index(Worksheets("Denton Contour Plots").Range("B34:B58"),  
Application.WorksheetFunction.Match(y8, Worksheets("Denton Contour Plots").Range("B34:B58"), 1))
```

Else

```
x81 = Application.WorksheetFunction.Index(Worksheets("Denton Contour Plots").Range("C33:AF33"),  
Application.WorksheetFunction.Match(x8, Worksheets("Denton Contour Plots").Range("C33:AF33"), 1))  
x82 = Application.WorksheetFunction.Index(Worksheets("Denton Contour Plots").Range("C33:AF33"),  
Application.WorksheetFunction.Match(x8, Worksheets("Denton Contour Plots").Range("C33:AF33"), 1) + 1)  
y81 = Application.WorksheetFunction.Index(Worksheets("Denton Contour Plots").Range("B34:B58"),  
Application.WorksheetFunction.Match(y8, Worksheets("Denton Contour Plots").Range("B34:B58"), 1))  
y82 = Application.WorksheetFunction.Index(Worksheets("Denton Contour Plots").Range("B34:B58"),  
Application.WorksheetFunction.Match(y8, Worksheets("Denton Contour Plots").Range("B34:B58"), 1) + 1)
```

End If

```
q811 = Application.WorksheetFunction.Index(Worksheets("Denton Contour Plots").Range("C34:AF58"),  
Application.WorksheetFunction.Match(y81, Worksheets("Denton Contour Plots").Range("B34:B58"), 0),  
Application.WorksheetFunction.Match(x81, Worksheets("Denton Contour Plots").Range("C33:AF33"), 0))  
q812 = Application.WorksheetFunction.Index(Worksheets("Denton Contour Plots").Range("C34:AF58"),  
Application.WorksheetFunction.Match(y82, Worksheets("Denton Contour Plots").Range("B34:B58"), 0),  
Application.WorksheetFunction.Match(x81, Worksheets("Denton Contour Plots").Range("C33:AF33"), 0))  
q821 = Application.WorksheetFunction.Index(Worksheets("Denton Contour Plots").Range("C34:AF58"),  
Application.WorksheetFunction.Match(y81, Worksheets("Denton Contour Plots").Range("B34:B58"), 0),  
Application.WorksheetFunction.Match(x82, Worksheets("Denton Contour Plots").Range("C33:AF33"), 0))  
q822 = Application.WorksheetFunction.Index(Worksheets("Denton Contour Plots").Range("C34:AF58"),  
Application.WorksheetFunction.Match(y82, Worksheets("Denton Contour Plots").Range("B34:B58"), 0),  
Application.WorksheetFunction.Match(x82, Worksheets("Denton Contour Plots").Range("C33:AF33"), 0))
```

Dim YtcD As Double

$$YtcD = (1 / ((x82 - x81) * (y82 - y81)) * (q811 * (x82 - x8) * (y82 - y8) + q821 * (x8 - x81) * (y82 - y8) + q812 * (x82 - x8) * (y8 - y81) + q822 * (x8 - x81) * (y8 - y81))) / 100$$

End If

Secondary Loss (YsD)

Dim a10 As Double

If i1 = 0 Then

a10 = 0

Else

a10 = nozzleout(0, 0)

End If

Dim ang\_m As Double

$$ang\_m = \text{Atn}(0.5 * (\text{Tan}(a10) + \text{Tan}(\text{alpha4}(i1, 0))))$$

Dim CLsc As Double

$$CLsc = 2 * (\text{Tan}(a10) - \text{Tan}(\text{alpha4}(i1, 0))) * \text{Cos}(ang\_m)$$

$$YsD = 0.375 * 0.0334 * ((rowdata(i1, 8) * 0.0254) / (LossCoeff.Item("bldhgt" & i1 & "") * 0.0254)) * (Cos(alpha4(i1, 0) / Cos(Application.WorksheetFunction.Radians(rowdata(i1, 7) * 0.3))) * CLsc ^ 2 * (Cos(alpha4(i1, 0)) ^ 2 / (Cos(ang_m)) ^ 3))$$

YpDc = YpD \* convert  
 YtcDc = YtcD \* convert

YtD = YpDc + YtcDc + YsD

Trailing Edge Loss (YteD)

Dynamic viscosity

Dim mu As Double

If i1 = 0 Then

$$\mu = ((((((((-6.0671918E-12 * (nozzleout(2, 0) - 273.15)) + 2.212997838519E-08) * (nozzleout(2, 0) - 273.15)) - 3.46909333623785E-05) * (nozzleout(2, 0) - 273.15)) + 4.95001977743888E-02) * (nozzleout(2, 0) - 273.15)) + 16.9760680267161) * 10 ^ -6$$

Else

$$\mu = ((((((((-6.0671918E-12 * (turbineout(2, 0) - 273.15)) + 2.212997838519E-08) * (turbineout(2, 0) - 273.15)) - 3.46909333623785E-05) * (turbineout(2, 0) - 273.15)) + 4.95001977743888E-02) * (turbineout(2, 0) - 273.15)) + 16.9760680267161) * 10 ^ -6$$

End If

Density

Dim rho As Double

If i1 = 0 Then

$$\rho = (nozzleout(3, 0) * 6.89 * 1000 + 100000) / (nozzleout(2, 0) * 287)$$

Else

$$\rho = (turbineout(3, 0) * 6.89 * 1000 + 100000) / (turbineout(2, 0) * 287)$$

End If

Dim Re As Double

$$Re = (\rho * (vo) * 0.3048 * (rowdata(i1, 8) * 0.0254)) / \mu$$

Dim theta As Double

$$\theta = 0.016 / Sqr(Re) ^ (1 / 7) * (rowdata(i1, 8) * 0.0254)$$

Dim sigma As Double

$$\sigma = 0.02 / Sqr(Re) ^ (1 / 7) * (rowdata(i1, 8) * 0.0254)$$

Dim YteD As Double

$$YteD = (((-0.15 * (rowdata(i1, 10) * 0.0254)) / (rowdata(i1, 0) * 0.0254)) + ((2 * \theta) / (rowdata(i1, 0) * 0.0254)) + ((\sigma + (rowdata(i1, 10) * 0.0254)) / (rowdata(i1, 0) * 0.0254)) ^ 2) / 100$$

YteDc = YteD \* convert

Yt = YtD + YteDc

## C.3 Craig and Cox VBA Code for Loss Model

Flow angle conversion

```
If i1 = 0 Then
alphacc1 = 90
Else
alphacc1 = 90 - Application.WorksheetFunction.Degrees(nozzleout(0, 0))
End If
```

```
If alphacc1 > 140 Then
alphacc1 = 140
End If
```

```
alphacc2 = (alpha2(i1, 0) + 90)
```

Backbone length

```
Bb = (0.5 * Sqr(rowdata(i1, 8) ^ 2 + 16 * rowdata(i1, 9) ^ 2) + (rowdata(i1, 8) ^ 2 / (8 * rowdata(i1, 9))) * Log((4 * rowdata(i1, 9) + Sqr(rowdata(i1, 8) ^ 2 + 16 * rowdata(i1, 9) ^ 2)) / rowdata(i1, 8))) * 0.0254
```

Contraction Ratio

```
Dim CRLossRngx As Range
Dim CRLossRngyA As Range
Dim CRLossRngyB As Range
Dim CRLossRngyC As Range
Dim CRLossRngyD As Range
Dim CRLossRngyE As Range
```

```
Set CRLossRngx = Worksheets("CraigCox Corr").Range("P5:P13")
Set CRLossRngyA = Worksheets("CraigCox Corr").Range("Q5:Q13")
Set CRLossRngyB = Worksheets("CraigCox Corr").Range("R5:R13")
Set CRLossRngyC = Worksheets("CraigCox Corr").Range("S5:S13")
Set CRLossRngyD = Worksheets("CraigCox Corr").Range("T5:T13")
Set CRLossRngyE = Worksheets("CraigCox Corr").Range("U5:U13")
```

1st Polynomial Factors

```
Dim CRLossA(6, 0) As Double
```

```
CRLossA(0, 0) = Application.Index(Application.LinEst(CRLossRngyA, Application.Power(CRLossRngx, Array(1, 2, 3, 4, 5, 6))), 1, 1)
CRLossA(1, 0) = Application.Index(Application.LinEst(CRLossRngyA, Application.Power(CRLossRngx, Array(1, 2, 3, 4, 5, 6))), 1, 2)
CRLossA(2, 0) = Application.Index(Application.LinEst(CRLossRngyA, Application.Power(CRLossRngx, Array(1, 2, 3, 4, 5, 6))), 1, 3)
CRLossA(3, 0) = Application.Index(Application.LinEst(CRLossRngyA, Application.Power(CRLossRngx, Array(1, 2, 3, 4, 5, 6))), 1, 4)
CRLossA(4, 0) = Application.Index(Application.LinEst(CRLossRngyA, Application.Power(CRLossRngx, Array(1, 2, 3, 4, 5, 6))), 1, 5)
CRLossA(5, 0) = Application.Index(Application.LinEst(CRLossRngyA, Application.Power(CRLossRngx, Array(1, 2, 3, 4, 5, 6))), 1, 6)
CRLossA(6, 0) = Application.Index(Application.LinEst(CRLossRngyA, Application.Power(CRLossRngx, Array(1, 2, 3, 4, 5, 6))), 1, 7)
```

```
Dim CRLossB(6, 0) As Double
```

```
CRLossB(0, 0) = Application.Index(Application.LinEst(CRLossRngyB, Application.Power(CRLossRngx, Array(1, 2, 3, 4, 5, 6))), 1, 1)
CRLossB(1, 0) = Application.Index(Application.LinEst(CRLossRngyB, Application.Power(CRLossRngx, Array(1, 2, 3, 4, 5, 6))), 1, 2)
CRLossB(2, 0) = Application.Index(Application.LinEst(CRLossRngyB, Application.Power(CRLossRngx, Array(1, 2, 3, 4, 5, 6))), 1, 3)
CRLossB(3, 0) = Application.Index(Application.LinEst(CRLossRngyB, Application.Power(CRLossRngx, Array(1, 2, 3, 4, 5, 6))), 1, 4)
CRLossB(4, 0) = Application.Index(Application.LinEst(CRLossRngyB, Application.Power(CRLossRngx, Array(1, 2, 3, 4, 5, 6))), 1, 5)
CRLossB(5, 0) = Application.Index(Application.LinEst(CRLossRngyB, Application.Power(CRLossRngx, Array(1, 2, 3, 4, 5, 6))), 1, 6)
CRLossB(6, 0) = Application.Index(Application.LinEst(CRLossRngyB, Application.Power(CRLossRngx, Array(1, 2, 3, 4, 5, 6))), 1, 7)
```

```
Dim CRLossC(6, 0) As Double
```

```
CRLossC(0, 0) = Application.Index(Application.LinEst(CRLossRngyC, Application.Power(CRLossRngx, Array(1, 2, 3, 4, 5, 6))), 1, 1)
CRLossC(1, 0) = Application.Index(Application.LinEst(CRLossRngyC, Application.Power(CRLossRngx, Array(1, 2, 3, 4, 5, 6))), 1, 2)
CRLossC(2, 0) = Application.Index(Application.LinEst(CRLossRngyC, Application.Power(CRLossRngx, Array(1, 2, 3, 4, 5, 6))), 1, 3)
```



CRLossC(3, 0) = Application.Index(Application.LinEst(CRLossRngyC, Application.Power(CRLossRngx, Array(1, 2, 3, 4, 5, 6))), 1, 4)  
 CRLossC(4, 0) = Application.Index(Application.LinEst(CRLossRngyC, Application.Power(CRLossRngx, Array(1, 2, 3, 4, 5, 6))), 1, 5)  
 CRLossC(5, 0) = Application.Index(Application.LinEst(CRLossRngyC, Application.Power(CRLossRngx, Array(1, 2, 3, 4, 5, 6))), 1, 6)  
 CRLossC(6, 0) = Application.Index(Application.LinEst(CRLossRngyC, Application.Power(CRLossRngx, Array(1, 2, 3, 4, 5, 6))), 1, 7)

Dim CRLossD(6, 0) As Double

CRLossD(0, 0) = Application.Index(Application.LinEst(CRLossRngyD, Application.Power(CRLossRngx, Array(1, 2, 3, 4, 5, 6))), 1, 1)  
 CRLossD(1, 0) = Application.Index(Application.LinEst(CRLossRngyD, Application.Power(CRLossRngx, Array(1, 2, 3, 4, 5, 6))), 1, 2)  
 CRLossD(2, 0) = Application.Index(Application.LinEst(CRLossRngyD, Application.Power(CRLossRngx, Array(1, 2, 3, 4, 5, 6))), 1, 3)  
 CRLossD(3, 0) = Application.Index(Application.LinEst(CRLossRngyD, Application.Power(CRLossRngx, Array(1, 2, 3, 4, 5, 6))), 1, 4)  
 CRLossD(4, 0) = Application.Index(Application.LinEst(CRLossRngyD, Application.Power(CRLossRngx, Array(1, 2, 3, 4, 5, 6))), 1, 5)  
 CRLossD(5, 0) = Application.Index(Application.LinEst(CRLossRngyD, Application.Power(CRLossRngx, Array(1, 2, 3, 4, 5, 6))), 1, 6)  
 CRLossD(6, 0) = Application.Index(Application.LinEst(CRLossRngyD, Application.Power(CRLossRngx, Array(1, 2, 3, 4, 5, 6))), 1, 7)

Dim CRLossE(6, 0) As Double

CRLossE(0, 0) = Application.Index(Application.LinEst(CRLossRngyE, Application.Power(CRLossRngx, Array(1, 2, 3, 4, 5, 6))), 1, 1)  
 CRLossE(1, 0) = Application.Index(Application.LinEst(CRLossRngyE, Application.Power(CRLossRngx, Array(1, 2, 3, 4, 5, 6))), 1, 2)  
 CRLossE(2, 0) = Application.Index(Application.LinEst(CRLossRngyE, Application.Power(CRLossRngx, Array(1, 2, 3, 4, 5, 6))), 1, 3)  
 CRLossE(3, 0) = Application.Index(Application.LinEst(CRLossRngyE, Application.Power(CRLossRngx, Array(1, 2, 3, 4, 5, 6))), 1, 4)  
 CRLossE(4, 0) = Application.Index(Application.LinEst(CRLossRngyE, Application.Power(CRLossRngx, Array(1, 2, 3, 4, 5, 6))), 1, 5)  
 CRLossE(5, 0) = Application.Index(Application.LinEst(CRLossRngyE, Application.Power(CRLossRngx, Array(1, 2, 3, 4, 5, 6))), 1, 6)  
 CRLossE(6, 0) = Application.Index(Application.LinEst(CRLossRngyE, Application.Power(CRLossRngx, Array(1, 2, 3, 4, 5, 6))), 1, 7)

Dim s\_b As Double

s\_b = rowdata(i1, 6) / rowdata(i1, 8)

Dim SINB\_SINA As Double

SINB\_SINA = 1 - (Sin(Application.WorksheetFunction.Radians(alphacc2)) / Sin(Application.WorksheetFunction.Radians(alphacc1)))

2nd Polynomial Factors

Dim CRLoss2(4, 0) As Double

CRLoss2(0, 0) = (((((((((CRLossA(0, 0) \* s\_b) + CRLossA(1, 0)) \* s\_b) + CRLossA(2, 0)) \* s\_b) + CRLossA(3, 0)) \* s\_b) + CRLossA(4, 0)) \* s\_b)  
 + CRLossA(5, 0)) \* s\_b) + CRLossA(6, 0)  
 CRLoss2(1, 0) = (((((((((CRLossB(0, 0) \* s\_b) + CRLossB(1, 0)) \* s\_b) + CRLossB(2, 0)) \* s\_b) + CRLossB(3, 0)) \* s\_b) + CRLossB(4, 0)) \* s\_b)  
 + CRLossB(5, 0)) \* s\_b) + CRLossB(6, 0)  
 CRLoss2(2, 0) = (((((((((CRLossC(0, 0) \* s\_b) + CRLossC(1, 0)) \* s\_b) + CRLossC(2, 0)) \* s\_b) + CRLossC(3, 0)) \* s\_b) + CRLossC(4, 0)) \* s\_b)  
 + CRLossC(5, 0)) \* s\_b) + CRLossC(6, 0)  
 CRLoss2(3, 0) = (((((((((CRLossD(0, 0) \* s\_b) + CRLossD(1, 0)) \* s\_b) + CRLossD(2, 0)) \* s\_b) + CRLossD(3, 0)) \* s\_b) + CRLossD(4, 0)) \*  
 s\_b) + CRLossD(5, 0)) \* s\_b) + CRLossD(6, 0)  
 CRLoss2(4, 0) = (((((((((CRLossE(0, 0) \* s\_b) + CRLossE(1, 0)) \* s\_b) + CRLossE(2, 0)) \* s\_b) + CRLossE(3, 0)) \* s\_b) + CRLossE(4, 0)) \* s\_b)  
 + CRLossE(5, 0)) \* s\_b) + CRLossE(6, 0)

CR

CR = (((((((((CRLoss2(0, 0) \* SINB\_SINA) + CRLoss2(1, 0)) \* SINB\_SINA) + CRLoss2(2, 0)) \* SINB\_SINA) + CRLoss2(3, 0)) \* SINB\_SINA) +  
 CRLoss2(4, 0))

Lift Parameter

Dim FLLossRngx As Range

Dim FLLossRngyA As Range

Dim FLLossRngyB As Range

Dim FLLossRngyC As Range

Dim FLLossRngyD As Range

Dim FLLossRngyE As Range

Set FLLossRngx = Worksheets("CraigCox Corr").Range("I5:I16")

Set FLLossRngyA = Worksheets("CraigCox Corr").Range("J5:J16")

Set FLLossRngyB = Worksheets("CraigCox Corr").Range("K5:K16")

Set FLLossRngyC = Worksheets("CraigCox Corr").Range("L5:L16")



FLoss2(4, 0) = ((((((((((FLossE(0, 0) \* alphacc1) + FLossE(1, 0)) \* alphacc1) + FLossE(2, 0)) \* alphacc1) + FLossE(3, 0)) \* alphacc1) + FLossE(4, 0)) \* alphacc1) + FLossE(5, 0)) \* alphacc1) + FLossE(6, 0)

FL

FL = (((((((FLoss2(0, 0) \* alphacc2) + FLoss2(1, 0)) \* alphacc2) + FLoss2(2, 0)) \* alphacc2) + FLoss2(3, 0)) \* alphacc2) + FLoss2(4, 0)

Profile Loss (PLoss)

Dim BasLossRngx As Range  
Dim BasLossRngyA As Range  
Dim BasLossRngyB As Range  
Dim BasLossRngyC As Range  
Dim BasLossRngyD As Range  
Dim BasLossRngyE As Range  
Dim BasLossA(6, 0) As Double  
Dim BasLossB(6, 0) As Double  
Dim BasLossC(6, 0) As Double  
Dim BasLossD(6, 0) As Double  
Dim BasLossE(6, 0) As Double  
Dim BasLoss2(4, 0) As Double  
Dim Loss As Double

If CR <= 2 Then

Set BasLossRngx = Worksheets("CraigCox Corr").Range("B5:B15")  
Set BasLossRngyA = Worksheets("CraigCox Corr").Range("C5:C15")  
Set BasLossRngyB = Worksheets("CraigCox Corr").Range("D5:D15")  
Set BasLossRngyC = Worksheets("CraigCox Corr").Range("E5:E15")  
Set BasLossRngyD = Worksheets("CraigCox Corr").Range("F5:F15")  
Set BasLossRngyE = Worksheets("CraigCox Corr").Range("G5:G15")

1st Polynomial Factors

BasLossA(0, 0) = Application.Index(Application.LinEst(BasLossRngyA, Application.Power(BasLossRngx, Array(1, 2, 3, 4, 5, 6))), 1, 1)  
BasLossA(1, 0) = Application.Index(Application.LinEst(BasLossRngyA, Application.Power(BasLossRngx, Array(1, 2, 3, 4, 5, 6))), 1, 2)  
BasLossA(2, 0) = Application.Index(Application.LinEst(BasLossRngyA, Application.Power(BasLossRngx, Array(1, 2, 3, 4, 5, 6))), 1, 3)  
BasLossA(3, 0) = Application.Index(Application.LinEst(BasLossRngyA, Application.Power(BasLossRngx, Array(1, 2, 3, 4, 5, 6))), 1, 4)  
BasLossA(4, 0) = Application.Index(Application.LinEst(BasLossRngyA, Application.Power(BasLossRngx, Array(1, 2, 3, 4, 5, 6))), 1, 5)  
BasLossA(5, 0) = Application.Index(Application.LinEst(BasLossRngyA, Application.Power(BasLossRngx, Array(1, 2, 3, 4, 5, 6))), 1, 6)  
BasLossA(6, 0) = Application.Index(Application.LinEst(BasLossRngyA, Application.Power(BasLossRngx, Array(1, 2, 3, 4, 5, 6))), 1, 7)

BasLossB(0, 0) = Application.Index(Application.LinEst(BasLossRngyB, Application.Power(BasLossRngx, Array(1, 2, 3, 4, 5, 6))), 1, 1)  
BasLossB(1, 0) = Application.Index(Application.LinEst(BasLossRngyB, Application.Power(BasLossRngx, Array(1, 2, 3, 4, 5, 6))), 1, 2)  
BasLossB(2, 0) = Application.Index(Application.LinEst(BasLossRngyB, Application.Power(BasLossRngx, Array(1, 2, 3, 4, 5, 6))), 1, 3)  
BasLossB(3, 0) = Application.Index(Application.LinEst(BasLossRngyB, Application.Power(BasLossRngx, Array(1, 2, 3, 4, 5, 6))), 1, 4)  
BasLossB(4, 0) = Application.Index(Application.LinEst(BasLossRngyB, Application.Power(BasLossRngx, Array(1, 2, 3, 4, 5, 6))), 1, 5)  
BasLossB(5, 0) = Application.Index(Application.LinEst(BasLossRngyB, Application.Power(BasLossRngx, Array(1, 2, 3, 4, 5, 6))), 1, 6)  
BasLossB(6, 0) = Application.Index(Application.LinEst(BasLossRngyB, Application.Power(BasLossRngx, Array(1, 2, 3, 4, 5, 6))), 1, 7)

BasLossC(0, 0) = Application.Index(Application.LinEst(BasLossRngyC, Application.Power(BasLossRngx, Array(1, 2, 3, 4, 5, 6))), 1, 1)  
BasLossC(1, 0) = Application.Index(Application.LinEst(BasLossRngyC, Application.Power(BasLossRngx, Array(1, 2, 3, 4, 5, 6))), 1, 2)  
BasLossC(2, 0) = Application.Index(Application.LinEst(BasLossRngyC, Application.Power(BasLossRngx, Array(1, 2, 3, 4, 5, 6))), 1, 3)  
BasLossC(3, 0) = Application.Index(Application.LinEst(BasLossRngyC, Application.Power(BasLossRngx, Array(1, 2, 3, 4, 5, 6))), 1, 4)  
BasLossC(4, 0) = Application.Index(Application.LinEst(BasLossRngyC, Application.Power(BasLossRngx, Array(1, 2, 3, 4, 5, 6))), 1, 5)  
BasLossC(5, 0) = Application.Index(Application.LinEst(BasLossRngyC, Application.Power(BasLossRngx, Array(1, 2, 3, 4, 5, 6))), 1, 6)  
BasLossC(6, 0) = Application.Index(Application.LinEst(BasLossRngyC, Application.Power(BasLossRngx, Array(1, 2, 3, 4, 5, 6))), 1, 7)

BasLossD(0, 0) = Application.Index(Application.LinEst(BasLossRngyD, Application.Power(BasLossRngx, Array(1, 2, 3, 4, 5, 6))), 1, 1)  
BasLossD(1, 0) = Application.Index(Application.LinEst(BasLossRngyD, Application.Power(BasLossRngx, Array(1, 2, 3, 4, 5, 6))), 1, 2)  
BasLossD(2, 0) = Application.Index(Application.LinEst(BasLossRngyD, Application.Power(BasLossRngx, Array(1, 2, 3, 4, 5, 6))), 1, 3)

BasLossD(3, 0) = Application.Index(Application.LinEst(BasLossRngyD, Application.Power(BasLossRngx, Array(1, 2, 3, 4, 5, 6))), 1, 4)  
 BasLossD(4, 0) = Application.Index(Application.LinEst(BasLossRngyD, Application.Power(BasLossRngx, Array(1, 2, 3, 4, 5, 6))), 1, 5)  
 BasLossD(5, 0) = Application.Index(Application.LinEst(BasLossRngyD, Application.Power(BasLossRngx, Array(1, 2, 3, 4, 5, 6))), 1, 6)  
 BasLossD(6, 0) = Application.Index(Application.LinEst(BasLossRngyD, Application.Power(BasLossRngx, Array(1, 2, 3, 4, 5, 6))), 1, 7)

BasLossE(0, 0) = Application.Index(Application.LinEst(BasLossRngyE, Application.Power(BasLossRngx, Array(1, 2, 3, 4, 5, 6))), 1, 1)  
 BasLossE(1, 0) = Application.Index(Application.LinEst(BasLossRngyE, Application.Power(BasLossRngx, Array(1, 2, 3, 4, 5, 6))), 1, 2)  
 BasLossE(2, 0) = Application.Index(Application.LinEst(BasLossRngyE, Application.Power(BasLossRngx, Array(1, 2, 3, 4, 5, 6))), 1, 3)  
 BasLossE(3, 0) = Application.Index(Application.LinEst(BasLossRngyE, Application.Power(BasLossRngx, Array(1, 2, 3, 4, 5, 6))), 1, 4)  
 BasLossE(4, 0) = Application.Index(Application.LinEst(BasLossRngyE, Application.Power(BasLossRngx, Array(1, 2, 3, 4, 5, 6))), 1, 5)  
 BasLossE(5, 0) = Application.Index(Application.LinEst(BasLossRngyE, Application.Power(BasLossRngx, Array(1, 2, 3, 4, 5, 6))), 1, 6)  
 BasLossE(6, 0) = Application.Index(Application.LinEst(BasLossRngyE, Application.Power(BasLossRngx, Array(1, 2, 3, 4, 5, 6))), 1, 7)

## 2nd Polynomial Factors

BasLoss2(0, 0) = ((((((((((BasLossA(0, 0) \* CR) + BasLossA(1, 0)) \* CR) + BasLossA(2, 0)) \* CR) + BasLossA(3, 0)) \* CR) + BasLossA(4, 0)) \* CR) + BasLossA(5, 0)) \* CR) + BasLossA(6, 0)  
 BasLoss2(1, 0) = ((((((((((BasLossB(0, 0) \* CR) + BasLossB(1, 0)) \* CR) + BasLossB(2, 0)) \* CR) + BasLossB(3, 0)) \* CR) + BasLossB(4, 0)) \* CR) + BasLossB(5, 0)) \* CR) + BasLossB(6, 0)  
 BasLoss2(2, 0) = ((((((((((BasLossC(0, 0) \* CR) + BasLossC(1, 0)) \* CR) + BasLossC(2, 0)) \* CR) + BasLossC(3, 0)) \* CR) + BasLossC(4, 0)) \* CR) + BasLossC(5, 0)) \* CR) + BasLossC(6, 0)  
 BasLoss2(3, 0) = ((((((((((BasLossD(0, 0) \* CR) + BasLossD(1, 0)) \* CR) + BasLossD(2, 0)) \* CR) + BasLossD(3, 0)) \* CR) + BasLossD(4, 0)) \* CR) + BasLossD(5, 0)) \* CR) + BasLossD(6, 0)  
 BasLoss2(4, 0) = ((((((((((BasLossE(0, 0) \* CR) + BasLossE(1, 0)) \* CR) + BasLossE(2, 0)) \* CR) + BasLossE(3, 0)) \* CR) + BasLossE(4, 0)) \* CR) + BasLossE(5, 0)) \* CR) + BasLossE(6, 0)

FL\_sb = FL \* ((rowdata(i1, 6) \* 0.0254) / Bb)

## Basic Loss

Loss = (((((((BasLoss2(0, 0) \* FL\_sb) + BasLoss2(1, 0)) \* FL\_sb) + BasLoss2(2, 0)) \* FL\_sb) + BasLoss2(3, 0)) \* FL\_sb) + BasLoss2(4, 0)

Else

Set BasLossRngx = Worksheets("CraigCox Corr").Range("B15:B30")  
 Set BasLossRngyA = Worksheets("CraigCox Corr").Range("C15:C30")  
 Set BasLossRngyB = Worksheets("CraigCox Corr").Range("D15:D30")  
 Set BasLossRngyC = Worksheets("CraigCox Corr").Range("E15:E30")  
 Set BasLossRngyD = Worksheets("CraigCox Corr").Range("F15:F30")  
 Set BasLossRngyE = Worksheets("CraigCox Corr").Range("G15:G30")

## 1st Polynomial Factors

BasLossA(0, 0) = Application.Index(Application.LinEst(BasLossRngyA, Application.Power(BasLossRngx, Array(1, 2, 3, 4, 5, 6))), 1, 1)  
 BasLossA(1, 0) = Application.Index(Application.LinEst(BasLossRngyA, Application.Power(BasLossRngx, Array(1, 2, 3, 4, 5, 6))), 1, 2)  
 BasLossA(2, 0) = Application.Index(Application.LinEst(BasLossRngyA, Application.Power(BasLossRngx, Array(1, 2, 3, 4, 5, 6))), 1, 3)  
 BasLossA(3, 0) = Application.Index(Application.LinEst(BasLossRngyA, Application.Power(BasLossRngx, Array(1, 2, 3, 4, 5, 6))), 1, 4)  
 BasLossA(4, 0) = Application.Index(Application.LinEst(BasLossRngyA, Application.Power(BasLossRngx, Array(1, 2, 3, 4, 5, 6))), 1, 5)  
 BasLossA(5, 0) = Application.Index(Application.LinEst(BasLossRngyA, Application.Power(BasLossRngx, Array(1, 2, 3, 4, 5, 6))), 1, 6)  
 BasLossA(6, 0) = Application.Index(Application.LinEst(BasLossRngyA, Application.Power(BasLossRngx, Array(1, 2, 3, 4, 5, 6))), 1, 7)

BasLossB(0, 0) = Application.Index(Application.LinEst(BasLossRngyB, Application.Power(BasLossRngx, Array(1, 2, 3, 4, 5, 6))), 1, 1)  
 BasLossB(1, 0) = Application.Index(Application.LinEst(BasLossRngyB, Application.Power(BasLossRngx, Array(1, 2, 3, 4, 5, 6))), 1, 2)  
 BasLossB(2, 0) = Application.Index(Application.LinEst(BasLossRngyB, Application.Power(BasLossRngx, Array(1, 2, 3, 4, 5, 6))), 1, 3)  
 BasLossB(3, 0) = Application.Index(Application.LinEst(BasLossRngyB, Application.Power(BasLossRngx, Array(1, 2, 3, 4, 5, 6))), 1, 4)  
 BasLossB(4, 0) = Application.Index(Application.LinEst(BasLossRngyB, Application.Power(BasLossRngx, Array(1, 2, 3, 4, 5, 6))), 1, 5)  
 BasLossB(5, 0) = Application.Index(Application.LinEst(BasLossRngyB, Application.Power(BasLossRngx, Array(1, 2, 3, 4, 5, 6))), 1, 6)  
 BasLossB(6, 0) = Application.Index(Application.LinEst(BasLossRngyB, Application.Power(BasLossRngx, Array(1, 2, 3, 4, 5, 6))), 1, 7)

BasLossC(0, 0) = Application.Index(Application.LinEst(BasLossRngyC, Application.Power(BasLossRngx, Array(1, 2, 3, 4, 5, 6))), 1, 1)  
 BasLossC(1, 0) = Application.Index(Application.LinEst(BasLossRngyC, Application.Power(BasLossRngx, Array(1, 2, 3, 4, 5, 6))), 1, 2)

BasLossC(2, 0) = Application.Index(Application.LinEst(BasLossRngyC, Application.Power(BasLossRngx, Array(1, 2, 3, 4, 5, 6))), 1, 3)  
 BasLossC(3, 0) = Application.Index(Application.LinEst(BasLossRngyC, Application.Power(BasLossRngx, Array(1, 2, 3, 4, 5, 6))), 1, 4)  
 BasLossC(4, 0) = Application.Index(Application.LinEst(BasLossRngyC, Application.Power(BasLossRngx, Array(1, 2, 3, 4, 5, 6))), 1, 5)  
 BasLossC(5, 0) = Application.Index(Application.LinEst(BasLossRngyC, Application.Power(BasLossRngx, Array(1, 2, 3, 4, 5, 6))), 1, 6)  
 BasLossC(6, 0) = Application.Index(Application.LinEst(BasLossRngyC, Application.Power(BasLossRngx, Array(1, 2, 3, 4, 5, 6))), 1, 7)

BasLossD(0, 0) = Application.Index(Application.LinEst(BasLossRngyD, Application.Power(BasLossRngx, Array(1, 2, 3, 4, 5, 6))), 1, 1)  
 BasLossD(1, 0) = Application.Index(Application.LinEst(BasLossRngyD, Application.Power(BasLossRngx, Array(1, 2, 3, 4, 5, 6))), 1, 2)  
 BasLossD(2, 0) = Application.Index(Application.LinEst(BasLossRngyD, Application.Power(BasLossRngx, Array(1, 2, 3, 4, 5, 6))), 1, 3)  
 BasLossD(3, 0) = Application.Index(Application.LinEst(BasLossRngyD, Application.Power(BasLossRngx, Array(1, 2, 3, 4, 5, 6))), 1, 4)  
 BasLossD(4, 0) = Application.Index(Application.LinEst(BasLossRngyD, Application.Power(BasLossRngx, Array(1, 2, 3, 4, 5, 6))), 1, 5)  
 BasLossD(5, 0) = Application.Index(Application.LinEst(BasLossRngyD, Application.Power(BasLossRngx, Array(1, 2, 3, 4, 5, 6))), 1, 6)  
 BasLossD(6, 0) = Application.Index(Application.LinEst(BasLossRngyD, Application.Power(BasLossRngx, Array(1, 2, 3, 4, 5, 6))), 1, 7)

BasLossE(0, 0) = Application.Index(Application.LinEst(BasLossRngyE, Application.Power(BasLossRngx, Array(1, 2, 3, 4, 5, 6))), 1, 1)  
 BasLossE(1, 0) = Application.Index(Application.LinEst(BasLossRngyE, Application.Power(BasLossRngx, Array(1, 2, 3, 4, 5, 6))), 1, 2)  
 BasLossE(2, 0) = Application.Index(Application.LinEst(BasLossRngyE, Application.Power(BasLossRngx, Array(1, 2, 3, 4, 5, 6))), 1, 3)  
 BasLossE(3, 0) = Application.Index(Application.LinEst(BasLossRngyE, Application.Power(BasLossRngx, Array(1, 2, 3, 4, 5, 6))), 1, 4)  
 BasLossE(4, 0) = Application.Index(Application.LinEst(BasLossRngyE, Application.Power(BasLossRngx, Array(1, 2, 3, 4, 5, 6))), 1, 5)  
 BasLossE(5, 0) = Application.Index(Application.LinEst(BasLossRngyE, Application.Power(BasLossRngx, Array(1, 2, 3, 4, 5, 6))), 1, 6)  
 BasLossE(6, 0) = Application.Index(Application.LinEst(BasLossRngyE, Application.Power(BasLossRngx, Array(1, 2, 3, 4, 5, 6))), 1, 7)

#### 2nd Polynomial Factors

BasLoss2(0, 0) = ((((((((((BasLossA(0, 0) \* CR) + BasLossA(1, 0)) \* CR) + BasLossA(2, 0)) \* CR) + BasLossA(3, 0)) \* CR) + BasLossA(4, 0)) \* CR) + BasLossA(5, 0)) \* CR) + BasLossA(6, 0)  
 BasLoss2(1, 0) = ((((((((((BasLossB(0, 0) \* CR) + BasLossB(1, 0)) \* CR) + BasLossB(2, 0)) \* CR) + BasLossB(3, 0)) \* CR) + BasLossB(4, 0)) \* CR) + BasLossB(5, 0)) \* CR) + BasLossB(6, 0)  
 BasLoss2(2, 0) = ((((((((((BasLossC(0, 0) \* CR) + BasLossC(1, 0)) \* CR) + BasLossC(2, 0)) \* CR) + BasLossC(3, 0)) \* CR) + BasLossC(4, 0)) \* CR) + BasLossC(5, 0)) \* CR) + BasLossC(6, 0)  
 BasLoss2(3, 0) = ((((((((((BasLossD(0, 0) \* CR) + BasLossD(1, 0)) \* CR) + BasLossD(2, 0)) \* CR) + BasLossD(3, 0)) \* CR) + BasLossD(4, 0)) \* CR) + BasLossD(5, 0)) \* CR) + BasLossD(6, 0)  
 BasLoss2(4, 0) = ((((((((((BasLossE(0, 0) \* CR) + BasLossE(1, 0)) \* CR) + BasLossE(2, 0)) \* CR) + BasLossE(3, 0)) \* CR) + BasLossE(4, 0)) \* CR) + BasLossE(5, 0)) \* CR) + BasLossE(6, 0)

FL\_sb = FL \* ((rowdata(i1, 6) \* 0.0254) / Bb)

If FL\_sb > 10 Then

FL\_sb = 10

End If

Basic Loss

Loss = (((((((BasLoss2(0, 0) \* FL\_sb) + BasLoss2(1, 0)) \* FL\_sb) + BasLoss2(2, 0)) \* FL\_sb) + BasLoss2(3, 0)) \* FL\_sb) + BasLoss2(4, 0)

End If

PLoss = Loss / (Bb / (rowdata(i1, 6) \* 0.0254) \* Sin(Application.WorksheetFunction.Radians(alphacc2)))

Trailing Edge Loss ( Pte)

Dim TELossRngx As Range

Dim TELossRngyA As Range

Dim TELossRngyB As Range

Dim TELossRngyC As Range

Dim TELossRngyD As Range

Dim TELossRngyE As Range

Set TELossRngx = Worksheets("CraigCox Corr").Range("B35:B45")

Set TELossRngyA = Worksheets("CraigCox Corr").Range("C35:C45")

Set TELossRngyB = Worksheets("CraigCox Corr").Range("D35:D45")



$TELoss2(2, 0) = ((((((((((TELossC(0, 0) * alphacc2) + TElLossC(1, 0)) * alphacc2) + TElLossC(2, 0)) * alphacc2) + TElLossC(3, 0)) * alphacc2) + TElLossC(4, 0)) * alphacc2) + TElLossC(5, 0)) * alphacc2) + TElLossC(6, 0)$   
 $TELoss2(3, 0) = ((((((((((TELossD(0, 0) * alphacc2) + TElLossD(1, 0)) * alphacc2) + TElLossD(2, 0)) * alphacc2) + TElLossD(3, 0)) * alphacc2) + TElLossD(4, 0)) * alphacc2) + TElLossD(5, 0)) * alphacc2) + TElLossD(6, 0)$   
 $TELoss2(4, 0) = ((((((((((TELossE(0, 0) * alphacc2) + TElLossE(1, 0)) * alphacc2) + TElLossE(2, 0)) * alphacc2) + TElLossE(3, 0)) * alphacc2) + TElLossE(4, 0)) * alphacc2) + TElLossE(5, 0)) * alphacc2) + TElLossE(6, 0)$

TE

Xte = (((((((TELoss2(0, 0) \* te\_s) + TElLoss2(1, 0)) \* te\_s) + TElLoss2(2, 0)) \* te\_s) + TElLoss2(3, 0)) \* te\_s) + TElLoss2(4, 0)

Dim PteLossRngx As Range  
Dim PteLossRngyA As Range

Set PteLossRngx = Worksheets("CraigCox Corr").Range("I50:I57")  
Set PteLossRngyA = Worksheets("CraigCox Corr").Range("J50:J57")

1st Polynomial Factors

Dim PteLossA(6, 0) As Double

$PteLossA(0, 0) = Application.Index(Application.LinEst(PteLossRngyA, Application.Power(PteLossRngx, Array(1, 2, 3, 4, 5, 6))), 1, 1)$   
 $PteLossA(1, 0) = Application.Index(Application.LinEst(PteLossRngyA, Application.Power(PteLossRngx, Array(1, 2, 3, 4, 5, 6))), 1, 2)$   
 $PteLossA(2, 0) = Application.Index(Application.LinEst(PteLossRngyA, Application.Power(PteLossRngx, Array(1, 2, 3, 4, 5, 6))), 1, 3)$   
 $PteLossA(3, 0) = Application.Index(Application.LinEst(PteLossRngyA, Application.Power(PteLossRngx, Array(1, 2, 3, 4, 5, 6))), 1, 4)$   
 $PteLossA(4, 0) = Application.Index(Application.LinEst(PteLossRngyA, Application.Power(PteLossRngx, Array(1, 2, 3, 4, 5, 6))), 1, 5)$   
 $PteLossA(5, 0) = Application.Index(Application.LinEst(PteLossRngyA, Application.Power(PteLossRngx, Array(1, 2, 3, 4, 5, 6))), 1, 6)$   
 $PteLossA(6, 0) = Application.Index(Application.LinEst(PteLossRngyA, Application.Power(PteLossRngx, Array(1, 2, 3, 4, 5, 6))), 1, 7)$

Pte = ((((((((((PteLossA(0, 0) \* te\_s) + PteLossA(1, 0)) \* te\_s) + PteLossA(2, 0)) \* te\_s) + PteLossA(3, 0)) \* te\_s) + PteLossA(4, 0)) \* te\_s) + PteLossA(5, 0)) \* te\_s) + PteLossA(6, 0)

Mach number Losses (MA)

Dim MALossRngx As Range  
Dim MALossRngyA As Range  
Dim MALossRngyB As Range  
Dim MALossRngyC As Range  
Dim MALossRngyD As Range  
Dim MALossRngyE As Range  
Dim MALossRngyF As Range  
Dim MALossRngyG As Range

Set MALossRngx = Worksheets("CraigCox Corr").Range("I35:I44")  
Set MALossRngyA = Worksheets("CraigCox Corr").Range("J35:J44")  
Set MALossRngyB = Worksheets("CraigCox Corr").Range("K35:K44")  
Set MALossRngyC = Worksheets("CraigCox Corr").Range("L35:L44")  
Set MALossRngyD = Worksheets("CraigCox Corr").Range("M35:M44")  
Set MALossRngyE = Worksheets("CraigCox Corr").Range("N35:N44")  
Set MALossRngyF = Worksheets("CraigCox Corr").Range("O35:O44")  
Set MALossRngyG = Worksheets("CraigCox Corr").Range("P35:P44")

1st Polynomial Factors

Dim MALossA(6, 0) As Double

$MALossA(0, 0) = Application.Index(Application.LinEst(MALossRngyA, Application.Power(MALossRngx, Array(1, 2, 3, 4, 5, 6))), 1, 1)$   
 $MALossA(1, 0) = Application.Index(Application.LinEst(MALossRngyA, Application.Power(MALossRngx, Array(1, 2, 3, 4, 5, 6))), 1, 2)$   
 $MALossA(2, 0) = Application.Index(Application.LinEst(MALossRngyA, Application.Power(MALossRngx, Array(1, 2, 3, 4, 5, 6))), 1, 3)$   
 $MALossA(3, 0) = Application.Index(Application.LinEst(MALossRngyA, Application.Power(MALossRngx, Array(1, 2, 3, 4, 5, 6))), 1, 4)$   
 $MALossA(4, 0) = Application.Index(Application.LinEst(MALossRngyA, Application.Power(MALossRngx, Array(1, 2, 3, 4, 5, 6))), 1, 5)$   
 $MALossA(5, 0) = Application.Index(Application.LinEst(MALossRngyA, Application.Power(MALossRngx, Array(1, 2, 3, 4, 5, 6))), 1, 6)$   
 $MALossA(6, 0) = Application.Index(Application.LinEst(MALossRngyA, Application.Power(MALossRngx, Array(1, 2, 3, 4, 5, 6))), 1, 7)$





$MA_{Loss2}(0, 0) = ((((((((((MA_{LossA}(0, 0) * ote\_s) + MA_{LossA}(1, 0)) * ote\_s) + MA_{LossA}(2, 0)) * ote\_s) + MA_{LossA}(3, 0)) * ote\_s) + MA_{LossA}(4, 0)) * ote\_s) + MA_{LossA}(5, 0)) * ote\_s) + MA_{LossA}(6, 0)$   
 $MA_{Loss2}(1, 0) = ((((((((((MA_{LossB}(0, 0) * ote\_s) + MA_{LossB}(1, 0)) * ote\_s) + MA_{LossB}(2, 0)) * ote\_s) + MA_{LossB}(3, 0)) * ote\_s) + MA_{LossB}(4, 0)) * ote\_s) + MA_{LossB}(5, 0)) * ote\_s) + MA_{LossB}(6, 0)$   
 $MA_{Loss2}(2, 0) = ((((((((((MA_{LossC}(0, 0) * ote\_s) + MA_{LossC}(1, 0)) * ote\_s) + MA_{LossC}(2, 0)) * ote\_s) + MA_{LossC}(3, 0)) * ote\_s) + MA_{LossC}(4, 0)) * ote\_s) + MA_{LossC}(5, 0)) * ote\_s) + MA_{LossC}(6, 0)$   
 $MA_{Loss2}(3, 0) = ((((((((((MA_{LossD}(0, 0) * ote\_s) + MA_{LossD}(1, 0)) * ote\_s) + MA_{LossD}(2, 0)) * ote\_s) + MA_{LossD}(3, 0)) * ote\_s) + MA_{LossD}(4, 0)) * ote\_s) + MA_{LossD}(5, 0)) * ote\_s) + MA_{LossD}(6, 0)$   
 $MA_{Loss2}(4, 0) = ((((((((((MA_{LossE}(0, 0) * ote\_s) + MA_{LossE}(1, 0)) * ote\_s) + MA_{LossE}(2, 0)) * ote\_s) + MA_{LossE}(3, 0)) * ote\_s) + MA_{LossE}(4, 0)) * ote\_s) + MA_{LossE}(5, 0)) * ote\_s) + MA_{LossE}(6, 0)$   
 $MA_{Loss2}(5, 0) = ((((((((((MA_{LossF}(0, 0) * ote\_s) + MA_{LossF}(1, 0)) * ote\_s) + MA_{LossF}(2, 0)) * ote\_s) + MA_{LossF}(3, 0)) * ote\_s) + MA_{LossF}(4, 0)) * ote\_s) + MA_{LossF}(5, 0)) * ote\_s) + MA_{LossF}(6, 0)$   
 $MA_{Loss2}(6, 0) = ((((((((((MA_{LossG}(0, 0) * ote\_s) + MA_{LossG}(1, 0)) * ote\_s) + MA_{LossG}(2, 0)) * ote\_s) + MA_{LossG}(3, 0)) * ote\_s) + MA_{LossG}(4, 0)) * ote\_s) + MA_{LossG}(5, 0)) * ote\_s) + MA_{LossG}(6, 0)$

MA

If m >= 1 Then

MA = ((((((((((MA\_{Loss2}(0, 0) \* m) + MA\_{Loss2}(1, 0)) \* m) + MA\_{Loss2}(2, 0)) \* m) + MA\_{Loss2}(3, 0)) \* m) + MA\_{Loss2}(4, 0)) \* m) + MA\_{Loss2}(5, 0)) \* m) + MA\_{Loss2}(6, 0)

Else

MA = 0

End If

Blade Back Radius Losses

Dim BBR\_{LossRngx} As Range

Dim BBR\_{LossRngyA} As Range

Dim BBR\_{LossRngyB} As Range

Dim BBR\_{LossRngyC} As Range

Dim BBR\_{LossRngyD} As Range

Set BBR\_{LossRngx} = Worksheets("CraigCox Corr").Range("B50:B62")

Set BBR\_{LossRngyA} = Worksheets("CraigCox Corr").Range("C50:C62")

Set BBR\_{LossRngyB} = Worksheets("CraigCox Corr").Range("D50:D62")

Set BBR\_{LossRngyC} = Worksheets("CraigCox Corr").Range("E50:E62")

Set BBR\_{LossRngyD} = Worksheets("CraigCox Corr").Range("F50:F62")

1st Polynomial Factors

Dim BBR\_{LossA}(6, 0) As Double

BBR\_{LossA}(0, 0) = Application.Index(Application.LinEst(BBR\_{LossRngyA}, Application.Power(BBR\_{LossRngx}, Array(1, 2, 3, 4, 5, 6))), 1, 1)

BBR\_{LossA}(1, 0) = Application.Index(Application.LinEst(BBR\_{LossRngyA}, Application.Power(BBR\_{LossRngx}, Array(1, 2, 3, 4, 5, 6))), 1, 2)

BBR\_{LossA}(2, 0) = Application.Index(Application.LinEst(BBR\_{LossRngyA}, Application.Power(BBR\_{LossRngx}, Array(1, 2, 3, 4, 5, 6))), 1, 3)

BBR\_{LossA}(3, 0) = Application.Index(Application.LinEst(BBR\_{LossRngyA}, Application.Power(BBR\_{LossRngx}, Array(1, 2, 3, 4, 5, 6))), 1, 4)

BBR\_{LossA}(4, 0) = Application.Index(Application.LinEst(BBR\_{LossRngyA}, Application.Power(BBR\_{LossRngx}, Array(1, 2, 3, 4, 5, 6))), 1, 5)

BBR\_{LossA}(5, 0) = Application.Index(Application.LinEst(BBR\_{LossRngyA}, Application.Power(BBR\_{LossRngx}, Array(1, 2, 3, 4, 5, 6))), 1, 6)

BBR\_{LossA}(6, 0) = Application.Index(Application.LinEst(BBR\_{LossRngyA}, Application.Power(BBR\_{LossRngx}, Array(1, 2, 3, 4, 5, 6))), 1, 7)

Dim BBR\_{LossB}(6, 0) As Double

BBR\_{LossB}(0, 0) = Application.Index(Application.LinEst(BBR\_{LossRngyB}, Application.Power(BBR\_{LossRngx}, Array(1, 2, 3, 4, 5, 6))), 1, 1)

BBR\_{LossB}(1, 0) = Application.Index(Application.LinEst(BBR\_{LossRngyB}, Application.Power(BBR\_{LossRngx}, Array(1, 2, 3, 4, 5, 6))), 1, 2)

BBR\_{LossB}(2, 0) = Application.Index(Application.LinEst(BBR\_{LossRngyB}, Application.Power(BBR\_{LossRngx}, Array(1, 2, 3, 4, 5, 6))), 1, 3)

BBR\_{LossB}(3, 0) = Application.Index(Application.LinEst(BBR\_{LossRngyB}, Application.Power(BBR\_{LossRngx}, Array(1, 2, 3, 4, 5, 6))), 1, 4)

BBR\_{LossB}(4, 0) = Application.Index(Application.LinEst(BBR\_{LossRngyB}, Application.Power(BBR\_{LossRngx}, Array(1, 2, 3, 4, 5, 6))), 1, 5)

BBR\_{LossB}(5, 0) = Application.Index(Application.LinEst(BBR\_{LossRngyB}, Application.Power(BBR\_{LossRngx}, Array(1, 2, 3, 4, 5, 6))), 1, 6)

BBR\_{LossB}(6, 0) = Application.Index(Application.LinEst(BBR\_{LossRngyB}, Application.Power(BBR\_{LossRngx}, Array(1, 2, 3, 4, 5, 6))), 1, 7)

Dim BBR\_{LossC}(6, 0) As Double

BBR\_{LossC}(0, 0) = Application.Index(Application.LinEst(BBR\_{LossRngyC}, Application.Power(BBR\_{LossRngx}, Array(1, 2, 3, 4, 5, 6))), 1, 1)

BBR\_{LossC}(1, 0) = Application.Index(Application.LinEst(BBR\_{LossRngyC}, Application.Power(BBR\_{LossRngx}, Array(1, 2, 3, 4, 5, 6))), 1, 2)

BBR\_{LossC}(2, 0) = Application.Index(Application.LinEst(BBR\_{LossRngyC}, Application.Power(BBR\_{LossRngx}, Array(1, 2, 3, 4, 5, 6))), 1, 3)

BBRLossC(3, 0) = Application.Index(Application.LinEst(BBRLossRngyC, Application.Power(BBRLossRngx, Array(1, 2, 3, 4, 5, 6))), 1, 4)  
 BBRLossC(4, 0) = Application.Index(Application.LinEst(BBRLossRngyC, Application.Power(BBRLossRngx, Array(1, 2, 3, 4, 5, 6))), 1, 5)  
 BBRLossC(5, 0) = Application.Index(Application.LinEst(BBRLossRngyC, Application.Power(BBRLossRngx, Array(1, 2, 3, 4, 5, 6))), 1, 6)  
 BBRLossC(6, 0) = Application.Index(Application.LinEst(BBRLossRngyC, Application.Power(BBRLossRngx, Array(1, 2, 3, 4, 5, 6))), 1, 7)

Dim BBRLossD(6, 0) As Double  
 BBRLossD(0, 0) = Application.Index(Application.LinEst(BBRLossRngyD, Application.Power(BBRLossRngx, Array(1, 2, 3, 4, 5, 6))), 1, 1)  
 BBRLossD(1, 0) = Application.Index(Application.LinEst(BBRLossRngyD, Application.Power(BBRLossRngx, Array(1, 2, 3, 4, 5, 6))), 1, 2)  
 BBRLossD(2, 0) = Application.Index(Application.LinEst(BBRLossRngyD, Application.Power(BBRLossRngx, Array(1, 2, 3, 4, 5, 6))), 1, 3)  
 BBRLossD(3, 0) = Application.Index(Application.LinEst(BBRLossRngyD, Application.Power(BBRLossRngx, Array(1, 2, 3, 4, 5, 6))), 1, 4)  
 BBRLossD(4, 0) = Application.Index(Application.LinEst(BBRLossRngyD, Application.Power(BBRLossRngx, Array(1, 2, 3, 4, 5, 6))), 1, 5)  
 BBRLossD(5, 0) = Application.Index(Application.LinEst(BBRLossRngyD, Application.Power(BBRLossRngx, Array(1, 2, 3, 4, 5, 6))), 1, 6)  
 BBRLossD(6, 0) = Application.Index(Application.LinEst(BBRLossRngyD, Application.Power(BBRLossRngx, Array(1, 2, 3, 4, 5, 6))), 1, 7)

Dim s\_e As Double  
 s\_e = rowdata(i1, 6) / rowdata(i1, 1)

#### 2nd Polynomial Factors

Dim BBRLoss2(4, 0) As Double  
 BBRLoss2(0, 0) = ((((((((((BBRLossA(0, 0) \* m) + BBRLossA(1, 0)) \* m) + BBRLossA(2, 0)) \* m) + BBRLossA(3, 0)) \* m) + BBRLossA(4, 0)) \* m) + BBRLossA(5, 0)) \* m) + BBRLossA(6, 0)  
 BBRLoss2(1, 0) = ((((((((((BBRLossB(0, 0) \* m) + BBRLossB(1, 0)) \* m) + BBRLossB(2, 0)) \* m) + BBRLossB(3, 0)) \* m) + BBRLossB(4, 0)) \* m) + BBRLossB(5, 0)) \* m) + BBRLossB(6, 0)  
 BBRLoss2(2, 0) = ((((((((((BBRLossC(0, 0) \* m) + BBRLossC(1, 0)) \* m) + BBRLossC(2, 0)) \* m) + BBRLossC(3, 0)) \* m) + BBRLossC(4, 0)) \* m) + BBRLossC(5, 0)) \* m) + BBRLossC(6, 0)  
 BBRLoss2(3, 0) = ((((((((((BBRLossD(0, 0) \* m) + BBRLossD(1, 0)) \* m) + BBRLossD(2, 0)) \* m) + BBRLossD(3, 0)) \* m) + BBRLossD(4, 0)) \* m) + BBRLossD(5, 0)) \* m) + BBRLossD(6, 0)

BBR

If s\_e < 1 Then  
 BBR = 0  
 Else  
 BBR = ((((((BBRLoss2(0, 0) \* s\_e) + BBRLoss2(1, 0)) \* s\_e) + BBRLoss2(2, 0)) \* s\_e) + BBRLoss2(3, 0)  
 End If

#### Incidence losses

##### Basic Positive stalling incidence

Dim BPSInclLossRngx As Range  
 Dim BPSInclLossRngyA As Range  
 Dim BPSInclLossRngyB As Range  
 Dim BPSInclLossRngyC As Range  
 Dim BPSInclLossRngyD As Range  
 Dim BPSInclLossRngyE As Range

Set BPSInclLossRngx = Worksheets("CraigCox Corr").Range("B67:B77")  
 Set BPSInclLossRngyA = Worksheets("CraigCox Corr").Range("C67:C77")  
 Set BPSInclLossRngyB = Worksheets("CraigCox Corr").Range("D67:D77")  
 Set BPSInclLossRngyC = Worksheets("CraigCox Corr").Range("E67:E77")  
 Set BPSInclLossRngyD = Worksheets("CraigCox Corr").Range("F67:F77")  
 Set BPSInclLossRngyE = Worksheets("CraigCox Corr").Range("G67:G77")

#### 1st Polynomial Factors

Dim BPSInclLossA(6, 0) As Double  
 BPSInclLossA(0, 0) = Application.Index(Application.LinEst(BPSInclLossRngyA, Application.Power(BPSInclLossRngx, Array(1, 2, 3, 4, 5, 6))), 1, 1)  
 BPSInclLossA(1, 0) = Application.Index(Application.LinEst(BPSInclLossRngyA, Application.Power(BPSInclLossRngx, Array(1, 2, 3, 4, 5, 6))), 1, 2)



```

BPSInclLossE(1, 0) = Application.Index(Application.LinEst(BPSInclLossRngyE, Application.Power(BPSInclLossRngx, Array(1, 2, 3, 4, 5, 6))), 1,
2)
BPSInclLossE(2, 0) = Application.Index(Application.LinEst(BPSInclLossRngyE, Application.Power(BPSInclLossRngx, Array(1, 2, 3, 4, 5, 6))), 1,
3)
BPSInclLossE(3, 0) = Application.Index(Application.LinEst(BPSInclLossRngyE, Application.Power(BPSInclLossRngx, Array(1, 2, 3, 4, 5, 6))), 1,
4)
BPSInclLossE(4, 0) = Application.Index(Application.LinEst(BPSInclLossRngyE, Application.Power(BPSInclLossRngx, Array(1, 2, 3, 4, 5, 6))), 1,
5)
BPSInclLossE(5, 0) = Application.Index(Application.LinEst(BPSInclLossRngyE, Application.Power(BPSInclLossRngx, Array(1, 2, 3, 4, 5, 6))), 1,
6)
BPSInclLossE(6, 0) = Application.Index(Application.LinEst(BPSInclLossRngyE, Application.Power(BPSInclLossRngx, Array(1, 2, 3, 4, 5, 6))), 1,
7)

```

Dim sin\_o\_s As Double

```
sin_o_s = Application.WorksheetFunction.Degrees(Application.WorksheetFunction.Asin((rowdata(i1, 0) / rowdata(i1, 6))))
```

#### 2nd Polynomial Factors

Dim BPSInclLoss2(4, 0) As Double

```

BPSInclLoss2(0, 0) = (((((((((BPSInclLossA(0, 0) * sin_o_s) + BPSInclLossA(1, 0)) * sin_o_s) + BPSInclLossA(2, 0)) * sin_o_s) + BPSInclLossA(3,
0)) * sin_o_s) + BPSInclLossA(4, 0)) * sin_o_s) + BPSInclLossA(5, 0)) * sin_o_s) + BPSInclLossA(6, 0)
BPSInclLoss2(1, 0) = (((((((((BPSInclLossB(0, 0) * sin_o_s) + BPSInclLossB(1, 0)) * sin_o_s) + BPSInclLossB(2, 0)) * sin_o_s) + BPSInclLossB(3,
0)) * sin_o_s) + BPSInclLossB(4, 0)) * sin_o_s) + BPSInclLossB(5, 0)) * sin_o_s) + BPSInclLossB(6, 0)
BPSInclLoss2(2, 0) = (((((((((BPSInclLossC(0, 0) * sin_o_s) + BPSInclLossC(1, 0)) * sin_o_s) + BPSInclLossC(2, 0)) * sin_o_s) + BPSInclLossC(3,
0)) * sin_o_s) + BPSInclLossC(4, 0)) * sin_o_s) + BPSInclLossC(5, 0)) * sin_o_s) + BPSInclLossC(6, 0)
BPSInclLoss2(3, 0) = (((((((((BPSInclLossD(0, 0) * sin_o_s) + BPSInclLossD(1, 0)) * sin_o_s) + BPSInclLossD(2, 0)) * sin_o_s) + BPSInclLossD(3,
0)) * sin_o_s) + BPSInclLossD(4, 0)) * sin_o_s) + BPSInclLossD(5, 0)) * sin_o_s) + BPSInclLossD(6, 0)
BPSInclLoss2(4, 0) = (((((((((BPSInclLossE(0, 0) * sin_o_s) + BPSInclLossE(1, 0)) * sin_o_s) + BPSInclLossE(2, 0)) * sin_o_s) + BPSInclLossE(3,
0)) * sin_o_s) + BPSInclLossE(4, 0)) * sin_o_s) + BPSInclLossE(5, 0)) * sin_o_s) + BPSInclLossE(6, 0)

```

i+bas

```
i_bas = (((((((BPSInclLoss2(0, 0) * alphacc1) + BPSInclLoss2(1, 0)) * alphacc1) + BPSInclLoss2(2, 0)) * alphacc1) + BPSInclLoss2(3, 0)) *
alphacc1) + BPSInclLoss2(4, 0)
```

#### Incidence correction CR

Dim IncCRLossRngx As Range

Dim IncCRLossRngyA As Range

Dim IncCRLossRngyB As Range

Dim IncCRLossRngyC As Range

Dim IncCRLossRngyD As Range

Dim IncCRLossRngyE As Range

```

Set IncCRLossRngx = Worksheets("CraigCox Corr").Range("I67:I69")
Set IncCRLossRngyA = Worksheets("CraigCox Corr").Range("J67:J69")
Set IncCRLossRngyB = Worksheets("CraigCox Corr").Range("K67:K69")
Set IncCRLossRngyC = Worksheets("CraigCox Corr").Range("L67:L69")
Set IncCRLossRngyD = Worksheets("CraigCox Corr").Range("M67:M69")
Set IncCRLossRngyE = Worksheets("CraigCox Corr").Range("N67:N69")

```

#### 1st Polynomial Factors

Dim IncCRLossA(3, 0) As Double

```
IncCRLossA(0, 0) = Application.Index(Application.LinEst(IncCRLossRngyA, Application.Power(IncCRLossRngx, Array(1, 2))), 1, 1)
```

```
IncCRLossA(1, 0) = Application.Index(Application.LinEst(IncCRLossRngyA, Application.Power(IncCRLossRngx, Array(1, 2))), 1, 2)
```

```
IncCRLossA(2, 0) = Application.Index(Application.LinEst(IncCRLossRngyA, Application.Power(IncCRLossRngx, Array(1, 2))), 1, 3)
```

Dim IncCRLossB(3, 0) As Double

```
IncCRLossB(0, 0) = Application.Index(Application.LinEst(IncCRLossRngyB, Application.Power(IncCRLossRngx, Array(1, 2))), 1, 1)
```

```
IncCRLossB(1, 0) = Application.Index(Application.LinEst(IncCRLossRngyB, Application.Power(IncCRLossRngx, Array(1, 2))), 1, 2)
```

```
IncCRLossB(2, 0) = Application.Index(Application.LinEst(IncCRLossRngyB, Application.Power(IncCRLossRngx, Array(1, 2))), 1, 3)
```

Dim IncCRLossC(3, 0) As Double

IncCRLossC(0, 0) = Application.Index(Application.LinEst(IncCRLossRngyC, Application.Power(IncCRLossRngx, Array(1, 2))), 1, 1)

IncCRLossC(1, 0) = Application.Index(Application.LinEst(IncCRLossRngyC, Application.Power(IncCRLossRngx, Array(1, 2))), 1, 2)

IncCRLossC(2, 0) = Application.Index(Application.LinEst(IncCRLossRngyC, Application.Power(IncCRLossRngx, Array(1, 2))), 1, 3)

Dim IncCRLossD(3, 0) As Double

IncCRLossD(0, 0) = Application.Index(Application.LinEst(IncCRLossRngyD, Application.Power(IncCRLossRngx, Array(1, 2))), 1, 1)

IncCRLossD(1, 0) = Application.Index(Application.LinEst(IncCRLossRngyD, Application.Power(IncCRLossRngx, Array(1, 2))), 1, 2)

IncCRLossD(2, 0) = Application.Index(Application.LinEst(IncCRLossRngyD, Application.Power(IncCRLossRngx, Array(1, 2))), 1, 3)

Dim IncCRLossE(3, 0) As Double

IncCRLossE(0, 0) = Application.Index(Application.LinEst(IncCRLossRngyE, Application.Power(IncCRLossRngx, Array(1, 2))), 1, 1)

IncCRLossE(1, 0) = Application.Index(Application.LinEst(IncCRLossRngyE, Application.Power(IncCRLossRngx, Array(1, 2))), 1, 2)

IncCRLossE(2, 0) = Application.Index(Application.LinEst(IncCRLossRngyE, Application.Power(IncCRLossRngx, Array(1, 2))), 1, 3)

## 2nd Polynomial Factors

Dim IncCRLoss2(4, 0) As Double

IncCRLoss2(0, 0) = (((IncCRLossA(0, 0) \* sin\_o\_s) + IncCRLossA(1, 0)) \* sin\_o\_s) + IncCRLossA(2, 0)

IncCRLoss2(1, 0) = (((IncCRLossB(0, 0) \* sin\_o\_s) + IncCRLossB(1, 0)) \* sin\_o\_s) + IncCRLossB(2, 0)

IncCRLoss2(2, 0) = (((IncCRLossC(0, 0) \* sin\_o\_s) + IncCRLossC(1, 0)) \* sin\_o\_s) + IncCRLossC(2, 0)

IncCRLoss2(3, 0) = (((IncCRLossD(0, 0) \* sin\_o\_s) + IncCRLossD(1, 0)) \* sin\_o\_s) + IncCRLossD(2, 0)

IncCRLoss2(4, 0) = (((IncCRLossE(0, 0) \* sin\_o\_s) + IncCRLossE(1, 0)) \* sin\_o\_s) + IncCRLossE(2, 0)

i+CR

i\_CR = ((((((IncCRLoss2(0, 0) \* CR) + IncCRLoss2(1, 0)) \* CR) + IncCRLoss2(2, 0)) \* CR) + IncCRLoss2(3, 0)) \* CR) + IncCRLoss2(4, 0)

Incidence correction s/b

Dim IncsbLossRngx As Range

Dim IncsbLossRngyA As Range

Dim IncsbLossRngyB As Range

Dim IncsbLossRngyC As Range

Dim IncsbLossRngyD As Range

Dim IncsbLossRngyE As Range

Set IncsbLossRngx = Worksheets("CraigCox Corr").Range("P67:P79")

Set IncsbLossRngyA = Worksheets("CraigCox Corr").Range("Q67:Q79")

Set IncsbLossRngyB = Worksheets("CraigCox Corr").Range("R67:R79")

Set IncsbLossRngyC = Worksheets("CraigCox Corr").Range("S67:S79")

Set IncsbLossRngyD = Worksheets("CraigCox Corr").Range("T67:T79")

Set IncsbLossRngyE = Worksheets("CraigCox Corr").Range("U67:U79")

## 1st Polynomial Factors

Dim IncsbLossA(6, 0) As Double

IncsbLossA(0, 0) = Application.Index(Application.LinEst(IncsbLossRngyA, Application.Power(IncsbLossRngx, Array(1, 2, 3, 4, 5, 6))), 1, 1)

IncsbLossA(1, 0) = Application.Index(Application.LinEst(IncsbLossRngyA, Application.Power(IncsbLossRngx, Array(1, 2, 3, 4, 5, 6))), 1, 2)

IncsbLossA(2, 0) = Application.Index(Application.LinEst(IncsbLossRngyA, Application.Power(IncsbLossRngx, Array(1, 2, 3, 4, 5, 6))), 1, 3)

IncsbLossA(3, 0) = Application.Index(Application.LinEst(IncsbLossRngyA, Application.Power(IncsbLossRngx, Array(1, 2, 3, 4, 5, 6))), 1, 4)

IncsbLossA(4, 0) = Application.Index(Application.LinEst(IncsbLossRngyA, Application.Power(IncsbLossRngx, Array(1, 2, 3, 4, 5, 6))), 1, 5)

IncsbLossA(5, 0) = Application.Index(Application.LinEst(IncsbLossRngyA, Application.Power(IncsbLossRngx, Array(1, 2, 3, 4, 5, 6))), 1, 6)

IncsbLossA(6, 0) = Application.Index(Application.LinEst(IncsbLossRngyA, Application.Power(IncsbLossRngx, Array(1, 2, 3, 4, 5, 6))), 1, 7)

Dim IncsbLossB(6, 0) As Double

IncsbLossB(0, 0) = Application.Index(Application.LinEst(IncsbLossRngyB, Application.Power(IncsbLossRngx, Array(1, 2, 3, 4, 5, 6))), 1, 1)

IncsbLossB(1, 0) = Application.Index(Application.LinEst(IncsbLossRngyB, Application.Power(IncsbLossRngx, Array(1, 2, 3, 4, 5, 6))), 1, 2)





NSInclLossF(1, 0) = Application.Index(Application.LinEst(NSInclLossRngyF, Application.Power(NSInclLossRngx, Array(1, 2, 3, 4, 5, 6))), 1, 2)  
 NSInclLossF(2, 0) = Application.Index(Application.LinEst(NSInclLossRngyF, Application.Power(NSInclLossRngx, Array(1, 2, 3, 4, 5, 6))), 1, 3)  
 NSInclLossF(3, 0) = Application.Index(Application.LinEst(NSInclLossRngyF, Application.Power(NSInclLossRngx, Array(1, 2, 3, 4, 5, 6))), 1, 4)  
 NSInclLossF(4, 0) = Application.Index(Application.LinEst(NSInclLossRngyF, Application.Power(NSInclLossRngx, Array(1, 2, 3, 4, 5, 6))), 1, 5)  
 NSInclLossF(5, 0) = Application.Index(Application.LinEst(NSInclLossRngyF, Application.Power(NSInclLossRngx, Array(1, 2, 3, 4, 5, 6))), 1, 6)  
 NSInclLossF(6, 0) = Application.Index(Application.LinEst(NSInclLossRngyF, Application.Power(NSInclLossRngx, Array(1, 2, 3, 4, 5, 6))), 1, 7)

## 2nd Polynomial Factors

Dim NSInclLoss2(6, 0) As Double

NSInclLoss2(0, 0) = ((((((((((NSInclLossA(0, 0) \* sin\_o\_s) + NSInclLossA(1, 0)) \* sin\_o\_s) + NSInclLossA(2, 0)) \* sin\_o\_s) + NSInclLossA(3, 0)) \*  
 sin\_o\_s) + NSInclLossA(4, 0)) \* sin\_o\_s) + NSInclLossA(5, 0)) \* sin\_o\_s) + NSInclLossA(6, 0)  
 NSInclLoss2(1, 0) = ((((((((((NSInclLossB(0, 0) \* sin\_o\_s) + NSInclLossB(1, 0)) \* sin\_o\_s) + NSInclLossB(2, 0)) \* sin\_o\_s) + NSInclLossB(3, 0)) \*  
 sin\_o\_s) + NSInclLossB(4, 0)) \* sin\_o\_s) + NSInclLossB(5, 0)) \* sin\_o\_s) + NSInclLossB(6, 0)  
 NSInclLoss2(2, 0) = ((((((((((NSInclLossC(0, 0) \* sin\_o\_s) + NSInclLossC(1, 0)) \* sin\_o\_s) + NSInclLossC(2, 0)) \* sin\_o\_s) + NSInclLossC(3, 0)) \*  
 sin\_o\_s) + NSInclLossC(4, 0)) \* sin\_o\_s) + NSInclLossC(5, 0)) \* sin\_o\_s) + NSInclLossC(6, 0)  
 NSInclLoss2(3, 0) = ((((((((((NSInclLossD(0, 0) \* sin\_o\_s) + NSInclLossD(1, 0)) \* sin\_o\_s) + NSInclLossD(2, 0)) \* sin\_o\_s) + NSInclLossD(3, 0)) \*  
 sin\_o\_s) + NSInclLossD(4, 0)) \* sin\_o\_s) + NSInclLossD(5, 0)) \* sin\_o\_s) + NSInclLossD(6, 0)  
 NSInclLoss2(4, 0) = ((((((((((NSInclLossE(0, 0) \* sin\_o\_s) + NSInclLossE(1, 0)) \* sin\_o\_s) + NSInclLossE(2, 0)) \* sin\_o\_s) + NSInclLossE(3, 0)) \*  
 sin\_o\_s) + NSInclLossE(4, 0)) \* sin\_o\_s) + NSInclLossE(5, 0)) \* sin\_o\_s) + NSInclLossE(6, 0)  
 NSInclLoss2(5, 0) = ((((((((((NSInclLossF(0, 0) \* sin\_o\_s) + NSInclLossF(1, 0)) \* sin\_o\_s) + NSInclLossF(2, 0)) \* sin\_o\_s) + NSInclLossF(3, 0)) \*  
 sin\_o\_s) + NSInclLossF(4, 0)) \* sin\_o\_s) + NSInclLossF(5, 0)) \* sin\_o\_s) + NSInclLossF(6, 0)

i-stall bas

i\_n\_bas = ((((((((((NSInclLoss2(0, 0) \* alphacc1) + NSInclLoss2(1, 0)) \* alphacc1) + NSInclLoss2(2, 0)) \* alphacc1) + NSInclLoss2(3, 0)) \*  
 alphacc1) + NSInclLoss2(4, 0)) \* alphacc1) + NSInclLoss2(5, 0)

## Negative Stalling Incidences s/b

Dim NSIncsbLossRngx As Range  
 Dim NSIncsbLossRngyA As Range  
 Dim NSIncsbLossRngyB As Range  
 Dim NSIncsbLossRngyC As Range  
 Dim NSIncsbLossRngyD As Range  
 Dim NSIncsbLossRngyE As Range  
 Dim NSIncsbLossRngyF As Range  
 Dim NSIncsbLossRngyG As Range

Set NSIncsbLossRngx = Worksheets("CraigCox Corr").Range("AE67:AE77")  
 Set NSIncsbLossRngyA = Worksheets("CraigCox Corr").Range("AF67:AF77")  
 Set NSIncsbLossRngyB = Worksheets("CraigCox Corr").Range("AG67:AG77")  
 Set NSIncsbLossRngyC = Worksheets("CraigCox Corr").Range("AH67:AH77")  
 Set NSIncsbLossRngyD = Worksheets("CraigCox Corr").Range("AI67:AI77")  
 Set NSIncsbLossRngyE = Worksheets("CraigCox Corr").Range("AJ67:AJ77")  
 Set NSIncsbLossRngyF = Worksheets("CraigCox Corr").Range("AK67:AK77")  
 Set NSIncsbLossRngyG = Worksheets("CraigCox Corr").Range("AL67:AL77")

## 1st Polynomial Factors

Dim NSIncsbLossA(6, 0) As Double

NSIncsbLossA(0, 0) = Application.Index(Application.LinEst(NSIncsbLossRngyA, Application.Power(NSIncsbLossRngx, Array(1, 2, 3, 4, 5,  
 6))), 1, 1)  
 NSIncsbLossA(1, 0) = Application.Index(Application.LinEst(NSIncsbLossRngyA, Application.Power(NSIncsbLossRngx, Array(1, 2, 3, 4, 5,  
 6))), 1, 2)  
 NSIncsbLossA(2, 0) = Application.Index(Application.LinEst(NSIncsbLossRngyA, Application.Power(NSIncsbLossRngx, Array(1, 2, 3, 4, 5,  
 6))), 1, 3)  
 NSIncsbLossA(3, 0) = Application.Index(Application.LinEst(NSIncsbLossRngyA, Application.Power(NSIncsbLossRngx, Array(1, 2, 3, 4, 5,  
 6))), 1, 4)  
 NSIncsbLossA(4, 0) = Application.Index(Application.LinEst(NSIncsbLossRngyA, Application.Power(NSIncsbLossRngx, Array(1, 2, 3, 4, 5,  
 6))), 1, 5)







Basic Negative Stalling Incidence > 90

Dim BNSInc90LossRngx As Range  
Dim BNSInc90LossRngyA As Range  
Dim BNSInc90LossRngyB As Range  
Dim BNSInc90LossRngyC As Range  
Dim BNSInc90LossRngyD As Range  
Dim BNSInc90LossRngyE As Range

Set BNSInc90LossRngx = Worksheets("CraigCox Corr").Range("AN67:AN79")  
Set BNSInc90LossRngyA = Worksheets("CraigCox Corr").Range("AO67:AO79")  
Set BNSInc90LossRngyB = Worksheets("CraigCox Corr").Range("AP67:AP79")  
Set BNSInc90LossRngyC = Worksheets("CraigCox Corr").Range("AQ67:AQ79")  
Set BNSInc90LossRngyD = Worksheets("CraigCox Corr").Range("AR67:AR79")  
Set BNSInc90LossRngyE = Worksheets("CraigCox Corr").Range("AS67:AS79")

1st Polynomial Factors

Dim BNSInc90LossA(6, 0) As Double  
BNSInc90LossA(0, 0) = Application.Index(Application.LinEst(BNSInc90LossRngyA, Application.Power(BNSInc90LossRngx, Array(1, 2, 3, 4, 5, 6))), 1, 1)  
BNSInc90LossA(1, 0) = Application.Index(Application.LinEst(BNSInc90LossRngyA, Application.Power(BNSInc90LossRngx, Array(1, 2, 3, 4, 5, 6))), 1, 2)  
BNSInc90LossA(2, 0) = Application.Index(Application.LinEst(BNSInc90LossRngyA, Application.Power(BNSInc90LossRngx, Array(1, 2, 3, 4, 5, 6))), 1, 3)  
BNSInc90LossA(3, 0) = Application.Index(Application.LinEst(BNSInc90LossRngyA, Application.Power(BNSInc90LossRngx, Array(1, 2, 3, 4, 5, 6))), 1, 4)  
BNSInc90LossA(4, 0) = Application.Index(Application.LinEst(BNSInc90LossRngyA, Application.Power(BNSInc90LossRngx, Array(1, 2, 3, 4, 5, 6))), 1, 5)  
BNSInc90LossA(5, 0) = Application.Index(Application.LinEst(BNSInc90LossRngyA, Application.Power(BNSInc90LossRngx, Array(1, 2, 3, 4, 5, 6))), 1, 6)  
BNSInc90LossA(6, 0) = Application.Index(Application.LinEst(BNSInc90LossRngyA, Application.Power(BNSInc90LossRngx, Array(1, 2, 3, 4, 5, 6))), 1, 7)

Dim BNSInc90LossB(6, 0) As Double  
BNSInc90LossB(0, 0) = Application.Index(Application.LinEst(BNSInc90LossRngyB, Application.Power(BNSInc90LossRngx, Array(1, 2, 3, 4, 5, 6))), 1, 1)  
BNSInc90LossB(1, 0) = Application.Index(Application.LinEst(BNSInc90LossRngyB, Application.Power(BNSInc90LossRngx, Array(1, 2, 3, 4, 5, 6))), 1, 2)  
BNSInc90LossB(2, 0) = Application.Index(Application.LinEst(BNSInc90LossRngyB, Application.Power(BNSInc90LossRngx, Array(1, 2, 3, 4, 5, 6))), 1, 3)  
BNSInc90LossB(3, 0) = Application.Index(Application.LinEst(BNSInc90LossRngyB, Application.Power(BNSInc90LossRngx, Array(1, 2, 3, 4, 5, 6))), 1, 4)  
BNSInc90LossB(4, 0) = Application.Index(Application.LinEst(BNSInc90LossRngyB, Application.Power(BNSInc90LossRngx, Array(1, 2, 3, 4, 5, 6))), 1, 5)  
BNSInc90LossB(5, 0) = Application.Index(Application.LinEst(BNSInc90LossRngyB, Application.Power(BNSInc90LossRngx, Array(1, 2, 3, 4, 5, 6))), 1, 6)  
BNSInc90LossB(6, 0) = Application.Index(Application.LinEst(BNSInc90LossRngyB, Application.Power(BNSInc90LossRngx, Array(1, 2, 3, 4, 5, 6))), 1, 7)

Dim BNSInc90LossC(6, 0) As Double  
BNSInc90LossC(0, 0) = Application.Index(Application.LinEst(BNSInc90LossRngyC, Application.Power(BNSInc90LossRngx, Array(1, 2, 3, 4, 5, 6))), 1, 1)  
BNSInc90LossC(1, 0) = Application.Index(Application.LinEst(BNSInc90LossRngyC, Application.Power(BNSInc90LossRngx, Array(1, 2, 3, 4, 5, 6))), 1, 2)  
BNSInc90LossC(2, 0) = Application.Index(Application.LinEst(BNSInc90LossRngyC, Application.Power(BNSInc90LossRngx, Array(1, 2, 3, 4, 5, 6))), 1, 3)  
BNSInc90LossC(3, 0) = Application.Index(Application.LinEst(BNSInc90LossRngyC, Application.Power(BNSInc90LossRngx, Array(1, 2, 3, 4, 5, 6))), 1, 4)  
BNSInc90LossC(4, 0) = Application.Index(Application.LinEst(BNSInc90LossRngyC, Application.Power(BNSInc90LossRngx, Array(1, 2, 3, 4, 5, 6))), 1, 5)

BNSInc90LossC(5, 0) = Application.Index(Application.LinEst(BNSInc90LossRngyC, Application.Power(BNSInc90LossRngx, Array(1, 2, 3, 4, 5, 6))), 1, 6)  
 BNSInc90LossC(6, 0) = Application.Index(Application.LinEst(BNSInc90LossRngyC, Application.Power(BNSInc90LossRngx, Array(1, 2, 3, 4, 5, 6))), 1, 7)

Dim BNSInc90LossD(6, 0) As Double  
 BNSInc90LossD(0, 0) = Application.Index(Application.LinEst(BNSInc90LossRngyD, Application.Power(BNSInc90LossRngx, Array(1, 2, 3, 4, 5, 6))), 1, 1)  
 BNSInc90LossD(1, 0) = Application.Index(Application.LinEst(BNSInc90LossRngyD, Application.Power(BNSInc90LossRngx, Array(1, 2, 3, 4, 5, 6))), 1, 2)  
 BNSInc90LossD(2, 0) = Application.Index(Application.LinEst(BNSInc90LossRngyD, Application.Power(BNSInc90LossRngx, Array(1, 2, 3, 4, 5, 6))), 1, 3)  
 BNSInc90LossD(3, 0) = Application.Index(Application.LinEst(BNSInc90LossRngyD, Application.Power(BNSInc90LossRngx, Array(1, 2, 3, 4, 5, 6))), 1, 4)  
 BNSInc90LossD(4, 0) = Application.Index(Application.LinEst(BNSInc90LossRngyD, Application.Power(BNSInc90LossRngx, Array(1, 2, 3, 4, 5, 6))), 1, 5)  
 BNSInc90LossD(5, 0) = Application.Index(Application.LinEst(BNSInc90LossRngyD, Application.Power(BNSInc90LossRngx, Array(1, 2, 3, 4, 5, 6))), 1, 6)  
 BNSInc90LossD(6, 0) = Application.Index(Application.LinEst(BNSInc90LossRngyD, Application.Power(BNSInc90LossRngx, Array(1, 2, 3, 4, 5, 6))), 1, 7)

Dim BNSInc90LossE(6, 0) As Double  
 BNSInc90LossE(0, 0) = Application.Index(Application.LinEst(BNSInc90LossRngyE, Application.Power(BNSInc90LossRngx, Array(1, 2, 3, 4, 5, 6))), 1, 1)  
 BNSInc90LossE(1, 0) = Application.Index(Application.LinEst(BNSInc90LossRngyE, Application.Power(BNSInc90LossRngx, Array(1, 2, 3, 4, 5, 6))), 1, 2)  
 BNSInc90LossE(2, 0) = Application.Index(Application.LinEst(BNSInc90LossRngyE, Application.Power(BNSInc90LossRngx, Array(1, 2, 3, 4, 5, 6))), 1, 3)  
 BNSInc90LossE(3, 0) = Application.Index(Application.LinEst(BNSInc90LossRngyE, Application.Power(BNSInc90LossRngx, Array(1, 2, 3, 4, 5, 6))), 1, 4)  
 BNSInc90LossE(4, 0) = Application.Index(Application.LinEst(BNSInc90LossRngyE, Application.Power(BNSInc90LossRngx, Array(1, 2, 3, 4, 5, 6))), 1, 5)  
 BNSInc90LossE(5, 0) = Application.Index(Application.LinEst(BNSInc90LossRngyE, Application.Power(BNSInc90LossRngx, Array(1, 2, 3, 4, 5, 6))), 1, 6)  
 BNSInc90LossE(6, 0) = Application.Index(Application.LinEst(BNSInc90LossRngyE, Application.Power(BNSInc90LossRngx, Array(1, 2, 3, 4, 5, 6))), 1, 7)

Dim sin\_o\_s As Double  
 sin\_o\_s = Application.WorksheetFunction.Degrees(Application.WorksheetFunction.Asin((rowdata(i1, 0) / rowdata(i1, 6))))

#### 2nd Polynomial Factors

Dim BNSInc90Loss2(4, 0) As Double  
 BNSInc90Loss2(0, 0) = ((((((((((BNSInc90LossA(0, 0) \* sin\_o\_s) + BNSInc90LossA(1, 0)) \* sin\_o\_s) + BNSInc90LossA(2, 0)) \* sin\_o\_s) + BNSInc90LossA(3, 0)) \* sin\_o\_s) + BNSInc90LossA(4, 0)) \* sin\_o\_s) + BNSInc90LossA(5, 0)) \* sin\_o\_s) + BNSInc90LossA(6, 0)  
 BNSInc90Loss2(1, 0) = ((((((((((BNSInc90LossB(0, 0) \* sin\_o\_s) + BNSInc90LossB(1, 0)) \* sin\_o\_s) + BNSInc90LossB(2, 0)) \* sin\_o\_s) + BNSInc90LossB(3, 0)) \* sin\_o\_s) + BNSInc90LossB(4, 0)) \* sin\_o\_s) + BNSInc90LossB(5, 0)) \* sin\_o\_s) + BNSInc90LossB(6, 0)  
 BNSInc90Loss2(2, 0) = ((((((((((BNSInc90LossC(0, 0) \* sin\_o\_s) + BNSInc90LossC(1, 0)) \* sin\_o\_s) + BNSInc90LossC(2, 0)) \* sin\_o\_s) + BNSInc90LossC(3, 0)) \* sin\_o\_s) + BNSInc90LossC(4, 0)) \* sin\_o\_s) + BNSInc90LossC(5, 0)) \* sin\_o\_s) + BNSInc90LossC(6, 0)  
 BNSInc90Loss2(3, 0) = ((((((((((BNSInc90LossD(0, 0) \* sin\_o\_s) + BNSInc90LossD(1, 0)) \* sin\_o\_s) + BNSInc90LossD(2, 0)) \* sin\_o\_s) + BNSInc90LossD(3, 0)) \* sin\_o\_s) + BNSInc90LossD(4, 0)) \* sin\_o\_s) + BNSInc90LossD(5, 0)) \* sin\_o\_s) + BNSInc90LossD(6, 0)  
 BNSInc90Loss2(4, 0) = ((((((((((BNSInc90LossE(0, 0) \* sin\_o\_s) + BNSInc90LossE(1, 0)) \* sin\_o\_s) + BNSInc90LossE(2, 0)) \* sin\_o\_s) + BNSInc90LossE(3, 0)) \* sin\_o\_s) + BNSInc90LossE(4, 0)) \* sin\_o\_s) + BNSInc90LossE(5, 0)) \* sin\_o\_s) + BNSInc90LossE(6, 0)

i-bas90

i\_nbas90 = ((((((((((BNSInc90Loss2(0, 0) \* alphacc1) + BNSInc90Loss2(1, 0)) \* alphacc1) + BNSInc90Loss2(2, 0)) \* alphacc1) + BNSInc90Loss2(3, 0)) \* alphacc1) + BNSInc90Loss2(4, 0)

Basic Positive Stalling Incidence > 90

Dim BPSInc90LossRngx As Range

Dim BPSInc90LossRngyA As Range  
Dim BPSInc90LossRngyB As Range  
Dim BPSInc90LossRngyC As Range  
Dim BPSInc90LossRngyD As Range  
Dim BPSInc90LossRngyE As Range

Set BPSInc90LossRngx = Worksheets("CraigCox Corr").Range("AU67:AU77")  
Set BPSInc90LossRngyA = Worksheets("CraigCox Corr").Range("AV67:AV77")  
Set BPSInc90LossRngyB = Worksheets("CraigCox Corr").Range("AW67:AW77")  
Set BPSInc90LossRngyC = Worksheets("CraigCox Corr").Range("AX67:AX77")  
Set BPSInc90LossRngyD = Worksheets("CraigCox Corr").Range("AY67:AY77")  
Set BPSInc90LossRngyE = Worksheets("CraigCox Corr").Range("AZ67:AZ77")

#### 1st Polynomial Factors

Dim BPSInc90LossA(6, 0) As Double  
BPSInc90LossA(0, 0) = Application.Index(Application.LinEst(BPSInc90LossRngyA, Application.Power(BPSInc90LossRngx, Array(1, 2, 3, 4, 5, 6))), 1, 1)  
BPSInc90LossA(1, 0) = Application.Index(Application.LinEst(BPSInc90LossRngyA, Application.Power(BPSInc90LossRngx, Array(1, 2, 3, 4, 5, 6))), 1, 2)  
BPSInc90LossA(2, 0) = Application.Index(Application.LinEst(BPSInc90LossRngyA, Application.Power(BPSInc90LossRngx, Array(1, 2, 3, 4, 5, 6))), 1, 3)  
BPSInc90LossA(3, 0) = Application.Index(Application.LinEst(BPSInc90LossRngyA, Application.Power(BPSInc90LossRngx, Array(1, 2, 3, 4, 5, 6))), 1, 4)  
BPSInc90LossA(4, 0) = Application.Index(Application.LinEst(BPSInc90LossRngyA, Application.Power(BPSInc90LossRngx, Array(1, 2, 3, 4, 5, 6))), 1, 5)  
BPSInc90LossA(5, 0) = Application.Index(Application.LinEst(BPSInc90LossRngyA, Application.Power(BPSInc90LossRngx, Array(1, 2, 3, 4, 5, 6))), 1, 6)  
BPSInc90LossA(6, 0) = Application.Index(Application.LinEst(BPSInc90LossRngyA, Application.Power(BPSInc90LossRngx, Array(1, 2, 3, 4, 5, 6))), 1, 7)

Dim BPSInc90LossB(6, 0) As Double  
BPSInc90LossB(0, 0) = Application.Index(Application.LinEst(BPSInc90LossRngyB, Application.Power(BPSInc90LossRngx, Array(1, 2, 3, 4, 5, 6))), 1, 1)  
BPSInc90LossB(1, 0) = Application.Index(Application.LinEst(BPSInc90LossRngyB, Application.Power(BPSInc90LossRngx, Array(1, 2, 3, 4, 5, 6))), 1, 2)  
BPSInc90LossB(2, 0) = Application.Index(Application.LinEst(BPSInc90LossRngyB, Application.Power(BPSInc90LossRngx, Array(1, 2, 3, 4, 5, 6))), 1, 3)  
BPSInc90LossB(3, 0) = Application.Index(Application.LinEst(BPSInc90LossRngyB, Application.Power(BPSInc90LossRngx, Array(1, 2, 3, 4, 5, 6))), 1, 4)  
BPSInc90LossB(4, 0) = Application.Index(Application.LinEst(BPSInc90LossRngyB, Application.Power(BPSInc90LossRngx, Array(1, 2, 3, 4, 5, 6))), 1, 5)  
BPSInc90LossB(5, 0) = Application.Index(Application.LinEst(BPSInc90LossRngyB, Application.Power(BPSInc90LossRngx, Array(1, 2, 3, 4, 5, 6))), 1, 6)  
BPSInc90LossB(6, 0) = Application.Index(Application.LinEst(BPSInc90LossRngyB, Application.Power(BPSInc90LossRngx, Array(1, 2, 3, 4, 5, 6))), 1, 7)

Dim BPSInc90LossC(6, 0) As Double  
BPSInc90LossC(0, 0) = Application.Index(Application.LinEst(BPSInc90LossRngyC, Application.Power(BPSInc90LossRngx, Array(1, 2, 3, 4, 5, 6))), 1, 1)  
BPSInc90LossC(1, 0) = Application.Index(Application.LinEst(BPSInc90LossRngyC, Application.Power(BPSInc90LossRngx, Array(1, 2, 3, 4, 5, 6))), 1, 2)  
BPSInc90LossC(2, 0) = Application.Index(Application.LinEst(BPSInc90LossRngyC, Application.Power(BPSInc90LossRngx, Array(1, 2, 3, 4, 5, 6))), 1, 3)  
BPSInc90LossC(3, 0) = Application.Index(Application.LinEst(BPSInc90LossRngyC, Application.Power(BPSInc90LossRngx, Array(1, 2, 3, 4, 5, 6))), 1, 4)  
BPSInc90LossC(4, 0) = Application.Index(Application.LinEst(BPSInc90LossRngyC, Application.Power(BPSInc90LossRngx, Array(1, 2, 3, 4, 5, 6))), 1, 5)  
BPSInc90LossC(5, 0) = Application.Index(Application.LinEst(BPSInc90LossRngyC, Application.Power(BPSInc90LossRngx, Array(1, 2, 3, 4, 5, 6))), 1, 6)  
BPSInc90LossC(6, 0) = Application.Index(Application.LinEst(BPSInc90LossRngyC, Application.Power(BPSInc90LossRngx, Array(1, 2, 3, 4, 5, 6))), 1, 7)

```

Dim BPSInc90LossD(6, 0) As Double
BPSInc90LossD(0, 0) = Application.Index(Application.LinEst(BPSInc90LossRngyD, Application.Power(BPSInc90LossRngx, Array(1, 2, 3, 4, 5, 6))), 1, 1)
BPSInc90LossD(1, 0) = Application.Index(Application.LinEst(BPSInc90LossRngyD, Application.Power(BPSInc90LossRngx, Array(1, 2, 3, 4, 5, 6))), 1, 2)
BPSInc90LossD(2, 0) = Application.Index(Application.LinEst(BPSInc90LossRngyD, Application.Power(BPSInc90LossRngx, Array(1, 2, 3, 4, 5, 6))), 1, 3)
BPSInc90LossD(3, 0) = Application.Index(Application.LinEst(BPSInc90LossRngyD, Application.Power(BPSInc90LossRngx, Array(1, 2, 3, 4, 5, 6))), 1, 4)
BPSInc90LossD(4, 0) = Application.Index(Application.LinEst(BPSInc90LossRngyD, Application.Power(BPSInc90LossRngx, Array(1, 2, 3, 4, 5, 6))), 1, 5)
BPSInc90LossD(5, 0) = Application.Index(Application.LinEst(BPSInc90LossRngyD, Application.Power(BPSInc90LossRngx, Array(1, 2, 3, 4, 5, 6))), 1, 6)
BPSInc90LossD(6, 0) = Application.Index(Application.LinEst(BPSInc90LossRngyD, Application.Power(BPSInc90LossRngx, Array(1, 2, 3, 4, 5, 6))), 1, 7)

```

```

Dim BPSInc90LossE(6, 0) As Double
BPSInc90LossE(0, 0) = Application.Index(Application.LinEst(BPSInc90LossRngyE, Application.Power(BPSInc90LossRngx, Array(1, 2, 3, 4, 5, 6))), 1, 1)
BPSInc90LossE(1, 0) = Application.Index(Application.LinEst(BPSInc90LossRngyE, Application.Power(BPSInc90LossRngx, Array(1, 2, 3, 4, 5, 6))), 1, 2)
BPSInc90LossE(2, 0) = Application.Index(Application.LinEst(BPSInc90LossRngyE, Application.Power(BPSInc90LossRngx, Array(1, 2, 3, 4, 5, 6))), 1, 3)
BPSInc90LossE(3, 0) = Application.Index(Application.LinEst(BPSInc90LossRngyE, Application.Power(BPSInc90LossRngx, Array(1, 2, 3, 4, 5, 6))), 1, 4)
BPSInc90LossE(4, 0) = Application.Index(Application.LinEst(BPSInc90LossRngyE, Application.Power(BPSInc90LossRngx, Array(1, 2, 3, 4, 5, 6))), 1, 5)
BPSInc90LossE(5, 0) = Application.Index(Application.LinEst(BPSInc90LossRngyE, Application.Power(BPSInc90LossRngx, Array(1, 2, 3, 4, 5, 6))), 1, 6)
BPSInc90LossE(6, 0) = Application.Index(Application.LinEst(BPSInc90LossRngyE, Application.Power(BPSInc90LossRngx, Array(1, 2, 3, 4, 5, 6))), 1, 7)

```

## 2nd Polynomial Factors

```

Dim BPSInc90Loss2(4, 0) As Double
BPSInc90Loss2(0, 0) = ((((((((((BPSInc90LossA(0, 0) * sin_o_s) + BPSInc90LossA(1, 0)) * sin_o_s) + BPSInc90LossA(2, 0)) * sin_o_s) + BPSInc90LossA(3, 0)) * sin_o_s) + BPSInc90LossA(4, 0)) * sin_o_s) + BPSInc90LossA(5, 0)) * sin_o_s) + BPSInc90LossA(6, 0)
BPSInc90Loss2(1, 0) = ((((((((((BPSInc90LossB(0, 0) * sin_o_s) + BPSInc90LossB(1, 0)) * sin_o_s) + BPSInc90LossB(2, 0)) * sin_o_s) + BPSInc90LossB(3, 0)) * sin_o_s) + BPSInc90LossB(4, 0)) * sin_o_s) + BPSInc90LossB(5, 0)) * sin_o_s) + BPSInc90LossB(6, 0)
BPSInc90Loss2(2, 0) = ((((((((((BPSInc90LossC(0, 0) * sin_o_s) + BPSInc90LossC(1, 0)) * sin_o_s) + BPSInc90LossC(2, 0)) * sin_o_s) + BPSInc90LossC(3, 0)) * sin_o_s) + BPSInc90LossC(4, 0)) * sin_o_s) + BPSInc90LossC(5, 0)) * sin_o_s) + BPSInc90LossC(6, 0)
BPSInc90Loss2(3, 0) = ((((((((((BPSInc90LossD(0, 0) * sin_o_s) + BPSInc90LossD(1, 0)) * sin_o_s) + BPSInc90LossD(2, 0)) * sin_o_s) + BPSInc90LossD(3, 0)) * sin_o_s) + BPSInc90LossD(4, 0)) * sin_o_s) + BPSInc90LossD(5, 0)) * sin_o_s) + BPSInc90LossD(6, 0)
BPSInc90Loss2(4, 0) = ((((((((((BPSInc90LossE(0, 0) * sin_o_s) + BPSInc90LossE(1, 0)) * sin_o_s) + BPSInc90LossE(2, 0)) * sin_o_s) + BPSInc90LossE(3, 0)) * sin_o_s) + BPSInc90LossE(4, 0)) * sin_o_s) + BPSInc90LossE(5, 0)) * sin_o_s) + BPSInc90LossE(6, 0)

```

i+bas90

```

i_pbas90 = (((((((BPSInc90Loss2(0, 0) * alphacc1) + BPSInc90Loss2(1, 0)) * alphacc1) + BPSInc90Loss2(2, 0)) * alphacc1) + BPSInc90Loss2(3, 0)) * alphacc1) + BPSInc90Loss2(4, 0)

```

## Minimum Loss

```

Dim MinLossRngx As Range
Dim MinLossRngyA As Range
Dim MinLossRngyB As Range
Dim MinLossRngyC As Range
Dim MinLossRngyD As Range
Dim MinLossRngyE As Range

```



```

MinLoss2(1, 0) = ((((((((((MinLossB(0, 0) * s_Bb) + MinLossB(1, 0)) * s_Bb) + MinLossB(2, 0)) * s_Bb) + MinLossB(3, 0)) * s_Bb) +
MinLossB(4, 0)) * s_Bb) + MinLossB(5, 0)) * s_Bb) + MinLossB(6, 0)
MinLoss2(2, 0) = ((((((((((MinLossC(0, 0) * s_Bb) + MinLossC(1, 0)) * s_Bb) + MinLossC(2, 0)) * s_Bb) + MinLossC(3, 0)) * s_Bb) +
MinLossC(4, 0)) * s_Bb) + MinLossC(5, 0)) * s_Bb) + MinLossC(6, 0)
MinLoss2(3, 0) = ((((((((((MinLossD(0, 0) * s_Bb) + MinLossD(1, 0)) * s_Bb) + MinLossD(2, 0)) * s_Bb) + MinLossD(3, 0)) * s_Bb) +
MinLossD(4, 0)) * s_Bb) + MinLossD(5, 0)) * s_Bb) + MinLossD(6, 0)
MinLoss2(4, 0) = ((((((((((MinLossE(0, 0) * s_Bb) + MinLossE(1, 0)) * s_Bb) + MinLossE(2, 0)) * s_Bb) + MinLossE(3, 0)) * s_Bb) +
MinLossE(4, 0)) * s_Bb) + MinLossE(5, 0)) * s_Bb) + MinLossE(6, 0)

```

Fi

Dim Fi As Double

```

Fi = (((((((MinLoss2(0, 0) * alphacc1) + MinLoss2(1, 0)) * alphacc1) + MinLoss2(2, 0)) * alphacc1) + MinLoss2(3, 0)) * alphacc1) +
MinLoss2(4, 0)

```

Incidence Loss

Dim i\_pstall As Double

Dim i\_nstall As Double

If alphacc1 > 90 Then

```

i_pstall = i_pbas90 + (1 - ((alphacc1 - 90) / (90 - sin_o_s))) * (i_CR + i_s_b)

```

```

i_nstall = i_nbas90 + (1 - ((alphacc1 - 90) / (90 - sin_o_s))) * (i_n_s_b)

```

Else

```

i_pstall = i_bas + i_CR + i_s_b

```

```

i_nstall = i_n_bas + i_n_s_b

```

End If

Dim i\_min As Double

```

i_min = ((i_pstall + (Fi * i_nstall)) / (1 + Fi))

```

Dim inc As Double

If i1 = 0 Then

```

inc = 0

```

Else

```

inc = Application.WorksheetFunction.Degrees(nozzleout(0, 0)) - rowdata(i1, 7)

```

End If

Dim incr As Double

If Abs(inc) < Abs(i\_min) Then

```

incr = (inc - i_min) / Abs(i_nstall - i_min)

```

Else

```

incr = (inc - i_min) / Abs(i_pstall - i_min)

```

End If

Dim incLossRngx As Range

Dim incLossRngyA As Range

```

Set incLossRngx = Worksheets("CraigCox Corr").Range("BI67:BI79")

```

```

Set incLossRngyA = Worksheets("CraigCox Corr").Range("BJ67:BJ79")

```

1st Polynomial Factors

Dim incLossA(6, 0) As Double

```

incLossA(0, 0) = Application.Index(Application.LinEst(incLossRngyA, Application.Power(incLossRngx, Array(1, 2, 3, 4, 5, 6))), 1, 1)

```

```

incLossA(1, 0) = Application.Index(Application.LinEst(incLossRngyA, Application.Power(incLossRngx, Array(1, 2, 3, 4, 5, 6))), 1, 2)

```

```

incLossA(2, 0) = Application.Index(Application.LinEst(incLossRngyA, Application.Power(incLossRngx, Array(1, 2, 3, 4, 5, 6))), 1, 3)

```

```

incLossA(3, 0) = Application.Index(Application.LinEst(incLossRngyA, Application.Power(incLossRngx, Array(1, 2, 3, 4, 5, 6))), 1, 4)

```

```

incLossA(4, 0) = Application.Index(Application.LinEst(incLossRngyA, Application.Power(incLossRngx, Array(1, 2, 3, 4, 5, 6))), 1, 5)

```

```

incLossA(5, 0) = Application.Index(Application.LinEst(incLossRngyA, Application.Power(incLossRngx, Array(1, 2, 3, 4, 5, 6))), 1, 6)

```

```

incLossA(6, 0) = Application.Index(Application.LinEst(incLossRngyA, Application.Power(incLossRngx, Array(1, 2, 3, 4, 5, 6))), 1, 7)

```



$Xi = ((((((((((incLossA(0, 0) * incr) + incLossA(1, 0)) * incr) + incLossA(2, 0)) * incr) + incLossA(3, 0)) * incr) + incLossA(4, 0)) * incr) + incLossA(5, 0)) * incr) + incLossA(6, 0)$

If inc < -5 Or inc > 10 Then

Xi = Xi

Else

Xi = 1

End If

If Xi > 3.5 Then

Xi = 3.5

End If

Corrected Profile Loss

$xpcc = 0.01 * (Xte * Xi * PLoss + BBR + MA + Pte) * (1 + 0.5 * g1 * m ^ 2)$

$Pte2 = 0.01 * Pte * (1 + 0.5 * g1 * m ^ 2)$

Secondary Losses

Aspect ratio factor

Dim LossCoeff As Collection

Dim Loss As Variant

Set LossCoeff = New Collection

LossCoeff.Add "" & 0.25 \* (rowgeom(i1 + 1, 1) + rowgeom(i1, 1) - rowgeom(i1 + 1, 0) - rowgeom(i1, 0)) & "", "bldhgt" & i1 & ""

Dim b\_h As Double

$b\_h = Bb / (LossCoeff.Item("bldhgt" & i1 & "")) * 0.0254$

Dim SecARLossRngx As Range

Dim SecARLossRngyA As Range

Set SecARLossRngx = Worksheets("CraigCox Corr").Range("B84:B94")

Set SecARLossRngyA = Worksheets("CraigCox Corr").Range("c84:c94")

1st Polynomial Factors

Dim SecARLossA(6, 0) As Double

SecARLossA(0, 0) = Application.Index(Application.LinEst(SecARLossRngyA, Application.Power(SecARLossRngx, Array(1, 2, 3, 4, 5, 6))), 1, 1)

SecARLossA(1, 0) = Application.Index(Application.LinEst(SecARLossRngyA, Application.Power(SecARLossRngx, Array(1, 2, 3, 4, 5, 6))), 1, 2)

SecARLossA(2, 0) = Application.Index(Application.LinEst(SecARLossRngyA, Application.Power(SecARLossRngx, Array(1, 2, 3, 4, 5, 6))), 1, 3)

SecARLossA(3, 0) = Application.Index(Application.LinEst(SecARLossRngyA, Application.Power(SecARLossRngx, Array(1, 2, 3, 4, 5, 6))), 1, 4)

SecARLossA(4, 0) = Application.Index(Application.LinEst(SecARLossRngyA, Application.Power(SecARLossRngx, Array(1, 2, 3, 4, 5, 6))), 1, 5)

SecARLossA(5, 0) = Application.Index(Application.LinEst(SecARLossRngyA, Application.Power(SecARLossRngx, Array(1, 2, 3, 4, 5, 6))), 1, 6)

SecARLossA(6, 0) = Application.Index(Application.LinEst(SecARLossRngyA, Application.Power(SecARLossRngx, Array(1, 2, 3, 4, 5, 6))), 1, 7)

Dim Nsh\_b As Double

$Nsh\_b = ((((((((((SecARLossA(0, 0) * b\_h) + SecARLossA(1, 0)) * b\_h) + SecARLossA(2, 0)) * b\_h) + SecARLossA(3, 0)) * b\_h) + SecARLossA(4, 0)) * b\_h) + SecARLossA(5, 0)) * b\_h) + SecARLossA(6, 0)$

Basic Loss Factor

Dim SecBasLossRngx As Range  
 Dim SecBasLossRngyA As Range  
 Dim SecBasLossRngyB As Range

Set SecBasLossRngx = Worksheets("CraigCox Corr").Range("B99:B105")  
 Set SecBasLossRngyA = Worksheets("CraigCox Corr").Range("C99:C105")  
 Set SecBasLossRngyB = Worksheets("CraigCox Corr").Range("D99:D105")

m

Dim SecBasLossA(1, 0) As Double  
 SecBasLossA(0, 0) = Application.Index(Application.LinEst(SecBasLossRngyA, Application.Power(SecBasLossRngx, Array(1))), 1, 1)  
 SecBasLossA(1, 0) = Application.Index(Application.LinEst(SecBasLossRngyA, Application.Power(SecBasLossRngx, Array(1))), 1, 2)

C

Dim SecBasLossB(1, 0) As Double  
 SecBasLossB(0, 0) = Application.Index(Application.LinEst(SecBasLossRngyB, Application.Power(SecBasLossRngx, Array(1))), 1, 1)  
 SecBasLossB(1, 0) = Application.Index(Application.LinEst(SecBasLossRngyB, Application.Power(SecBasLossRngx, Array(1))), 1, 2)

Velocity Ratio

vel\_ratio = 0

If vel\_ratio > 1 Then  
 vel\_ratio = 1  
 End If

Dim secm As Double  
 secm = (SecBasLossA(0, 0) \* FL\_sb) + SecBasLossA(1, 0)

Dim secc As Double  
 secc = (SecBasLossB(0, 0) \* FL\_sb) + SecBasLossB(1, 0)

Dim Sec\_bas As Double  
 Sec\_bas = (secm \* vel\_ratio) + secc

xsc = 0.01 \* (Nsh\_b \* Sec\_bas) \* (1 + 0.5 \* g1 \* m ^ 2)

a1 = nozzleout(0, 0)

am = Atn(0.5 \* (Tan(a1) + Tan(alpha4(i1, 0))))

xtcc = 0.47 \* (rowdata(i1, 2) / rowdata(i1, 8) ^ 0.78 \* rowdata(i1, 8) / LossCoeff.Item("bldhgt" & i1 & "")) \* ((Tan(a1) - Tan(alpha4(i1, 0))) \* Cos(alpha4(i1, 0))) ^ 2 / Cos(am)

End If

If i1 = 0 Then  
 xtcc = 0  
 End If

Yt = xpcc + xsc + xtcc

Profile Loss Reynolds number

Dynamic Viscosity

Dim mu As Double  
 If i1 = 0 Then  
 mu = ((((((((-6.0671918E-12 \* (nozzleout(2, 0) - 273.15)) + 2.212997838519E-08) \* (nozzleout(2, 0) - 273.15)) - 3.46909333623785E-05) \* (nozzleout(2, 0) - 273.15)) + 4.95001977743888E-02) \* (nozzleout(2, 0) - 273.15)) + 16.9760680267161) \* 10 ^ -6

```

Else
mu = ((((((((-6.0671918E-12 * (turbineout(2, 0) - 273.15)) + 2.212997838519E-08) * (turbineout(2, 0) - 273.15)) - 3.46909333623785E-05) *
(turbineout(2, 0) - 273.15)) + 4.95001977743888E-02) * (turbineout(2, 0) - 273.15)) + 16.9760680267161) * 10 ^ -6
End If

Density

Dim rho As Double

If i1 = 0 Then
rho = (nozzleout(3, 0) * 6.89 * 1000 + 100000) / (nozzleout(2, 0) * 287.04)
Else
rho = (turbineout(3, 0) * 6.89 * 1000 + 100000) / (turbineout(2, 0) * 287.04)
End If

If i1 = 0 Then
Re = (rho * (nozzleout(2, 0)) * 0.3048 * (rowdata(i1, 8) * 0.0254)) / mu
Else
Re = (rho * (vo) * 0.3048 * (rowdata(i1, 8) * 0.0254)) / mu
End If

ReO = Re * rowdata(i1, 0) / rowdata(i1, 8)

Xre = 21.945740773485 * ReO ^ -0.261777855254533

xpcc = 0.01 * (Xre * Xte * Xi * PLoss + BBR + MA + Pte) * (1 + 0.5 * g1 * m ^ 2)

Velocity Ratio

Dim a7 As Double
a7 = Application.WorksheetFunction.Pi() * ((rowgeom(0, 0) * 0.0254) ^ 2) / 4

Dim a8 As Double
a8 = Application.WorksheetFunction.Pi() * ((rowgeom(0, 1) * 0.0254) ^ 2) / 4

Dim Annulus As Double
Annulus = a8 - a7

Dim rhoi As Double
rhoi = (Pi * 6.89 * 1000) / (ti * 287.04)

v7 = w / (rhoi * Annulus)

If i1 = 0 Then
vel_ratio = (v7 / vo) ^ 2
Else
vel_ratio = (nozzleout(1, 0) / vo) ^ 2
End If

If vel_ratio > 1 Then
vel_ratio = 1
End If

secm = (SecBasLossA(0, 0) * FL_sb) + SecBasLossA(1, 0)

secc = (SecBasLossB(0, 0) * FL_sb) + SecBasLossB(1, 0)

Sec_bas = (secm * vel_ratio) + secc

xsc = 0.01 * (Xre * Nsh_b * Sec_bas) * (1 + 0.5 * g1 * m ^ 2)

If i1 = 0 Then

```

xtcc = 0  
End If

$Y_t = xpcc + xsc + xtcc$